Universidad de Santiago de Compostela

THE DEVELOPMENT OF PLASMATIC GLUTAMATE GRABBERS FOR THE TREATMENT OF ISCHEMIC STROKE

Desarrollo de atrapadores de glutamato plasmático como terapia para el ictus isquémico

Memoria para optar al grado de doctor presentada por

María Pérez Mato

Directores de tesis:

Prof. José Castillo Sánchez

Dr. Tomás Sobrino Moreiras

Dr. Francisco Campos Pérez

Santiago de Compostela, Septiembre 2015

USC
UNIVERSIDADE
DE SANTIAGO
DE COMPOSTELA

Prof. José Castillo Sánchez
Catedrático de Neurología

Servicio de Neurología
Hospital Clínico Universitario
Travesía de la Choupana s/n
15706 Santiago de Compostela

El **Prof. Dr. José Castillo Sánchez**, Catedrático y Director del Departamento de Medicina de la Universidad de Santiago de Compostela, Jefe del departamento de Neurología del Hospital Clínico Universitario de Santiago de Compostela y Director Científico del Instituto de Investigación Sanitaria de Santiago de Compostela (IDIS), el **Dr. Francisco Campos Pérez**, Investigador Miguel Servet y colaborador docente del Departamento de Medicina de la Universidad de Santiago de Compostela y el **Dr. Tomás Sobrino Moreiras**, Investigador Miguel Servet y colaborador docente del Departamento de Medicina de la Universidad de Santiago de Compostela,

CERTIFICAN:

Que el presente trabajo titulado **"Desarrollo de atrapadores de glutamato plasmático como terapia para el ictus isquémico"** ha sido realizado bajo su dirección, por la licenciada en biología **Dña. María Pérez Mato**, y se encuentra en condiciones de ser presentado y defendido como Tesis Doctoral ante el tribunal correspondiente en la Universidad de Santiago de Compostela.

Santiago de Compostela, Septiembre 2015

Prof. José Castillo Dr. Francisco Campos Dr. Tomás Sobrino

USC
UNIVERSIDADE
DE SANTIAGO
DE COMPOSTELA

Prof. José Castillo Sánchez
Catedrático de Neurología

Servicio de Neurología
Hospital Clínico Universitario
Travesía de la Choupana s/n
15706 Santiago de Compostela

Prof. Dr. José Castillo Sánchez, Professor of Neurology and Director of the Department of Medicine of the University of Santiago de Compostela, Chief of Neurology Department of the University Clinical Hospital of Santiago de Compostela and Scientific Director of Health Research Institute of Santiago de Compostela (IDIS), **Dr. Francisco Campos Pérez**, PhD and Miguel Servet researcher and **Dr. Tomás Sobrino Moreiras**, PhD and Miguel Servet researcher

CERTIFY:

That the present research study entitled "**The development of plasmatic glutamate grabbers for the treatment of ischemic stroke**" has been carried out under their supervision by **María Pérez Mato**, graduated in Biology, and the document fulfill all requisites for its defense under the corresponding committee proposed by the University of Santiago de Compostela.

Santiago de Compostela, September 2015

Prof. José Castillo Dr. Francisco Campos Dr. Tomás Sobrino

USC
UNIVERSIDADE
DE SANTIAGO
DE COMPOSTELA

Agradecimientos

Me ha llevado mucho tiempo danzar esta danza, 7 años concretamente, pero seguro que me hubiera llevado el doble si no hubiera sido por la ayuda de muchas personas a las que tengo mucho que agradecer, tanto profesional como personalmente, haber formado parte de este proyecto.

En primer lugar me gustaría agradecer al Prof. Castillo haberme dado la gran oportunidad de formar parte de su grupo de investigación. También mostrarle mi gratitud por toda su ayuda y enseñanzas, que van desde la “Bioquímica de la isquemia cerebral” hasta que los colores claros no son adecuados en las presentaciones. Por todo esto y mucho más, muchas gracias.

Seguidamente a mis codirectores, Dr. Francisco Campos y Dr. Tomás Sobrino, a quienes tengo que agradecerles su implicación y dedicación en este trabajo. Además de ello, me gustaría agradecerles la confianza depositada en mí, así como su apoyo diario.

Agradecer también a mis compañeros de laboratorio que han hecho posible este trabajo, tanto los que están como a los que ya no están. Muchas gracias Miguel, Manuel, Rogelio, Susana, Juan, Ana, María, José, Emilio, Iria, Isabel, María Pouso y María Sabucedo por vuestra colaboración. Muchas gracias también a Alba, Héctor, Andrés, Joserra, Esteban, Tania, Nacho, Manuel, Clara, Esteban, Raquel, Pedro, Jesús, Octavio, David Barral, Iván, David Brea y Esther por hacer más fácil el día a día y por vuestra contribución. Quería agradecer especialmente a mis físicos preferidos, a Ramón y Bárbara. Gracias Ramón por hacer la mayor parte de las resonancias de este trabajo. Y muchas gracias Bárbara por tu paciencia infinita para explicarme todas las dudas científicas y no científicas, por tu ayuda con las resonancias, múltiples correcciones y el desarrollo gráfico de este trabajo, por compartir conmigo tu vida y brindarme tu amistad.

He tenido la suerte de poder realizar parte de este trabajo en otros laboratorios y contar con la colaboración de grandes

profesionales. Gracias Amparo y Emi del grupo de investigación de Biofarma de la USC por vuestra cooperación con los experimentos de captación de glutamato. También agradecer a Esther, Ángela, Mari, Sihara y Joana del grupo de investigación de Neoplasia y Diferenciación de Células Endocrinas de la USC por vuestra ayuda con los protocolos de electroporación y por hacerme sentir una más. Muchas gracias a Manuela por tu disponibilidad para la resolución de dudas respecto a protocolos de western blot y a Pili del grupo de Células Madre en Cáncer y Envejecimiento de la USC por tu colaboración en la expansión del plásmido. Asimismo, agradezco al Prof. Christoph Fahlke por aceptarme en Zelluläre Biophysik y especialmente al Prof. Baumann por su orientación y atención a mis consultas. Gracias a mis compañeros Arne, Anne, Nadine, Sabine and Annika por vuestra ayuda y a Georgia por tu compañía durante largos días en Jülich.

Este trabajo es también fruto del apoyo vital de los amigos que siempre están ahí, sin el cual no tendría la fuerza y energía para seguir. Muchas gracias a Noelia, Nuria, Carmen, Marcos, Cris, Ana, David, Jesse, María José, Marisa, Natalia, Silvia, Javier, Patry, Ara, Paul, Belén, Nora, Naty, Fer, Víctor, Cris Rey y Marta.

Gracias a Javi, a quien no encontraré la forma de agradecerle su apoyo, ayuda comprensión y confianza a lo largo de estos 7 años. Siempre has estado en los logros y fracasos, haciendo que este trabajo también sea tuyo.

Finalmente muchas gracias a toda mi familia, Maricarmen, Anita, Denis, Yesika, Bea, Joaquín, María del Carmen, Constantino, Francisco, Herminda, Paco, Pili, Bebo Fina y María por todos los momentos tan felices compartidos. Y especialmente, a mis padres Carmen y Vicente y a mi hermano Jorge, porque sin ellos este trabajo no habría sido posible.

A todos, muchas gracias.

María

USC
UNIVERSIDADE
DE SANTIAGO
DE COMPOSTELA

USC
UNIVERSIDADE
DE SANTIAGO
DE COMPOSTELA

Abbreviations

ADC: Apparent Diffusion Coefficient

A-KG: α Ketoglutarate

ALS: Amyotrophic Lateral Sclerosis

AMPAr: α-Amino-3-Hydroxy-5-Methyl-4-Isoxazol Receptors

ATP: Adenosine Tri-Phosphate

BBB: Blood-Brain Barrier

bFGF: Fibroblast Growth Factor

BMSCs: Bone Marrow Stem Cells

BNDF: Brain-Derived Neurotrophic Factor

CBF: Cerebral Blood Flow

CNS: Cerebral Nervous System

COX-2: Cycloxigenase-2

CSD: Cortical Spreading Depression

CSF: Cerebral Spinal Fluid

CSPGs: Chondroitin Sulfate Proteoglycans

CVOs: Circumventricular Organs

DC: Dendritic Cells

DWI: Diffusion Weighted Images

EAATs: Excitatory Amino Acid Transporters

EC: Endothelial Cells

EGF: Epidermal Growth Factor

ESCs: Embryonic Stem Cells

FGF: Fibroblast Growth Factor

GABA: Gamma-Aminobutyric Acid

GAPDH: Glyceraldhyde 3-Phosphate Deshydrogenase

GM-CSF: Granulocyte-Macrophage Colony-Stimulating Factor

GOT: Glutamate-Oxaloacetate Transaminase

GPT: Glutamic Piruvic Transaminase

hESCs: Human Embryonic Stem Cells

HGF: Platelet-Derived Growth Factor

HIV-1: Human Immune-Deficiency Virus Type 1

HSCs: Hematopoietic Stem Cells

HSV-1: Herpes Simplex Virus Type 1

HUCBCs: Human Umbilical Cord Blood Cells

IBZ: Ischemic Border Zone

ICAM-1: Intercellular Adhesion Molecule

IDO: Dioxygenase

IGF-1: Insulin-Like Growth Factor-1

iGluR: Ionotropic Glutamate Receptor

IL10: Interleukin 10

iNOS: Inducible NO Synthase Enzymes

iPSCs: Induced Pluripotent Cells

ITR: Inverted Terminal Repeat

MC: Mast Cells

MCAO: Middle Cerebral Artery

mGluR: Metabotropic Glutamate Receptor

MMPs: Matrix Metalloproteinases

MRA: Magnetic Resonance Angiography

MRS: Magnetic Resonance Spectroscopy

MSCs: Mesenchymal Stem Cells

NK: Natural Killers

NMDAr: N-Methyl-D-Aspartate Glutamatergic Receptors

nNOS: Nitric Oxide Synthase

NO: Nitric Oxide

NSCs: Neural Stem Cells

OPCs: Oligodendrocyte Progenitor Cells

ORFs: Open Reading Frames

PAI-1: Plasminogen Activator Inhibitor

PGE2: Prostaglandin E2

PI3-AKT: Phosphatidylinositol-3-Kinase

rAAV: Recombinant Adeno Associated Viral Vectors

rt-PA: Recombinant Tissue Plasminogen Activator

SAH: Subarachnoid Hemorrhage

SAT1: System A Trasnporter

SDF-1: Stromal Cell-Derived Factor-1

SE: Status Epilepticus

SEPs: Somatosensory Evoked Potentials

SGZ: Subgranular Zone

SN1: System N Transporter

SNAREs: Soluble N-Ethylmaleimide-Sensitive Factor Attachement Factor

SVZ: Subventricular Zone

TBI: Traumatic Brain Injury

TCA cycle: Tricarboxylic Acids Cycle

TGF-β: Transforming Growth Factor Beta

TIA: Trasiente Ischemic Attack

TLRs: Toll-Like Receptors

TNFα: Tumor Necrosis Factor-α

TSG-6: Tumor Necrosis Factor-Stimulated Gene-6

VEGF: Vascular Endothelial Growth Factor

VEGFr2: Vascular Endothelial Growth Fractor Receptor

VGLUT: Vesicular Glutamate Transporters

USC
UNIVERSIDADE
DE SANTIAGO
DE COMPOSTELA

USC
UNIVERSIDADE
DE SANTIAGO
DE COMPOSTELA

USC
UNIVERSIDADE
DE SANTIAGO
DE COMPOSTELA

Introduction

USC
UNIVERSIDADE
DE SANTIAGO
DE COMPOSTELA

1.Stroke

1.1. Definition

Stroke is a cerebrovascular disease, consequence of the alteration of normal cerebral blood flow, which results in a transient or permanent deficit of the function of one or more parts of the brain. This alteration of normal cerebral blood flow induces metabolic or biochemical alterations and would lead to cell death, and consequently, the alteration of the nervous system. The World Health Organization (WHO) has defined stroke as the fast clinical development of focal signs of alteration of cerebral function without any other apparent origin than the vascular one.[1]

1.2. Epidemiology

Stroke is the major cause of mortality and morbidity worldwide. According to the World Health Organization, the world average incidence of cerebrovascular disease is around 200 new cases per 100.000 inhabitants [2]. In Europe exist differences between northern and southern populations, being the most high figures in Nordic countries such as Finland (270 per 100.000 in men), and less in others such as Italy and Portugal (100 per 100.000 men).[3] The incidence of Spain is 167 per 100.000 / year (181 for men and 153 for women), being higher in Galicia by the aging population.[4]

In developed countries, the prevalence of stroke adjusted by age in people over 64 years is between 4.6 and 7.3%. It is higher in men (5.9 to 9.3%) than females (3.2 to 6.1%) and increases with age.[5] In Spain, the rate of prevalence specifies-age was 4.9% for the total of cerebrovascular disease and 3.5% for ischemic stroke.[6] Due to the progressive aging of Europe's population in general, and the Spanish and Galician in particular, the incidence and

prevalence of stroke increase progressively, which will lead to a serious social health.

Therefore, the stroke is a health problem that requires establishing better guidelines for prevention and treatment to reduce their incidence as the degree of disability that originates. Considering that the incidence increases in people over 65 years and, based on an improvement in the quality of life, is taking a significant increase in life expectancy and a progressive aging of the world population, the prevalence of this disease increases, and with it, the magnitude of the this social problem.

1.3. Classification of stroke

Focusing on the nature of the lesion, stroke can be classified in two main groups, ischemic and hemorrhagic stroke. However, alternative classifications of this cerebrovascular disease can be used looking at other parameters such as stroke subtype, progression profile, neuroimaging characteristics, size and topography of the lesion, nature, and the mechanisms of induction and etiology.[7, 8]

1.3.1. Ischemic Stroke

Ischemic stroke is the most common type of stroke, and represents about the 80% of all strokes.[7, 9-11] Among the focal brain ischemia, we can differentiate between transient ischemic attack (TIA) and cerebral infarction. TIA is defined as the focal or monocular cerebral dysfunction with symptoms that last for less than 1h, whose origin is a vascular insufficiency caused by an arterial thrombus or embolism, associated to arterial, cardiac or hematologic disease.[12] TIA patients present higher risk of subsequent major stroke and other vascular episodes, mainly coronary, and the outcome of each individual is extraordinarily variable. Cerebral infarction is defined as the lesion caused by an intense or prolonged ischemia, which produce irreversible loss of cells.

In case of cerebral infarction and attending to the etiology, different ischemic stroke subtypes can be divided:[11]

- Atherothrombotic infarction: (~20%) generally middle or large sized infarcts with cortical, subcortical, carotid or vertebro-basilar topography, in patients with presence of one or several cerebrovascular risk factors. It is imperative the presence of clinically generalized atherosclerosis, or the demonstration of occlusion or stenosis (> 50% occlusion or <50% plus two or more vascular risk factors) in cerebral arteries, with an established correlation to the patient's clinic.
- Lacunar infarction or small vessel disease: (~25%) small sized infarct (<15 mm of diameter), localized in the distribution territory of the penetrating arterioles. Although micro-atheromatosis and lipohialinosis of penetrating arterioles are the most frequent pathologic substrate in lacunar infarcts, other less frequent potential causes are cardiac embolism, arterial embolism, infectious arthritis or prothrombotic state.
- Cardioembolic infarction: (~20%) generally medium (1.5-3 cm of diameter) or large (>3 cm of diameter) sized infarcts, with symptoms frequently started during awakening. It is mandatory the presence of a demonstrated embolic origin, and the absence of significant concomitant arterial occlusion or stenosis.
- Infarction of undetermined etiology: (~30%) brain infarcts of medium or large size with more than two potential etiologies or unknown origin.
- Other causes (~5%).

1.3.2. Hemorrhage stroke

Among all cerebrovascular diseases, the pathologic group of hemorrhages corresponds to approximately 15% of all strokes. This percentage excludes those derived from cranioencephalic trauma. In essence, it consists in a blood

extravasation, secondary to the breakage of a blood vessel, either arterial or venous, by diverse mechanisms.

The most common cause of hemorrhage is arterial hypertension. For other causes, except amyloidal angiopathy (typical in elderly people and perhaps the most frequent cause after hypertension), the list of potential origins in infant and young individuals can be summarized in: vascular malformations (aneurisms, arteriovenous malformations), drugs (antiplatelet, adrenergic stimulants), toxics (alcohol, cocaine, poison), hematological diseases (blood dyscrasia, coagulopathy), brain vasculopathy, primary or mestastatic tumors, and others.[13]

1.4. Biochemistry of cerebral ischemia

The acute obstruction of one of the large brain arteries induces an instantaneous reduction of blood flow in the corresponding irrigation area (focal ischemia). But that reduction of blood supply is not homogeneous in the affected area, and can change within min or h, especially if blood supply is not reinstated.[14]

Two regions can be distinguished: the ischemic core is the portion of tissue closest to the affected blood vessel and where the ischemia becomes severe, and the so-called penumbra, where the reduction of blood flow is less severe, due to the blood supply carried out by collateral arteries of the non-ischemic neighbor tissue.[15] The impact of brain ischemia will depend on the level of the artery occlusion and duration of the reduction of blood flow, which is why time is a very important parameter in this disease.

After the onset of brain ischemia, a sequence of molecular events are triggered in the short and the long term, initiated with an energetic failure in cells, related to the interruption of oxidative phosphorylation processes and the deficient production of adenosine tri-phosphate (ATP) (Figure 1).

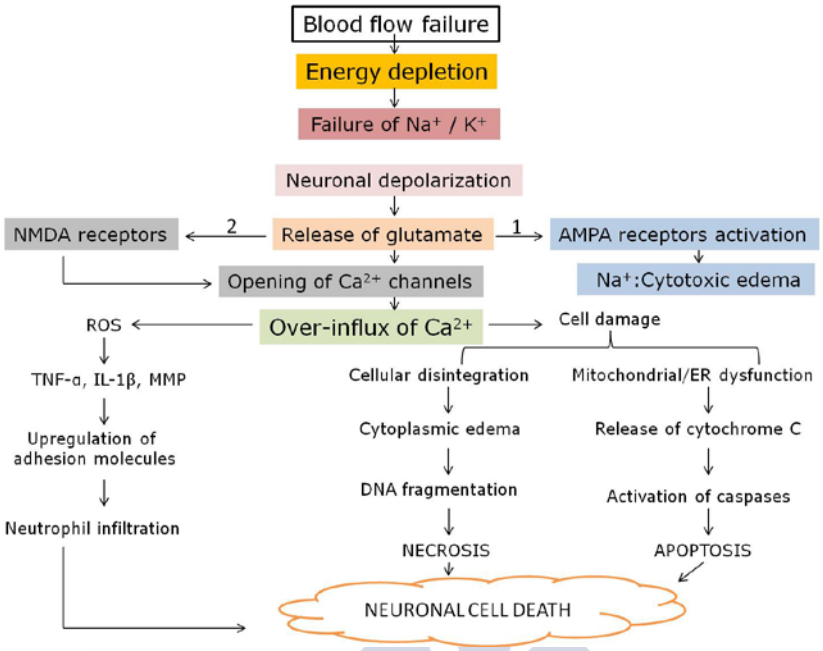

Figure 1: Sequence of main physiopathological events in cerebral ischemia.

The cessation of transmembrane ionic gradients due to the failure of sodium-potassium-ATPase pumps, and other ATP-dependent ionic pumps, is the key step of the physiopathological mechanisms in stroke, especially of cell death in the ischemic core, when the vascular occlusion lasts for few min.[16] Neurons and glial cells suffer an extreme depolarization because of the entrance of sodium, chloride, calcium and water into the cytoplasm[17] and in addition, potassium leaves the cell, inducing a sudden increment of its extracellular levels.[18] The energetic failure and the associated ionic changes, originate an increment in glutamate, a hyperexcitability of N-methyl-D-aspartate glutamatergic (NMDA) receptors (NMDAr), and of α-amino-3-hydroxy-5-methyl-4-isoxazol propionic acid (AMPA) receptors (AMPArs), which induces an even higher increase of intracellular calcium (Figure 2).[19-21]

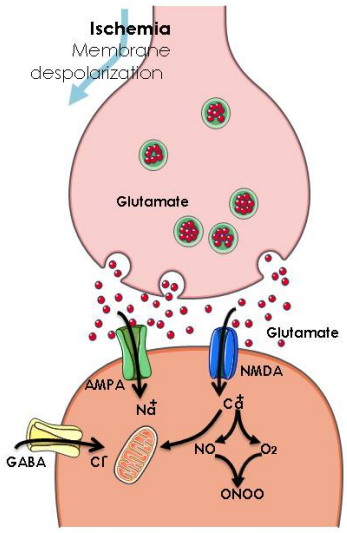

Figure 2: Role of glutamate on the stimulation of AMPA and NMDA receptors.

The increase of intracellular calcium does not exclusively depend on the activation of glutamate receptors, but also in the stimulation of calcium voltage-dependent channels. Hyperexcitability causes a depolarization phenomenon in the periphery of the infarct, which increases the energetic cost while the membrane tries to re-polarize itself.[15, 22, 23] Calcium increment, together with acidosis and peri-infarct depolarization, contributes to initiate the damage, and after it, inflammation and activation of apoptotic phenomena contribute to increment the lesion.[21, 24] During ischemia, and particularly during reperfusion, free radicals are generated. These are highly reactive species produced at the initial and late stages of brain ischemia, following different physiopathological mechanisms. In first place, oxygen reactive species are produced by the metabolism of arachidonic acid and the activity of neuronal Nitric Oxide (NO) synthase (nNOS). During intermediate stages, free oxygen radicals are provided by the infiltration of neutrophils in the ischemic area. At later stages, they are produced via

the synthesis and activation of inducible NO synthase enzymes (iNOS) and cycloxigenase-2(COX-2).[25, 26] Ischemic stroke triggers a series of complex molecular events, where the activation and the expression of genes are included.

However, ischemic cellular death can take place in two different ways. The most common one is necrosis,[27] which is the result of the acute energetic failure, mainly located in the core region of the lesion zone, and it is characterized by morphology changes and, at the end, cellular lysis, which also triggers inflammatory processes.[28] On the other hand, apoptotic or programmed cell death, in the region around the core region, can be observed when energy-dependent intracellular mechanisms are activated, leading to cell degradation.[24, 29]

1.5. Therapeutic approaches for the treatment of stroke.

1.5.1. Thrombolysis and neuro-interventionism in acute phase of stroke.

Pharmacological or mechanical (thrombectomy) thrombolysis are the strategies that report higher benefits for the patient, in terms of neurological outcome. The most common thrombolytic agent is the recombinant tissue plasminogen activator or rt-PA, and enzyme involve in the clot degradatadion of the occluded vessel. The thrombectomy is a technique which allows the extraction of the thrombus by a mechanical device. Both therapies have pushed for the creation of stroke units inside hospitals, which have improved the management of stroke patients. Nevertheless only 3-7% of stroke patients are currently treated by these procedures in most developed countries. Such reduced numbers may be due to different factors, including the narrow therapeutic window and the high risks of hemorrhage transformation. Current neuroprotective strategies are required to work at both stages, by widening the therapeutic window and by

reducing the associated risk factors.[30-34] The therapeutic window associated with intravenous thrombolytic treatment is 4.5 h. The extension of this window may be possible by selecting candidate patients with a large penumbral area (the area of the brain susceptible to damage unless otherwise protected within the first 24-48 h).[35]

1.5.2. Neuroprotection

Neuroprotection is a term that conglomerates a variety of strategies focused in reducing cell death after an ischemic event, without affecting tissue reperfusion. So far, several compounds have been proposed to block the pathway leading to ischemia-induced cell death at different steps of the ischemic cascade. Most of these compounds have shown positive effects in experimental studies, although unfortunately none of them have shown beneficial effect in clinical trials.[36] Figure 3 shows clinical trials of neuroprotectans in acute ischemic stroke with failed results, data provide by the Internet Stroke Center and Stroke Trials Registry.[37]

Neuroprotective drugs can be classified mainly into different groups regarding their action mechanism.

a. Calcium blockers

Calcium plays an important role in stroke pathophysiology. The blockage of calcium channels stops neuronal calcium intake, hence reducing cell death. Nimodipine is an example of this family of compounds. Over 250 animal studies of nimodipine in cerebral ischemia have been published, but only 10 of these studies reported a positive outcome.[36] None of the members of this family of compounds have demonstrated a clear neuroprotective activity on clinical trials. Among the reasons for this fact, overall the studies that generated positive results, animals were mostly treated within the first 15 min post-ischemia, which is not translatable to the clinical settings.

b. Glutamate antagonists

It is well established that glutamate, the major excitatory CNS neurotransmitter, is also capable of inducing excitotoxic neural injury in the setting of cerebral ischemia and other disorders. Glutamate and related excitatory amino acids interact with several receptor-classes, which are relevant to neuroprotection. These include the NMDA and AMPA receptors.[37]

Antagonists of NMDA receptors reduce infarct size and neurological deficit in animal models of focal cerebral ischemia, but its clinical use has presented several side effects, especially cardiovascular and psychiatric effects. For example, selfotel, a competitive antagonist of NMDA receptors has shown improve of outcome and no significant increase of mortality in a phase III study, but a high incidence of psychiatric adverse effects conditioned its withdrawal from clinical phases. Likewise, dextromethorphan and its metabolites dextrorphan and aptiganel were discontinued by an unfavorable relationship between risk and benefit and increased adverse effects. Eliprodil reduces the action of glutamate by interfere with sensor polyamine site on the NMDA receptor, but showed no difference with placebo. The gavestinel, antagonist of the NMDA receptor glycine, showed excellent tolerance, but no efficacy.[38]

On the other hand several AMPA antagonists showed neuroprotective efficacy in preclinical studies of both focal and global cerebral ischemia, but successful in larger clinical trials has not been reported.[37]

c. Antioxidants

Oxidative stress is another mechanism implicated on cell death after an ischemic event. Antioxidants could therefore play a role as neuroprotective drugs. The most successful antioxidant tested has been NXY-059. This drug reduced brain infarct by 66% in animal models, when injected even 5 h after occlusion. The first clinical trial generated positive

results, improving patient's functional outcome. However a second clinical trial showed negative results.[39]

Another antioxidant that reached clinical phase is uric acid, an antioxidant with neuroprotective effects in experimental models of stroke. A recent clinical trial[40] assessed whether uric acid therapy would improve functional outcomes at 90 days in patients with acute ischaemic stroke. The results showed that uric acid treatment is safe but did not increase the proportion of patients who achieved excellent outcome after stroke compared with placebo.

d. Phospholipid precursors: citicoline

Citicoline or CDP-choline is a precursor on the synthesis of phosphate-choline, which is integrated in the membrane of neurons. It has been shown that citicoline inhibits norepinephrine and dopamine levels on the CNS, and restores mitochondrial ATPase activity.[41] On animal models, citicoline lowered the phospholipase 2 activation after brain ischemia, reducing arachidonic acid formation and the production of free radicals; therefore lowering the oxidative stress. Another effects claimed for this drug are its capacity to reduce excitotoxicity and the stimulation of brain plasticity.[42] In preclinical studies, the treatment with citicoline immediately after reperfusion led to an improvement on functional deficits after a period of 28 days.[43] A pool-data analysis published in 2002 showed a 33% increment in complete recovery after mild or severe stroke (NIHSS ≥ 8) when the treatment was started within the first 24 hours and maintained for 6 weeks,[44] however a recent clinical trial have demonstrated the lack of protective in stroke patients.[45]

e. Inhibitors of glutamate release

Inhibitors of glutamate release work by blocking presynaptic channels, preventing membrane depolarization and glutamate release. One example of this kind of drugs is Lubezol, a compound capable of deregulate the glutamate-

induced nitric oxide synthase pathway. This compound has shown hippocampal neuroprotection from nitric oxide toxicity. In experimental studies it has shown a 50 % infarct volume reduction upon injecting the drug 3 hours after ischemia induction. Nevertheless no clinical trial rendered positive results, and one of them was cancelled due to the mortality increase experimented in the treated group.[46]

f. GABA agonists

This mechanism of action involves potentiation of the activity of GABA, the brain´s major inhibitory neurotransmitter. They attempt to counteract cellular depolarization caused by ischemia. Clomethiazole, which increases the activity of GABA, was negative in the first study and a second study of patients with total anterior circulation infarcts. The MaxiPost, getting hyperpolarisation of neurons by opening potassium channels, also showed no benefit.[37]

g. Anti-inflammatory

The anti-inflammatory compounds act by inhibiting any of the mechanisms of extensive inflammatory cascade of cerebral ischemia. The enlimomab, a monoclonal antibody against ICAM-1, which inhibits leukocyte adhesion and migration through the vascular endothelium, able to reduce infarct size in animal models of transient focal cerebral ischemia; however, in a Phase III, the result has been negative with a high number of complications. The UK279,276, a recombinant protein inhibitor of the CD11b/CD18 receptor, showed a low efficacy in clinical trial.[36]

h. Others

Several studies have been performed using other neuroprotective agents such as neuronal potassium channel activators (BMS-204352), membrane fluidity modifiers (Piracetam), opioid antagonists (Namefene), growth factors employes as intracellular calcium regulators, and much more.

None of them have shown the definitive efficacy of pharmacological neuroprotection.[37] Figure 3 provides an overview of categories of neuroportective strategies that have progressed to some stage of clinical trial.

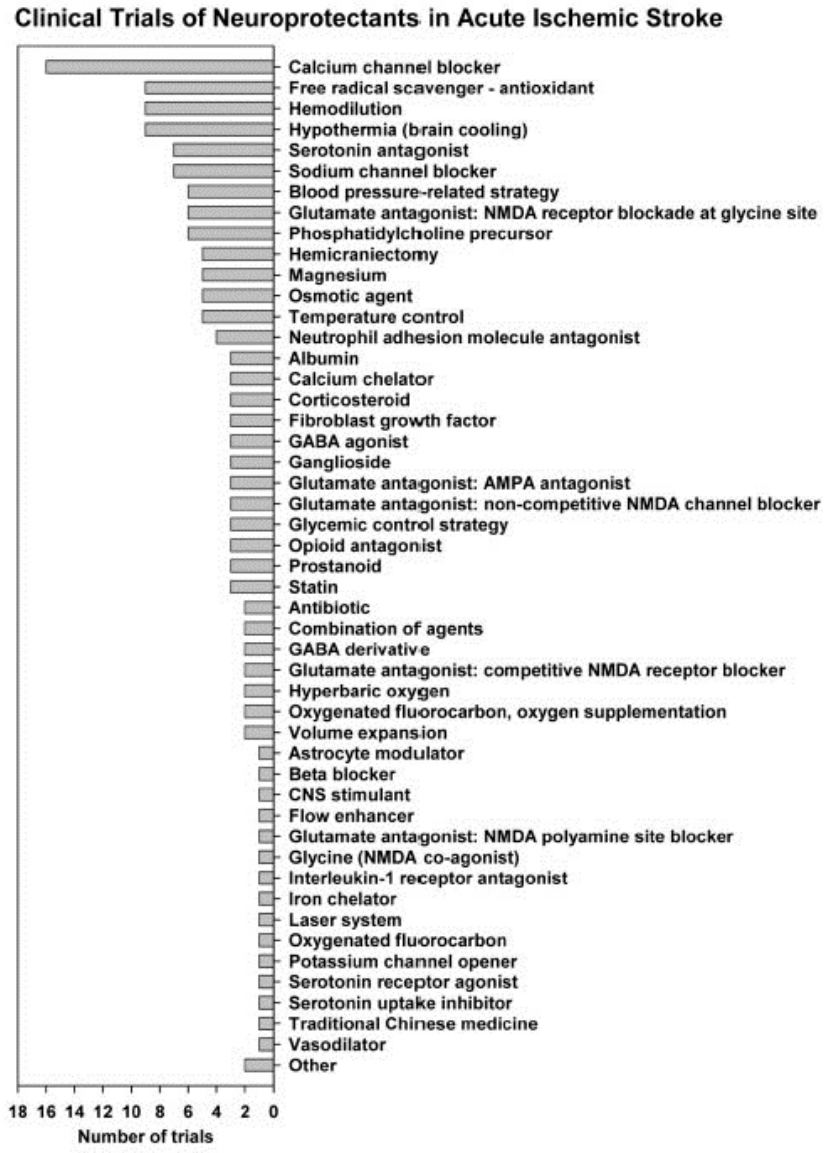

Figure 3: Clinical trials of neuroprotectans in acute ischemic stroke with failed results. Internet Stroke Center. Stroke Trials Registry.[37]

1.5.3. Neurorepair

Neurorepair strategies involve the restoration of brain function, either by regeneration of damaged cerebral tissue (neurogereneration) or by the establishment of alternative neural pathways or synapses (brain plasticity). However, therapeutic window for those therapies is wider than for thrombolytic or neuroprotective approaches. The aim of the treatments for neurological function recovery after stroke is not restricted to neurons; it is more focused on the neurovascular unit, including procedures that enhance synaptogenesis and angiogenesis. Thus, neurorepair treatments may use stem cells, pro-neurogenic, pro-angiogenic and/or pro-synaptogenic drug delivery, among others.

a. Neurogenesis after brain ischemia

In the adult brain there are niches for the production of neural stem cells,[47] localized in the subventricular region of the lateral ventricles (SVZ) and the dentate gyrus of the hippocampus. Under normal physiological conditions, the neuroblasts produced in the SVZ migrate to the olfactory bulb to differentiate in new neurons. After the induction of focal brain ischemia in the rat, an increase in neuroblast formation occurs in the ipsilateral hemisphere, and these neuroblasts migrate to regions surrounding the lesion.[48] This effect has been also shown in humans.[49] The enhancement of endogenous neurorepair mechanisms is one of the main goals on new therapies for the treatment of stroke.

Even though newborn stem cells are recruited after an ischemic insult, most of them do not get integrated into neuronal circuits. Several strategies have been used to enhance endogenous neurogenesis. Thus, a great number of newly differentiated neurons would be available, increasing the chance of survival and integration in neuronal networks, therefore improving functional recovery. Both cellular and pharmacological therapies have been used to achieve this

goal by activating the phosphatidylinositol-3-kinase (PI3-Akt) pathway. This pathway is involved in cell survival, proliferation, differentiation and migration.[50]

b. Angiogenesis after brain ischemia

The development of the cerebral vascular system occurs mainly due to angiogenic processes. During adult life, endothelial cell proliferation ceases under normal physiological conditions. However, after an ischemic event brain capillaries surrounding the lesion proliferate, and new vessels are formed between 2 and 28 days after the onset of stroke.[51-54]

The angiogenic process involves a multi-step procedure that comprises endothelial cell proliferation and migration, tubule formation, branching and anastomosis. Vascular Endothelial Growth Factor (VEGF) and its receptor (VEGFr2) initiate the angiogenic process, being angiopoietin 1 and 2 and their receptor (TIE-2) responsible for the maturation, stabilization and vascular remodeling.[55] VEGF and VEGF2 expression promotes vascular ramification, and the newly formed vessels are highly permeable. Meanwhile angiopoietins and TIE2 expression stimulate vessel maturation leading to the formation of fully functional brain blood vessels. VEGF treatment or therapies focused in producing VEGF, VEGF2, angiopoietin or TIE2 expression could increase the angiogenesis in the peri-infarct region.

The angiogenic process is essential for brain recovery after cerebral ischemia. In experimental studies both cellular and pharmacological therapies have been used to increase angiogenesis, promoting the functional recovery of ischemic animals.[56]

c. Neurogenesis & angiogenesis

Neurogenesis and angiogenesis after cerebral ischemia are not separated processes. Neurogenesis in the peri-infarct region cannot occur without angiogenesis, since the ultimate is responsible for restoring the oxygen and nutrient supply. Furthermore, endothelial cells produce growth factors that allow the neurons to survive, and that regulate metabolic activity of neural precursors. Endothelial cells secrete Stromal Cell-Derived Factor-1 (SDF-1), VEGF and Matrix Metalloproteinases (MMPs) that induce and facilitate neural progenitor cell migration to the injured site. On the other hand, neural progenitor cells overexpress angiopoietin 2 and VEGFR2 leading to an increase in angiogenesis.[57]

Several *in vitro* and *in vivo* studies have shown the relationship between angiogenesis and neurogenesis.[57, 58] In animal models of ischemia, Tie2 inhibitors not only reduce angiogenesis, but also neuroblast migration to the peri-infarct area. On the other hand, neural progenitor cell grafted in the infarct region have demonstrated the induction of angiogenesis. These and other studies have reported that neurogenesis and angiogenesis are highly connected, and both promote neural remodeling and improve neurologic function after brain ischemia.[59, 60]

d. The role of oligodendrocytes, astrocytes and axons in neurorepair

In the brain parenchyma there are not only neurons, but other cellular components as well oligodendrocytes, astrocytes and the development of functional axons are also involved on neurorepair. After an ischemic event, astrocytes proliferate forming a glial scar that surrounds the lesion and release proteoglycans that inhibit axonal growth. Hence there should be mechanisms for reducing glial scar formation, and also to stimulate axonal growth, leading to an efficient neurorepair.[61]

2.Glutamate

2.1. Glutamate

The glutamate is considered to be the major mediator of excitatory signals in the mammalian central nervous system and is probably involved in most aspects of normal brain function including cognition, memory and learning. Glutamate also plays major roles in the development of the central nervous system, including synapse induction. Glutamate plays a signaling role also in peripheral organs and tissue as well as a in endocrine cells.[62]

The brain contains huge amounts of glutamate (about 5-15 mM per kg wet weight depending on the region),[63] but only a tiny fraction of this glutamate is normally present extracellular space. In fact, the glutamate in the brain is primarily maintained intracellular.[64] The concentrations in the extracellular fluids and plasma are normally around 1-10 μM and around 40-60 μM, respectively.[65, 66] It should be noted that the distribution of glutamate is in a dynamic equilibrium which is highly sensitive to changes in the energy supply.

2.2. Compartmentalization of glutamate

In the brain, glutamate exists as a free amino acid divided between two separate metabolic compartments located in astrocytes and neurons.[67] In this sense, different studies reveal the existence of one separate pool in astrocytes, which containing a small glutamate pool that is rapidly metabolized to glutamine. While the neuronal glutamate is contained in ≥2 pools, one composed of neuronal soma and dendrites and the one of nerve terminals (vesicles). Nerve impulses trigger the release of glutamate from the presynaptic cell, which in turn binds to the glutamate receptors on the opposing postsynaptic cell. Neurotransmission is terminated by

astrocytes and neurons that take up glutamate. Very little glutamate is believed to diffuse away from the synapse.[68-70]

2.3. Gutamate transporters

2.3.1. Excitatory amino acid transporters (EAATs)

EAATs (to date described 5 subtypes) are polypeptides in the range of 500-600 amino acid residues and exhibit 50-60% amino acid homology. The transmembrane topology of EAATs is thought to consist of six to eight putative transmembrane domains, one to two re-entrant loops, and cytoplasmic N- and C-terminal.[71] EAATs action involves the transport of glutamate across the cellular membrane couples to the inwardly directed electrochemical potential gradients of sodium and one H^+, and the outwardly directed potassium gradient. The initiation of this process involves the recruitment of glutamate and three sodium and one H^+ from the extracellular space to an outward-facing conformation of the transporter. The binding of these substrates triggers a conformational change, which adopts an inward-facing conformation of EAATs, followed by cargo release into the cytoplasm of the cell. The subsequent step involves the recruitment of potassium ions to an EAAT transporter from the cytoplasm, which evokes the return to an outward-facing conformation and release outside the cell.[72]

a. Location in the brain

EAAT (1-3) are widely distributes in the CNS, while $EAAT_4$ and $EAAT_5$ are predominantly expresses in the cerebellum and retina, respectively.[72] $EAAT_1$ and $EAAT_2$ are in the astrocyte membranes, being the highest densities of both in the astrocytes membrane facing neuropil. $EAAT_1$ is selective for astrocytes, while $EAAT_2$ is predominantly expressed in astrocytes, but there is also some (about 10%) in hippocampal nerve terminals. $EAAT_3$ is selective for neurons, but is expressed at levels two orders of magnitude lower

than $EAAT_2$ and is targeted to dendrites and cell bodies.[73] Besides of the location describe above, different studies indicate that EAATs are present in brain capillary endothelial cells,[74] where participate in cellular mechanism for brain glutamate efflux.

b. Function of EAATs

The general function of EAATs (Figure 4) is to regulate the extracellular glutamate concentration and maintain the concentration of glutamate at low physiological levels to avoid toxic effects. After release into the synaptic cleft, glutamate is rapidly removed through EAATs into glial cells and neurons. The major transporter is the $EAAT_2$, which is responsible for more than 90% of total glutamate uptake.[75] The role of the $EAAT_4$ is to regulate neuronal excitability through counteracting the depolarization of neurons. Both $EAAT_4$ and $EAAT_5$ possess a thermodynamically uncouple chlorine flux, which involves high chloride conductance with relatively low glutamate uptake.[72]

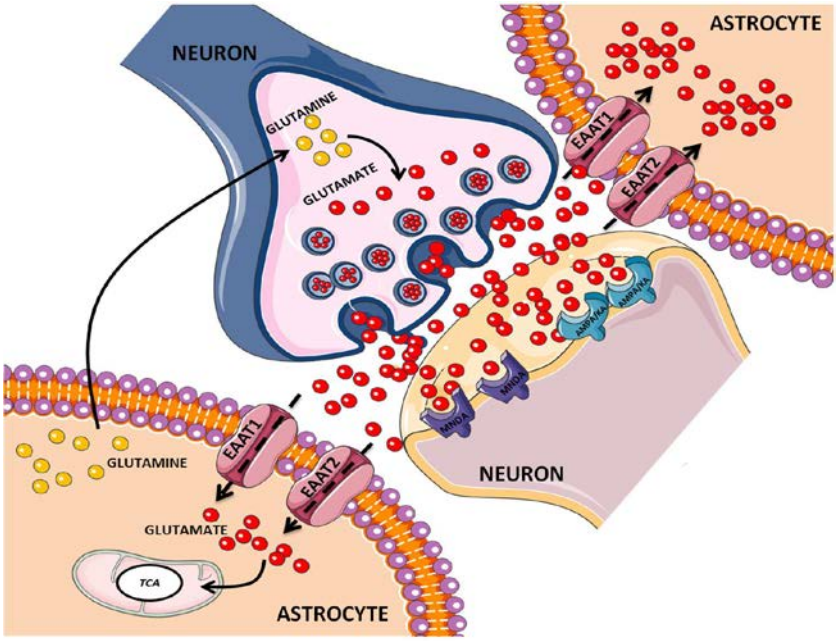

Figure 4: EAATs regulate the extracellular glutamate concentration and maintain it at low physiological levels to avoid toxic effects.

c. Potential aplicactions of EAATs.

Regulation of extracellular glutamate levels in the brain is crucial for maintenance of its normal functions. Abnormalities in this process are implicated in several neurodegenerative diseases including Alzheimer's disease, Huntington's disease, and amyotrophic lateral sclerosis. Since the major regulator of extracellular glutamate levels in the brain is the $EAAT_2$ promoter, proper expression and regulation of this promoter is critical for maintaining brain homeostasis and survival of neurons. The critical role of $EAAT_2$ and glutamate in neurodegeneration, suggest that this transporter can be use for developing screening protocols to identify molecules capable of physiologically and safely regulating glutamate levels *in vitro* and *in vivo* in animals, with ultimate applications in humans. Thus, it has identified β-lactam antibiotics, as transcriptional activators of $EAAT_2$ that are capable of providing neuronal protection through facilitating

glutamate uptake by astroglial cells. This finding suggests potential applications for these types of drugs as therapeutic agents to limit and prevent glutamate excitotoxicity. A thorough understanding of the mechanism(s) underlying transcriptional activation of $EAAT_2$ may help identify potentially new molecules and targets for drug discovery leading to compounds that can ameliorate and potentially prevent neurodegeneration. Through chemical modeling, it may be possible to develop new derivatives of β-lactam antibiotics with enhanced pharmacological and bioactivity properties that can be orally delivered and pass more readily through the blood brain barrier to decrease the severity and progression of specific neurodegenerative diseases. Use of the $EAAT_2$ promoter as a screening paradigm also provides an entry point for identifying potentially new classes of neuroprotective drugs that function by controlling glutamate levels in the synaptic region of neurons.[76]

2.3.2. Vesicular glutamate transporters (VGLUSTs)

a. Function of VGLUST

VGLUTs are responsible for transport of glutamate into the synaptic vesicles. The vesicular uptake is dependent on a proton gradient that they created by hydrolyzing ATP with H^+-ATPase. This enables the flow of H^+ into the interior of the synaptic vesicle making it more acidic and generating a pH gradient across the vesicle membrane.[72]

The vesicular glutamate transporters are polypeptides consisting of about 600 amino acid residues. Three subtypes of VGLUTs (1, 2 and 3) have been identified and appear to share more than 70% homology with one another. The transmembrane topology of VGLUTs is thought to consist of 8-10 putative transmembrane domains. A highly conserved glycosylation site between transmembrane domains 1 and 2, and numerous consensus sequences for phosphorylation by various protein kinases are also predicted.[71]

b. Localization in the brain

The isoforms VGLUT1 and VGLUT2 are expressed mainly in glutamatergic neurons and their expression in CNS seems to be largely complementary with only a limited overlap. VGLUT1 is localized in the neocortex, hippocampus and amygdale. VGLUT2 can be observed in olfactory bulb, cerebral cortex, dentate gyrus, thalamus and hypothalamus. VGLUT3 is localized in a limited number of glutamatergic neurons in multiple brain regions: neocortex, hippocampus, olfactory bulb, hypothalamus, sustantia nigra. Additionally, VGLUT3 has been found in hippocampal and cortical GABAergic neurons.[72]

2.4. Glutamate metabolism and cycling

There are a few ways for the body to produce glutamate molecules:

a. Glu-glutamine cycle
b. Synthesis in neurons and astrocytes from glucose
c. Synthesis inside neurons from lactate delivered from astrocytes

A fraction of glutamate present in the brain participates in the glutamate-glutamine cycle in neurons and astrocytes. However, de novo synthesis is necessary because glutamate can be oxidized and cannot be entirely regenerated through this cycle. Glutamate also does not cross the blood brain barrier and hence is not delivered to the CNS through the ingestion of food.

Glucose is the major substrate for glutamate synthesis in astrocytes and neurons,[77] and the influx of sodium stimulates glucose uptake in astrocytes and neurons by GLUT1 and GLUT3, respectively. Glucose is metabolized via glycolysis to pyruvate, which can be reduced to lactate or enters the tricarboxylic acids cycle (TCA cycle) and provides α-ketoglutarate (α-KG) as a carbon backbone of glutamate.

Glutamate in neurons can also be synthesized from lactate delivered from astrocytes. In some neurons, glutamate might be converted to gamma-aminobutyric acid (GABA) through the action of glutamate decarboxylase. Glutamate is released from presynaptic neurons into the synaptic cleft, where this compound binds to specific ionotropic (iGluR) or metabotropic receptors (mGluR) located on postsynaptic and presynaptic neurons. Besides, EAATs start uptake glutamate direct into astrocytes ($EAAT_1$ and $EAAT_2$) and neurons ($EAAT_3$),[78] to maintain adequate extracellular glutamate concentrations. Through $EAAT_1$ and $EAAT_2$, glutamate is taken up through the inward co-transport of three sodium molecules, one H^+ molecule and the counter transport of one K^+.[79, 80] The sodium-dependent neuronal glutamate transporters include $EAAT_3$, which exhibits a similar mechanism of action. In astrocytes, glutamate is converted to glutamine through glutamine synthetase (a specific enzyme in astrocytes and oligodendrocytes) in an ATP-dependent process. Notably, not every molecule of glutamate is converted to glutamine, as a small fraction of glutamate is degraded to α-KG and enters the TCA cycle. The glutamine produced from astrocytes is released through the glutamine transporter system N transporter 1 (SN1) and reaches neurons via system A transporter (SAT1) (Figure 5). Here, glutamine is converted to glutamate through phosphate-activated glutaminase.[81] Subsequently, transmitter is loaded into vesicles through VGLUTs, and after interaction with soluble N-ethylmaleimide-sensitive factor attachment protein receptors (SNAREs), glutamate is released into the synaptic cleft where it binds to glutamate receptors and EAATs. There is demonstrated mechanism of action cysteine/glutamate antiporter (X_c^-), which by means of this transporter L-cystine is uptaken from synaptic space to astrocyte where is converted to L-cysteine which may be transporter to neurons and serve as a substrate to glutathione synthesis, or this synthesis may take place in astrocytes.[82]

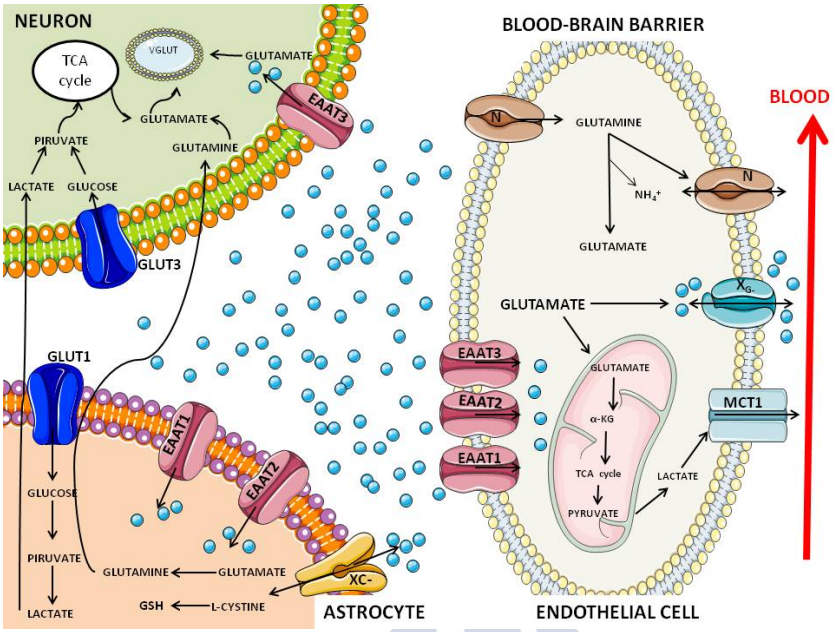

Figure 5: Glutamate cycling and metabolism.

It seems evident that uptake of extracellular glutamate into endothelial cells (EC) via EAATs is an important step in the glutamate metabolism. The presence of EAATs in the abluminal membrane of EC in the brain, indicates that EC are able to accumulate glutamate. The following fate of accumulated glutamate may involve both transport of intact glutamate, metabolism of glutamate and transport of resulting metabolites or a combination of the two.[80] The transport of intact glutamate is supported *in vivo* studies, which indicate the presence of a facilitative glutamate transporter at the luminal membrane of the Scathe transporter was named X_G^- and has been shown to be sodium independent.[83] As regards the metabolism of glutamate in the EC, studies demonstrated a high mitochondria density in brain endothelial cells. It has been suggested that endothelial cells may utilize glutamate as an energy substrate to fuel the ABC-transporters.[84] Furthermore, endothelial cells express branched chain aminotransferases, which may catalyze the conversion of glutamate to α-KG, this go through the Krebs

cycle in the mitochondria. From there, the α-KG can appear on pyruvate, which may be converted to lactate in the cytosol and transported through MCT-1 in the luminal membrane to the blood.[74] Besides, in the abluminal size of EC there are transporters capable of pumping glutamine from the extracellular fluid into endothelial cells and glutaminase within EC may also hydrolyze glutamine to glutamate and NH_4^+(Figure 3).[67]

2.5. Mechanism of glutamate excitotoxicity

The mechanisms of glutamate excitotoxicity have been well studied in both animals and humans. Though the precise genes and proteins involved are still being elucidated, it is well known some of the major pathways that glutamate contributes to neuronal damage.[85, 86] The disruption of glutamate homeostasis is implicates in both acute central nervous system (CNS) injuries such as stroke,[87-90] trauma, in chronic neurodegenerative disorders including multiple sclerosis, amyotrophic lateral sclerosis and Parkinson´s disease[88, 91-93] as well as in surgery interventions that produce brief period of cerebral blood flow interruption.[94]

In the event of CNS injury such as stroke, cell membrane depolarization from ATP break down increases the release of glutamate, while also blocking the reuptake of the neurotransmitter due to the consumption of the energy source.[95] The massive release of glutamate overwhelms regulating mechanisms leading to a buildup of the neurotransmitter in the extracellular milieu. The excess glutamate in turn activates a series of downstream mediators in the affected tissue that ultimately leads to neuroexcitotoxicity. Cellular death causes also more increase in extracellular glutamate, which feeds into the cycle of further cellular death.[96]

Ionotropic glutamate receptors include the NMDA, AMPA, and kainite types. The major receptor involve in glutamate mediated neuronal damage is NMDAr, an important tri-

subunit-receptor essential to neuronal plasticity (i.e. learning and memory formation).[97] Studies have shown that increase of activation of NMDAr by high levels of glutamate plays a significant role in neuronal excitotoxicity by receptor-mediated influx of calcium.[98] The increased intracellular calcium, may then lead to the activation of other mechanisms including NOS and mitochondrial toxicity.[64, 99, 100]

Nitric oxide production plays also a significant role in glutamate-mediated neuronal damage. Neuron injuries have been show to induce translocation of nNOS from the cytosol to the cell membrane where it can interact with NMDAr.[100] Studies have demonstrated that NMDAr are spatially linked with nitric oxide synthase via the postsynaptic density protein of 95kDa (PSD-95).[101-103] During the glutamate binding to NMDAr, the influx of calcium leads to the activation of the nearby NOS resulting in the production of NO.[64, 86] NO can in turn lead to formation of harmful oxidants, causing protein nitration, protein oxidation, lipid peroxidation, direct DNA damage and Glyceraldehyde 3-phosphate deshydrogenase (GAPDH) depletion.[103] Neuron degeneration can also arise from formation of free radicals via damage of mitochondrial after massive NMDAr mediate glutamate insult. Again, increase in calcium is implicated.[86, 104] Studies by Dykens *et al.* demonstrated that the increase in calcium concentrations after NMDA activation leads to increase in the mitochondria sequestration through high capacity sodium/calcium exchangers.[105] The elevated utilization of these exchanges, however, can result in metabolic acidosis as well as the activation of superoxide and other free radical production. Mitochondrial injury also initiates calpain cleavage of key regulatory proteins and activation of pro-apoptotic genes leading to cell death.[96]

2.6. Pharmacological findings to combat glutamate excitotoxity

The elucidation of the mechanisms behind glutamate excitotoxicity ushered in a wave of pharmacological advances aimed to exploit this newfound knowledge. In the beginning, the major focus of research centered on NMDAr antagonism. NMDAr provided a logical target for drug design as it represented a major gateway for the myriad of other downstream effects of glutamate excitotoxicity. Moreover, during this period, progress in protein biochemistry and small molecule design yielded a wealth of information regarding the structure and function of these receptors.[106]

Several classes of NMDAr antagonists with different sites of action were developed, namely the competitive NMDAr antagonists acting on glutamate or glycine binding sites; noncompetitive allosteric inhibitors acting at other extracellular sites; and NMDAr channel blockers, which acted on sites in the receptor channel pore.[107] Though showing promise in animal studies, antagonist drugs such as Selfotel, Gavestinel and Traxoprodil have largely failed in randomized, controlled clinical trials in humans. A variety of reasons have postulated in explaining the lack of success for these NMDAr-targeting therapies. Many of these compounds lack sufficient brain penetrance while exhibiting significant dose-limiting side effects.[37, 107] The adverse events profile included hallucinations, agitations, catatonia, peripheral sensory loss, nausea, and elevation in blood pressure.[108] Moreover, in the setting of acute CNS insults, such as strokes or traumatic brain injuries, glutamate excitotoxicity is thought to cause harm within a narrow time frame after which the neurotransmitter reassumes its normal function. Therefore, the use of agents acting on NMDAr, a major receptor of glutamate, may have not only missed the window for therapeutic efficacy but also led to undesired side effects from prolonged receptor blockade.[109]

Research has continued on NMDAr antagonism despite initial disappointments. Agents such as Amantadine and Memantine have proved to be valuable in Parkinson's disease and Alzeheimer's diseased.[103] However, studies in the last two decades have expanded beyond the NMDAr with newer experiments seeking ways to control the upstream glutamate concentration as well as downstream protein signals.

2.7. Blood glutamate grabbing: new potential agents against glutamate excitotoxicity

Blood to brain homeostasis of glutamate is mediated by several glutamate transporters as previously has mentioned. Danbolt *et al*. suggested that high glutamate concentration at the synaptic cleft are rapidly (up to 1000 fold) reduced by the action of glutamate transporters present on both nerve terminal and surrounding astrocytes to prevent glutamate excitotoxicity.[110] There is an unfavorable gradient between brain (1-10μM) and blood (40-60μM) glutamate concentration into the EC[95] and when endothelial glutamate concentration becomes higher than the blood glutamate concentration, glutamate is transported into the blood by mechanism that facilitates blood excretion of glutamate from the brain of glutamate. The presence of EAATs in the blood-brain barrier and their ability to accumulate large intracellular glutamate concentrations started the hypothesis that lowering blood-glutamate levels could increase the concentration gradient from endothelium to blood and thereby increase elimination of glutamate from the brain, known as blood glutamate grabbing hypothesis (Figure 6). To demonstrate this glutamate grabbing hypothesis, the blood resident enzyme glutamate-oxaloacetate transaminase (GOT), which transforms glutamate into α-ketoglutarate and aspartate in the presence of oxaloacetate, was used. This enzyme, when oxaloacetate is artificially increased shifts the equilibrium of the reaction to the right side, thereby decreasing glutamate levels in blood (Figure 7). In this

sense, Gottlied *et al*. demonstrated when radioactive glutamate were injected into the lateral ventricles in experimental animals and the effect of oxaloacetate were studied, the results of the study showed that oxaloacetate induced a decrease in blood glutamate levels followed by an increase of the diffusion of radioactive brain glutamate into the blood. Similar effects were observed in other studies using two microdialysis probes, where the first one infusing, and the other collecting glutamate; oxaloacetate treatment reduced the rate of radioactive glutamate collection by the second probe.

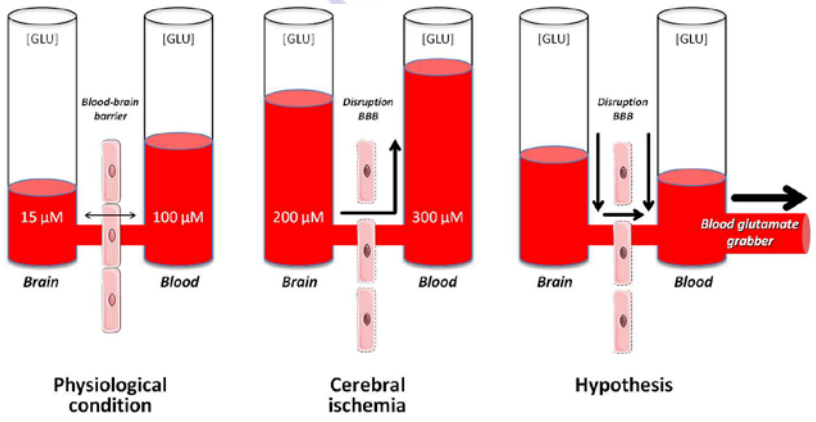

Figure 6: Mechanism of glutamate diffusion between brain and blood circulation through endothelial cells. (A) Under physiological conditions the brain blood barrier (BBB) acts as a semi-permeable membrane preventing the diffusion of glutamate from blood to brain. (B) During ischemia, glutamate concentrations in brain rise to levels 10 times above normal, leading to increased blood levels. (C) Oxaloacetate administration reduces blood glutamate levels facilitating the lowering of extracellular levels in brain.

Alternatively, malate pretreatment, a GOT blocker, has also demonstrated inhibition of the oxaloacetate-dependent lowering of blood glutamate, confirming that the effect of oxaloacetate on blood glutamate levels was mediated by blood glutamate lowering.

These studies inspired several investigations of the effects of blood glutamate grabbing during pathological conditions such

as ischemia, subarachnoid hemorrhage, closed head injury, traumatic brain injury and paraoxon intoxication. The studies utilized different approaches to reduce blood glutamate levels. All these studies came to the same general conclusion that lowering blood glutamate levels decreases the morbidity of the disease states, for instance through better recovery, better neuron survival or smaller stroke volumes.[74] The blood glutamate grabbers show potential for the development of novel, effective and safe therapeutic agents. Whereas NMDAr antagonists were ineffective or potentially harmful, blood glutamate grabbers do not act on glutamate receptors nor do they interfere with normal cellular signaling processes. Their action is only in the blood, and they accelerate a physiological mechanism of removing glutamate only from areas in which glutamate is pathologically elevated.[64]

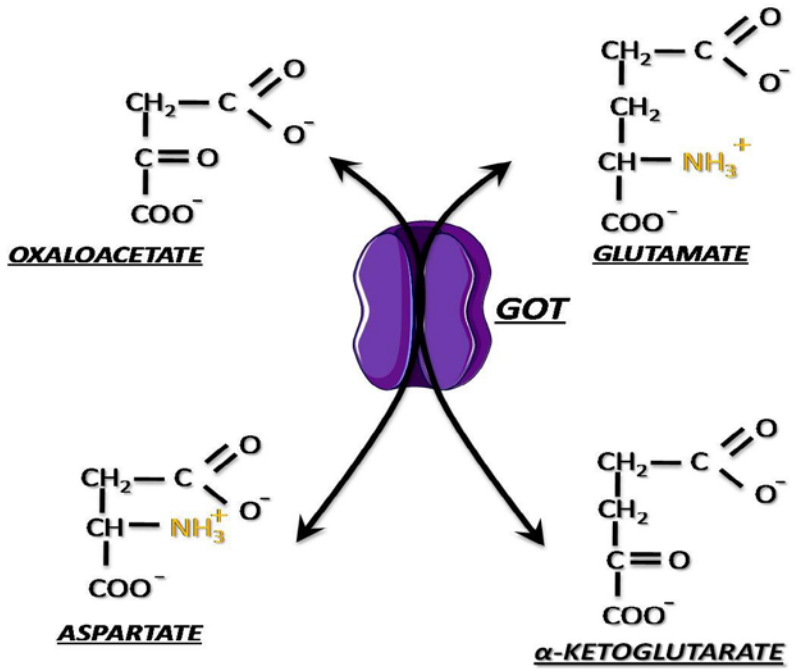

Figure 7: Blood resident enzyme glutamate-oxaloacetate transaminase (GOT) transforms glutamate into α-ketoglutarate and aspartate in the presence of oxaloacetate.

2.8. Therapeutics applications of blood brain glutamate grabbers

2.8.1. Ischemic stroke

It is well established that during brain ischemia, glutamate plays an important role in mediating neuronal damage,[111] and higher glutamate concentration in the blood and CSF are associated with an increased neurological deterioration after stroke in humans.[88, 89] Castillo *et al*. had described in clinical patients that glutamate acted as a critical key in the neuronal damage after ischemic stroke.[87-90, 112] Thus, the ischemic patients presented higher blood and CFS glutamate levels than control subjects at admission,[112]suggesting that, glutamate concentrations above of 200µM in plasma acted an import predictor of neuronal damage progression at 48 h, with a sensitivity of 85% and a specificity of 97%.[89]

This studies have also demonstrated that high levels of glutamate in plasma for at least 24 h was associated with early neurological deterioration, while in patients with stable ischemic stroke, glutamate levels dropped to normal values in less than 6 h from onset.[89] All these clinical data demonstrated for first time the critical role of glutamate in stroke pathology, and suggested a source of new strategies for the research of new protective therapies based on the inhibition of glutamate toxicity.

The central role of glutamate on ischemic pathology and the failure of glutamate antagonists, opened in 2009 a new line of investigation focused on blood glutamate grabbing hypothesis, that purpose the lowering of blood glutamate as new strategy to reduce the excitotoxic effect of glutamate after stroke, by means of the used of blood glutamate grabbers (Figure 8).

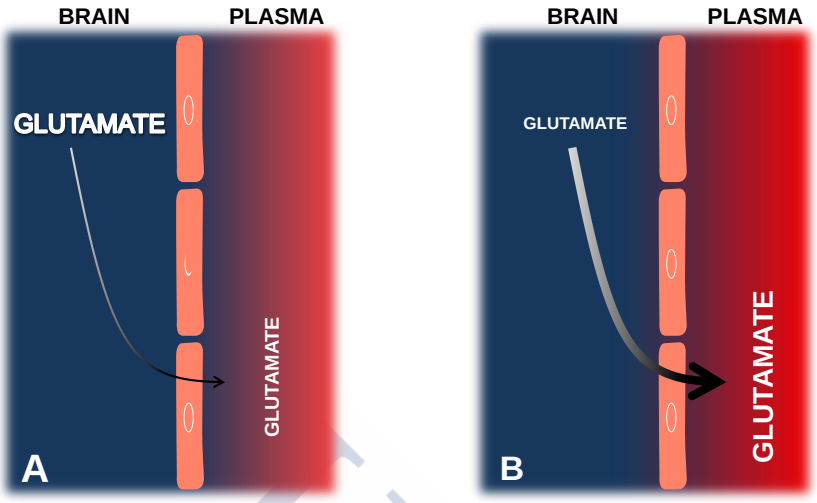

Figure 8: (A) Under ischemic conditions happens an accumulation of glutamate in the extracelluar space. (B) The increase of glutamate gradients between brain and blood facilitates the dumpling of glutamate from the extracellular space to circulating blood.

Based on this mechanism, when glutamate levels in brain fluids are elevated, oxaloacetate treatment causes a decrease in blood glutamate levels; this leads to a larger glutamate gradient between the brain and blood, which facilitates a decrease in extracellular levels of brain glutamate reflected in a reduction of ischemic damage.

The first evidence of the protective effect with oxaloacetate in ischemia was observed in rats submitted to photothrombotic lesion.[113,114] In this study, rats were subjected to a photothrombotic lesion and treated with a single 30-min-long administration of oxaloacetate (1.2 mg/100g, i.v.). Following induction of the lesion, the infarct size was measured and the amplitudes of the somatosensory evoked potentials (SEPs). The photothrombotic lesion resulted in appreciably decreased amplitudes of the evoked potentials, but oxaloacetate administration significantly attenuated this reduction, and also the infarct size assessed histologically. Oxaloacetate further prevented the long-term potentiation impairment in the rat CA1 hippocampal region induced by 2-vessel occlusion.[115] In the same way, Campos

et al. under the STAIR guidelines (Philip et al., 2009), demonstrated that a bolus intravenous injection of oxaloacetate (3.5 mg/100g), 90 min after occlusion, decreased blood glutamate levels, inducing an 60% decrease in infarct volume at 7 days after ischemia; edema was also reduced. These effects were associated with reduced motor deficit. To confirm that the neuroprotective effect was due to decreased brain glutamate levels, we performed magnetic resonance spectroscopy (MRS) in the infarct region. Spectroscopic analysis revealed that the increase in brain glutamate seen in control animals after MCAO was clearly reduced in animals treated with oxaloacetate, demonstrating its mechanism of action.[116] Similarly, infusion of peripheral pyruvate (with or without GPT) after MCAO resulted in reduced blood glutamate concentrations, smaller volume of infarction, reduced brain edema, improved neurological outcome, and reduced mortality compared with controls.[117]

In patients with ischemic stroke, Campos *et al.* also reported an association between higher concentrations of GOT and GPT in the blood and good outcomes (GOT having a stronger association than GPT levels).[118] In fact, patients with lower GOT levels and higher blood glutamate levels were independently associated with a worsened neurological outcome at 3 months and a higher infarct volume, which emphasizes the role that GOT plays in blood glutamate regulation.[114, 119] However the therapeutic effect of GOT administration in ischemic model animals have not been tested so far.

Godino et al[120] has reported another alternative method to decrease blood glutamate levels by peritoneal dialysis. In a rat model of cerebral ischemia, peritoneal dialysis was able to reduce the transient increase of glutamate levels induced by ischemia, decreasing the size of the infarct area and preventing the functional deficit. Nonetheless, more preclinical and clinical studies are needed in order to demonstrate that peritoneal dialysis is an effective and safe procedure for treating acute ischemic stroke patients.

- Limitations of glutamate grabbers in stroke

From a clinical point of view, glutamate grabbers may have some important limitations for their use as stroke therapy, as, glutamate increases immediately after neuronal damage, inducing a rapid effect, and therefore exhibits a short therapeutic window. Oxaloacetate showed a therapeutic window of no longer than 2 h after insult; therefore, the efficacy of this protective mechanism depends of the time-point of drug administration. However, in a recently published model of brain hemorrhage, oxaloacetate decreased the blood glutamate levels but did not affect the hemorrhagic hematoma, suggesting that this treatment can be given as early as possible, without neuroimaging, in case of suspected stroke, which may potentially increases the number of patients treated within the therapeutic window.[121]

2.8.2. Traumatic brain injury

Traumatic brain injury (TBI) is caused by a blow or jolt to the head or a penetrating head injury that disrupts the normal function of the brain. It is one of the most important cause of death and disability in the US and Europe and constitutes a major health and socioeconomic problem throughout the world.[122, 123] According to a report from the Centers for Disease Control and Prevention, an average of 1.7 million TBIs occurred annually from 2002 to 2006 in the US, with the majority of these cases being considered mild TBIs. Approximately 275,000 patients with TBI are hospitalized per year in the US, including 52,000 deaths. The leading causes of TBI include falls, struck by/against events, motor-vehicle traffic crashes, and assaults. In addition, a large population of military personnel has suffered some degree of TBI, and blast injury is a major cause of TBI for soldiers in modern wars.[124]For example, according to the Joint Theater Trauma Registry, compiled by the US Army Institute of Surgical Research, soldiers with head or neck injuries, including severe brain trauma, accounted for one quarter of total service members who have been evacuated from Iraq and Afghanistan.[124, 125] The long-term effect of mild traumatic

brain injury among soldiers deployed in Iraq is strongly associated with post-traumatic stress disorder and depression after soldiers return home, which may also induce physical health problems.[126] Moreover, the economic and social burden of traumatic brain injury has implications on a global scale, particularly with increasing motor-vehicle use in developed and developing countries.[127]

TBI can manifest clinically from concussion to coma and death depending on the extent of brain damage. Two major pathophysiological processes contribute to brain injury after trauma: primary injury, in which damage is caused as a direct result of the mechanical impact; and secondary injury, which is initiated immediately after trauma due to further cellular damage from the effects of primary injuries and continues to develop over a period of h or days following the initial traumatic assault.[128]The primary injury is usually irreversible since neural cell death occurs at the moment of injury. On the contrary, the secondary injury is likely a reversible process because delayed neural cell death is a protracted event that can be regulated at many points in the death pathway. Therefore, intervention in the program of delayed neural cell death has become a therapeutic target for the treatment of Tibia present, neurotransmitter release, calcium over-load, free radical-mediated damage, proapoptotic gene activation, mitochondrial dysfunction, and inflammatory responses are the major known mechanisms of secondary injury pathogenesis.[129, 130] These mechanisms are all induced via synaptic transmission and subsequent activation of postsynaptic receptors. Several proteins on the postsynaptic membrane are believed to form a special postsynaptic structure known as the postsynaptic density that serves as a multi-protein complex that mediates a molecular network among neural cells after injury.

Is well described that following TBI, brain CSF concentrations of glutamate increase in humans[131, 132] and rats.[133] Within min after TBI, experimental and clinical studies have found the extracellular glutamate levels to rise sharply.[131-133] This

increase in extracellular glutamate is mainly a consequence of massive neuron depolarization due to the traumatism and the associated energy failure commented above. Similar than stroke pathology, excess of glutamate in turn induces increased sodium and calcium influx to the cell, and the resulting intracellular calcium overload triggers cell damage mechanisms that finally lead to apoptosis through caspase activation.[134]

The importance of glutamate in TBI led to test the potential application of blood glutamate reduction as therapy of this brain lesion. The results observed showed that peripheral administration of oxaloacetoate,[91, 135, 136] 60 min after TBI in rats caused a significant reduction in blood glutamate concentrations and concomitant improvement in neurological outcome.

Interestingly, results from TBI model animals[135] (rats) demonstrated that the blood glutamate-reducing effect of oxaloacetate was dose-dependent, and that the administration of very low doses (5 mM) of oxaloacetate did not result in a reduction of blood glutamate. However, when low doses of oxaloacetate were administered with rGOT, the blood glutamate-lowering effects were restored. Seeing as rGOT is too large to penetrate the blood brain barrier, this finding suggested that the therapeutic effects of oxaloacetate was mediated by blood glutamate grabbing and not by direct effects in the brain. In line with previous data, in recent studies, oxaloacetate treatment resulted in an increased number of surviving neurons in five different regions of the hippocampus, with preserved cellularity, 30 days after Trico-administration of oxaloacetate with maleate, a GOT-blocker, was shown to prevent this glutamate reduction and improvement neurological outcome. Again, this provided strong evidence that the neuroprotective properties of oxaloacetate and GOT are primarily the result of blood glutamate grabbing, and not by some other mechanism.[91, 114]

2.8.3. Subarachnoid hemorrhage (SAH)

SAH is a common condition that is associated with significant mortality and morbidity. The mortality rate for SAH approaches 45 % at 30 days, and 10 to 15 % of cases are fatal before hospitalization.[137-140] At the time of the initial bleed, there is a critical reduction in cerebral blood flow as the regional intracranial pressure increases and approaches the systemic arterial pressure. The persistent lack of blood flow results in cerebral vasospasm and subsequent swelling of perivascular astrocytes, neuronal cells, and capillary endothelium.[64] Although a great deal of knowledge exists regarding the delayed effects of SAH, the pathophysiology of early brain injury has yet to be fully understood and essential early treatment remains to be a challenge.[141] Previously it has been described that elevated glutamate levels in the interstitial fluid and cerebrospinal fluid (CSF) of the brain may play a significant role in the mechanism for various acute brain insults.[85, 88,89, 142]

In agreement with these studies, later investigations also confirmed that after SAH, there is a massive release of glutamate that leads to overstimulation of NMDArs.[143, 144]

The level of glutamate concentration correlates with patients' neurological status after SAH.[145] A significant loss of blood–brain barrier (BBB) integrity after SAH has also been described to cause cerebral swelling and disturbance of intracranial hemodynamics,[146] which may in turn disrupt the BBB, causing a vicious cycle. A number of studies have demonstrated that the NO pathway is pathologically altered after SAH, contributing to early ischemic injury.[147] The NO produced from L-arginine by NOS through its three isozymes, nNOS, endothelial NOS, and inducible NOS, plays an important role in maintaining cerebrovascular tone and CBF. It is known that a calcium sensitive nNOS enzyme is physically associated with NMDAr and is activated after SAH causes glutamate excitotoxicity and subsequent neuronal death.[147, 148] Based on the excitotoxicity theory, NMDAr

antagonists may provide neuroprotection to limit secondary neuronal damage in different animal models of brain disease. However, the clinical potential of most NMDA antagonists demonstrated to be limited due to their indiscriminate blocking of the physiologic effects of NMDAr activation, as well as undesirable side effects like neuro-psychotic symptoms and memory deficits.

In line with our previous evidences in stroke and TBI, recent experiments suggested that glutamate grabbers also may be therapeutically useful in the treatment of SAH. Thus, in a rat model of SAH, oxaloacetate (250 mg/kg) was infused for 30, 60 min after induction of SAH,[64, 117] observing that infusion of the treatment was associated with a significant reduction in blood and CSF glutamate. Furthermore, there was an improvement in neurological outcome 24 h after SAH demonstrated by blood brain barrier disruption, neurological severity score, and brain edema.[64, 117]

2.8.4. Epilepsy

One of the most severe acute neurological conditions, associated with excessive glutamate release, is the status epilepticus (SE). SE is defined as an epileptic seizure lasting more than 30 min or as intermittent seizures, lasting for more than 30 min, during which the patient does not recover consciousness between repeated episodes.[149] SE is one of the most common neurological emergencies and several prospective studies have reported an incidence of 10–20/100,000 amongst whites in Europe and the US.[150] Convulsive SE is the commonest form, representing 40–60% of all SE cases. Mortality is high, with one out of five dying in the first 30 days.[150] The main neurological sequels of SE reported in the literature are cognitive impairment, brain damage-related deficits, and long-term development of recurrent seizures.[149]

There is much evidence that abnormally elevated glutamate is present in the brain of patients with medically refractory

temporal lobe epilepsy.[151, 152] As such, treatment with glutamate grabbers may provide a novel therapeutic modality in the treatment of such medically refractory seizures. With such purpose, rats submitted to a single injection of peripheral oxaloacetate 30 min after being subjected to pilocarpine-induced SE resulted in complete prevention of SE-induced neuronal loss in the CA1 region of the hippocampus with a significant reduction in apoptosis.[153] Despite evidence for neuroprotection, a reduction in seizure severity was not observed in that study. This concluded that the acute neuronal cell loss in the hippocampus (CA1 subfield) induced by SE was completely prevented in rats treated with oxaloacetate.

Moreover, the late caspase-1 activation was significantly reduced when rats were treated with oxaloacetate. These data supported the idea that the treatment with oxaloacetate causes a neuroprotective effect in rats subjected to pilocarpine-induced SE.[153]

2.8.5. Migraine headache

Migraine is a neurobiological disorder that affects 14.7 % of Europeans and its attacks manifest themselves from childhood to old age, with a decline among women during the postmenopausal years.[154] Although the molecular mechanisms of migraine are not completely understood, it has been suggested that glutamatergic homeostasis is involved.[112, 155-157] An excessive glutamatergic signal induces an over-activation of NMDAr, which seems to be implicated in the triggering, propagation and duration of cortical spreading depression (CSD).[157] Furthermore, NMDA-mediated glutamatergic transmission is probably implicated in the activation of the trigemino-vascular system[158] and may cause the clinical symptoms of migraine attack and central sensitization.[159] In this regard, NMDAr antagonists have been used as the most effective compounds for CSD suppression in experimental models[160], however their use in humans has failed mainly, because of unacceptable side effects.[161]

The role of glutamate in migraine suggested that systemic modifications of blood glutamate levels could reduce the excessive glutamatergic signal in brain and therefore to be used as a potential prophylactic treatment against migraine attacks.[155]

To test this hypothesis, the association of GOT activity in blood with serum glutamate levels and clinical parameters in patients with migraine[99] was performed. The results exhibited that migraine patients showed increased glutamate levels and lower GOT activity than control subjects. Furthermore, GOT activity was inversely associated with glutamate levels during interictal period, while increased glutamate levels was associated with the duration of the pain during ictal period, but not relationship was found for GOT activity levels and clinical parameters in patients with migraine.[99]

This has led to suggest that new therapeutic modalities in migraine prophylaxis may involve blood glutamate reduction.[155] Thus far, however, there are no experimental studies that demonstrate the use of blood glutamate grabbers in the treatment or prophylaxis of migraine headaches.

2.8.6. Glioma

In the last few years, it has been suggested that glutamate plays a crucial role in the growth of malignant gliomas, and may play an important role in the development of seizures that often accompany gliomas.[162-166] Studies with glioma cells in culture have shown that the cells release massive amounts of glutamate resulting in elevations of the extracellular concentrations higher than 100 μM within h in a space that is 1,000-fold larger than the cellular volume.[166] Significant increases were also demonstrated in the peritumoral space surrounding experimental brain tumors in rats[167] and in malignant gliomas and oligodendrogliomas in human patients.[168, 169] Since gliomas appear release glutamate, this pathology can be added to the long list of neurological

diseases in which glutamate excitotoxicity is the common destructive pathway, and therefore susceptible to be treated with blood glutamate grabbers.

In fact, a recent study demonstrated that rats and mice subjected to oxaloacetate treatment displayed a smaller tumor volume, reduced tumor invasiveness, and prolonged survival.[170] Suggesting the use of glutamate grabbers as a new treatment against gliomas.

2.8.7. Organophosphate intoxication

Organophosphate compounds are highly toxic chemicals widely used as pesticides [e.g. malathion and paraoxon (PO)] and as chemical warfare nerve agents (e.g. soman, sarin). Pesticide poisoning is one of the most common poisonings worldwide, estimated at one million cases each year with several hundred thousand deaths.[171] Organophosphates inactivate the enzyme acetylcholine esterase, a serine protease that hydrolyzes the neurotransmitter acetylcholine. Exposure to organophosphates leads to acetylcholine accumulation that causes the overstimulation of cholinergic receptors, which consequently results in the rapid and profound excitotoxicity and dysfunction of cholinergic neurons.[172]

Exposure to organophosphates damages several brain areas including the entorhinal and piriform cortex, amygdale, and hippocampus CA1/CA3.[173] Much of the brain damage does not typically occur at the time of the initial lesion, making secondary neuronal damage a major contributor to the neuronal loss. The degree of brain damage depends on the severity of the convulsions and is in direct relation to the increase in peripheral benzodiazepine receptors density.[174] The density of PBRs increases when microglia is activated in response to tissue damage such as organophosphates exposure.[175]

Glutamate has a substantial role in the propagation and maintenance of organophosphate-induced seizures, thus contributing to the secondary brain damage.[176] Gutamate was shown to be releases in excess in the brain under some intoxication and has prominent role during seizures.[177] Furthermore, glutamate receptor antagonists in general, NMDA blockers in particular, were proposes as potential antidotes against organophophates intoxication.[177] The standard treatment for organophophates intoxication consists of pretreatment with pyridostigmine, a reversible inhibitor of AChE and anticholinergic agents such as atropine sulfate.[178] In addition, it was reported that benactyzine (combined with anticholinergic and anti-NMDA properties), or benzodiazepines, could reduce some of the brain damage if administered early enough.[179]

Based on the important role of glutamate on organophosphate toxicity and the efficacy of blood glutamate grabbers, in a recent study Ruban *et al*.[180] showed that 10 min after paraoxon exposure in rats, followed by oxaloacetate and GOT infusion significantly reduced neuronal damage and prevented the peripheral benzodiazepine receptor density elevation. This study showed promise that glutamate grabbers may be useful in the treatment of secondary brain damage in the setting of organophosphate toxicity.

2.8.8. Fetal hypoxic–ischemic asphyxia

Fetal asphyxia or hypoxic–ischemic encephalopathy remains an important cause of perinatal death and long-term developmental disability. Among the different biochemical mechanisms that can damage the neuronal tissue after fetal asphyxia, it has been established that the release of excessive amounts of glutamate into the cerebral extracellular space plays as well a central role in pathology. In this regard, glutamate antagonists have been proposed as potential therapeutic agents to reduce the effects of asphyxia in the affected infants.[181] However, their use has important

limitations in newborn infants because of the critical role of the glutamatergic system during brain development. In this line, previous clinical studies reported that GOT was presented in higher concentration in fetal blood than maternal blood.[182] In addition, it was also observed that elevated concentration of GOT in fetal blood was directly correlated with the concentration of blood glutamate. These findings led to hypothesize that mechanisms such as GOT activity could participate in maintenance of non-toxic concentrations of glutamate during brain development, suggesting that GOT could be used as a potential treatment for the increased concentration of glutamate after fetal asphyxia. To test this hypothesis, and based on the well-known increase of glutamate after fetal asphyxia, it was studied the relationship between GOT and glutamate levels in arterial umbilical cord blood samples from control newborn infants and newborn infants with symptoms of hypoxia–ischemia. The results demonstrated that glutamate concentration and GOT activity in umbilical blood samples were higher in newborn infants with symptoms of hypoxia-ischemia compared to newborn infants without fetal distress. Analysis of Apgar scores and blood pH values (markers of perinatal distress) exhibited that conditions of severe distress were associated with higher glutamate and GOT levels. Then, this study suggested that during fetal development, based on the ability of GOT to metabolize glutamate this enzyme can act as an endogenous protective mechanism in the control of glutamate homeostasis.[183]

2.8.9. Amyotrophic Lateral Sclerosis (ALS)

The role of glutamate excitotoxicity in ALS has been extensively documented and remains one of the prominent hypotheses of ALS pathogenesis. In light of this evidence, the availability of a method to remove excess glutamate from brain and spinal cord extracellular fluids without the need to deliver drugs across the blood-brain barrier and with minimal or no adverse effects may provide a major therapeutic asset. Ruban *et al*.[184] demonstrated the therapeutic efficacy of the

combined treatment with recombinant glutamate-oxaloacetate-transaminase (rGOT) and its co-factor oxaloacetic acid in an animal model of sporadic ALS. This study showed that oxaloacetic acid/rGOT treatment provides significant neuroprotection to spinal cord motor neurons.

3.Stem cells in stroke

3.1. Classification of stem cells

Stem cells represent the building blocks of our bodies, functioning as the natural units of embryonic generation during development, and adult regeneration following tissue damage. They are defined by two distinct characteristics: the ability to maintain themselves through cell division, sometimes after long periods of inactivity (self-renewal), and the ability to give rise to more specialized cell types (differentiation). Stem cells are broadly classified as embryonic and adult stem cells.[185] Recently, there has been an exciting development in generation of a new class of pluripotent stem cells, induced pluripotent cells (iPSCs).[186]

3.1.1. Embryonic stem cells

The functional definition of embryonic stem cells (ESCs) includes four criteria: origin from a pluripotent cell population, capable of self-renewal indefinitely in the undifferentiated state, capable of maintaining normal karyotype during growth and clonally derived cells capable of differentiation in to all three embryonic germ layers *in vitro* or in to teratomas *in vivo*.[187]

In culture, ESCs appears as tightly packed colonies with distinct borders. Within the colonies, individual stem cells have a high nucleus and the cytoplasm with distinctive nucleoli. The pluripotent ESCs express transcription factors

Oct 4, Nanog and Sox 2 as well as tumor rejection antigens Tra–1–81 and Tra–1–60. It is important that any newly derived ESCs line be rigorously tested to unequivocally identify it as pluripotent. This should also include demonstration of differentiation capability and positive identification of all three germ layers in embryoid bodies formed *in vitro* or by teratoma formation *in vivo*. Karyotypic stability during culture needs also to be established.[188]

Human embryonic stem cells (hESCs) have emerged as exciting candidates for cell therapies in regenerative medicine due to their capacity to self-renew and differentiate into lineages of all three embryonic germ layers. Studies have demonstrated the ability of hESCs to differentiate into a number of pathologically relevant cell types, including insulin-producing cells, neural precursor cells, cardiomyocytes and hepatocyte-like cells[189189], highlighting their potential to be used as a renewable cell source to treat major diseases such as type I diabetes, Parkinson's disease, cardiovascular disease and liver diseases, among many others. Thus holding a high potencial for biomedical research and clinical applications as an allogeneic cell source.[188] However, the broader differentiation potential also presents a challenge in directing/ controlling the cell fate, and a higher risk of tumor formation after transplantation of ESCs derived tissue progenitors compared to adult stem cells.[189] Another controversial point of the application of ESCs in translational medicine it is difficult to suppress immunologic rejection in ESCs-based therapies.[190]

3.1.2. Induced pluripotent stem cells

The ethical controversies involving isolation of ESCs and the need for an autologous pluripotent stem cell source have fueled intense investigations into cellular reprogramming, leading to the generation (iPSCs).

Two groups (Yamanaka group in Kyoto University and Thomson group in University of Wisconsin) separately

reported that somatic cells can be successfully reprogrammed into iPSCs, marking a major landmark in stem cell research.[191, 192] In each study, four transcription factors were used for induction. Yamanaka's group selected Oct3/ 4, Sox2, Klf, and c-Myc[191], while Thomson's group used Oct3/4, Sox2, Nanog, and Lin28.[192] This allowed researches to reprogram mature somatic cells harvested from patients and generate an unlimited supply of iPSCs which in turn could be differentiated into various cell types needed such as neurons, cardiac cells, pancreatic cells, liver cells, blood cells or enterocytes for disease modeling, drug screening and cell therapy.

iPSCs cells have a couple of key advantages: they avoid the ethical concerns that have plagued the embryonic stem cell field, and they are patient-specific, thus providing a powerful tool for translational medicine.[193]

3.1.3. Adult stem cell

Adult stem cells, also called somatic stem cells, prompt tissue homeostasis throughout life and ensure tissue regeneration following damage. They reside in specific anatomic locations "stem cell niches" and are regulated by a combination of cellular, molecular and physical signals. Numerous types of adult stem cells have been identified, including hematopoietic, mesenchymal, endothelial, intestinal and neuronal stem cells, each displaying different properties and potency.

3.2. Cell therapies in stroke

Research on stem cell therapies has been increasing from the last 40 years. These kinds of therapies are especially attractive because stem cells interact directly to brain parenchyma cells whereas classical or pharmacological treatments depend on their pharmacokinetic profiles.[194] In this way, stem cells have emerged with a double role, not only as the key for revealing the insights of the neuroscience

as well as new promising therapies for stroke, due to their self-renewal and multipotentiality properties.[195] However, the mechanisms mediating ischemic stroke recovery using stem cells are still poorly understood.[196]

One of the potential mechanisms of stem cell therapy is cell replacement. Early studies have reported that after stem cell transplantation the number of grafted cells differentiated into mature neurons formed can vary. The origin of this variation lies in the source of the stem cell and also in the injection site. In this way, in recent preclinical studies, 34-60% of the injected cells were Neural Stem Cells (NSCs),[197] 30% ESCs[198] or 2-20% for Mesenchymal Stem Cells (MSCs).[199, 200] But sometimes, grafted cells remain undifferentiated close to the injury site, releasing growth and trophic factors[201, 202] or even without entering the Cerebral Nervous System (CNS) inducing also benefits after stroke.[203] Regardless of this effect, this systemic cell administration can provoke that administered cells stay also in other organs, like spleen or liver, interacting with other cells from the immune system and leading into modulatory functions,[204] reducing at the same time, the post-ischemic inflammatory damage in stroke.[205-207] Nevertheless, apart from cell replacement, enhanced trophic support and immunomodulatory response, there are endogenous brain repair processes that stem cell can stimulate, such as angiogenesis, neurogenesis, synaptogenesis and white matter remodeling[48, 208-211] inducing neurorestorative effects after ischemia.

In contrast to other pathologies, in stroke there is affected more than one brain cell population, involving also vascular cells in the ischemic region. This heterogeneity means that not only functional neuronal connections have to be reestablished; the vascular system has to be restored as well. In consequence, there is not an unique type of stem cells for stroke therapy, many of them have been tested demonstrating beneficial effects: ESCs,[212-214] Neural Stem Cells (NSCs),[209, 215, 216] iPSCs[217, 218] Human Umbilical Cord Blood Cells (HUCBCs)[219, 220] and MSCs.[200, 221, 222] Recent

studies with iPSCs have shown powerful new opportunities for modeling human diseases offering hope for personalized regenerative cell therapies. However, the field is racing ahead, and some researchers are pausing to evaluate whether induced pluripotent stem cells are indeed the true equivalents of ESCs and whether subtle differences between these cells might affect their research applications and therapeutic potential.[223, 224]

But, there are several parameters to take into account to elucidate the effective time point for stem cell therapy in preclinical or even clinical studies. An important factor to be considered is the use of autologous versus allogenic stem cells. In spite of this, the less lineage specific the cells are, the less chances to have an immune response,[225] in fact, for example MSCs which can be harvested from a variety of mesenchymal tissues have different immune response depending on their origin.[226]

Very few preclinical studies have compared different routes of administration, and the choice among them depends on the organ target. First studies for cerebrovascular diseases explored the intraparechymal route with the main goal of determine the feasibility of replacing lost neurons and rebuilding neural circuits,[227] meanwhile later studies showed that stem cells were not only able to survive after injection, as well as proliferate, differentiate and even migrate to the site of the injury.[228, 229] However, intraparenchymal cell delivery normally is not the first choice because the injection is focused in one region and to reach that point it is necessary to damage brain tissue. On the other hand, vascular routes, intravenous (i.v.) and intra-arterial (i.a.) solve these pitfalls and they are becoming the most common cell delivery method. Tail vein, femoral and jugular veins are the most common ones for stem cell administration. Several groups have demonstrated that i.v. administration can reduce infarct size or induce functional recovery [200, 219] when administrated 24h after stroke. Later studies also studied the biodistribution after i.v. injection and found out that depend

on the cell type, between 1-5% of the injected cells reached arterial circulation.[230] One of the most interesting i.v. applications was for NSCs delivery. It's known that this kind of stem cells has the ability to differentiate into neurons, astrocytes and oligodendrocytes. At the early beginning of stem cell therapies their repairing mechanisms were assumed to be related to rebuild the neural structure, but in recent years it has been observed that the injured brain environment is not optimal for cell integration, so the recovery works through growth factor mediation or anti-inflammatory processes.[231] Nevertheless, it seems that if the brain is the target, it would be desirable to reach it with the most of the injected cells, and to achieve it the best delivery route is the i.e. administration. The first study showed that 21% of the injected Bone Marrow Stem Cells (BMSCs) were observed in the affected hemisphere, and this was also related with functional recovery in behavioral tests but not as an infarct volume reduction in the treated group. However, administration route efficiency is also conditioned by the safety of the procedure and attending to this, i.a. administration has shown higher mortality than i.v. delivery. In a recent study, 41% of the animals died after an i.a. injection compared to 8% for i.v. delivery.[232] That's why this delivery route has been more explored recently and many studies have developed different injection strategies to minimize the risks.[233-236]

All these promising preclinical results progressed into early clinical trials of stem cell therapy in stroke. The effectiveness of different types of stem cells and delivery routes is also reflected in clinical studies which are exploring different combinations. So far, there is four published clinical trials of intracerebral cell therapy for stroke and one that is still ongoing,[237-239] one of intravenously administration[231, 240-242] and three following intra-arterial delivery.[243-245] The main goals of these clinical trials were to demonstrate the safety and feasibility of stem cell therapy using different types of stem cells and routes of administration. Published results

have reported that there were not enough patients enrolled in these studies to show benefits in terms of functional recovery after the treatment, but all of them demonstrated that stem cells are a promising, feasible and safe therapy for stroke.

However, the optimal conditions for applying stem cell therapies are still under discussion, fundamental questions related to cell type, characterization and dosage, therapeutic timing versus toxicity, or the relationship between biodistribution, fate and outcome are still on the bench, and preclinical studies should answer it first.

3.3. Mesenchymal stem cells

In 1970, Friedenstein *et al*.[246] demonstrated that bone marrow contains a population of hematopoietic stem cells (HSCs) and a rare population of plasti-adherent stromal cells (1 in 10000 nucleated cells in BM). These plastic adherent cells, initially referred to as stromal cells and now commonly called MSCs, were capable of forming single-cell colonies.

No exist an unique cell surface marker unequivocally distinguishes MSC from other HSC, which makes a uniform definition difficult. The International Society for Cell Therapy proposed criteria[247] that comprise: adherence to plastic in standard culture conditions, expression of the surface molecules CD73, CD90 and CD105 in the absence of CD 34, CD 45, HLA-DR, CD 14 or CD 11b, CD 79a or CD19 surface molecules as assessed by fluorescences-activated cell sorter analysis and a capacity for differentiation to mesodermal lineages (adipocytes, chondrocytes, osteocytes, fibroblasts and myocytes)[248]. Besides this lineage, according to environmental factors such as growth factors, hypoxia and the extracellular three-dimensional environment, MSCs may differentiate into other different cell types.

MSCs have been isolated from multiple tissues: skeletal muscle, adipose tissue, synovial membranes, dental pulp,

periodontal ligaments, cervical tissue, menstrual blood, Wharton´s jelly (WJ), umbilical cord (UC), umbilical cord blood (UCB), amniotic fluid, placenta and fetal tissues such as blood, liver and bone marrow (BM). In most cases, isolated MSCs are heterogeneous in proliferation and differentiation, although all express the characteristic MSC marker profile.[246]

Numerous reports have described therapeutic benefits in various disease models after administration of the MSCs. The therapeutic benefits of MSCs were initially associated by their migration, engraftment, and differentiation into target tissues.[249] However, remarkable anatomical structural repairs and functional improvements were increasingly observed with a small number or even no MSCs in the injured tissues. This suggests that most beneficial effects are largely due to secretory factors (neurotrophins, chemokines, cytokines) which mediate paracrine action and effects involving modulation of inflammatory and immune responses.[250]

Studies has shown that the therapeutic effects of MSC depend on their potency to secrete various factors to enhance tissue regeneration, modulate the local environment and stimulate the proliferation, migration, differentiation, survival and functional recovery of resident cells.[251] The MSC transplantation had a dual role, decreases the expression of factors deleterious to tissue and upregulate the beneficial lead to tissue regeneration a few days later. Angiogenesis process[252] and endothelial cell proliferation[251251] are related with the secretion of epidermal growth factor (EGF), fibroblast growth factor (FGF), platelet-derived growth factor (HGF), insulin-like growth factor-1 (IGF-1) and VEGF. Another variety of cytokines, like transforming growth factor beta (TGF-β), tumor necrosis factor-stimulated gene-6 (TSG-6), prostaglandin E2 (PGE2), galectin 1 and 9, interleukin 10 (IL10), indoleamine-1,3, dioxygenase (IDO), intercellular adhesion molecule (ICAM-1) and granulocyte-macrophage colony-stimulating factor (GM-CSF), are implicated in the paracrine action of MSC.[253, 254] Besides of the mechanism

described above, a large number of studies have indicated that MSCs have low inherent immunogenicity and possess an immunomodulation and immunosuppression function, which makes them attractive candidates for autologous and allogeneic transplantation.[255, 256255, 256] MSCs affect immune response through their interactions with the cellular components of the innate and adaptive immune system, which can occur through cellular contact and the secretion of diverse factors.[255-257] In response to pro-inflammatory stimuli, MSC develop an anti-inflammatory profile through the secretion of soluble factors (Table 1) these licensed cells can act on numerous innate immune cells.

Cytokines secreted by MSCs	Target cells
IL-10	Mph,Neu,DCs,Th1,Tregs,Tr1, tumor cells
IL-6	Neu,Mo,DCs,Th2,Tregs,Th17,CD8+FoxP3+
TGFβ	Mph,NK,DCs,B,T,Tregs
Chemokines	Neu,Mo,NK,Eo,Baso,DCs,Ly
CCL-2/MCP-1	Mph,EC,PL,Th2,Th17
CCL-5/RANTES	Neu,Mo,DCs,Th1,Tregs,CD8+FoxP3+
IDO	Mo,DCs,B,T,Tregs
VEGF	DCs,EC,Th1,Th17,Tregs
ICAM	T,MSCs
PGE2	Mph,Mo,NK,DCs,T,Tr1

Table 1: Cytokines secreted by MSCs and the corresponding target cells

So is that, MSC secretion of IL-6, IL-8, IFNβ, MIF and GM-CSF increase neutrophil migration to the site of injury, enhancing their activation and phagocytosis whilst promoting their survival. The cytokines CCL2, CCL3 and CCL12 recruits monocytes to the site of injury where they differentiate into M1 pro-inflammatory macrophages. In Figure 9 is summarized molecules secreted by the MSC and the innate immune cells that are involved. MSC exert different effects, quite so MSC produce an inhibitory effect on natural killers (NK) cells, affecting different aspects of NK cell function such as proliferation, cytotoxic activity and cytokine production. Relating to dendritic (DC) cells (DC), MSC have been demonstrated to interfere with DC differentiation, maturation and function. Another affected cells are the mast (MC) cells,

the MSC can effectively suppress MC activation both *in vitro* and *in vivo*.[258]

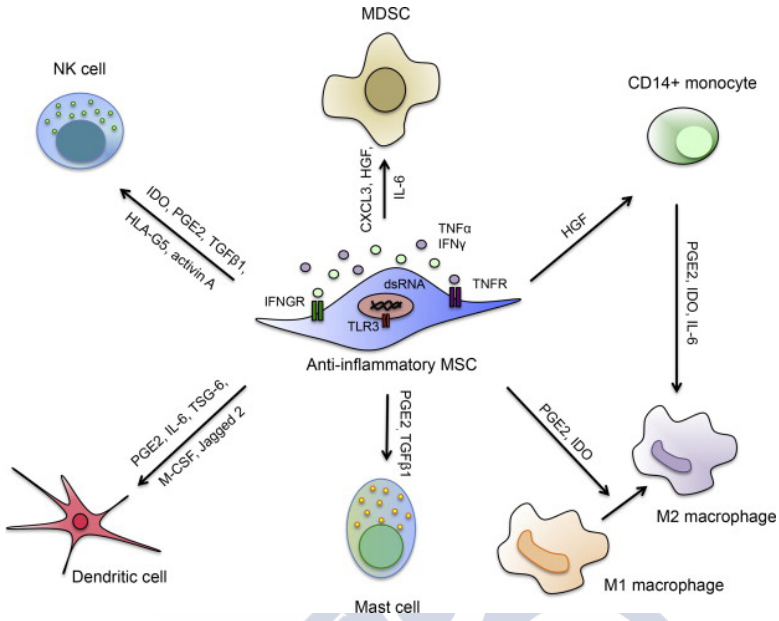

Figure 9: The multi-faceted anti-inflammatory actions of mesenchymal stem cells (Adapted from [291]).

But the activation of the immunoregulatory properties of MSC requires the presence of proinflammatory cytokines derived from T lymphocytes, macrophages and NK cells, thus indicating that there are bidirectional regulatory mechanisms between MSCs and immune cells. Cytokines, such as IFNγ, are necessary in this process, either alone or in combination with TNFα, IL-1α, IL-1β or IL-17. The expression of toll-like receptors (TLRs) in MSC has led to the involvement of TLRs in the activation of the MSC. The studies suggested that the activated MSC by TLR is getting a proinflammatory or anti-inflammatory phenotypes depending on TLR which is enabled. The importance of an inflammatory environment for MSC immunosuppressive capacity has been shown both *in vitro* and *vivo*.[257]

3.4. The use of mesenchymal stem cells in stroke

3.4.1. Route and time of transplantation of MSCs

Preclinical studies addresses questions related to route of transplantation and optimum time administration.

Different routes of administration, like intracerebral, intra-arterial (IA), intravenous (IV), intranasal, intrathecal and intraventricular were tested.[259, 260] The IA and IV transplantation presents the advantages of safety and wide distribution of stem cells within the ischemic penumbra as compared to other method. Experimentally, IA administration was superior to intravenous IV due to lower cell trapping by systemic organs such as lung, liver and spleen.

The optimal time of transplantation depends on the dynamically changed environment in injured brain. Early delivery of MSCs probably plays neuroprotective roles because of it are counteract against increased toxicity and inflammatory response. Transplantation of cells at 2-3 weeks after ischemia probably is superior in enhancing endogenous neuronal repair such as plasticity, angiogenesis and neurogeneis. In order to determine the optimal time for MSCs administration, Ishikaza *et al*.[261] infused IA human MSCs at 1,4 and 7 days after stroke and observed that MSCs were distributed both in peri-infarct and core area in 1 days group and dominantly in peri-infarct area in 4 days group and very few cells were observed on 7 days group.

3.4.2. Mechanism of action of MSCs in stroke

The mechanisms of action of MSCs have been explored on two levels: a peripheral level accounting for reduction of inflammation and immunomodulation and a central level expressed by the effects on neurogenesis, astrocytes, oligondendrocytes, axons and angiogenesis.

a. Immunomodulation and effect on inflammation in stroke

The current state of knowledge regarding activation of the immune response to focal cerebral ischemia is not complete even if it is known that immune responses play a pivotal role in the pathogenesis of ischemic stroke.

In settings of transient or focal cerebral ischemia the immune system is activated in response to damage of components of the neurovascular unit. Immediately after stroke the innate immune response that leads to inflammation is activated. The inflammatory mediators in turn lead to recruitment of inflammatory cells and the production of more inflammatory mediators that result in activation of the adaptive immune response. In the ischemic brain, inflammation acts as a "double edge sword": gives way to tissue repair and attempts at regeneration but also, due to "bystander toxicity" and scar formation, is a major impediment of regeneration and plasticity.[262, 263]

MSCs have been found capable of attenuating both innate and adaptive immune responses *in vitro* studies. Studies on neuronal cells subjected to oxygen-glucose deprivation and on animal models of ischemic stroke, showed that MSCs generate reduction of tumor necrosis factor-α (TNFα) through a mechanism involving interleukin (IL)-6 and VEGF signaling and inhibit NF-κB, finally producing an anti-inflammatory and anti-apoptotic effect.[264]

Human cord blood MSCs significantly decrease expression of IL-2 mRNA and IL-6 mRNA, attenuate IL-23 and IL-17 expression both in serum and around infarct lesion, reduce infarct size and improve functional deficits in a rat model of middle cerebral artery occlusion.[265]

b. Increased neurogenesis

It is now widely accepted that neural stem cells (NSCs) residing in the subventricular zone (SVZ) of the lateral ventricle and the subgranular zone (SGZ) of the hippocampal dentate gyrus are capable of producing new neurons in the adult brain. In addition it has been suggested the existence of an adult human neurogenic system that rises from the circumventricular organs (CVOs) and follows, at minimum, the circuitry of the hypothalamus and limbic system.[261, 266] Ischemic stroke injury triggers a dramatic and long-lasting (14 days) up regulation in NSC proliferation, inducing neurogenesis and gliogenesis in the SVZ and CVOs.[267-269]

Although neurogenesis in stroke has been characterized in detail, its role in recovery is mostly unknown. Only a very small fraction of newly formed cells in fact integrate into the lesioned tissue, so that the prevailing idea is that newly formed cells support the lesioned tissue.[270, 271]

Cell-based therapies activate the phosphatidylinositol-3-kinase (PI3K)/Akt pathway in neural progenitor cells that influence cell survival, proliferation, differentiation and migration. BM-MSCs stimulate the brain parenchyma cells to produce neurotrophic factors such as the fibroblast growth factor (bFGF) and the brain-derived neurotrophic factor (BNDF).[272, 273]

c. Effects on astrocytes, microglia, oligodendrocytes and axons

In the acute phase after ischemic stroke, the glial reaction to injury results in recruitment of microglia, olygodendrocyte precursors, meningeal cells and astrocytes to the lesion site. Some of these responses have beneficial effects, isolating the injury site and minimizing the area of inflammation and cellular degeneration, whereas other mechanisms inhibit axonal regeneration by participating in the formation of the glial scar.[274]

After ischemic stroke astrocytes become "reactive" and certain astrocytes release inhibitory extracellular matrix molecules known as chondroitin sulfate proteoglycans (CSPGs), a major barrier against axonal regeneration and produce a variety of proinflammatory cytokines. Other populations of astrocytes have important roles in neuroprotection and neurorestoration. They protect spared tissue from further damage, rebuild the blood–brain barrier (BBB), take up excess glutamate and produce neurotrophic factors. Astrocytes have also prominent roles in modifying synaptic plasticity and formation of new synapses.[275, 276]

In the setting of brain ischemia, the administration of MSCs stimulates astrocytes to release neurotrophins and growth factors including VEGF, vFGF and BDNF. MSCs reduce astrocyte apoptosis and inhibit ischemia-induced aquaporin-4 upregulation contributing to maintenance of BBB integrity after cerebral ischemia.[277]

MSCs decrease TGFβ1 expression in microglia/macrophages from the ischemic border zone (IBZ) contributing to the regulation of plasminogen activator inhibitor 1 (PAI-1) level in astrocytes. PAI-1 is associated with neurite remodeling after stroke.[278]

Oligodendrogenesis and remyelination play a crucial role in behavior and functional restoration post-ischemia. Oligodendrocyte progenitor cells (OPCs) present in the corpus callosum, striatum and SVZ of the adult mouse brain differentiate into mature oligodendrocytes. Oligodendrocytes are highly vulnerable to ischemic stress. Mature oligodendrocytes form myelin sheaths for sprouting axons in ischemic tissue. Transplantation of BM-MSCs increases both the number of oligodendrocyte progenitors in these areas of the ischemic stroke hemisphere and the number of mature oligodendrocytes at the periphery of the lesion.[279]

In the induced experimental stroke, BM-MSCs increase axon density in the perilesional zone, this phenomenon continuing

for at least 1 year after the stroke. MSCs reduce the expression of a protein called reticulon (Rtn4 or Nogo) and the production of a proteoglican named neurocan (Ncan), identified as axonal growth inhibitors.[280]

d. Increased angiogenesis

Angiogenesis is a process which involves endothelial cell proliferation, migration, tube formation, branching and anastomosis. The VEGF and VEGFr initiate the angiogenesis and angiopoietin 1 and 2 and their receptor Tie2 are involved in vessel maturation, stabilization and remodeling. Angiogenesis is essential for ischemic brain repair because it stimulates the blood flow and the metabolism in the ischemic boundary zone.[281]

Intravenous administration of BM-MSCs leads to a time dependent release of neurotrophins and angiogenic growth factors such BDNF, VEGF, bFGF, NGF, hepatocyte growth factor (HGF) and glial cell derived neurotrophic factor (GDNF) which stimulates angiogenesis and neurogenesis after stroke. These cytokines and growth factors have both autocrine and paracrine effects, regulating differentiation, proliferation and cell survival. Several studies showed that BM-MSCs increase the expression of SDF-1, VEGF, angiopoietin 1, Tie2, tight junction proteins and BDNF in the peri-infarct region.[282]

Other studies compared different routes of administration as well as various sources of MSCs in terms of bioactive molecules secretion, effects on angiogenesis and functional recovery after experimental stroke. In a rat stroke model, intra-arterial and intravenous delivery of BM-MSCs improved brain perfusion and metabolism as evaluated by SPECT and PET. Especially in rats treated with cells delivered via intra-arterial infusion, promoted angiogenesis and improved functional recovery. No micro-strokes were detected after intra-arterial injection. Another study reported that adipose tissue-derived from MSCs were found to be as effective as BM-MSCs in promoting functional recovery, reducing cell

death, as well as increasing cellular proliferation, neurogenesis and the expression of angiogenesis markers (such as VEGF) at 14 days post-infarction in a rat stroke model.[283]

In order to enhance growth factor delivery, certain groups used genetically modified MSCs to express growth factors known to stimulate differentiation and survival of host neurons. Miki *et al*.[284] uses the genetically modified MSC with herpes simplex virus Type 1 (HSV-1) vector to carry VEGF and obtained a 10% reduction of the infarct volume and improved functional deficit. Onda *et al.*[285] employed MSCs modified with adenoviral vector containing angiopoietin 1, which reduced by 30% the infarct size and improved motor deficit.

3.4.3. Safety in preclinical studies

The use of MSCs on animal stroke models was generally safe and showed favorable effects on behavioral outcome, yet several studies reported adverse events such as embolization, infection and tumorigenesis, as well as accumulation of amyloid β and calcium in the thalamus.[286]

3.4.4. Clinical experience with MSCs

In order to evaluate the safety profile of MSCs, Lalu *et al*. conducted a meta-analysis of prospective clinical trials, published in MEDLINE, EMBASE and the Cocrane Central Register of Controlled Trials, regarding trials using intravascular administration of MSC in adult or mixed populations (adult and pediatric population). The meta-analysis of the randomized controlled trials did not detect any association between the administration of MSC and acute infusional toxicity, systemic organ complications, infection, malignancy or death. Only a significant association between the administration of MSCs and transient fever syndrome was detected.[287]

Lalu *et al.* described a total of 9 clinical trials, which used autologous MSCs administered once or twice mostly systemically in a dose ranging from $50x10^6$ to $159x10^6$. The maximum follow-up period was 1 year and no significant side effects were reported.[286] The only three trials (NCT01678534, NCT01297413, NCT01091701) employing allogeneic MSCs are still ongoing and no partial results are published yet.

4.Expression of exogenous genes in cells

Due to in the present study, experimental procedures of trasnsfection and viral infection were used, a previous explanation of transfection categories, viral biology and infection were included in this section, with the aim to clarify the protocols described in Material and Methods section.

4.1. Transfection

Transfection, the delivery of DNA or RNA into eukaryotic cells, is a powerful tool used to study and control gene expression. Cloned genes can be transfected into cells for biochemical characterization, mutational analyses, investigation of the effects of gene expression on cell growth, investigation of gene regulatory elements, and to produce a specific protein. There are two types of transfection: transient and stable.

When cells are transiently transfected with plasmids, the DNA is introduced into the nucleus of the cell, but does not integrate into the chromosome. This means that many copies of the gene of interest are present, leading to high levels of expressed protein. Transcription of the transfected gene can be analyzed within 24–96 h after introduction of the DNA depending on the construct used. Transient transfection is

most efficient when supercoiled plasmid DNA is used. siRNAs miRNAs and mRNAs can be used for transient transfection and are effective in the cytoplasm, without the need to be transferred to the nucleus.

In the stable or permanent transfection, the transfected DNA is either integrated into the chromosomal DNA or maintained as an episome. Stably transfected cells can be selected by an antibiotic-resistance gene.

Several transfection methods have been employed and it can be classified in chemical methods and physical methods.

- Chemical transfection

Chemical transfection methods are the most widely used methods in contemporary research and were the first to be used to introduce foreign genes into mammalian cells. Chemical methods commonly use cationic polymer (one of the oldest chemicals used), calcium phosphate, cationic lipid and cationic amino acid.[288-290] The underlying principle of chemical methods is similar. Positively charged chemicals make nucleic acid/ chemical complexes with negatively charged nucleic acids. These positively charged nucleic acid/chemical complexes are attracted to the negatively charged cell membrane. The exact mechanism of how nucleic acid/chemical complexes pass through the cell membrane is unknown but it is believed that endocytosis and phagocytosis are involved in the process. Transfected DNA must be delivered to the nucleus to be expressed and again the translocation mechanism to the nucleus is not known. The transfection efficiency of chemical methods is largely dependent on factors such as nucleic acid/chemical ratio, solution pH, and cell membrane conditions, so the process results in low transfection efficiency, especially *in vivo*, compared with virus-mediated methods. However, these methods have merits of relatively low cytotoxicity, no mutagenesis, no extra-carrying DNA, and no size limitation

on the packaged nucleic acid. Chemical transfection efficiency also varies depending on cell type.

- Physical methods

The physical transfection[291] methods are the most recent methods and use diverse physical tools to deliver nucleic acids. The methods include direct micro injection, biolistic particle delivery, electroporation, and laser-based transfection.[291291] In brief, the micro injection method directly injects nucleic acid into the cytoplasm or nucleus.[292, 293] This method deliver nucleic acids into cells but demands skill, often causes cell death, and is very labor-intensive. Biolistic particle delivery employs gold particles that conjugate with nucleic acids. The nucleic acid/particle conjugates are then shot into recipient cells at a high velocity ("gene gun"). This method is straightforward and reliable but it requires expensive instruments and causes physical damage to samples. Electroporation is the most widely used physical method. The exact mechanism is unknown but it is supposed that a short electrical pulse disturbs cell membranes and makes holes in the membrane through which nucleic acids can pass.[294] Because electroporation is easy and rapid, it is able to transfect a large number of cells in a short time once optimum electroporation conditions are determined. Laser-mediated transfection (also known as optoporation or phototransfection) uses a pulse laser to irradiate a cell membrane to form a transient pore.[295-298] When the laser induces a pore in the membrane, nucleic acids in the medium are transferred into the cell because of the osmotic difference between the medium and the cytosol. The laser method enables one to observe the transfecting cell and to make pores at any location on the cell. This method can be applied to very small cells, because it uses a laser, but it requires an expensive laser-microscope system. In addition to those mentioned above, there are other physical methods using ultrasound (sonoporation) and magnetic field (magnetofection).[299-301]

4.2. Viral Vectors

Viral vectors is the most effective means of gene transfer to modify specific cell type or tissue and can be manipulated to express the therapeutic genes. Several virus types are currently being investigated for use to deliver genes to cells to provide either transient or permanent transgene expression. These include adenoviruses (Ads), retroviruses (γ-retroviruses and lentiviruses), poxviruses, adeno-associated viruses, baculoviruses and herpes simplex viruses.

- Adenoviruses

This virus has since been classified into six species that infect humans, and these species are subdivided into over 50 infective serotypes. The Ad capsid is a non-enveloped, icosahedral protein shell (70-100 nm in diameter) that surrounds the inner DNA-containing core. The genome of the Ad is a linear, double-stranded DNA (dsDNA) ranging from 26 to 40 kb in length. This linear form is organized into a compact, nucleosome-like structure within the viral capsid and is known to have inverted terminal repeat (ITR) sequences.

- Retroviruses

Retroviruses are known for their ability to reverse the transcription of their single-stranded RNA genome, thus creating dsDNA to replicate after infecting host cells. These viruses are most generally categorized as either simple (oncogenic retroviruses) or complex (lentiviruses and spumaviruses). The retroviral capsid is an enveloped protein shell that is 80-100 nm in diameter and contains the viral genome. The envelope structure surrounding the capsid is actually a lipid bilayer that originates from the host cell and contains both virus-encoded surface glycoproteins and transmembrane glycoproteins. The genome of the retrovirus is a linear, non-segmented, single-stranded RNA, 7-12kb in length.

- Lentiviruses

Lentiviruses, a subcategory of the retrovirus family, are known as complex retroviruses based on the details of the viral genome. The most common example of a lentivirus is the human immune-deficiency virus type 1 (HIV-1). The lentiviral capsid is the same as that of the simple retroviruses describe above. The lentiviral genome, like other retroviruses, contains a single-stranded RNA, 7-12 kb in length.

- Baculoviruses

The most commonly studied baculovirus is known as the Autographa californica multiple nucleoplyhedrovirus (AcMNPV). It was originally thought that virus was incapable of infecting mammalian cells; however, in 1983 several studies showed that baculovirus could be internalized by mammalian cells, and they were used for the expression of human interferon β. The baculoviral capsid is a rod-shaped protein shell (40-50nm in diameter and 200-400nm in length) that is naturally protected by a polyhedron coat.

- Herpes simplex viruses (HSV)

Actually, many different varieties of the HSV have been discovered. The most common of these, known as HSV-1, is well known by the average person as the viral cause for cold sores. The HSV has an icosohedral protein shell that is covered by a viral envelope. Embedded within the envelope are a variety of glycoproteins important for the viral attachment to host cellular receptors. The HSV genome consists of a dsDNA (152kb in length) that code for up to 90 different proteins important for viral attachment and replication.

- Recombinant adeno associated viral (rAAV) vectors

AAV is a small (25-nm), non-enveloped virus that packages a linear single-stranded DNA genome. It belongs to the family

Parvoviridae and is placed in the genus *Dependovirus,* because productive infection by AAV occurs only in the presence of a helper virus, either adenovirus or herpesvirus. In the absence of helper virus, AAV (serotype 2) can set up latency by integrating into chromosome 19q13.4, establishing itself as the only mammalian DNA virus know to be capable of site-specific integration.[302]

The rAAV genome is a linear, single-stranded DNA of 4.7 kb. Both sense and antisense strands of AAV DNA are packaged into AAV capsids with equal frequency. The genome is structurally characterized by 145-bp ITRs that flank two open reading frames (ORFs).[303]

The AAV life cycle have two stages after a successful infection, a lytic stage (Figure 10) and a lysogenic stage. During the lytic stage in the presence of helper virus (adenovirus or herpesvirus), AAV undergoes productive infection characterized by genome replication, viral gene expression and virion production. However, the lysogenic stage is characterized by the absence of adenovirus or herpesvirus, there is limited AAV replication, viral gene expression is repressed and the AAV genome can establish latency by integration into a 4-kb region on chromosome 19, termed AAVS1.[304]

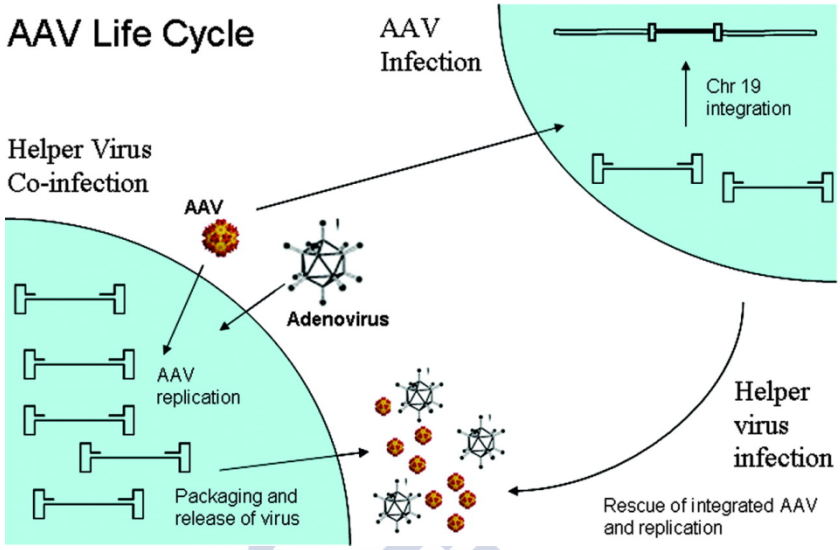

Figure 10: AAV life cycle (Adapted from [302]).

AAV entry into target cells by using the cellular receptor heparin sulfate proteoglycan. Internalization is enhanced by interactions with one or more of at least six known co-receptores including integrins, fibroblast growth factor receptor 1, hepatocyte growth factor receptor and laminin receptor. Cell defective for this receptors, the AAV infection is produced by endocytosed into clathrin-coated vesicles. The AAV trafficking postentry and AAV enters the nucleus are not completely characterized.[302]

AAV has become increasingly common as a vector for use in human clinical trials; as of now, 38 protocols have been approved by the Recombinant DNA Advisory Committee and the Food and Drug Administration (FDA). The factors that have played a role in encouraging the use of AAV vectors include the low pathogenicity of the virus, the persistence of the virus and the many available serotypes. In Table 2 are summarized some trials, some of the them have been concluded or are in progress.[302]

Condition	Gene product(s)	Phase
Monogenic disease	CFTR	I/II
Canavan´s disease	Aspartoacylase	I
Parkinson´s disease	GAD65,AADC,neurturin	I
Alzheimer´s disease	Beta nerve growth factor	I
Alpha-1-antitrypsin deficiency	AAT	I
Arthritis	TNFR:Fc	I
Leber congenital amaurosis	RPE65	I
Hemophilia B	Factor IX	I
Late infantile neuronal lipofuscinosis	CLN2	I
Muscular dystrophy	Minidystrophin, sarcolycan	I
Heart failure	SERCA-2a	I
Prostate cancer	GMCSF	I/II/III
Epilepsy	Neuropeptide Y	I

Table 2: Clinical trials involving rAAV vectors.

Hypothesis

USC
UNIVERSIDADE
DE SANTIAGO
DE COMPOSTELA

After cerebral ischemia, there is a rapid but transient raise of glutamate into the extracellular space mediating excitotoxicity mechanisms. Therefore, several therapies have been tested in order to mitigate the deleterious effects of glutamate. Unfortunately, all of them have failed by lack of efficacy or displayed severe side effects in clinical trials. In this regard, the decrease of brain glutamate levels by lowering blood glutamate have been described as a new an effective protective mechanism against cerebral ischemia; therefore, blood glutamate grabbers may establish a novel and attractive therapeutic strategy for acute ischemic stroke. Based on this mechanism, previous studies by our group have demonstrated that oxaloacetate treatment mediated a decrease of blood glutamate levels, which reflected in the lowering of extracellular levels of brain glutamate and a reduction of brain injury. However, oxaloacetate interferes in Krebs cycle and the large dose required may lead to side effects in human clinical practice. Therefore, new alternatives of blood glutamate grabbers are necessary. We hypothesized the following:

- The use of recombinant GOT1 as a new blood glutamate grabber
- The use of cell line transfected with $EAAT_2$ able to act as novel glutamate grabbers cells.
- Mesenchymal Stem Cells transfected with $EAAT_2$ that could have a dual role: a) neuroprotective effect due to their role of blood glutamate grabber through $EAAT_2$ expression; and b) neurorepair effect associated with their endogenous features of stem cell.

USC
UNIVERSIDADE
DE SANTIAGO
DE COMPOSTELA

Objectives

USC
UNIVERSIDADE
DE SANTIAGO
DE COMPOSTELA

The present work will be structured in 2 sections, and the main objectives are the following:

1. Analysis of protective effect of rGOT1 in ischemia
   - Analyze the protective effect of human rGOT1 administrated alone and in combination with a low dose (non-effective dose) of oxaloacetate in the rat model of ischemia.

2. Test the effect of glutamate grabbers cells on ischemic damage.
   - Induce the exogenous expression of $EAAT_2$ in mesenchymal stem cells and other types of cells.
   - Characterization of $EAAT_2$ expression in transfected cells.
   - Validate the functionality of the $EAAT_2$ in cells transfected.
   - Demonstrate in healthy animals that transfected cells with $EAAT_2$ have capacity for uptaking plasma glutamate.
   - Confirm that the transfected cells with $EAAT_2$ induce neuroprotection in an animal model of cerebral ischemia.
   - Determinate the additional beneficial effect of $EAAT_2$ expression on mesenchymal stem cells.

USC
UNIVERSIDADE
DE SANTIAGO
DE COMPOSTELA

Materials & Methods

USC
UNIVERSIDADE
DE SANTIAGO
DE COMPOSTELA

5. Section I. Analysis of protective effect of rGOT in ischemia

The purpose of this study was to test the efficacy of GOT administration on blood and brain glutamate lowering and the subsequent potential protective effect on cerebral ischemic damage. For that, recombinant GOT1 (rGOT1) were administered in ischemic animal model and their effect were compared with oxaloacetate,[116] used as a positive control of blood glutamate reduction.

This study was divided into two steps: a dose-response study and therapeutic study.

5.1. rGOT1 dose-response study

In the first place, a dose-response study was performed in healthy animals, with the aim to determine the highest effective dose of rGOT1 on blood glutamate reduction. As glutamate is metabolized by GOT in combination with oxaloacetate, the effect of rGOT1 supplemented with a non-effective oxaloacetate was also tested in with healthy animals.

With this purpose, healthy rats were first subjected to an artificial increase in serum glutamate concentration in order to determine the effective dose of rGOT1 able to induce a reduction in glutamate concentration (n=6 per dose). The artificial increase in serum glutamate concentration was induced by means of the administration of glutamate 15 mM (1 ml per 300 g weight of the animal). This procedure was used to mimic the increase in serum glutamate observed after an ischemic insult[116]. Glutamate 15 mM was injected in jugular at the beginning of the experiment (after animal anesthesia induction), and 30 min later rGOT1 was given. Serum samples (500 ml) were taken (from vein tail) under basal conditions (before glutamate injection), and 1, 2, 4, 6

and 24 h after glutamate injection. Glutamate 15mM and treatments were administered through the jugular vein in a bolus form. All rGOT1 doses were dissolved in saline (0.9% of NaCl) and the concentration was adjusted to inject 1ml per animal. pH was adjusted to 7.4. Pure human rGOT1 (stock 5800 U/l)) was provided by Professor David Mirelman from Weizmann Institute, Israel.

The following experimental groups were designed:

a) Group 1 (n=6): rats treated with saline (1mL).
b) Group 2 (n=6): rats treated with glutamate 15mM (1mL).
c) Group 3 (n=6): rats treated with oxaloacetate 1.5mg/100g (1mL).
d) Group 4 (n=6): rats treated with glutamate 15mM + rGOT1 6.44 µg/100g (1mL).
e) Group 5 (n=6): rats treated with glutamate 15mM + rGOT1 12.88 µg/100g (1mL).
f) Group 6 (n=6): rats treated with glutamate 15mM + rGOT1 25.76 µg/100g (1mL).
g) Group 7 (n=6): rats treated with glutamate 15mM + rGOT1 12.88 µg/100g supplemented with oxaloacetate 1.5mg/100g (1mL).

The dose of rGOT that induces a greater decrease in blood glutamate in healthy animals will be selected for use in the protective study.

5.2. Protective study

In this phase, the protective optimal dose selected in previous the dose–response study was tested in an ischemic model. Four experimental groups were studied:

a) Group 1(n=11): animals treated with saline (1mL).
b) Group 2 (n=11): animals treated with oxaloacetate 3.5 mg/100g (1mL).

c) Group 3 (n=11): animals treated with rGOT1 12.88 µg/100g (1mL).
d) Group 4 (n=11): animals treated with rGOT 12.88 µg/100g supplemented with oxaloacetate 1.5 mg/100g (1mL).

To determine the capacity of the treatments to induce a blood and brain glutamate reduction and a protective effect, two different studies were performed. On one hand serum glutamate determination through ELISA (Figure 11) and on the other hand, brain glutamate determination through MRS (Figure 12). Moreover, other parameters as serum GOT activity, infarct volume and functional deficit were also measured. Treatments were administered immediately after reperfusion (80 min after occlusion) or 1 hour after reperfusion (140 min after occlusion).

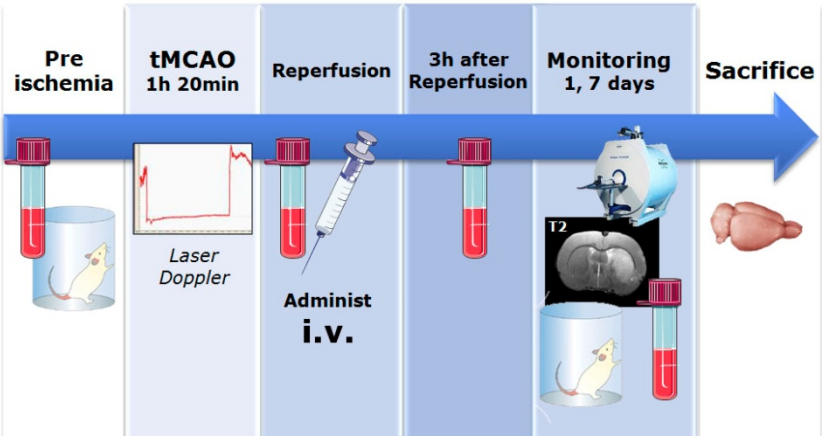

Figure 11: Protocol used to determinate the effect of the treatments used on serum glutamate. Serum glutamate levels were measured before tCMAO surgery, after artery reperfusion (80 min) and 1, 2, 3 and 24 h after artery reperfusion.

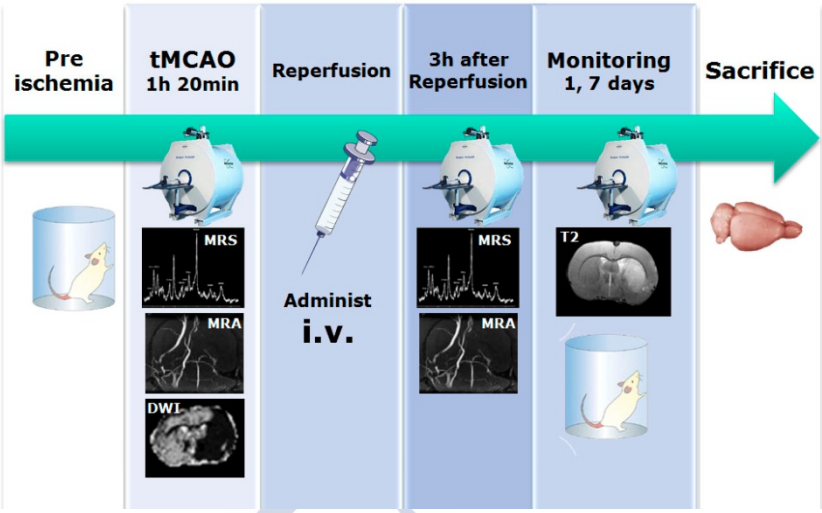

Figure 12: Protocol used to determinate the effect of the treatments on brain glutamate levels.

Serum glutamate concentration were determined under basal conditions (before surgery), immediately after reperfusion (80 min after occlusion) and 1, 2 and 3 h after reperfusion. GOT activity was measured under basal conditions (before surgery) and 1, 3 and 24 h after reperfusion. Brain glutamate levels were measured during occlusion (80 min) and during reperfusion (180 min) using the Magnetic Resonance Spectroscopy (MRS) technique (Figure 12). As it was not technically accurate to measure the serum and brain glutamate levels after reperfusion at the same time in the same animal, treatments were tested in two independent groups of animals (n=6 each).

One group (Figure 12) was used to measure brain glutamate levels and in the other group (Figure 11) to determine the serum glutamate concentration and GOT activity. Infarct volume was determined during occlusion (only in those animals subjected to spectroscopy analysis), 24 h and 7 days after ischemia. Sensorimotor test was performed under basal conditions (1 day before surgery) and 7 days after ischemia.

5.3. Animal procedures

5.3.1. Animal management

In this study we have used 119 male Sprague Dawley rats (Harlan Laboratories, Barcelona, Spain) with a weight of 275±25g. Animals were kept at controlled conditions of temperature (22±1ºC) and humidity (60±5%), with a 12/12 h light/ dark cycle for a period of one week prior to surgery and up to 14 days after surgery. The rats were granted free access to food (commercial chow pellets) and tap water. For surgery and MRI, rats were anesthetized with sevoflurane (3% in 70% N_2O and 30% O_2). Rectal temperature was monitored and maintained at 37±0.5ºC with a feedback controlled heating system (1025 system, SA Instruments). At the end of the procedures animals were sacrificed under deep anesthesia (8% sevoflurane). Experimental protocols were approved by the local Animal Care Committee according to the Spanish and European Union (EU) rules (86/609/CEE, 2003/65/CE, 2010/63/EU, RD 1201/2005 and RD53/2013).

5.3.2. Model of focal transient ischemia in rat

Transient focal ischemia was induced in rats by intraluminal occlusion of the middle cerebral artery (MCAO), performed as previously described[305] with several modifications. In order to monitor the relative cerebral blood flow (CBF) during the surgery, a laser-Doppler flow probe (tip diameter 1mm) attached to a flow meter (PeriFlux 5000; Perimed AB) was located over the thinned skull, and over the middle cerebral artery territory (approximately 4mm lateral to bregma). Under a surgical microscope, common carotid, external carotid, and the internal carotid arteries of the left side were dissected from connective tissue through a midline neck incision. Left external carotid and pterygopalatine arteries were separated and tied with 6-0 silk sutures. A silicon rubber-coated monofilament (403512PK5Re; Doccol Corporation, USA) was inserted through the external carotid into the left common carotid artery and advanced into the

internal carotid from the bifurcation to occlude the origin of the Macbeth vertebral arteries remained intact in all surgical procedures. In those animals subjected to spectroscopy analysis, once the artery was occluded, determined by Doppler signal reduction, the animals were carefully moved from the surgical bench to a Magnetic Resonance (MR), with the aim to determine the basal ischemic lesion by means of apparent diffusion coefficient (ADC) maps. Angiography imaging was also performed to confirm the artery remained occluded over the MR study, and finally brain glutamate by MRS was analyzed. After basal MR analysis, animals were returned to the surgical bench and Doppler probe was repositioned. Reperfusion was performed 80 min after the occlusion onset. Animals were subsequently randomized in experimental groups performed, by using computer-generated random numbers.

5.3.3. Inclusion criteria

Only animals with a cerebral serum flow reduction of over 70% and with reperfusion after occlusion were included in the study.

5.4. Treatment administration

Animals were intravenously injected into the jugular vein. First, animals were anesthetized with sevoflurane 3% in O_2:N_2O/30:70. Then a 0.5 cm incision was made in the animal´s neck just above the clavicle 1cm to both left and right of the midline. Subcutaneous fat was cut out, and the jugular vein was exposed. A 30g needle was used for every injection after withdrawal, the puncture is rapidly closed to preventing bleeding.

5.5. Blood glutamate analysis

Venous blood was collected from the tail vein at different times specified in 5.1. Blood samples were collected in test

tubes and centrifuged at 3,000 rpm for 7 min. Serum was removed and immediately frozen and stored at 80 °C. Serum glutamate concentration was determined by means of Glutamate Assay Kit (Abnova, Taiwan) following the manufacturer´s technical specifications.

5.6. GOT activity analysis

GOT activity was determined by means of Reflotron GOT (AST). Tests followed the manufacturer´s technical specifications (Roche, Basel, Swizerland).

5.7. Functional test

In all animals, cylinder test[306] was performed before MCAO and 7 days after MCAO by a researcher who was blinded to the experimental groups.

The Cylinder test is designed to evaluate locomotor asymmetry in rodent models of CNS disorders. In this test while the animal moves within a clear plastic cylinder, its forelimb activity is recorded. Forelimb use is defined by the placement of the whole palm on the wall of the arena, which indicates its use for body support. Forelimb contacts while rearing are scored with a total of 10 contacts recorded for each animal. The number of impaired and non-impaired forelimb contacts is calculated as a percentage of total contacts.

5.8. Magnetic resonance studies

5.8.1. MR equipment

Magnetic resonance imaging studies were conducted on a 9.4 T horizontal bore magnet (Bruker BioSpin, Germany) with 20 cm wide actively shielded gradient coils (440mT/m). Radio-frequency transmission was achieved with a birdcage volume resonator; signal was detected using a four-element surface

coil, positioned over the head of the animal, which was fixed with a teeth bar, earplugs, and adhesive tape. Transmission and reception coils were actively decoupled from each other. Gradient-echo pilot scans were performed at the beginning of each imaging session for accurate positioning of the animal inside the magnet bore.

5.8.2. Imaging protocol

- Magnetic resonance angiography

Magnetic resonance angiography (MRA) was used to identify the circle of Willis and to evaluate the relative blood flow during tMCAO. Axial MRA images of rat brain are a stack of 58 slices where all brain is mapped. In Figure 13A and Figure 13B it is shown a MRA Z-projection of a healthy and a tMCAO rat respectively. The parameters used for TOF-MRA 3D Flash sequence were FOV 30.72 x 30.72 x 14 mm3, image matrix 256 x 256 x 58 (in plane resolution 120 mm/pixel x 120 mm/pixel x 241 mm/pixel), repetition time 15 ms, 2 averages and echo time 2.5 ms.

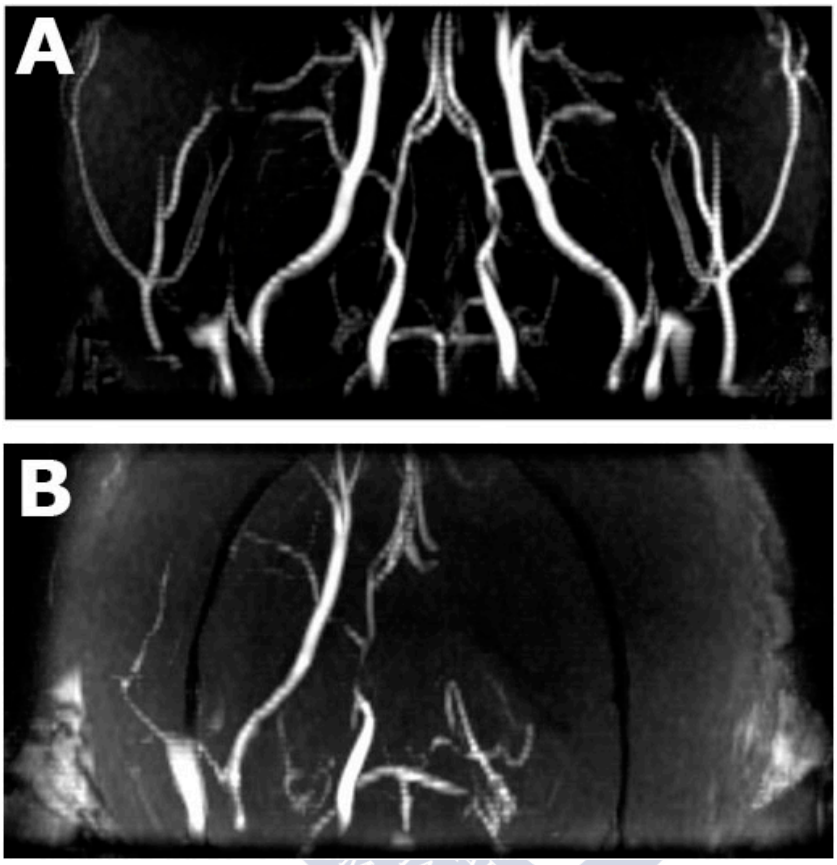

Figure 13: Z-projection of MRA. (A) Healthy animal. (B) Animal under tMCAO.

- Diffusion weighted images & Apparent diffusion coefficients maps

In order to evaluate the extent and localization of the hypoperfunded brain region during the occlusion, MR Diffusion Weighted images (DWI) were performed. It is important to note that in clinical practice MR DWI infarct region are displayed as hyperintense signal in MRI while preclinical displays are normally hypoinense. This is because clinical MR images normally present the image for the higher "b" value of the sequence (DWI) while preclinical images are normally maps (Apparent diffusion coefficient, ADC), resulted from the adjustment of all "b" values to an exponential

decay. So, for the previous animal, ADC maps are shown in grayscale in Figure 14A and color scale in Figure 14B. Attending to these maps, tMCAO is affecting to MCA territory where a reduction of the cerebral blood flow (CBF) can be noted in cortex and striatum (dark in grayscale, black-purple-blue in color scale). During tMCAO the Apparent diffusion coefficient maps were acquired using a spin-echo echo-planar imaging sequences with the following acquisition parameters: FOV 24 x 16 mm2, image matrix 96 x 64 (in plane resolution 200mm/pixel x 200mm/pixel), 14 consecutive slices of 1mm thickness, repetition time 4 s, 4 averages, echo time 26.91 ms, spectral bandwidth 200.000 Hz and 7 diffusion b values: 0; 300; 600; 900; 1200; 1600 and 2000. Diffusion-weighted images were acquired during the ACM occlusion.

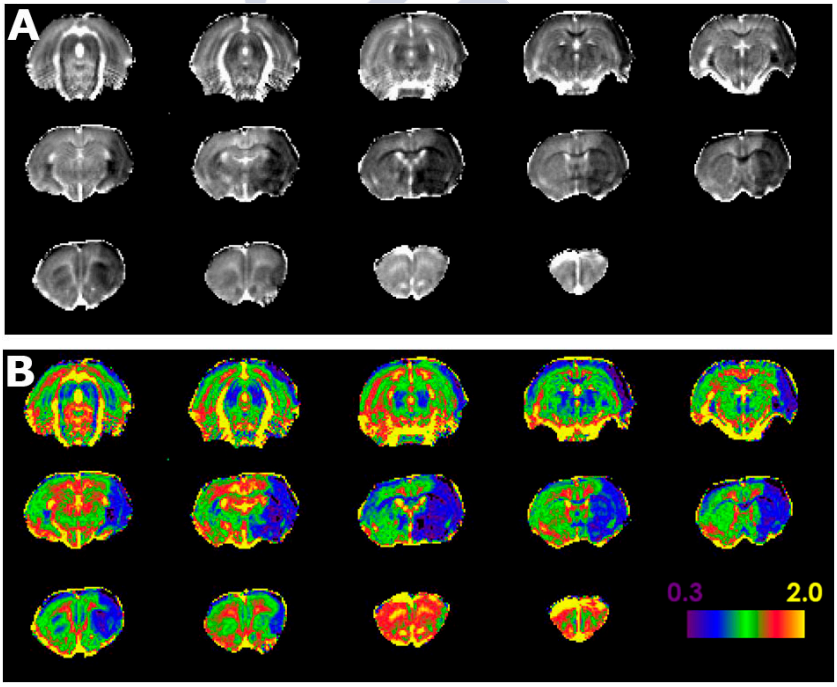

Figure 14: ADC of an rat during tMCAO. Coefficient diffusion values (0.3-2.0·10^{-3} mm^2/s. (A) Grayscale. (B) Color scale.

- MR T_2

In order to evaluate the efficacy of the treatments studied in this work, MRI T2 weighted images were acquired and T2 maps were calculated to quantify the infarct volume over time. MRI T2-weighted images were acquired using a multislice multiecho spin-echo sequence with the following acquisition parameters: FOV 19.2 x 19.2 mm2, image matrix 192 x 192 (isotropic in-plane resolution of 100 µm/pixel x 100 µm/pixel), 14 consecutive slices of 1mm thickness, repetition time of 3 s, and 16 echoes with 9 ms of echo time. T2-weighted images were acquired at different timepoints (normally, 24h, 1, 3, 7 and 14 days) after the onset of the ischemia.

5.8.3. Magnetic resonance spectroscopy

Magnetic resonance spectroscopy (MRS) was acquired to compare the metabolite change in the ischemic region during and after tMCAO by comparing the obtained spectrum over time and also with the non ischemic brain region. Technically, MRS was acquired as previously described.[307, 308] Briefly, local shimming was performed by manual adjustment of first- and second-order shim coil currents using a proton-stimulated-echo acquisition mode (STEAM)-waterline sequence. The field homogeneity in a 3-mm^3 voxel typically (FIG XX) resulted in signal line widths of 10-20 Hz for the water signal. Water signal was suppressed by variable power RF pulses with optimized relaxation delays (VAPOR). *In vivo* 1 hour magnetic resonance spectra of the rat brain were acquired by using a STEAM sequence with echo time=3ms, mixing time (TM)= 5ms, repetition time= 2500ms, 176 averages, cubic voxel=3x3x3 mm^3 (27 µl). Spectra were processed using MNOVA 7 (Mestrelab Research, Santiago de Compostela, Spain). For the quantitative analysis, glutamate signals were normalized to the creatine peak areas for each single spectrum. MRS was acquired during the occlusion (80min) and during 180 min after reperfusion in different part of the brain, cortex and striatum from the ischemic and non

ischemic region to compare metabolite differences between them.

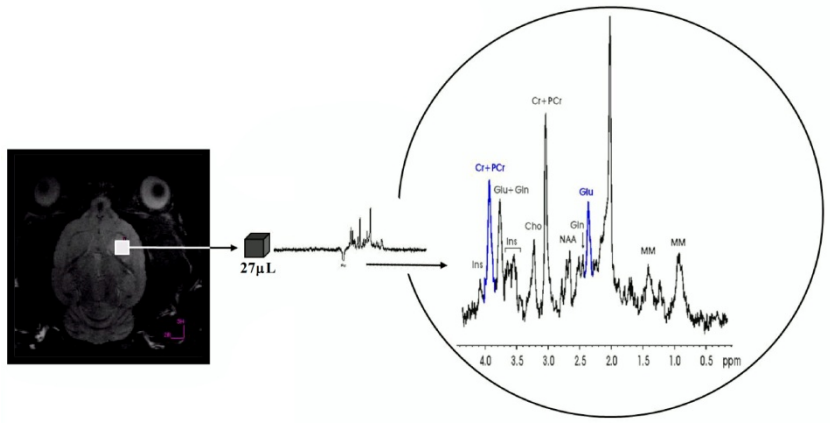

Figure 15: Schematic view of the MRS acquisition procedure. Here, 27µL voxel in the ischemic hemisphere is studied and for it the areas of Cr+PCr and Glu peaks (noted as blue in the spectrum) are determined and compared.

5.8.4. Image analysis

All images were processed using ImageJ (Rasband WS, ImageJ, NIH, http://rsb.info.nih.gov/ij). Infarct volumes were determined from ADC maps and T2 maps by manually selecting areas of reduced ADC values or hyperintense T2 signal by a researcher blinded to the animal protocol.

5.9. Statistical analysis.

All data are presented as the mean and standard error of the mean (mean ± SEM). One-way or two-way analysis of variance (ANOVA) followed by post-hoc Bonferroni evaluation was used for multiple groups to determine significant differences. Student's t-test was used to test the differences between two groups. Statistical significance was set at $*p<0.05$, $**p<0.01$ and $***p<0.001$. The statistical analysis was conducted using PASW Statistics 18 for MAC (SPSS Inc., Chicago, CA, USA).

6. Section II: Effect of glutamate grabbers cells on ischemic damage.

In this section it is described all *in vitro* protocols used to induce the artificial expression of EAATs in the cells, and the *in vivo* procedures to test the protective effect of these transgenic cells in ischemic model animals.

6.1. *In vitro* studies

6.1.1. Cell culture

Four types of cell cultures were used in this experimental section, rat astrocytes, rat neurons, HEK and MSC. HEK (KEK 293) and MSC were used to induce the expression of EAATs while astrocytes and neurons for additional experiments.

a. Rat astrocytes isolation and culture

Astrocytes were obtained as described before[309] with minimal modifications. Briefly, brains were removed, meninges were separated and cortical area was dissected from one-day old Sprague–Dawley rat pups. The digestion of cortices was performed with 0.25% trypsin-EDTA (Gibco-Invitrogen, USA). Cells were mechanically dissociated in Dulbecco's Modified Eagle Medium (DMEM) containing 25 mM glucose, 2 mM glutamine, 10% (v/v) horse serum, 10% (v/v) penicillin and 100 mg/ml streptomycin (all from Gibco-Invitrogen, USA). Dissociated cells were seeded in 75 cm^2 flasks (Corning, USA) and maintained in an incubator at 37ºC with a humidified atmosphere containing 95% air and 5% CO_2. Medium was replaced every 3 days to fresh growth medium until cells reached confluence.

b. Rat neuron isolation and culture

Cortical neurons were obtained from embryos (E16-17) (Sprague Dawley rats). Embryos rats were decapitated and the brains were removed, the meninges were separated and the cortical area was dissected and collected. The digestion of cortices was performed with 0.25% trypsin-EDTA (Gibco-Invitrogen, USA) for 10 min at 37ºC. The tissues were mechanically dissociated in Dulbecco´s Modified Eagle Medium (DMEM) containing 25 mM glucose, 2 mM glutamine, 10% horse serum, 10% fetal bovine serum, 1% antibiotic solution (penicillin/streptomycin) all from Gibco-Invitrogen, USA. Afterwards, the tissue was treated with 0.4 mM DNAase (Sigma-Aldrich, USA) for 10 min at 37ºC and centrifuged for 10 min at 800 rpm. Neurons were resuspended in Neurobasal medium supplemented with 0.5% B27, 1% penicillin/streptomycin, 1% L-glutamine (all from Gibco-Invitrogen, USA). After counting, neurons were seeded at a density of $2x10^5$ cells/cm^2 in the previously described medium supplemented with cytosine arabinoside 10 mM (Sigma-Aldrich, USA) to prevent the astroglial proliferation.

All procedures were conformed to the Committee of Animal Care of the Hospital Clínico Universitario of Santiago de Compostela, according to E.U. rules (86/609/EEC, 2003/65/EC and RD 1201/2005).

c. Rat Mesenchymal Stem Cells (rMCSs) culture and expansion

rMSCs were purchased from Trevigen (Cultrex, USA). These cells were plated in 75 cm^2 flasks at a density of $1x10^6$ per dish. The culture medium used was Iscovec Dulbecco modified medium (1x) (IMDM, Gibco-Invitrogen, USA) and supplemented with 10% Fetal Bovine Serum (FBS, Gibco-Invitrogen, USA), 10% Horse Serum (HS, Gibco-Invitrogen, USA), 1% antibiotic solution (penicillin/streptomycin; Gibco-Invitrogen) and 1% antimycotic solution (amphotericin; Sigma-Aldrich, USA). The cells were incubated at 37°C in a

humidified atmosphere of 95% air and 5% CO_2. Medium was replaced every 3 days. When MSCs reached to 80-90% of confluence, they were trypsinized (0.25% trypsin-EDTA; Gibco-Invitrogen, USA). Cell passage numbers between 7 and 18 were used in the experiments.

d. HEK cell line cultivation

HEK cells were obtained from the Institute of Zelluläre Biophysik of Forschungszentrum (Jülich, Germany). Cells were cultured in Minimun Essential Medium GlutaMAX I (Gibco-Invitrogen, USA) supplemented with 10% Fetal Bovine Serum (FBS, Gibco-Invitrogen, USA), 1% MEM Non Essential Amino Acids (Gibco-Invitrogen, USA), 1% antibiotic solution (penicillin/streptomycin; Gibco-Invitrogen, USA) and 1% antimycotic solution (amphotericin; Sigma-Aldrich, USA). The cells were maintained at 37ºC in a humidified atmosphere of 95% air and 5% CO_2, changing the medium every 2-3 days. When the cells achieved the 80-90% confluence, these were detached with 0.25% trypsin-EDTA (Gibco-Invitrogen, USA). Cell passage numbers between 7 and 25 were used in these experiments.

6.2. Exogenous expression of EAATs on cells

To induce the exogenous expression of EAATs on cells, two molecular procedures were probed, transfection and virus infection.

6.2.1. Cellular *in vitro* transfection

To induce the EAATs expression in cells, a plasmid containing the $EAAT_2$ sequence was used. Previous to explain the transfection protocol, an explanation about the plasmid DNA expansion will be described.

Plasmid DNA pRcCMVmYFPEAAT$_2$ (Figure 16) encoding the constructs YFP-$EAAT_2$ was obtained from the Institute of

Zelluläre Biophysik of Forschungszentrum (Jülich, Germany) and was propagated in competent *Escherichia Coli*. Ultrapure, endotoxin free plasmid DNA was prepared using a QIA filter kit (Qiagen, Germany) according to the manufacturer´s instructions. Purified plasmid was resuspended in sterile TE buffer (Tris/HCL 10mM, EDTA 1mM, pH 7.6). For analysis of the fractions at each stage of the plasmid purification procedure, the plasmid was restricted with the enzyme EcoRI (New England BioLabs, UK) and checked by gel electrophoresis. The plasmid concentration and its purity were measured by ultraviolet (UV) absorbance at 280 and 260 nm on a Nanodrop (Thermo Scientific, USA)

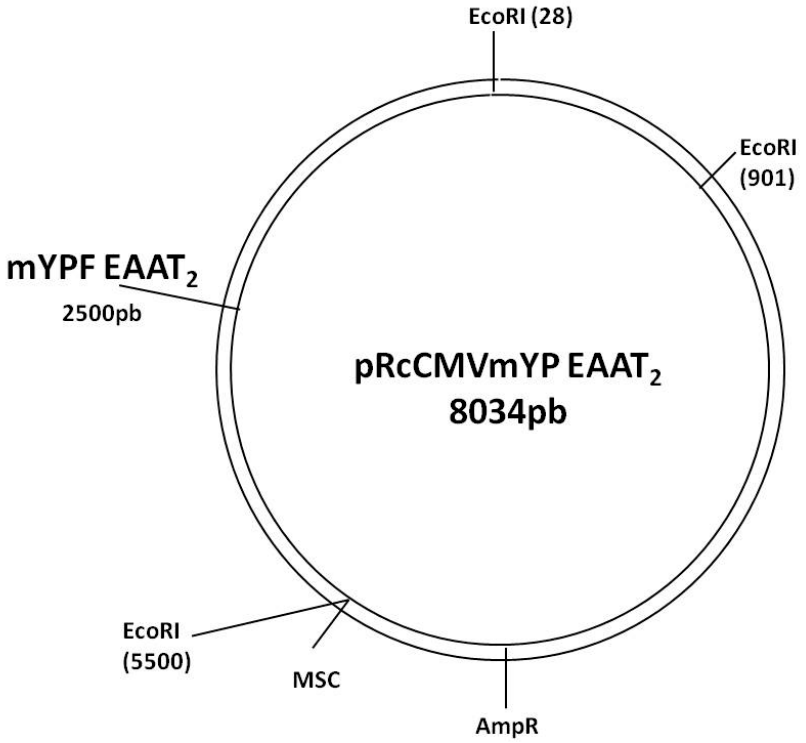

Figure 16: Plasmid DNA pRcCMVmYFPEAAT$_2$

Three different transfection protocols were probed to induce the plasmid expression: calcium phosphate transfection, electroporation transfection and lipofectamine transfection.

a. Calcium phosphate transfection

This method requires the preparation of the transfection buffers. For that, N, N-bis (2-hydroxethyl)-2-aminoethanesulfonic acid (BES) was obtained from Calbiochem-Behring, German; $CaCl_2$ was purchased from Sigma-Aldrich, USA. Stock solutions of 1 M $CaCl_2$ was prepared, filter through a polyethersulfone filter with a 0.22µm pore size (Millipore, Germany) and stored at room temperature. Then 2xBES-buffered saline (2xBBS) containing 50 mM BES, 280 mM NaCl and 1.5 mM Na_2HPO_4 was prepared, filter again and stored at room temperature. The pH was adjusted at 6.95 with HCl at room temperature.

The day before of the transfection, cells were seeded at a density of $5x10^4$ cells per cm^2 and incubated overnight in the suitable medium and conditions. Then 124 µl of H_2O, which contained 15 µg of plasmid DNA, was mixed with 41 µl of 1M $CaCl_2$ and 165 µl 2xBBS and the mixture was incubated for 20 min at room temperature. Calcium phosphate-DNA solution was added dropwise to the plate of cells, and the mixtures were swirled gently and incubated for 15 to 24 h at 35ºC under 4% CO_2. After this time, the medium was removed and the cells were rinsed twice with PBS and once with PBS-EDTA and split with trypsin (0.25% trypsin-EDTA).[310]

A little percentage of transfected cells with this method can integrate the gen properly. To select the stably transfected cells, the gentamicin (G418) (Gibco-Invitrogen, USA) was used. Then, the transfected cells were split and planted at density (1x104) into $10cm^2$ dishes 24 h prior to selection. Cells were selected for 2 to 3 weeks in growth medium containing 1 mg/ml of G418, except the second day of selection, in which G418 concentration was 1.2 mg/ml.

b. Electroporation transfection

Electroporation of cells were performed according to the optimized protocols provided by the manufacturer (Amaxa Biosystem, Germany). Cells were detached by incubation in 0.25% trypsin-EDTA (Gibco-Invitrogen, USA) and centrifuged at 800 rpm for 5 Minford electroporation, the cells were counted and resuspended in 100 µl of Human MSC Nucleofector Solution (Amaxa Biosystem, Germany) at a concentration of $1x10^6$ cells/lathe cell suspension was mixed with 4 µg of plasmid DNA in a sterile electroporation cuvette (Amaxa Biosystem, Germany) and pulsed with the U-23 program. Immediately after, the cells were transferred into pre-warmed fresh medium in 6-well plates preteated with poly-D-lysine hydrobromide (Sigma-Aldrich, USA).

c. Lipofectamine transfection

Lipofectamine 2000 (Gibco by Life Technologies, USA) was used as the lipid vehicle. For harvesting transfected cells with high efficiency and low cytotoxicity, different concentration of DNA, cell density and lipofectamine was tested in order to optimize transfection protocol. For this purpose, 24 h before transfection, the cells were planted at a density of $0.5–2×10^5$ cells per cm^2 on 24 well plates and maintained in growth medium, which was replaced with medium without antibiotics and antimycotics before of the transfection. Different amounts of reagent Lipofectamine (1-5 µl) and plasmid DNA (1-5 µg) were tested. Each amount of Lipofectamine was dissolved in Opti-MEM (Gibco-Life Technologies, USA) without serum to a final volume of 50 µlathe same procedure was done for the plasmid DNA (pDNA). The pDNA-Lipofectamine complexes were prepared by combining the 50 µl of the Lipofectamine 2000 solution with the 50 µl of pDNA solution. The mix was left to stand at room temperature for 20 min. The solution was stable for 6 h at room temperature. Meanwhile, the medium antibiotics and antimycotics in each well of the cells cultures were changed to Opti-MEM (without serum). The 100 µl complex solution was added to each well

and mixed gently by rocking the plate back and forth. The cells were incubated for 18-48 h at 37°C under 5% CO_2. After lipofection, the medium was replaced with growth medium.

6.2.2. Viral infection: rAAV

In addition to transfection, the cell-induction EAATs expression was tried with recombinant adeno-associated virus (rAAV) as well.

The first step in the production of rAAV is the design of the constructs. For that, we must take into account that rAAV has a packaging capacity of ~4.7Kb. The length of two ITRs (inverted terminal repeat sequences) of rAAV is about 0.2-0.3Kb in total and the foreign DNA that could be introduced between these ITRs should be <4.4Kb. In addition, when the length of inserted DNA between the ITRs is close to the maximal allowed, i.e., 4-4.4Kb, the packaging efficiency decreases significantly. For instance, for gene over-expression from cDNA, since the CMV-poly(A) element is about 1 Kb, therefore the maximal allowable cDNA length is about 3Kb. Considering this, it is expected to be package the YFP-$EAAT_2$ construct, whose length is 2.5Kb, to a size which is very close to the limit of packaging. Due to this, another short construct was also designed. The short construct consisted of the $EAAT_2$ sequence and a region encoding the Ha-tag sequence, thus the size of this construct being shorter and therefore providing an expected better efficiency of packaging.

1. Long construct rAAV: YFP-$EAAT_2$

We used the plasmid pRcCMVmYFPEAAT2 contain the gen EAAT2 linked in tandem to the gen YFP. The plasmid was digested by EcoRI (New England BioLabs, UK) to create two fragments: the YFP-EAAT2 sequence (2500 bp) and the backbone of the vector (5500 bp). Equal amounts of digested DNA were electrophoresed on 0.75% agarose gels to test the

digestion was successful. The gel was stained with SYBR Safe DNA (Life Technologies, USA) gel stain (1:10,000 dilution) for 15 min, and then viewed using the blue-light transilluminator (Bio-Rad, USA). The insert DNA YFP-EAAT2 were excised from the gels and purified using the Nucleospin Gel and PCR clean up (Macherey-Nagel, Germany) according to the optimized protocols provided by the manufacture. The insert was cloned in the vector viral ccCMVm (kindly donated by Prof. A. Baumann), which in the multiple cloning site contained restriction sites as XabI, HindIII, EcoRV, EcoRI, BamHI. The ccCMVm was linearized by digestion with the enzyme EcoRI (New England BioLabs, UK). The linearized vector was subjected to an electrophoresis process similar to that performed in the fragment YFP-EAAT2. Likewise, the vector ccCMVm was excised from the gel and purified with the same protocol mentioned above. Besides the vector was submitted to dephosphorylate using the Rapid DNA Dephos & Ligation Kit (Roche, Switzerland), thereby preventing the viral vector becoming circular by binding of sticky ends. After that, the ligation of insert into linearized vector ccCMVm was done with the Rapid DNA Dephos & Ligation Kit (Roche, Switzerland) following the protocol provided by the manufacture. Competent cells were transformed with the mix of ligation (Table 3) and planted on a selective medium for growth. Only cells containing the insert cloned in the vector ccCMVm formed colonies, which were picked and grown in liquid culture. The purification of the DNA from the culture was performed following the protocol described in the kit NucleoSpin Plasmid (Macherey-Nagel, Germany). The purified DNA was digested with the enzymes EcoRI (New England BioLabs, UK) to verify that the insert had the expected size and with Sami (New England BioLabs, UK) and Audi (New England BioLabs, UK) to corroborate that cloning of the insert into the viral vector was performed in the right direction.

Ligation 1	Ligation 2	Ligation 3
0 µl DNA insert	4 µl DNA insert	4 µl DNA insert
2 µl DNA vector	0 µl DNA vector	2 µl DNA vector
2 µl DNA dilution Buffer 5x	2 µl DNA dilution Buffer 5x	2 µl DNA dilution Buffer 5x
6 µl Water	4 µl Water	2 µl Water
10 µl T4 DNA ligation buffer	10 µl T4 DNA ligation buffer	10 µl T4 DNA ligation buffer
1 µl DNA lipase	1 µl DNA lipase	1 µl DNA lipase

Table 3: Mix of ligation

2. Short construct rAAV: Ha-tag-$EAAT_2$

The fragment YFP-EAAT2 was obtained with the same procedure as previously was described. Due to the design of this construct, only the gen $EAAT_2$ was necessary, which was linked to the gen Ha-tag. For that, $EAAT_2$ amplification was carried out using 2 primers: 5´accatctagaccaccatggcatctacggaaggtgc 3´ (contains a Kozak sequence, a recognition sequence of the enzyme XbaI and free sequence) and 3´accagaattcggcatagtcggggacgtcatagggatatttatcacgttccaaggt ttc 5´include the Ha-tag sequence, a recognition sequence of the enzyme EcoRI and a free sequence ended in cytosine, both of them were acquired from Applied Biosystems, USA. Amplification process was performed using the kit T4 DNA Polymerase (New Englands BioLabs, UK) and according to the following protocol: (1) polymerase activation for 2 min at T=95ºC, (2) denature for 20s at T=95ºC, (3) annealing for 10s at T=56ºC and (4) extension for 4s at T=70ºC, the steps 2-4 were repeated in 30 cycles. The PCR product was submitted to an electrophoresis, excision and purification process similar to that described above. The purified PCR fragment was digested with the restriction enzymes XbaI (New Englands BioLabs, UK) and EcoRI (New Englands BioLabs, UK), electrophoresed, excised and purified according to the previously described protocols.

The PCR fragment was cloned into the viral vector scCMVm (Figure 17), which was necessary linearized. For that, the viral vector was digested with EcoRI (New Englands BioLabs,

UK) and XbaI (New Englands BioLabs, UK) enzymes. The product of the digestion was subjected to electrophoresis, excised and purified following the same protocol as in the previous section.

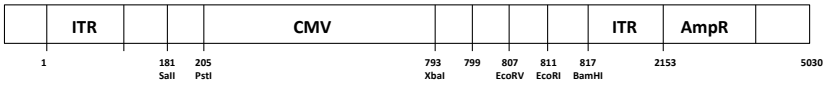

Figure 17: Viral vector scCMVm

The ligation of construct into the vector, the transformation of competent cells, the selection of a clone and purification of DNA was performed following the protocol described in previous section. To verify that insertion of the sequence $EAAT_2$-HaTag in the vector was successful, the following controls of restriction were conducted: EcoRI, XbaI, SmaI and AhdI (New Englands BioLabs, UK).

- Production and purification of recombinant adeno-associated viruses (rAAVs)

The most commonly used method for production of AAV vectors in research laboratories consists of a 2 or 3 plasmid transfection of adherent HEK cells. The triple transfection method described below uses the plasmid with the gene of interest, plasmids of different serotypes and helper plasmid providing the adenoviral gene products necessary for replication and packaging. The protocol includes the processes for transfecting of cells with the 3 plasmids, harvesting the crude cells lysate, preparing the lysate for viral vector purification by iodixanol gradient and the titration by real-time PCR of the viral genome.

- Production of AAV vector by transient transfection

The day before the transfection, $1x10^7$ HEK cells per 14.5 cm^2 dish were seeded out in a total volume of 25 ml complete medium. At a time point of 2 h before transfection, the medium was replaced with fresh complete medium. The HEK cells were transfected using the calcium phosphate-transfection method[310] and the next transfection cocktail: 1

ml $CaCl_2$ (250mM), 7,5 µg helper plasmid pRC, 22,5 µg adeno helper plasmid pXX (both plasmid were kindly provided by Prof. Dr. A. Baumann), 7.5 µg virus plasmid (pAAV-YFP-$EAAT_2$ or pAAV-Ha-Tag-$EEAT_2$) and 1ml HBS 2x (50mM HEPES, 280 mM NaCl, 1.5 mM Na_2HPO_4, pH 7.12). After 24 h of the transfection, the medium was changed and HEK cells were maintained at 37ºC, 5% CO_2 and 95% of humidified atmosphere for 48h. At this point, the cells were harvested. To do this, the medium was removed and 10 ml PBS M/K (sterile PBS, substituted with 1mM $MgCl_2$ and, 2.5 mM KCl) was placed per dish. The cells were collected by scraping and the cell suspension was transferred to a falcon tube, which was centrifuged at 300g for 5 menthe supernatant was removed and the pellet was resuspended in a lysis buffer (NaCl 150 mM, Tris/HCl 50 mM, pH 8.5) and incubated at room temperature for 10 min. Immediately, the cell lysate was subjected to three cycles of freezing in liquid nitrogen and thawing at 37ºC. Finally, 2 µl benzonase (25 kU/µl/ml) was added to the cell lysate and incubated at 37ºC for at least 30 menthe, the cell homogenate was centrifuged for 30min at 5000g and the clarified supernatant was collected.

- Purification of rAAV vectors by iodixanol gradient sedimentation

In order to purificate the rAAV suspension, a iodixanol gradient was performed by filling the volume of each iodixanol solution (15%, 25%, 40% and 60%) in a ultra-centrifugation tube (Polycarbonate, 26.3 ml, Beckmann Coulter) with a peristaltic pump. The supernatant obtained in the previous section formed the uppermost layer of the iodixanol gradient until the tube was filled to the top. The tube was ultracentrifuged 120 min at 60,000 rpm in a Beckman 70 Ti Rotor. To complete the process, the 40% iodixanol solution (clear band, contains the virus particles) was transferred with a syringe connected to a 40 mm canula to a fresh tube and was frozen at -80ºC.

- Determination of rAAV titers by real-time PCR

Viral genomes were isolated from purified virus for titer determination. The genetic material was isolated using the Dneasy Blood & Tissue Kit (Qiagen, Germany), according to the manufacturer instructions. The titer values were determined via qPCR analysis. For this, the QuantiTect SYBR Green PCR (Qiagen, Germany) was used for qPCR reactions. The qPCR reaction mixture, a total of 18 µl was composed as indicated Table 4.

Component	Volume	
SYBR Green	10 µl	
Primer 1 (10pmol/ µl)	1 µl	To 18 µl qPCR reaction
Primer 2(10pmol/ µl)	1 µl	mixture:add 2 µl of sample
H_2O	6 µl	in LightCycler capillary
Total	18 µl	

Table 4: qPCR reaction mixture

The qPCR running protocol is summarized in Table 5.

Program	Step	Tª	Duration	Cycles	Detection
Pre incubation	Denaturing	95ºC	10min	1	-
Amplification	Denaturing	95ºC	10 sec		-
	Annealing	62ºC	15 sec	50-80	-
	Synthesis	72ºC	15 sec		Single
Melting curve	Denaturing	95ºC	1 sec		-
	Annealing	62ºC	15 sec	1	-
	Melting	65-95ºC	0.1ºC/sec		Continuous
Cooling	-	40ºC	30 sec	1	-

Table 5: qPCR running protocol.

6.2.3. Infection of cells

a. Transduction with rAAV-GFP of different serotypes in cells and the best MOI (multiplication of infection) determination

Cells were plated at $5x10^4$ cells/well onto a 24 well plate and cultured at 37ºC in an atmosphere containing 5% CO_2 for 24 h before rAAV infection. A total of 7 serotypes was tested (rAAV1, rAAV2, rAAV4, rAAV5, rAAV6, rAAV8 and rAAV9), all of them donated by Prof. A. Baumann (Germany). The viral stocks were used at 3 MOI gradients: $5x10^5$, $2.5x10^5$ and $4x10^4$vp/cell. Each dilution was performed in triplicate. A no-viral well and iodixanol 40% well were included as negative controls. Two days later, after infection, the medium was replaced with complete medium. The YFP expression was analyzed 5 days after infection using fluorescence microscopy and FACS analysis.

b. Infection with rAAV-YFP-$EAAT_2$ (serotypes 2, 6) and rAAV-Ha-tag-$EAAT_2$ (serotypes 2, 6) in MSC and HEK cells

Cells ($5x10^4$cells/well) were seeded onto a 24 well plate for 24 h before rAAV infection. The cells were transduced with the next MOI gradients: $1x10^{10}$, $5x10^9$, $1x10^9$ vp/cell of rAAV2YFP-$EAAT_2$, rAAV2Ha-tag-$EAAT_2$, rAAV6YFP-$EAAT_2$ and rAAV6Ha-tag-$EAAT_2$ in triplicate. Uninfected cells were used as a negative control. Virus infection was performed for 48 h and the medium was changed. Seven days after infection, YFP and Ha-tag expression was analyzed by fluorescence microscopy and FACS analysis.

6.3. Analysis of YFP and Ha-tag expression

To confirm the integration and the expression of the $EAAT_2$ used in the transfection and viral infection, YFP and Ha-tag (used as gene expression reporters) were analyzed by flow cytometry and fluorescence microscopy.

6.3.1. Flow cytometry

We used flow cytometry techniques for the analysis of the YFP expression in transfected and infected cells. Cells were dissociated with 0.25% Trypsin-EDTA (Sigma-Aldrich, USA) and centrifuged at 800 rpm during 5 min to remove the Trypsin-EDTA. Subsequently, cells were washed with PBS (Life Technologies, USA) and centrifuged at 800 rpm during 5 min to form a cell pellet, which was finally resuspended at concentration of $1x10^5$ cells per 100µl. For the analysis, 30000 gated events (cells) were collected. A cell was counted as positive for YFP expression when its fluorescence was higher than the threshold settings of the negative control sample (non-fluorescing cells). For the cytometry analysis we used a FACSAria IIu analyzer (BD, USA), and the PC FACSDiva software program (BD, USA). Cell counts were always expressed as percentage.

In case of the Ha-tag-EAAT2 infected cells, $1x10^6$ cells, infected which the virus Ha-tag-$EAAT_2$ (serotypes 2, 6) were detached whit 0.25% Trypsin-EDTA and centrifuged at 800 rpm for 5 min the cells were washed and stained by incubation (30 min) with Anti-Ha-tag-Fluorescein clone 3F10 (20 µl per $1x10^6$ cells, Roche, Switzerland) antibody at 2-8ºC during 30min. Then, cells were suspended in 200 µl of PBS and the analysis was performed. The unlabelled cells were used as a negative control. The analysis was done using a BD FACS Aria I (BD Bioscience, USA) and data were analyzed with the use of FACSDiva software (BD Biosciences, USA).

6.3.2. Fluorescence microscopy

The cells were observed under inverted microscope (Olympus IX51) during the infection and the efficiency of YFP expression was detected using a fluorescence microscopy. For analysis of the Ha-tag sequence by fluorescence microscopy, cells were planted at a density of $2x10^4$ cells on glass coverslips, which were previously treated with 0.1

mg/ml poly-D-lysine hydrobromide (Sigma-Aldrich, USA). The next day, the medium was removed and the cells were rinsed in PBS 3 times. Following on, the cells were fixed in 4% PFA solution methanol free (Thermo Scientific, USA) for 5 min at room temperature. After that, the washing process described above was repeated. Then, the cells were incubated with 0.5% BSA (GE Healthcare, UK) in PBS for 30 min, in order to block unspecific antibody binding sites. Then, the washing process was repeated and a rat monoclonal antibody (Roche, Switzerland) against the sequence Ha-tag was used at a dilution 5 µg/ml in 0.5% BSA and PBS for 24 h at 4ºC. After this time, the washing process was performed and cells were incubated with 1:6000 Hoescht (Invitrogen, USA) for 5 min. Afterwards a coverslip was mounted. For this purpose, the coverslip was removed from the well and the edge of the coverslip was touched with a paper to aspirate as much buffer as possible. Then, ensuring that the place coverslip with the cells were side down, a drop of Aqua Polymount (Polysciences, USA) was added and kept in the dark at room temperature for 2 h and after the samples were stored at 4ºC for further analysis.

Images were captured randomly using Nikon digital camera.

6.4. Analysis of $EAAT_2$ expression in cells

6.4.1. Immunostaining of $EAAT_2$ in MSCs and HEK cells

Cells were planted at a density of $2x10^4$ on glass coverslips, which were previously treated with 0.1 mg/ml poly-D-lysine hydrobromide (Sigma-Aldrich, USA). The next day, the medium was removed and the cells were rinsed in PBS 3 times. Following on, the cells were fixed in 4% PFA solution methanol free (Thermo Scientific, USA) for 5 min at room temperature. After that, the washing process described above was repeated. Then the cells were incubated with 0.5% BSA (GE Healthcare UK) in PBS for 30 min, in order to

block unspecific antibody binding sites. Then, the washing process was repeated and a mouse primary monoclonal antibody (Millipore, USA) against the protein $EAAT_2$ (Millipore, USA) was used at a dilution 1:100 in 0.5% BSA and PBS for 24h at 4ºC. After this time, the washing process was performed and incubation with a biotinylated horse anti-mouse IgG antibody rat adsorbed (1:200, Vector Laboratories, USA) was done, followed again by a 10 minute wash, applied 3 times. Next, a 1:100 dilution of both avidin and biotin (Vector Laboratories) in PBS was made and used for incubation for 30 min. After, 3 washes of 10 min with PBS, samples were incubated with dylight 594 streptavidin 1:500 (Vector Laboratories, USA) for 30 min. After another 3 step washes of 10 min, cells were incubated with 1:6000 Hoescht (Invitrogen, USA) for 5 min. Afterwards a coverslip was mounted to determine whether $EAAT_2$ expression colocalize with the transfected cells with YFP, the colocalization was analyzed by means of a confocal microscope (LEICA AOBS-SP5X).

6.5. Characterization of transfected MSCs

The infection and transfection processes described above could induce chances in MSC phenotype, as well as the capacity associated with MSCs to secrete growth factors and their angiogenic ability. Because of this, the following experiments in order to verify that MSCs maintains their characteristics were realized.

6.5.1. Flow cytometry of MSCs

To confirm that transfected MSCs (cells which were expressed YFP) did not lose the MSC phenotype after the experimental procedure, cells were analyzed by flow cytometry analysis. For that, specific membrane makers of rMCSs as CD90, CD73 and CD45 were analyzed.

Cells ($1x10^5$) were washed and stained by incubation (15 min) with CD90-PerCP-Cy5 (5 µl per $1x10^5$ cells,

Immunostep, Spain), CD73-APC (1 µl per $1x10^5$ cells, Immunostep, Spain) and CD45-PE (2.5 µl per $1x10^5$ cells, BD Pharmigen, USA) antibodies. Then, cells were suspended in 100 µl of PBS and the analysis was performed. The unlabelled MSCs were used as a negative control and the phenotype of MSC was characterized as CD90+/CD73+/CD45-. The analysis was performed using a BD FACS Aria I (BD Bioscience, USA) and data were analyzed with the use of FACSDiva software (BD Biosciences, USA).

6.5.2. *In vitro* matrigel angiogenesis assay.

To determine the angiogenic capacity of the transfected MSCs (a specific characteristic of these cells), a tube formation assay was performed in transfected and non-trasnfected cells.

Matrigel reduced growth factor (BD Biosciences, USA) was used as a substrate to assess tube formation capacity as an *in vitro* measurement of functional angiogenesis, in MSC control and transfected MSC. Standard 24-well plates were coated with 200 µl of cold Matrigel and allowed to solidify at 37ºC for 30 min. Afterwards, outgrown MSC were added onto matrigel-coated wells at seeding of $1x10^4$ per well in IMDM (Gibco-Invitrogen, USA) supplemented with 5% Fetal Bovine Serum (FBS, Gibco-Invitrogen, USA), 1% antibiotic solution (penicillin/streptomycin; Gibco-Invitrogen, USA) and 1% antimycotic solution. Cells were incubated for 12 h at 37ºC, 5% CO_2 and in a humidified atmosphere of 95%. After removal of the medium, the cells were fixed in 4% PFA and images were captured using an inverted microscope (Olumpus IX51). The tube formation was assessed by counting the number of circular structures (rings) and number of branching points (tube joints). Five random fields were measured for each well.

6.5.3. Vascular endothelial growth factor (VEGF) determination:

VEGF, a specific growth factor produced by MSCs was also analyzed to determine that artificial $EAAT_2$ expression does not affect to the MSCs properties.

VEGF concentrations of MSC control and transfected MSC were measured with a Quantikine VEGF ELISA kit (R&D Systems, USA) following the manufacturer's protocol. VEGF values are corrected for the amount of total cell protein calculated by Bradford (Bio-Rad, USA) techniques.

6.6. *In vitro* test of toxicity

For assessing the cellular mortality caused in cells after transfection and infection, the LDH assay and proliferation rate were performed.

6.6.1. Lactate dehydrogenase (LDH) assay

Supernatants from last 24 h (fresh medium incubation) were collected in Eppendorf tubes. A negative control of lysated cells was also included (death control) following manufacturer protocol. After a mild centrifugation of the supernatants, 75 µl were mixed in a 96 well plate with 150 µl LDH reagents following the manufacturer protocol (Lactate Dehydrogenase Assay Kit Sigma-Aldrich, USA). After 20 min incubation, the plate was read on Synergy2 (Biotek, USA) at 490 nm. To calculate the viability rate respect to control, next equation was applied.

$$Viability[control] = \frac{LDH_{lysed} - LDH_{exposed}}{LDH_{lysed} - LDH_{control}} \cdot 100$$

6.6.2. Proliferation rate

To determine the proliferation rate, total cell count was performed with Trypan Blue staining and a Neubauer chamber.

6.7. Characterization the functionality of the $EAAT_2$

To determine the functionality of the $EAAT_2$-induced expression, a glutamate uptake assay was performed in both types of cells used, HEK and MSCs.

6.7.1. Glutamate uptake assay

Uptake of radiolabeled glutamate was performed using a competitivity assay. Transfected cells (HEK and MSCs) with $EAAT_2$ were planted in triplicate at $1.5x10^5$ on 24-well tissue culture plates treated with poly-D-lysine hydrobromide (Sigma-Aldrich, USA). Non-transfected cells were used as negative control and astrocytes were employed as positive control. After 24h, the medium was aspirated and cells were washed 3 times with 250 µl PBS buffer at room temperature. Then 500 µl PBS buffer, supplemented with 13 nM L-[^{3}H] glutamate (1 µCi/ µl; Sigma-Aldrich USA; specific activity=51.1 Ci/mmol) and various concentrations of glutamate (1µM, 10 µM, 50 µM, 100 µM, 250 µM, 500 µM, 1 mM and 10 mM) was added to each well, and the plate was incubated at 37ºC for 10min. After this time, the plates were placed on ice and cells were washed 3 times with ice-cold PBS. Through microscopy it was verified that the cells continued to be fixed to the bottom of the well, and the cells were lysed with 200 µl of 0.2 M NaOH for 4 h in shaking. After four h, 50 µl of cell lysate was transferred to a 96-well multiplex plate and 150 µl of Optiphase buffer were added to each well. The multiplex plate was shaken for 30min at RT. Cell-associated radioactivity was determined in cell lysates by scintillation counting (PerkinElmer, Germany) and the total

protein content in lysates was determined by the Bradfor assay (Bio-Rad, USA). The results were expressed in DPM per µg of cellular protein.

To determine the specificity of glutamate uptake, two selective inhibitors of $EAAT_2$, DHK and TFB-TBOA, (Tocris, Bioscience, USA) were employed. Both inhibitors were used individually and jointly at the next concentrations: 300µM (DHK) and 500µM (TFB-TBOA)[311]. For doing the assay, the cells were prepared as described above and the medium was removed. Three washes were performed with PBS and the cells were incubated with inhibitors for 10 min at 37ºC. After this time, the labeled and unlabeled glutamates, at the same concentrations described above, were added. The protocol employed was the same as that made in the previous section.

6.8. *In vivo* experiments

With the aim to test the efficacy of $EAAT_2$ transfected cells on blood glutamate lowering and their protective effect on ischemic damage, cells were administered in ischemic animal model and their effect were compared with non-transfected cells and with oxaloacetate, used a positive control of blood glutamate reduction. Control group was treated with saline.

6.8.1. Timeline of the study

This study was divided into two steps: a dose-response study and protective study.

a. Dose-response study

Previously a dose-response study was performed in healthy animals, with the aim to determine the optimal cell dose able to induce a reduction in serum glutamate levels. For that, the following experimental groups were done:

a) Control group (n=3): treated (i.v.) with 1ml of PBS.
b) Oxaloacetate group (n=3): treated (i.v.) with 1ml of 3.5 mg/100g.
c) $3x10^6$ HEK cells non-transfected cells (n=3), defined as HEK- (1 mL).
d) $3x10^6$ HEK cells transfected with $EAAT_2$ (n=3), defined as HEK+ (1 mL).
e) $3x10^6$ and $9x10^6$ MSCs non-transfected (n=3), defined as MSCs- (1mL).
f) $3x10^6$ and $9x10^6$ MSCs transfected with the $EAAT_2$ (n=3), defined as MSCs+ (1 mL).

To determine the effect of the treatments on blood glutamate, blood samples (500 µl) were taken (from vein tail) under basal conditions (before treatment injection), and 1, 2, 3, 5, 4, 6 and 24 h after treatment injection. Treatments were administered through the jugular vein in a bolus during 10 wingover treatment administration, the animals were maintained under sevoflurane 1% in O_2:N_2O/30:70.

b. Protective study

In order to evaluate the protective properties of the cellular treatments in an animal model of ischemic stroke, 8 groups were studied:

a) Control group (n=6): treated (i.v.) with 1ml of PBS.
b) Oxaloacetate group (n=6): treated (i.v.) with 1ml of 3.5mg/100g.
c) HEK- group (n=6): treated (i.v.) with 1ml of $3x10^6$ control HEK- cells.
d) HEK+ group (n=6): treated (i.v.) with 1ml of $3x10^6$ HEK+ cells.
e) MSC- group (n=6): treated (i.v.) with 1ml of $3x10^6$ HEK- cells.
f) HEK+ group (n=6): treated (i.v.) with 1ml of $9x10^6$ HEK+ cells.
g) MSC- group (n=6): treated (i.v.) with 1ml of $9x10^6$ HEK- cells.

To determine the capacity of the treatments to induce a blood glutamate reduction and a protective effect, serum glutamate levels, infarct volume and functional deficit were measured in the experimental animals. Treatments were administered immediately after reperfusion (45 min after occlusion). Serum glutamate concentration was determined under basal conditions (before surgery), and 1, 2, 3, 4, 5, 6 h after treatment administration and 1, 7 and 14 days after ischemia for further glutamate determinations. Infarct volume was determined during occlusion (to determine the basal lesion before treatment administration), 1, 7 and 14 days after ischemia. Sensorimotor test (Cylinder test and Modified Neurological Severity Scores; mNSS) was performed under basal conditions (1 day before surgery) and 14 days after ischemia. Finally, on the 14^{th} day, animals were transcardially perfused and their brains processed as described previously for future histology analysis. Experimental protocol can be observed in Figure 18.

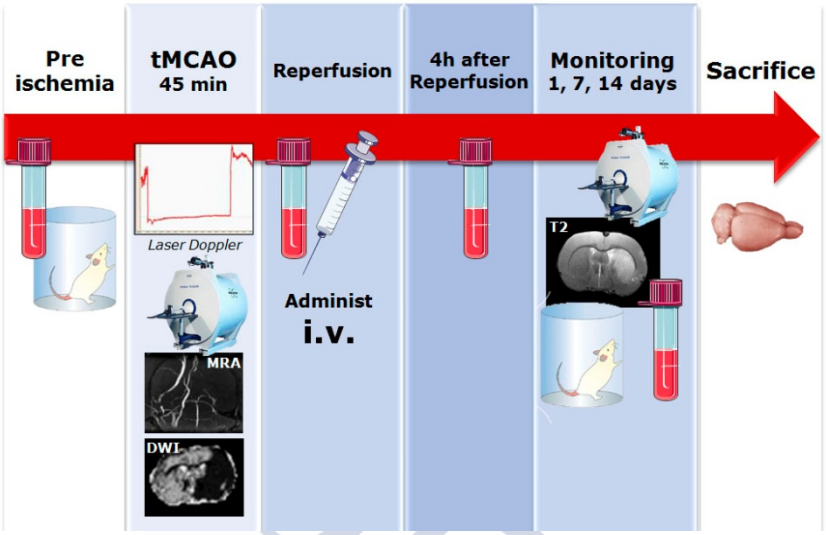

Figure 18: Timeline evaluation of the therapeutic benefits of the different treatments in an animal model of ischemic stroke.

6.8.2. Animal procedures

a. Animal management

In this study we have used 202 male Wistar rats (Harlan Laboratories, Barcelona, Spain) with a weight of 300±25 g. Of the total number of Wistar animals, 72 animals were discarded for not meeting the inclusion criteria and 11 animals died. Animals were kept at controlled conditions of temperature (22±1ºC) and humidity (60±5%), with a 12/12 h light/ dark cycle for a period of one week prior to surgery and up to 14 days after surgery. The rats were granted free access to food (commercial chow pellets) and tap water. For surgery and MRI, rats were anesthetize with sevoflurane (3% in 70% N_2O and 30% O_2). Rectal temperature was monitored and maintained at 37±0.5ºC with a feedback controlled heating system (1025 system, SA Instruments). At the end of the procedures animals were sacrificed under deep anesthesia (8% sevoflurane). Experimental protocols were approved by the local Animal Care Committee according to

the Spanish and European Union (EU) rules (86/609/CEE, 2003/65/CE, 2010/63/EU, RD 1201/2005 and RD53/2013).

b. Model of focal transient ischemia in rat

Transient focal ischemia was induced in rats by intraluminal occlusion of the middle cerebral artery (tMCAO), performed as previously described[305] with several modifications. In order to monitor the relative cerebral blood flow (CBF) during the surgery, a laser-Doppler flow probe (tip diameter 1mm) attached to a flow meter (PeriFlux 5000; Perimed AB) was located over the thinned skull, and over the middle cerebral artery territory (approximately 4mm lateral to bregma). Under a surgical microscope, common carotid, external carotid, and the internal carotid arteries of the left side were dissected from connective tissue through a midline neck incision. Left external carotid and pterygopalatine arteries were separated and tied with 6-0 silk sutures, showing a CBF reduction of 20%, measured by laser Doppler. A silicon rubber-coated monofilament (403512PK5Re; Doccol Corporation, USA) was inserted through the external carotid into the left common carotid artery and advanced into the internal carotid from the bifurcation to occlude the origin of the Macbeth vertebral arteries remained intact in all surgical procedures. Once the artery was occluded, determined by Doppler signal reduction, the animals were carefully moved from the surgical bench to a Magnetic Resonance (MR), with the aim to determine the basal ischemic lesion by means of apparent diffusion coefficient (ADC) maps. Angiography imaging was also performed to confirm the artery remained occluded over the MR study. After basal MR analysis, animals were returned to the surgical bench and Doppler probe was repositioned. Reperfusion was performed 45 min after the occlusion onset. Animals were subsequently randomized in experimental groups performed, by using computer-generated random numbers.

c. Inclusion criteria

Only animals with a cerebral blood reduction (CBR) higher than 60% and with reperfusion after occlusion, MCA occluded on MR angiography and an infarct volume during the occlusion between 35-45% of the hemisphere were included in this study.

6.8.3. Blood serum determinations: glutamate analysis

Venous blood was collected from the tail vein at different times which are specified in the section 6.8.1. Blood samples were collected in test tubes (BD Microtainer), centrifuged at 3,000 rpm for 7 min; serum was removed and immediately frozen and stored at –80°C. Serum glutamate concentration was determined by means of Glutamate Assay Kit (Abnova, Taiwan) following the manufacturer's technical specifications.

6.8.4. Treatment administration

Animals were intravenously injected into the jugular vein. First, animals were anesthetized with sevoflurane 3% in O_2:N_2O/30:70. Then a 0.5 cm incision was made in the animal´s neck just above the clavicle 1cm to both left and right of the midline. Subcutaneous fat was cut out, and the jugular vein was exposed. A 30g needle was used for every injection after withdrawal, the puncture is rapidly closed to preventing bleeding.

6.8.5. Functional test

In all animals, a battery of behavioral tests was performed before MCAO and 7, 14 days after MCAO by a researcher, who was blinded to the experimental groups. The battery of tests consisted of the Cylinder test and the Modified Neurological Severity Score (mNSS)[306].

a. Cylinder test

The Cylinder test was performed as described in the section.5.7.

b. Modified Neurological Severity Scores (mNSS)

One of the most common neurological scales used in animal studies of stroke is the modified neurological severity scores (mNSS Neurological function was graded on a scale of 0 to 12 (normal score, 0; maximal deficits core, 12). The mNSS is a composite of motor, sensory, reflex, and balance tests. In the severity scores of injury, 1 score point is awarded for the inability to perform the test or for the lack of a tested reflex; thus, the higher the score, the more severe is the injury. Table shows a set of the mNSS.

Placing rat on floor	
Normal walk	3
Inability to walk straight	1
Circling toward paretic side	1
Falls down to paretic side	1
Proprioceptive test (deep sensation, pushing paw against table edge to stimulate limb muscles)	
Posterior limb	1
Anterior limb	1
Raising rat by tail	
No flexion of forelimb	1
Head moved 10º to vertical axis within 30s	1
Lack of visual placing	1
Suspension of the half posterior of the body	
Turn to the side of the lesion	1
Maximum points	12

Table 6: One point is awarded for inability to perform the tasks or for lack of a tested reflex: 1-3, mild injury; 6-9, moderate injury; 9-12, severe injury.

6.8.6. Magnetic resonance studies

Magnetic resonance imaging studies were conducted on a 9.4 T horizontal bore magnet (Bruker BioSpin, Ettligen, Germany) with 20 cm wide actively shielded gradient coils (440mT/m). Radio-frequency transmission was achieved with a birdcage volume resonator; signal was detected using a four-element surface coil, positioned over the head of the animal, which was fixed with a teeth bar, earplugs, and adhesive tape. Transmission and reception coils were actively decoupled from each other. Gradient-echo pilot scans were performed at the beginning of each imaging session for accurate positioning of the animal inside the magnet bore.

a. Imaging protocol

Infarct size and angiography were assessed by magnetic resonance imaging. For this purpose, MRA and DWI-ADC during the occlusion, and MR T_2 on the 1st, 7th and 30th days after the ischemia described in 5.8.2 were employed.

b. Image analysis

All images were processed using ImageJ (Rasband WS, ImageJ, NIH, http://rsb.info.nih.gov/ij). Infarct volumes were determined from ADC maps and T2 maps by manually selecting areas of reduced ADC values or hyperintense T2 signal by a researcher blinded to the animal protocol.

6.9. Statistical analysis

All data are presented as the mean and standard error of the mean (mean ± SEM). One-way or two-way analysis of variance (ANOVA) followed by post-hoc Bonferroni evaluation was used for multiple groups to determine significant differences. Student's t-test was used to test the differences between two groups. Statistical significance was set at $*p<0.05$, $**p<0.01$ and $***p<0.001$. The statistical analysis

was conducted using PASW Statistics 18 for MAC (SPSS Inc., Chicago, CA, USA).

6.10. Summary procedure

In Figure 19 is described all experimental procedures necessary to obtain and characterize $EAAT_2$-cells used to test their effect on blood glutamate reduction and protection on ischemic animal model.

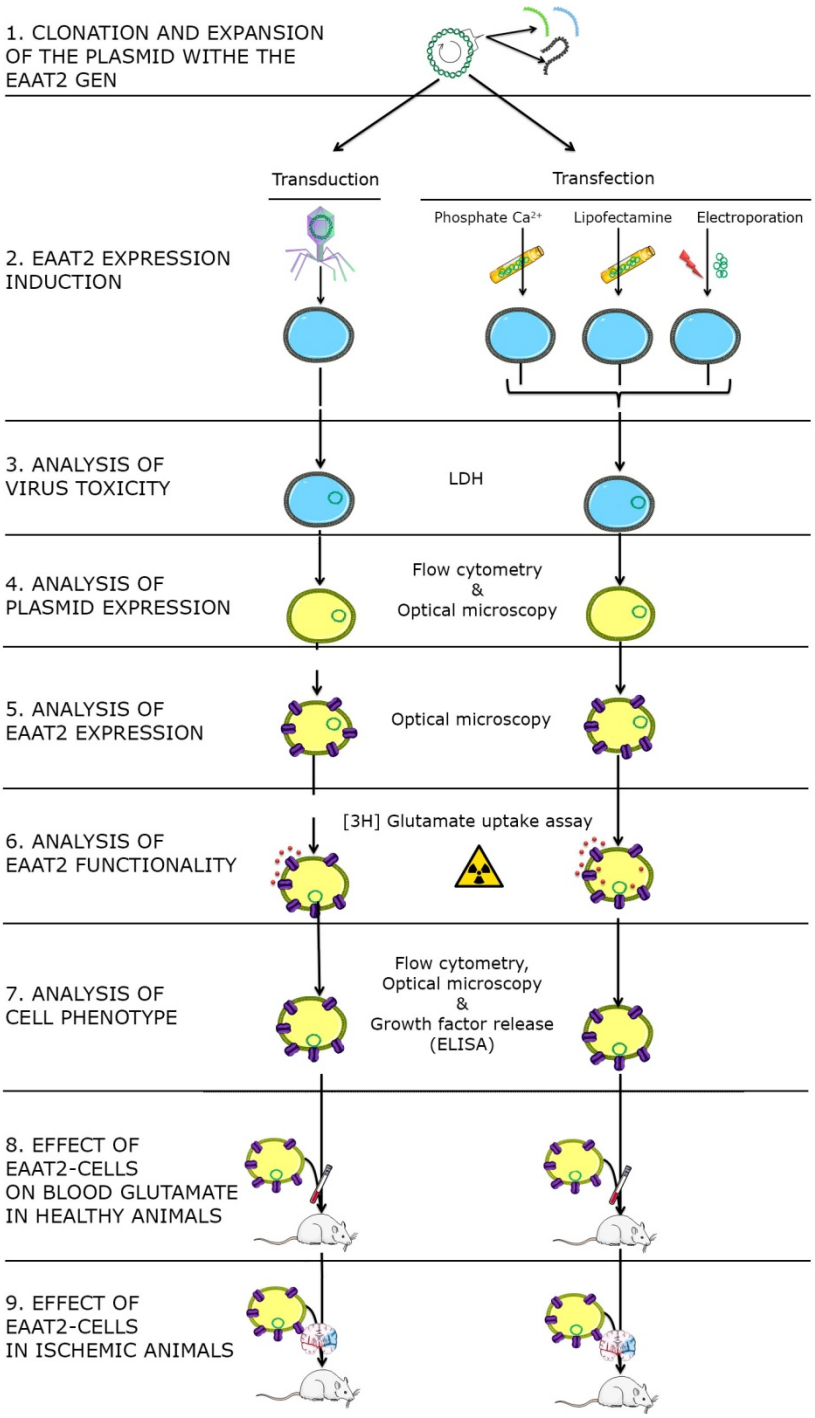

Figure 19: Summary of the experimental procedure.

USC
UNIVERSIDADE
DE SANTIAGO
DE COMPOSTELA

Results

USC
UNIVERSIDADE
DE SANTIAGO
DE COMPOSTELA

7.Section I: Analysis of protective effect of rGOT in ischemia

7.1. Animals included in the study.

A total of 119 animals were used in this study. Thirty-six animals were used in the rGOT1 dose–response study, six animals per group (six groups of treatments). In this study, no animal deaths were observed within the first 24 h after treatments administration. In the protective study, 60 animals were included, six animals/group (four groups in the spectroscopic study and other six groups in the non-spectroscopic study). Eighteen animals were excluded, 16 of them were not included because of unsuccessful MCA occlusion or reperfusion and 2 animals died 24 h after surgery (1 treated with saline and 1 treated with rGOT1). Finally, 5 animals were used as sham-operated control rats (sham) without MCAO.

7.2. rGOT1 dose-response study

7.2.1. Dose-response effect of oxaloacetate and rGOT1 treatments on serum glutamate concentration in healthy animals.

Administration of saline (control group) did not affect (p=0.373) the basal concentration of glutamate during 24 h after the i.v. administration (Table 7 and Figure 20A), demonstrating that the surgical procedure did not interfere with the serum glutamate concentration. Injection of glutamate (15 mM) induced a significant (p<0.05) increase in serum glutamate concentration 1 h after administration (Table 7 and Figure 20B). Basal concentration was normalized 3 h after treatment administration. This effect shows that the administration of glutamate in healthy

animals could be used to simulate the increase in serum glutamate, a hallmark biochemical parameter after ischemia.

	Saline (A)	Glutamate 15mM (B)
Basal	160±15	150±23
1h	155±23	196±27
2h	151±30	168±22
4h	158±18	152±17
6h	162±22	145±23
24h	150±20	156±14

Table 7: Blood glutamate levels after i.v. administration of (A) saline and (B) Glutamate (15mM).

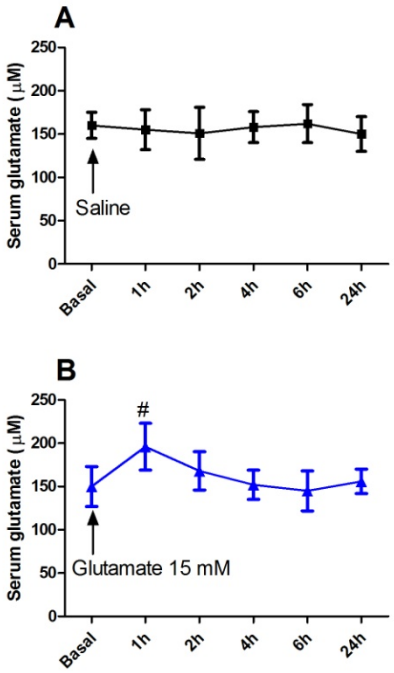

Figure 20: Blood glutamate levels after i.v. administration of (A) saline and (B) Glutamate (15mM).

On the basis of previous reports where rGOT1 has been used to study other pathologies, we started with a dose of 6.44 µg/100g to analyze the capacity of the enzyme to metabolize serum glutamate. Administration of 6.44 µg/100g of rGOT1 induced a reduction (p<0.01) (Table 8 and Figure 21A) in

serum glutamate concentration with respect to the maximum increase observed after glutamate injection. The maximum effect appeared between 2 and 4 h after administration of treatment. A higher dose of 12.88 µg/100g rGOT1 induced a robust reduction (p<0.01) in serum glutamate concentration (Table 8 and Figure 21B). Similar to the previous dose, the maximum lowering effect appeared between 2 and 4 h after administration of treatment; however, in this case, the capacity to reduce serum glutamate concentration was much higher. Administration of rGOT1 25.76 µg/100g induced a significant (p=0.007) reduction in serum glutamate concentration (Table 8 and Figure 21C). The maximum effect appeared between 2 and 4 h after administration of the treatment; however, the capacity of this dose to reduce serum glutamate concentration was similar to the 12.88 µg/100g dose. These findings showed that 12.88 µg/100g seems to be the most appropriate dose of rGOT1 to achieve a significant reduction in the serum glutamate concentration in the animals. Of note, serum glutamate concentrations were normalized 4–6 h after rGOT1 administration, demonstrating that the effect of the enzymatic treatment is transient.

In order to determine whether the effect of the enzyme could be potentiated by oxaloacetate (co-substrate of the enzymatic reaction), the dose of rGOT1 (12.88 µg/100g) was supplemented with a non-effective dose of oxaloacetate (1.5 mg/100g). In our previous study (already published[6]), we had described that a dose of 1.5 mg/100g of oxaloacetate did not affect the serum glutamate levels. Similar results were observed again in this study (Table 8 and Figure 21D). Administration of rGOT1 12.88 µg/100g with oxaloacetate (1.5 mg/100g) induced an immediate and significant (p<0.01) lowering of serum glutamate concentration, which is the gold standard approach for reducing increased glutamate levels after brain ischemia. The decrease in glutamate appeared 30 min (with respect to the basal values) after treatment administration and remained during at least 3 h (Table 8 and Figure 21E); however, no significant differences

with respect to rGOT1 12.88 µg/100g alone were observed. These results led us to examine whether the protective efficacy of rGOT1 (12.88 µg/100g) or rGOT1 (12.88 µg/100g) supplemented with oxaloacetate (1.5 mg/100g) in ischemic animals was higher than that observed previously with oxaloacetate 3.5 mg/100g.[6]

	Untreat	**rGOT 6.44** mg/100g	**rGOT 12.88** mg/100g	**rGOT 25.76** mg/100gr	**rGOT 12.88** mg/100g **+Oxal 1.5** mg/100g	**Oxal 1.5** mg/100g
Basal	150±23	145±34	156±42	147±25	145±34	145±21
1h	196±27	140±14	123±31	114±56	96±12	185±32
2h	168±22	110±23	98±19	100±63	74±12	170±24
4h	152±17	107±20	75±23	74±34	68±21	165±29
6h	145±23	148±18	150±31	158±20	132±34	155±14
24h	156±14	159±27	152±23	161±34	144±24	145±20

Table 8: Effect of rGOT and oxaloacetate (Oxal) on serum glutamate levels in healthy rats. Glutamate 15mM was injected i.v. 30 min prior to treatments. **(A)** Comparison between rats treated with glutamate 15mM (blue line) and rats treated with glutamate 15mM and rGOT1 6.44 µg/100g (black line).**(B)** Comparison between rats treated with glutamate 15mM (blue line) and rats treated with glutamate 15mM and rGOT1 µg/100g (black line).**(C)** Comparison between rats treated with glutamate (15 mM) (blue line) and rats treated with glutamate (15 mM) and with rGOT1 (25.76 µg/100g).**(D)** Comparison between rats treated with glutamate 15mM (blue line) and rats treated with glutamate (15 mM) and oxaloacetate (Oxal) (1.5 mg/100g).**(E)** Comparison between rats treated with glutamate (15 mM) (blue line) and rats treated with glutamate (15 mM) and rGOT1 (12.88 µg/100g) plus oxaloacetate (Oxal) (1.5 mg/100g).

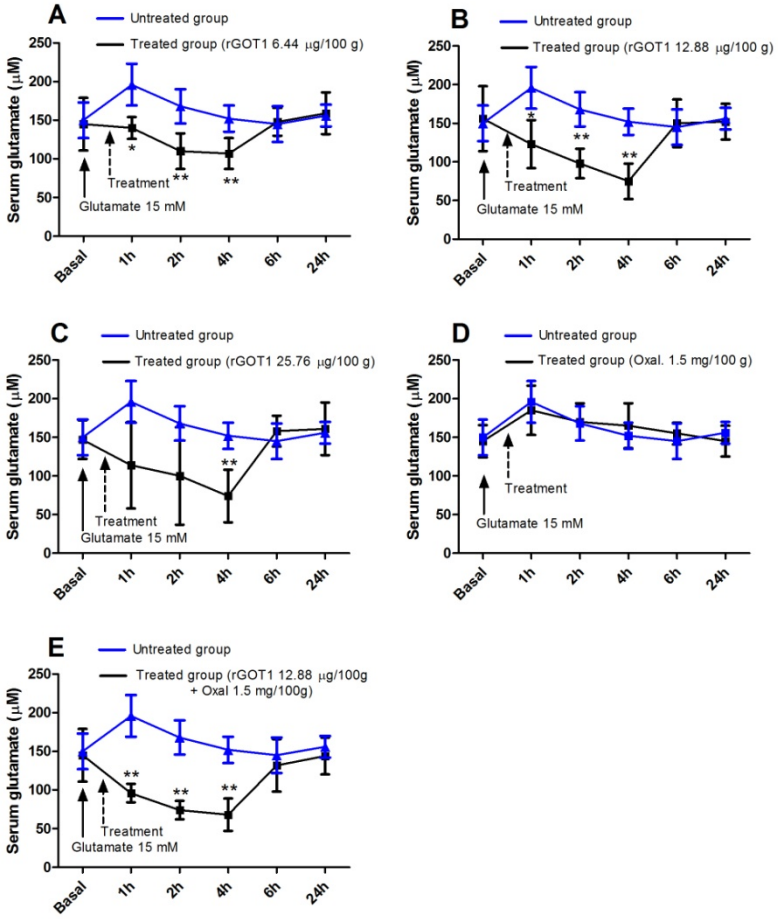

Figure 21: Effect of rGOT and oxaloacetate (Oxal) on serum glutamate levels in healthy rats. Glutamate 15mM was injected i.v. 30 min prior to treatments. **(A)** Comparison between rats treated with glutamate 15mM (blue line) and rats treated with glutamate 15mM and rGOT1 6.44 µg/100g (black line).**(B)** Comparison between rats treated with glutamate 15mM (blue line) and rats treated with glutamate 15mM and rGOT1 µg/100g (black line).**(C)** Comparison between rats treated with glutamate (15 mM) (blue line) and rats treated with glutamate (15 mM) and with rGOT1 (25.76 µg/100g).**(D)** Comparison between rats treated with glutamate 15mM (blue line) and rats treated with glutamate (15 mM) and oxaloacetate (Oxal) (1.5 mg/100g).**(E)** Comparison between rats treated with glutamate (15 mM) (blue line) and rats treated with glutamate (15 mM) and rGOT1 (12.88 µg/100g) plus oxaloacetate (Oxal) (1.5 mg/100g).

7.3. Protective study

7.3.1. Study of the protective effect of rGOT1 with or without supplementation of oxaloacetate on ischemic animals

MCAO induced an increase of 30% of serum glutamate concentration 1 h after reperfusion (Table 9 and Figure 22), returning to normal levels 3 h later. In sham operated rats in which MCA was not occluded, no changes in serum glutamate concentration were detected (data not shown).

	Saline	Oxal	rGOT 1	Oxal+rGOT1
Basal	149,7 ±25,7	149,7±45,8	153,2±21,9	132,3±37,8
0	172,0±60,4	166,1±64,6	168,3±29,9	154,8±43,1
60 min	190,5±37,8	113,4±46,4	100,5±21,1	101,3±41,9
120 min	188,5±20,9	130,4±33,1	111,2±52,7	124,6±39,0
180 min	163,7±24,3	130,5±23,1	106,5±56,1	134,7±43,2

Table 9: Serum glutamate concentration (µM) in MCAO rats. MCAO rats were treated with saline (control group) (n=6), oxaloacetate (Oxal) 3.5 mg/100g (n¼6), rGOT1 12.88 µg/100g (n=6) and rGOT1 12.88 µg/100g plus oxaloacetate 1.5 mg/100g (n=6).

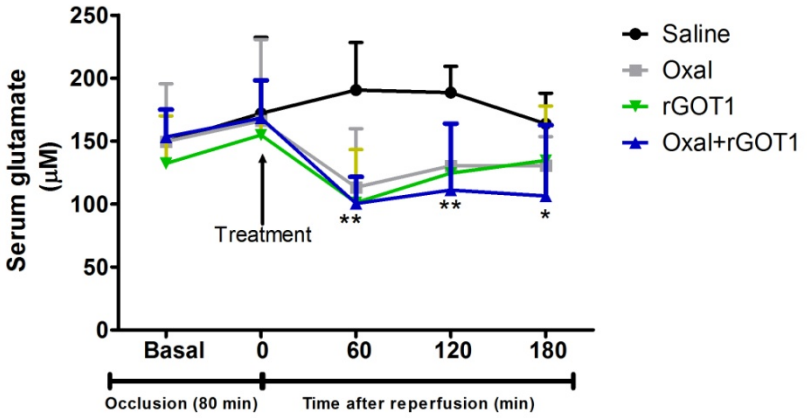

Figure 22: Time course of serum glutamate concentration (μM) in MCAO rats. MCAO rats were treated with saline (control group) (n=6), oxaloacetate (Oxal) 3.5 mg/100g (n¼6), rGOT1 12.88 μg/100g (n=6) and rGOT1 12.88 μg/100g plus oxaloacetate 1.5 mg/100g (n=6). Solid arrow indicates the time of treatment injection, administered at the moment of reperfusion (80 min after occlusion). Serum glutamate concentration was measured under basal conditions (before surgery), at the moment of the reperfusion (before treatment administration), and 1, 2 and 3 h after reperfusion. Data are shown as mean±S.E.M.*p<0.05, **p<0.01 compared with control group.

The increase in serum glutamate concentration after cerebral ischemia was inhibited (p<0.05) by each one of the three treatments; rGOT1 (12.88 μg/100g), oxaloacetate (3.5 mg/100g) and rGOT1 plus oxaloacetate (12.88 μg/100g and 1.5 mg/100g, respectively) (Table 9 and Figure 22). The small differences observed between the treatments were not statistically significant.

To confirm that treatment with rGOT1 induced an increase in systemic GOT1 activity, their levels were measured at different time points (Table 10 and Figure 23). GOT1 activities in the control and oxaloacetate groups were not altered after treatment, whereas rGOT1 treatments induced a significant (p<0.01) increase in serum GOT activity 1 h after administration, which returned close to normal levels 24 h after treatment administration.

	Saline	Oxal	rGOT 1	Oxal+rGOT1
Basal	80 ±13	75±10	79±8	82±9
1 h	75 ± 10	78±8	1400±45	1555±35
3 h	110±12	130±10	1367±67	1600±78
24 h	120±15	150±20	300±25	350±30

Table 10: Time course of serum GOT activity in MCAO rats. MCAO rats were treated with saline (control group) (n=6), oxaloacetate (Oxal) 3.5 mg/100g (n=6), rGOT1 12.88 µg/100g (n=6) and rGOT1 12.88 µg/100g plus oxaloacetate 1.5 mg/100g (n=6). Treatments were administered at the moment of reperfusion (80 min after occlusion). GOT activity was measured under basal conditions (before surgery), and 1, 3 and 24 h after reperfusion. Data are shown as percentage compared with basal levels±S.E.M.

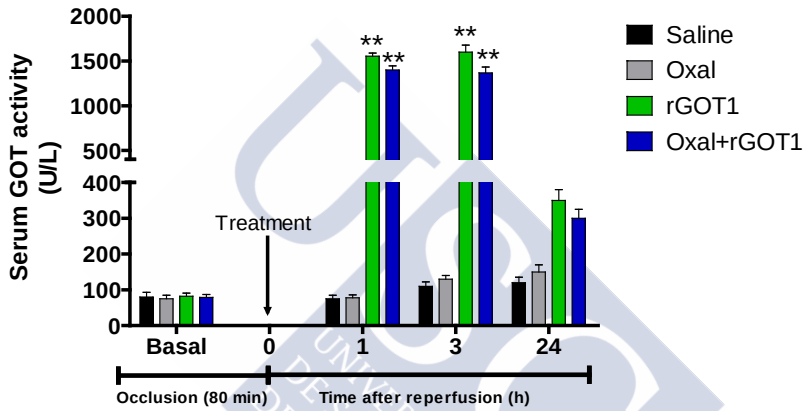

Figure 23: Time course of serum GOT activity in MCAO rats. MCAO rats were treated with saline (control group) (n=6), oxaloacetate (Oxal) 3.5 mg/100g (n=6), rGOT1 12.88 µg/100g (n=6) and rGOT1 12.88 µg/100g plus oxaloacetate 1.5 mg/100g (n=6). Treatments were administered at the moment of reperfusion (80 min after occlusion). GOT activity was measured under basal conditions (before surgery), and 1, 3 and 24 h after reperfusion. Data are shown as percentage compared with basal levels±S.E.M. $^{**}p$ <0.01 with respect to control group.

To confirm that serum glutamate reduction caused by the three treatments led a reduction of brain glutamate, MRS was performed on brain ischemic animals. Quantitative analysis of MRS revealed a persistent increase in brain glutamate levels after the occlusion of MCA in the control group. Glutamate levels in the brain parenchyma were significantly decreased (p<0.05 relative to the control animals), with each of the three treatments tested (Table 11, Figure 24 and Figure 25).

	Saline	Oxal	rGOT 1	Oxal+rGOT1
25 min	1,4±0,3	1,4±0,1	1,6±0,4	1,5±0,3
50 min	1,5±0,3	1,6±0,3	1,6±0,4	1,6±0,4
80 min	1,8±0,2	1,7±0,3	1,7±0,1	1,8±0,2
25 min	1,8±0,4	1,6±0,5	1,3±0,1	1,4±0,2
50 min	1,7±0,5	1,2±0,1	0,9±0,1	1,1±0,1
75 min	1,6±0,4	1,1±0,4	1,0±0,1	1,0±0,1
100 min	1,7±0,4	1,0±0,4	0,8±0,1	0,8±0,1
125 min	1,6±0,3	0,8±0,2	0,8±0,2	0,9±0,1
150 min	1,5±0,3	0,9±0,2	0,8±0,1	0,9±0,1
175 min	1,3±0,5	1,0±0,1	1,0±0,1	1,1±0,2

Table 11: Magnetic resonance spectroscopy of the time course of brain glutamate levels in MCAO rats treated with saline (control group) (n=6), oxaloacetate (Oxal) 3.5 mg/100 g (n=6), rGOT1 12.88 µg/100g (n=6) and rGOT1 12.88 µg/100g plus oxaloacetate 1.5 mg/100g (n=6).

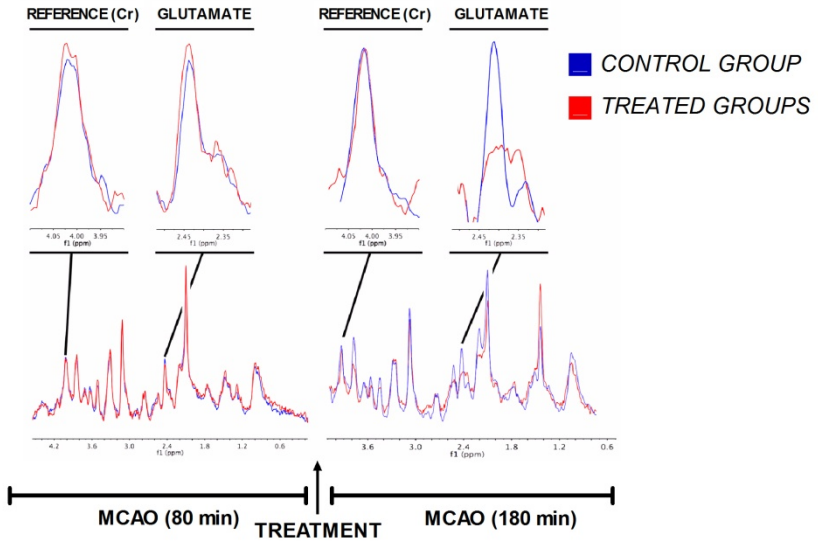

Figure 24: MRS analysis. Quantitative analysis of glutamate signals were normalized to creatine (Cr) peaks for each single spectra. Brain glutamate levels were analyzed during the occlusion (80 min) and during reperfusion (180 min). Brain glutamate levels were similar in treated (before treatment) and control (treated with saline) ischemic animals during occlusion. However, during reperfusion glutamate levels were lower in treated animals compared with the control.

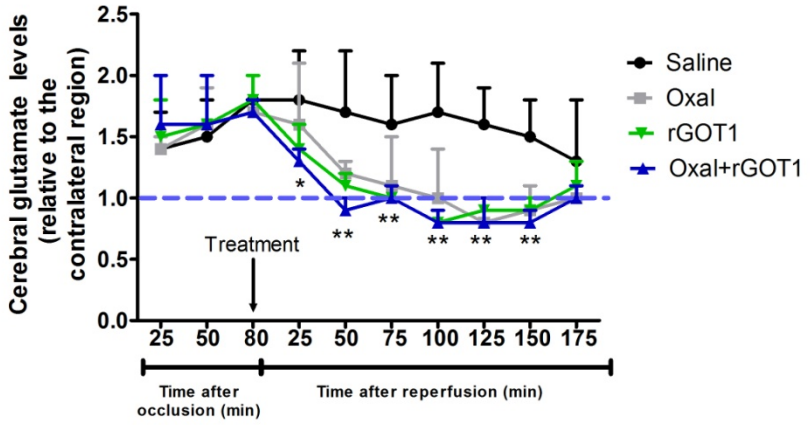

Figure 25: MRS analysis. Time course of brain glutamate levels in MCAO rats treated with saline (control group) (n=6), oxaloacetate (Oxal) 3.5 mg/100 g (n=6), rGOT1 12.88 µg/100g (n=6) and rGOT1 12.88 µg/100g plus oxaloacetate 1.5 mg/100g (n=6). Solid arrow indicates the moment of i.v treatment. Cerebral glutamate levels were measured during occlusion (80 min) and reperfusion (180 min). MRS analysis was performed in an independent group of animals. Data are shown as the mean of cerebral glutamate levels relative to the contralateral region±S.E.M. Blue dashed line indicates the levels of brain glutamate in the contralateral region.*p<0.05, **p<0.01 compared with control group.

In order to demonstrate that the reduction in serum and brain glutamate levels observed after treatment administration produced a protective effect in our animal model of cerebral ischemia, infarct volumes were measured at 24 h and 7 days after ischemia and were compared with the control group. Table 13 and Figure 26 show that, although all treatments were able to induce a significant (p<0.05) protection against the ischemic damage both 24 h and 7 days after the onset of ischemia, rGOT1+oxaloacetate revealed to be the more effective treatment (p<0.01, with respect to the control group). Analysis of infarct volumes adjusted to the ipsilateral hemisphere showed a similar protective profile (data not shown). Infarct volumes measured in those animals subjected to the spectroscopy protocol (Table 12 and Figure 27) showed the same protective results for the 3 treatments. Diffusion images revealed that all animals subjected to spectroscopy

presented the same ischemic damage before the treatment administration.

	Saline	Oxal	rGOT 1	Oxal+rGOT1
Basal	100	100	100	100
24d	98±17	77±16	74±11	47±15
7d	66±19	52±11	42±7	29±19

Table 12: Infarct size assessed by means of MRI in MCAO rats. MCAO rats were treated with saline (control group), oxaloacetate (Oxal) 3.5 mg/100g, rGOT1 12.88 µg/100g and rGOT1 12.88 µg/100g plus oxaloacetate 1.5 mg/100g. Treatments were administered at the moment of the reperfusion. Infarct size was assessed in ischemic rats subjected to spectroscopy analysis. Infarct sizes were measured at 24 h and 7 days after ischemia. ADC basal volumes were determined before the administration of treatment. Data is shown as the percentage relative to the basal infarct volume.

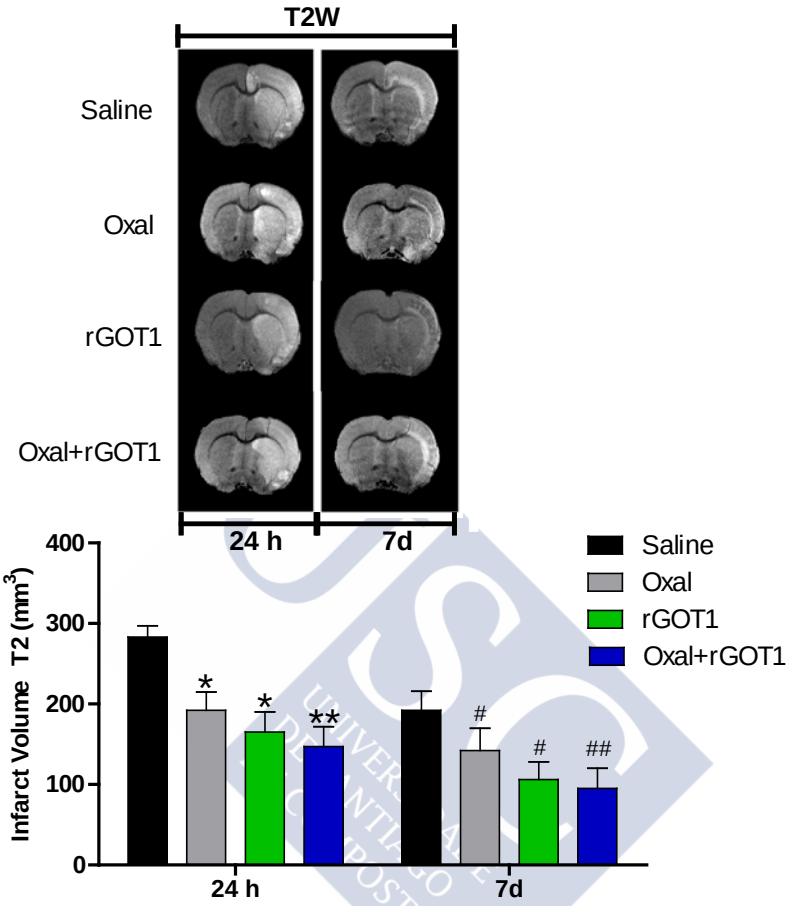

Figure 26: Infarct size assessed by means of MRI in MCAO rats. MCAO rats were treated with saline (control group), oxaloacetate (Oxal) 3.5 mg/100g, rGOT1 12.88 µg/100g and rGOT1 12.88 µg/100g plus oxaloacetate 1.5 mg/100g. Treatments were administered at the moment of the reperfusion. Infarct size was assessed in ischemic rats not subjected to spectrocopy analysis. Infarct sizes were measured at 24 h and 7 days after ischemia. Data are shown as the mean of infarct volume (mm3) ± S.E.M.*$p<0.05$, **$p<0.01$ with respect to the control group at 24 h; $^{\#}p<0.05$, $^{\#\#}p<0.01$ as well as on day 7.

	Saline	Oxal	rGOT 1	Oxal+rGOT1
24h	283±47	192±56	165±62	147±61
7d	192±79	142±68	106±54	95±62

Table 13: Infarct size assessed by means of MRI in MCAO rats. MCAO rats were treated with saline (control group), oxaloacetate (Oxal) 3.5 mg/100g, rGOT1 12.88 µg/100g and rGOT1 12.88 µg/100g plus oxaloacetate 1.5 mg/100g. Treatments were administered at the moment of the reperfusion. Infarct size was assessed in ischemic rats not subjected to spectrocopy analysis. Data is shown as the mean of infarct volume (mm^3) ± S.E.M.

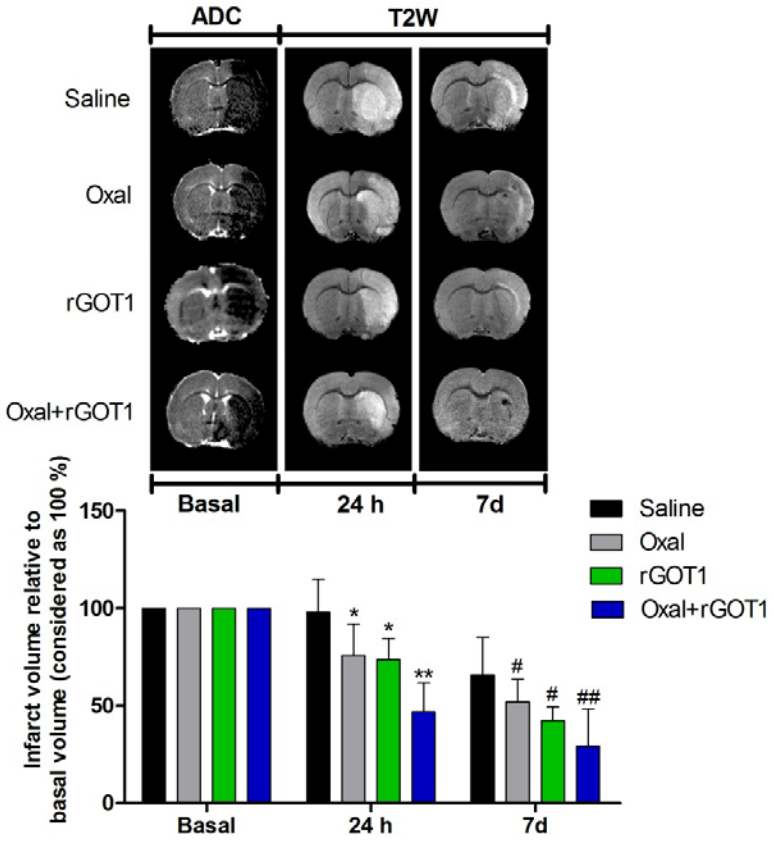

Figure 27: Infarct size assessed by means of MRI in MCAO rats. MCAO rats were treated with saline (control group), oxaloacetate (Oxal) 3.5 mg/100g, rGOT1 12.88 µg/100g and rGOT1 12.88 µg/100g plus oxaloacetate 1.5 mg/100g. Treatments were administered at the moment of the reperfusion. Infarct size was assessed in ischemic rats not subjected to spectrocopy analysis. Infarct sizes were measured at 24 h and 7 days after ischemia. Data are shown as the percentage relative to the basal volume. $*p<0.05$, $**p<0.01$ with respect to the control group at 24 h; $^{\#}p<0.05$, $^{\#\#}p<0.01$ as well as on day 7.

To determine the therapeutic window of rGOT1 treatments, 2 groups of animals were treated 1 h after reperfusion (140 min after occlusion). Analysis of serum glutamate concentration in animals treated with rGOT1 (12.88 µg/100g) or rGOT1 plus oxaloacetate (12.88 µg/100g and 1.5 mg/100g, respectively) showed that both treatments caused a significant (p<0.05) inhibition of the increase in glutamate observed in the control group (Table 14 and Figure 28).

	Saline	rGOT1 (+1h)	Oxal+rGOT1 (+1h)
Basal	149,7±25,7	153,2±21,9	132,3±37,8
0	172,0±60,4	168,3±29,9	154,8±43,1
60	190,5±37,8	189,0±21,1	197,0±41,9
120	188,5±20,9	111,2±52,7	124,6±39,0
180	163,7±24,3	112,0±67,0	134,7±43,2

Table 14: Serum glutamate concentration (µM) in MCAO rats. MCAO rats were treated with saline (control group) (n=6), rGOT1 12.88 µg/100g (n=6) and rGOT1 12.88 µg/100g plus oxaloacetate 1.5 mg/100g (n=6) 1 h after reperfusion. Serum glutamate concentration was measured under basal conditions (before surgery), at the time of reperfusion (before treatment administration), and 1, 2 and 3 h after reperfusion. Data are shown as mean±S.E.M.

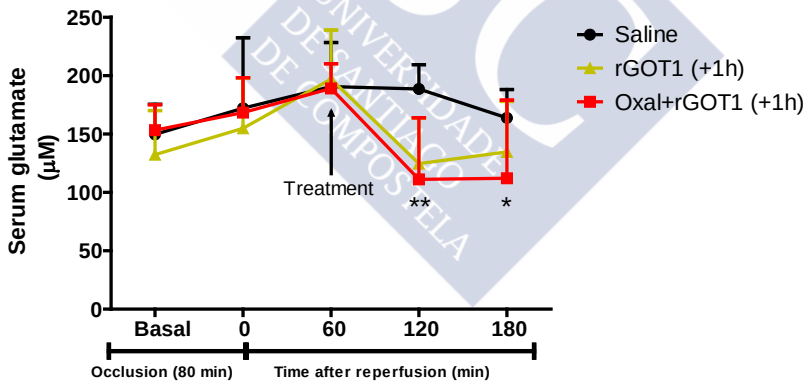

Figure 28: Time course of serum glutamate concentration (µM) in MCAO rats. MCAO rats were treated with saline (control group) (n=6), rGOT1 12.88 µg/100g (n=6) and rGOT1 12.88 µg/100g plus oxaloacetate 1.5 mg/100g (n=6) 1 h after reperfusion. Solid arrow indicates the time of the i.v. treatments. Serum glutamate concentration was measured under basal conditions (before surgery), at the time of reperfusion (before treatment administration), and 1, 2 and 3 h after reperfusion. Data are shown as mean±S.E.M.*p<0.05, **p<0.01 with respect to the control group.

Analysis of infarct volume determined that both treatments displayed similar infarct volume reduction at 24 h when administered immediately after reperfusion (Table 15, Table 16, Figure 29 and Figure 30), however, while the protective effect induced for rGOT1 disappears when this treatment is given 1 h after reperfusion on day 7; when rGOT1 is administered in combination with oxaloacetate, the effect persists beyond 1 h after reperfusion (p<0.05, with respect to the control).

	Saline	**rGOT 1**	**rGOT1 (+1h)**
24h	283±47	165±62	176±56
7d	192±79	106±54	153±27

Table 15: Infarct size measured by MRI in MCAO rats. MCAO rats were treated at 2 different times, at the moment of reperfusion and 1 h after reperfusion.(A) Saline (control group) (n=6), rGOT1 12.88 µg/100g (rGOT1) (n=6) at the moment of reperfusion, and rGOT1 12.88 µg/100g (rGOT1+1 h) (n=6) 1 h after reperfusion. Data are shown as the mean of infarct volume (mm^3) ±S.E.M.

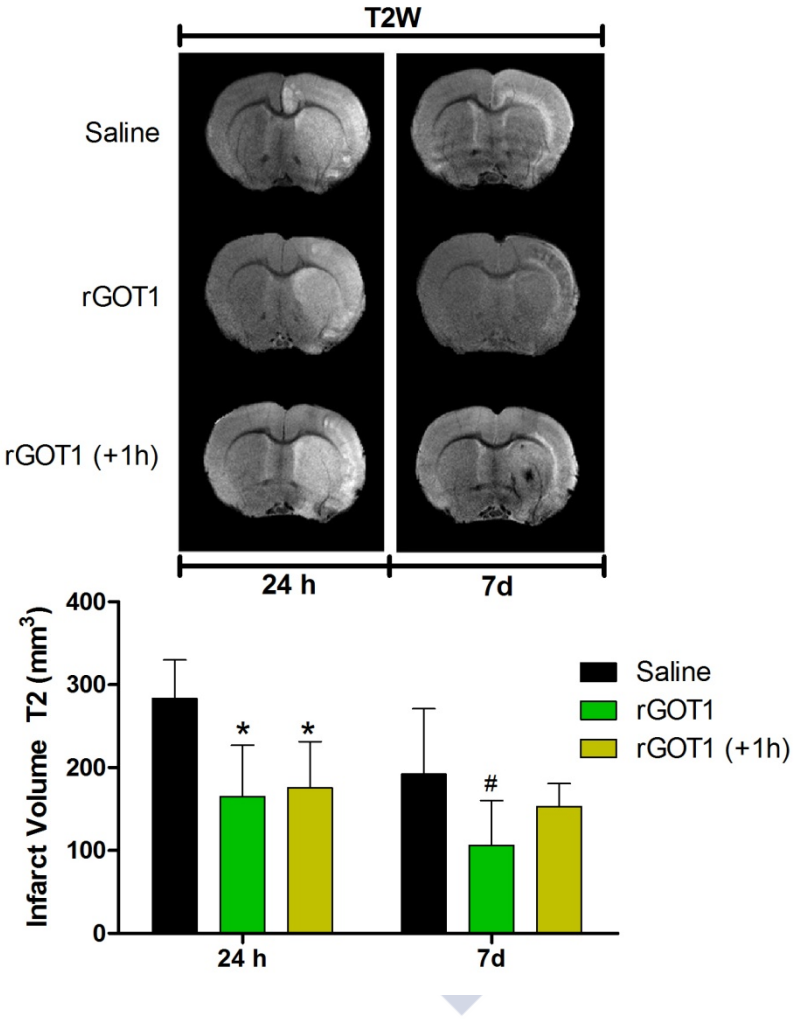

Figure 29: Infarct size assessed by means of MRI in MCAO rats. MCAO rats were treated at 2 different times, at the moment of reperfusion and 1 h after reperfusion.(A) Saline (control group) (n=6), rGOT1 12.88 µg/100g (rGOT1) (n=6) at the moment of reperfusion, and rGOT1 12.88 µg/100g (rGOT1+1 h) (n=6) 1 h after reperfusion. Data are shown as the mean of infarct volume (mm3) ±S.E.M.*p<0.05, **p<0.01 compared with control group at 24 h; #p<0.05, ##p<0.01 with respect to control group at day 7.

	Saline	rGOT 1	rGOT1 (+1h)
24h	283±47	147±61	152±35
7d	192±79	95±62	133±32

Table 16: Infarct size determined by MRI in MCAO rats. MCAO rats were treated at 2 different times, at the moment of reperfusion and 1 h after reperfusion. Saline (control group) (n=6), rGOT1 12.88 µg/100g plus oxaloacetate 1.5 mg/100g (Oxal+rGOT1) (n=6) at the time of the reperfusion and rGOT1 12.88 µg/100g plus oxaloacetate 1.5 mg/100g (Oxal+rGOT1 +1 h) (n=6) 1 h after reperfusion. Data are shown as the mean of infarct volume (mm^3) ±S.E.M.

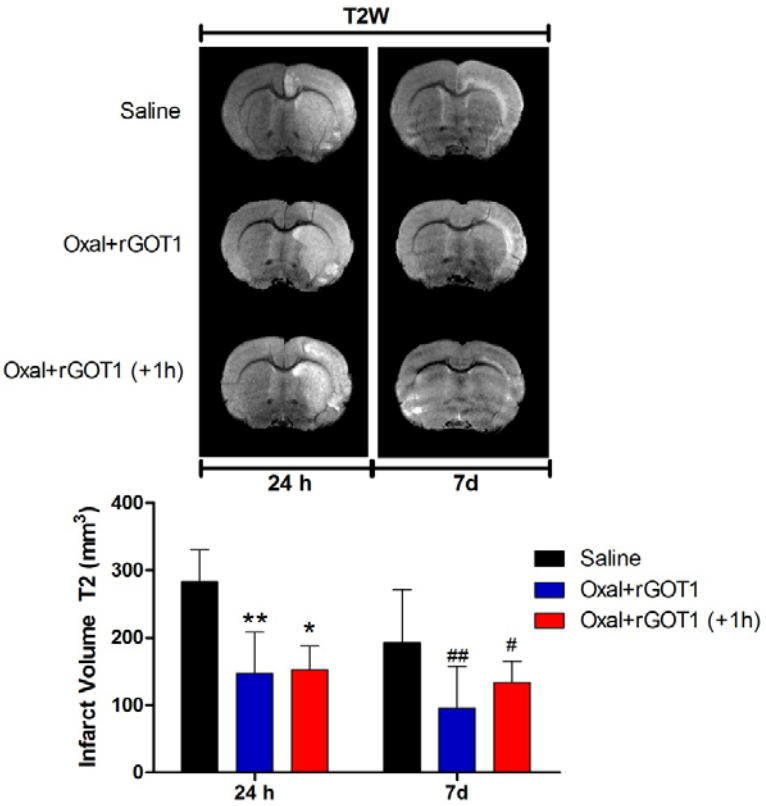

Figure 30: Infarct size assessed by means of MRI in MCAO rats. MCAO rats were treated at 2 different times, at the moment of reperfusion and 1 h after reperfusion. Saline (control group) (n=6), rGOT1 12.88 µg/100g plus oxaloacetate 1.5 mg/100g (Oxal+rGOT1) (n=6) at the time of the reperfusion and rGOT1 12.88 µg/100g plus oxaloacetate 1.5 mg/100g (Oxal+rGOT1 +1 h) (n=6) 1 h after reperfusion. Data are shown as the mean of infarct volume (mm3) ±S.E.M.*p<0.05, **p<0.01 compared with control group at 24 h; #p<0.05, ##p<0.01 with respect to control group at day 7.

Somatosensory test, an important end point assay of drug screening in stroke, confirmed that reduction in infarct volume observed with each of the 3 treatments was associated with a better neurological outcome measured 7 days after ischemia, showing the treatment rGOT1 oxaloacetate to be a superior effect (p<0.01, with respect to the control) (Table 17 and Figure 31).

Group	Laterality index (7days)
Baseline	48,99±0,06
Saline	94,29±0,12
Oxal	74,17±0,20
rGOT1	63,77±0,13
Oxal+rGOT1	56,67±0,16
rGOT1 (+1h)	70,00±0,23
Oxal+rGOT1(+1h)	65,00±0,15

Table 17: Effect of treatments on somatosensory test. Sensorimotor deficits after an ischemic insult were assessed using the cylinder test and quantified by laterality index. +1 h denotes that those treatments were administered 1 h after reperfusion. Other treatments were administered at the moment of the reperfusion. Somatosensory tests were performed 1 day before surgery (baseline) and on day 7 after MCAO. Values represent the mean±S.E.M, n=6.

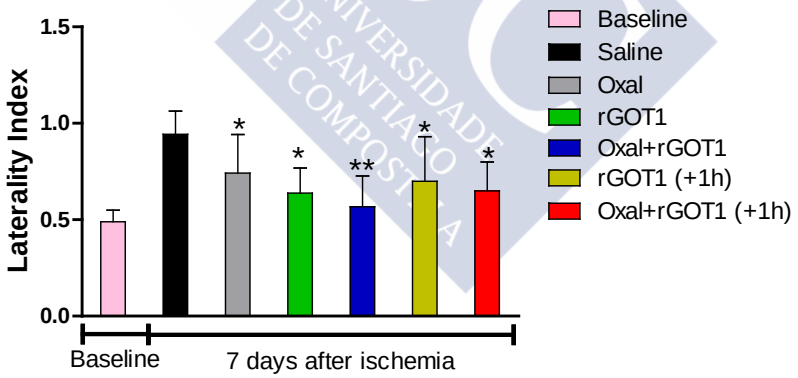

Figure 31: Effect of treatments on somatosensory test. Sensorimotor deficits after an ischemic insult were assessed using the cylinder test and quantified by laterality index. +1 h denotes that those treatments were administered 1 h after reperfusion. Other treatments were administered at the moment of the reperfusion. Somatosensory tests were performed 1 day before surgery (baseline) and on day 7 after MCAO. Values represent the mean±S.E.M, n=6.*p<0.05, **p<0.01 relative to control group.

8. Section II: Effect of glutamate grabbers cells on ischemic damage.

8.1. Plasmid $EAAT_2$ production for virus cell infection.

Previously, in this section, it will be explained those results regarding to the plasmid $EAAT_2$ production used for virus cell infection.

- Long construct production: YFP-$EAAT_2$

The sequence YFP-$EAAT_2$ was obtained from the digestion of the original plasmid pRcCMVmYFPEAAT$_2$ with the restriction enzyme EcoRI (Figure 32A). The digested DNA was electrophoresed on agarose gels and 3 fragments were obtained. In Figure 32B we can observe the fragments of the YPF-$EAAT_2$ sequence (~2500 bp) and other 2 sequences (~5000 bp and ~900 bp) after enzymatic digestion, which belongs to the backbone of the plasmid.

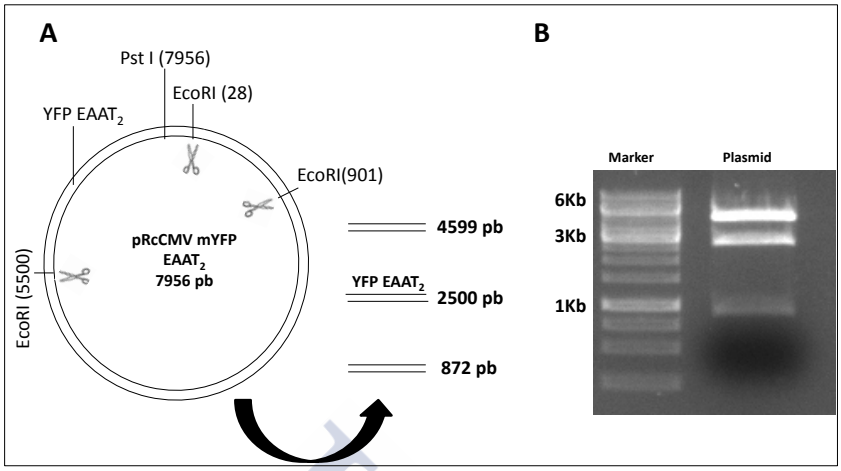

Figure 32: (A) Digestion of the plasmid pRcCMVmYFPEAAT$_2$ with EcoRI, that should originate 3 fragments: One sequence of ~5000 pb other of ~900 pb corresponding to backbone of the plasmid and 1 sequence of ~2500pb belongs to the YFP-EAAT$_2$, long construct.(B)The result of the electrophoresis of the digested plasmid showed 3 fragments, which corresponding with the expected sequences.

Once obtained the YFP-EAAT$_2$ sequence, this was inserted in the viral vector to be used in the production of rAAV virus. The viral vector used was csCMV, which was subjected to EcoRI digestion process for its linearization. Next, the vector was electrophoresed and the fragment obtained was excised and purified. In addition, the linearizated vector was dephosphorylated for preventing the circulation. Once the vector was ready, it was carried out the ligation process (Figure 33).

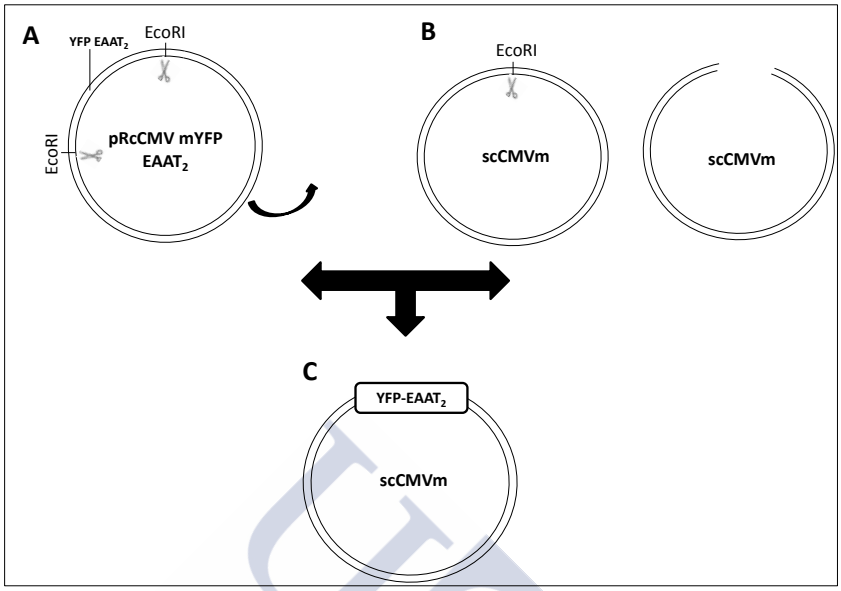

Figure 33: (A) The long construct YFP-$EAAT_2$ was obtained by the restriction of the plasmid pRcCMVmYFP-$EAAT_2$ with EcoRI. (B)The viral vector (sCCMVm) was submitted to restriction with EcoRI for linearization; C) YFP-$EAAT_2$ inserted in the viral vector.

After ligation process (insertion of YFP-$EAAT_2$ sequence in viral vector), 18 colonies were grown and picked in LB medium. The isolation of plasmid DNA, which consists of the insert YFP-$EAAT_2$ and the viral vector, was done with the kit NucleoSpin Plasmid. The DNA obtained was subjected to the following restriction controls (EcoRI, SmaI and AhdI) to ensure that the insert was cloned successfully in the viral vector.

The result of the restriction with EcoRI (Figure 35) should generate 2 fragments (the insert YFP-$EAAT_2$ ~2500pb and the backbone of the viral vector ~5000 bp) (Figure 34). The electrophoresis of digested DNA demonstrated that the DNA isolated from 16 independent colonies containing the insert cloned into the viral vector, however 2 of them showed incorrect ligation as it is indicated in the Figure 35.

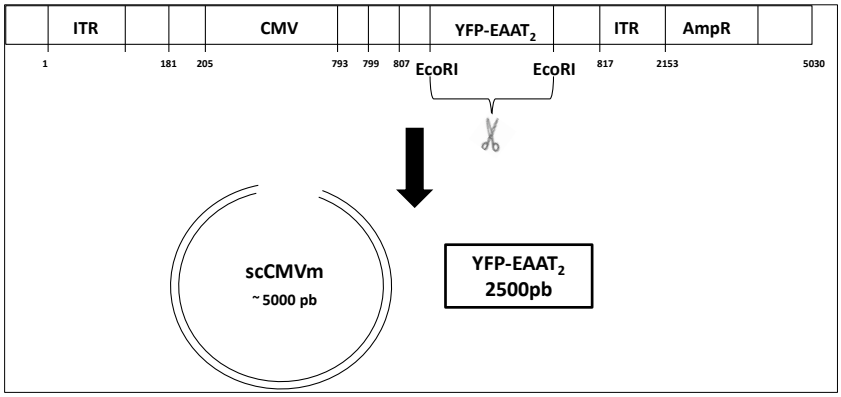

Figure 34: Restriction with EcoRI enzyme of the viral vector that contained the insert YFP-$EAAT_2$ resulted in 2 fragments: the insert YFP-$EAAT_2$ (~2500pb) and the backbone of the viral vector (~5000 bp).

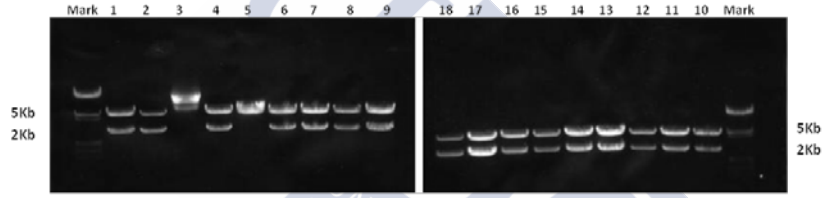

Figure 35: Electrophoresis of digested DNA demonstrated that the DNA isolated from 16 independent colonies containing the insert cloned into the viral vector. Only 2 colonies, 3 and 5, showed incorrect ligation as the size of the band did not correspond with 2 and 5 Kb.

The 14 clones selected were subjected to restriction with HindIII to certify that the insert was attached in the right direction. This restriction control with HindIII should generate 2 fragments corresponding with the sequence of YFP-$EAAT_2$ (2500pb) and the backbone of the viral vector (5000pb) (Figure 36). As it can see in Figure 37, the clones 4, 8 and 10 contained the insert (YFP-$EAAT_2$), but unfortunately the insert was not in the correct direction, because of the 2 fragments obtained corresponds to the fragment of 5000 bp (backbone of the viral vector), however the fragment had 1000bp, when the correct size of the insert should be around 2500pb.

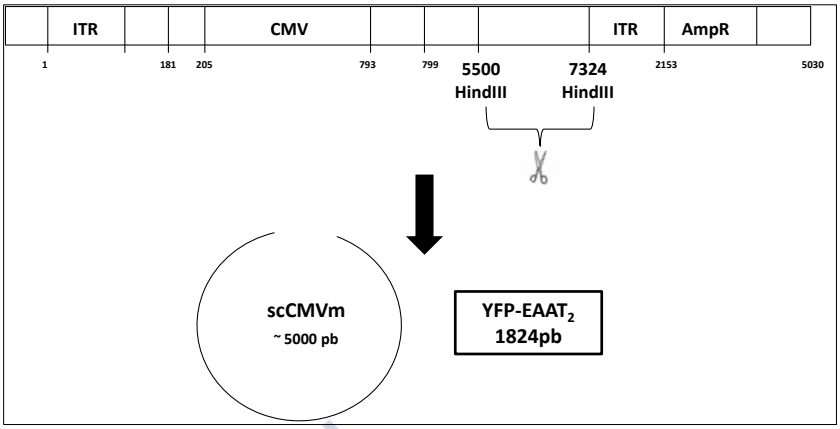

Figure 36: Restriction control with HindIII should generate 2 fragments corresponding with the sequence of YFP-EAAT$_2$ (2500pb) and the backbone of the viral vector (5000pb).

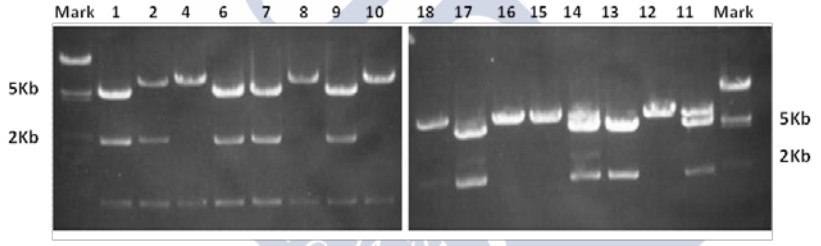

Figure 37: Plasmid DNA containing the viral vector and YFP-EAAT$_2$ was cut with HindIII enzyme restriction. Only colonies 4, 8 and 10 showed 2 fragments, one corresponded to the fragment of 5000 bp (backbone of the viral vector) and other of 1000 bp.

To solve this problem, the clone 4 (that was analyzed by DNA sequencing to verify that the YFP-EAAT$_2$ was correct) that contained the insert YFP-EAAT$_2$ in the wrong direction into the viral vector csCMVm was used to isolate the insert. For that, the clone 4 was submitted to restriction with EcoRI, electrophoresis and purification process. The DNA of the insert was ligated again with the viral vector (csCMVm) and the ligation mixture was used to transform competent cells. After ligation, 10 colonies were grown and picked in LB medium, following the protocol described above. Once, the plasmid DNA was isolated and submitted to the same control restriction with EcoRI, HindIII, SmaI and AhdI.

Analyses of EcoRI and HindIII were successful (data not show). Then AhdI and SmaI digestion were performed. The digestion of the viral vector (csCMV) with the same enzymes was carried out as a control restriction. The restriction of the viral vector with SmaI should generate 4 fragments (~ 3702 pb, ~1300 pb and 2 of 11pb) (Figure 38A). While the same digestion for the clones (from clone 4) should produce 5 fragments (with sizes of ~3758 pb, ~2000 pb, ~767 pb and 2 of 11pb) (Figure 38B). The digestion with AhdI of the viral vector should generate 3 fragments (~1239pb, ~2629 pb and ~1128 pb) (Figure 39A) and the restriction with AhdI for the clones should be 3 fragments (~3700pb, ~2629 pb and ~1128 pb) (Figure 39B).

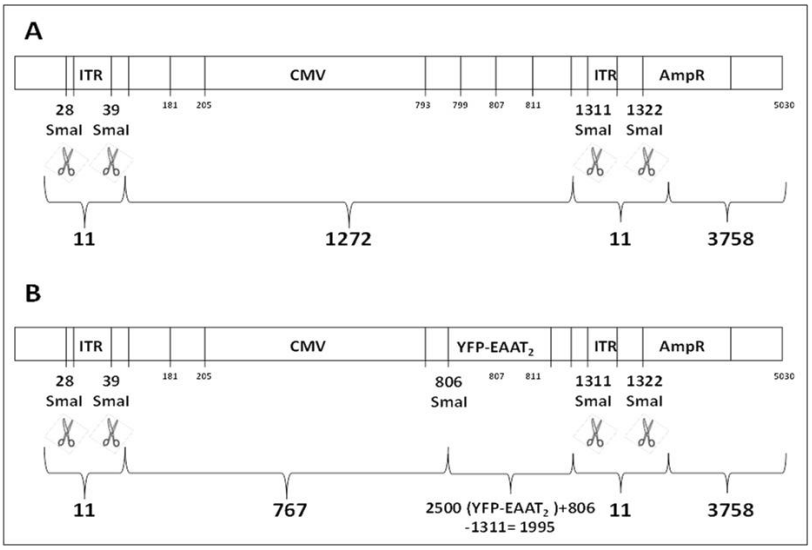

Figure 38: (A) Restriction of the viral vector with SmaI should generate 4 fragments (~ 3702 pb, ~1300 pb and 2 of 11pb).(B) Digestion with SmaI for the different clones (from clone 4) should produce 5 fragments (with sizes of ~3758 pb, ~2000 pb, ~767 pb and 2 of 11pb)

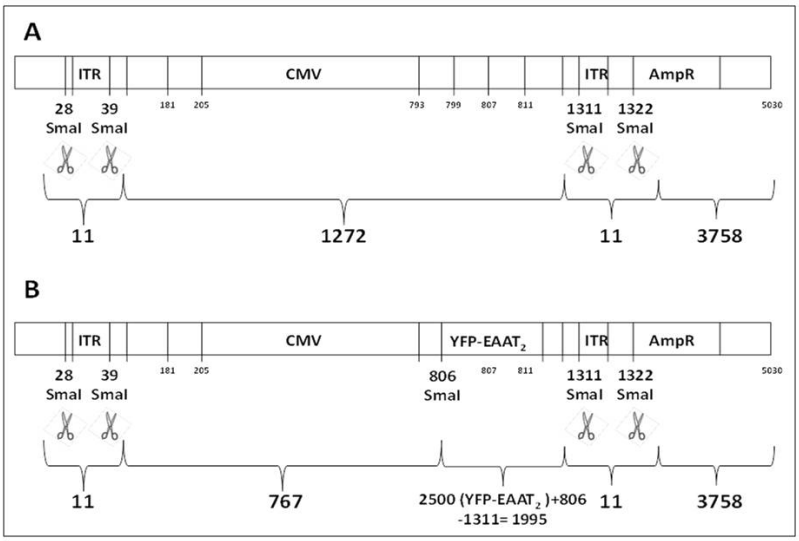

Figure 39: (A) The digestion with AhdI of the viral vector should generate 3 fragments (~1239pb, ~2629 pb and ~1128 pb). (B) The restriction with AhdI for the clones should produce 3 fragments (~3700pb, ~2629 pb and ~1128 pb).

The results of restrictions with SmaI showed that the viral vector was digested correctly, as the number and the sizes of the fragments were expected. The restriction was right for all the clones (3 fragments with the size correct) (Figure 40A).

Regarding to the restriction with AhdI, the viral vectors generated the expected fragments. However, the digestion of the clones showed that only the clones 3, 5 and 6 originated the 3 fragments (~3700pb, ~2629pb and ~1128 pb) (Figure 50B).

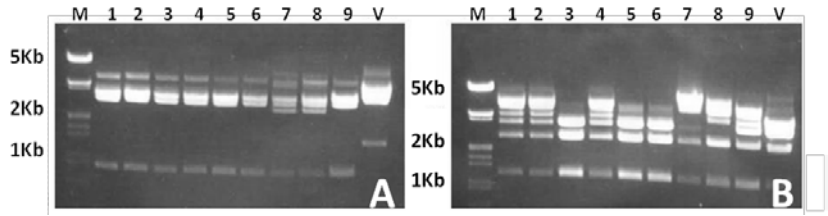

Figure 40: (A) Restriction with SmaI. (B) Restriction with AhdI. Only the clones 3, 5 and 6 had the insert YFP-EAAT$_2$ cloned in the right direction.

Then, the clones 3, 5 and 6 had the insert YFP-$EAAT_2$ cloned in the right direction. This final result indicated that this plasmid-DNA (viral vector and YFP-$EAAT_2$) was ready for viral encapsulation.

8.1.1. Short construct: Ha-tag-$EAAT_2$

Due to the viral packaging limitation (see Material and Methods), besides of to produce YFP-$EAAT_2$ for viral encapsulation, a shorter sequence with $EAAT_2$ (Ha-tag-EAAT2) was also produced.

To obtain the Ha-tag-$EAAT_2$ insert, previously the sequence YFP-$EAAT_2$ was isolated from the clone 4 (already tested in the YFP-$EAAT_2$ production) through the restriction with EcoRI, electrophoresis and purification.

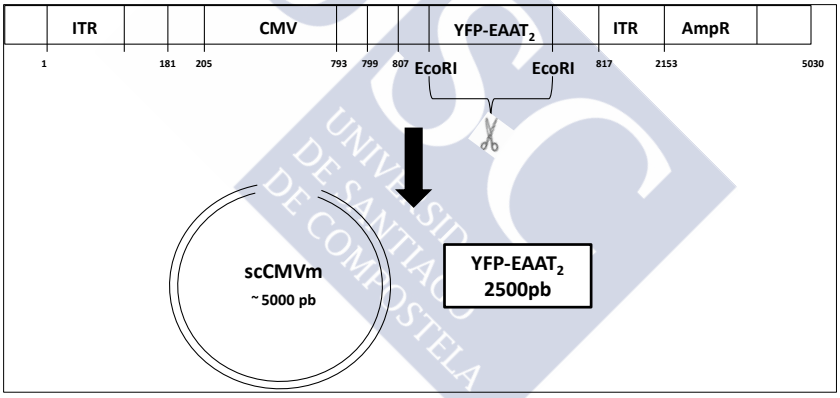

Figure 41: Isolation of the sequence YFP-EAAT2 from the clone 4 with EcoRI.

Then the fragment of interest ($EAAT_2$) was amplificated by means of PCR in combination with the probe Ha-tag and 2 restriction sites for EcoRI and XbaI, indicated in the Figure 42.

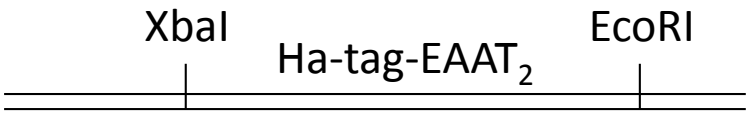

Figure 42: Representation of the sequence Ha-tag-$EAAT_2$.

The PCR-fragment was composed of $EAAT_2$-gen bound to the probe Ha-tag and to the restriction sites for EcoRI and XbaI. Then, this fragment was purified, digested with EcoRI and XbaI, submitted to electrophoresis and purificated again (Figure 43A). Later, the insert Ha-tag-$EAAT_2$ was obtained and it was ready for cloning in the viral vector (scCMV). Previously to the clonation, the viral vector was linearized with EcoRI and XbaI (Figure 43 B). Then, the appropriate ligation reaction mixtures were done (Figure 44) and used to the transformation of competent cells, which were grown in selective medium with ampicillin (see Material and Methods).

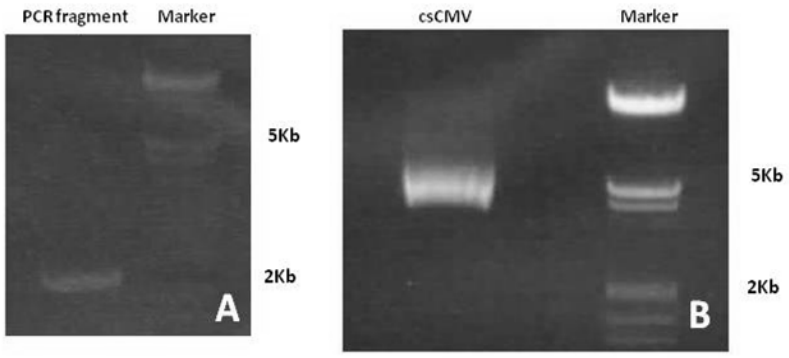

Figure 43: (A) Electrophoresis of PCR fragment composed of $EAAT_2$-gen bound to the probe Ha-tag and to the restriction sites for EcoRI and XbaI. (B) scCMV vector linearized by restriction with EcoRI and XbaI.

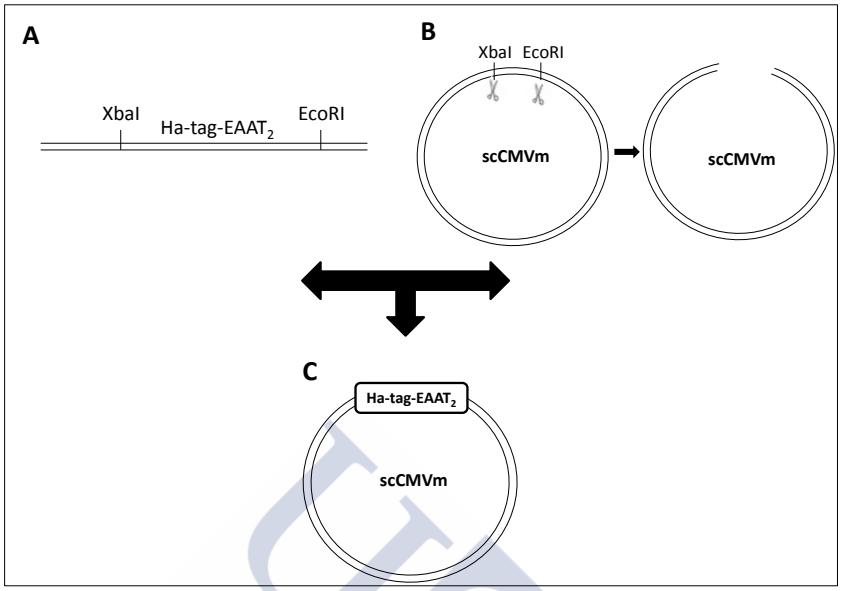

Figure 44:(A)The sequence of XbaI-Ha-tag-$EAAT_2$-EcoRI was created by means PCR amplification.(B)Linearization of the viral vector with XbaI and EcoRI.(C)Ligation process in which the Ha-Tag-$EAAT_2$ was inserted in the scCMVm.

Apparently those colonies that grew as a result of the ligation (100 colonies) had the insert Ha-Tag-$EAAT_2$ cloned in the viral vector scCMV. Fourteen colonies were picked and seemed in LB medium. Later, the plasmid DNA from the different colonies were isoleted and digested with the following restriction enzymes: EcoRI, XbaI, SmaI and AhdI.

The restriction with XbaI and EcoRI should created 2 fragments: ~1500pb (Hag-tag-$EAAT_2$) and ~5000pb (backbone of the viral vector) (Figure 45). The result of the digestion with EcoRI and XbaI showed that all the clones had the sequence Ha-Tag-$EAAT_2$ (except the clones 8, 10 and 12) (Figure 46).

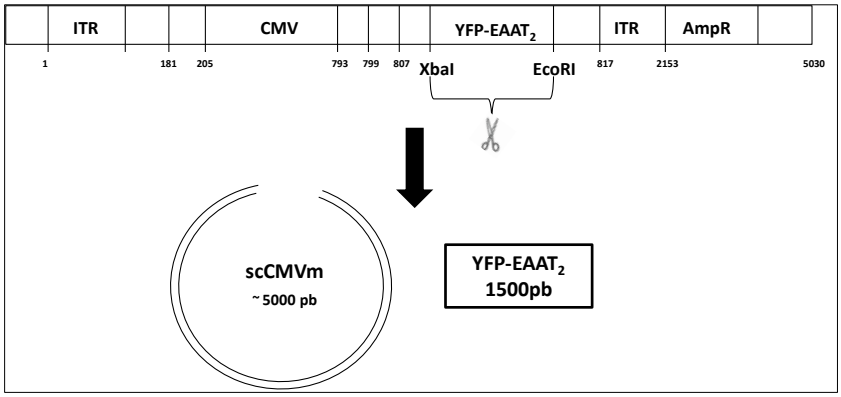

Figure 45: The restriction with XbaI and EcoRI should create 2 fragments: ~1500pb (Hag-tag-EAAT$_2$) and ~5000pb (backbone of the viral vector).

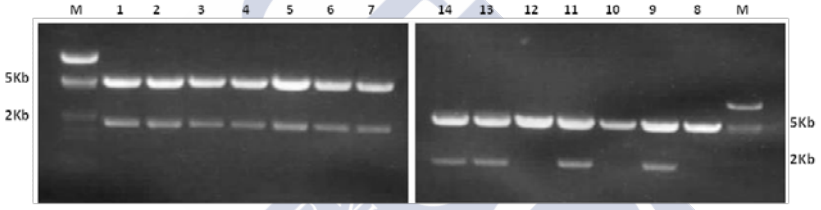

Figure 46: Resctriction with EcoRI and XbaI showed that all the clones had the sequence Ha-Tag-EAAT$_2$ (except the clones 8, 10 and 12).

Then, the selected clones, which contained the insert Ha-tag-EAAT$_2$, were submitted to digestion with SmaI and AhdI to verify that the insert was in the right direction. Again the viral vector was digested with the same enzymes as a control restriction. The restriction with SmaI for scCMVm should originate the same fragments mentioned in section 0. SmaI should produce fragments with a size of ~2772pb, ~3758pb and 2 fragments of 11 pb for the clone digestion (Figure 47:

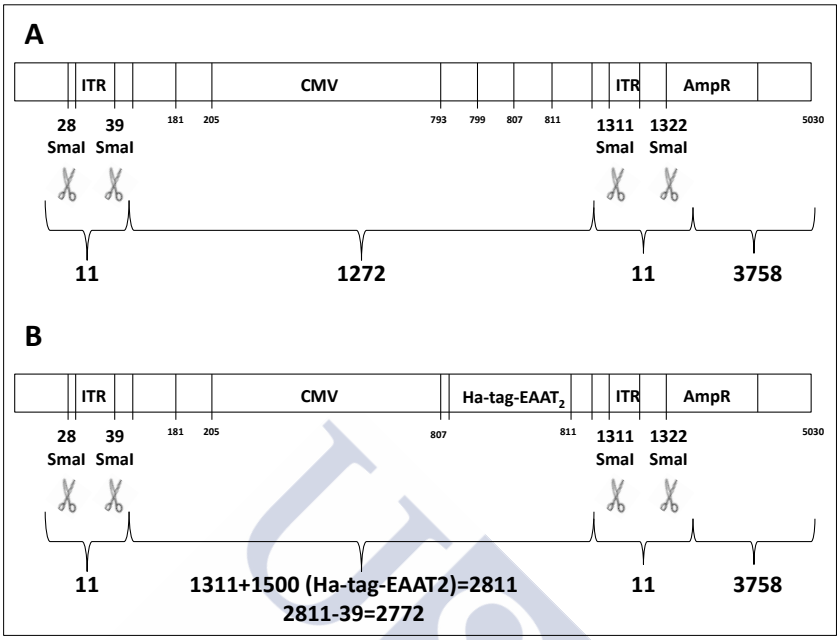

Figure 47: (A)The restriction of the vector with SmaI should generate 4 fragments (~ 3702 pb, ~1300 pb and 2 of 11pb).(B)Digestion with SmaI for the different clones should produce 4 fragments (which sizes were ~3758 pb, ~2772 pb and 2 of 11pb).

The digestion of the viral vector with AhdI produced the same fragments that were mentioned above. Three fragments were generated (~2739pb, ~2629pb and ~1128pb) (Figure 48 and 18).

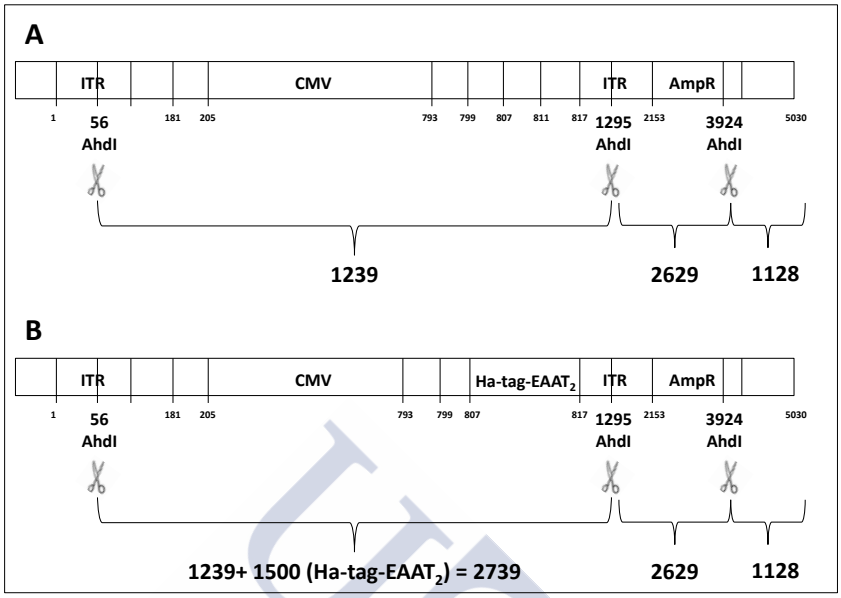

Figure 48: (A) The digestion with AhdI of the viral vector should generate 3 fragments (~1239pb, ~2629 pb and ~1128 pb).(B)The restriction with AhdI for the clones should produce 3 fragments (~2739pb, ~2629 pb and ~1128 pb).

The results of restrictions with AhdI showed that the viral vector was digested correctly, because the number and size of the fragments were the expected. The restriction was right for the clones 3, 5, 6, 9 and 11 (Figure 49A).

In case of SmaI enzymatic analysis, the viral vectors generated the expected fragments (~3758pb, ~2772pb). All clones studied contained both fragments (Figure 49B).

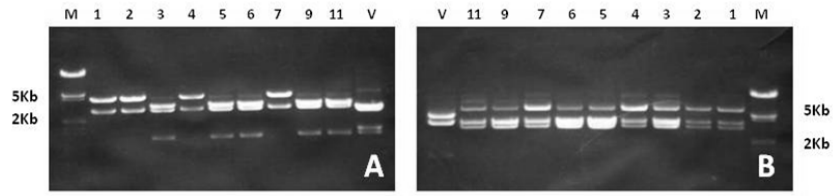

Figure 49: (A) Restriction with AhdI showed that clones 3, 5, 6, 9 and 11 originated the expected fragments.(B) The result of the restriction with SmaI exhibit that all the clones produced the correct fragments.

The results indicated that the clones 3, 5, 6, 9 and 11 had the insert in the right position (Figure 49). Again, this final result indicated that this plasmid-DNA (viral vector and Hag-tag-EAAT$_2$) was prepared for viral encapsulation.

8.2. Infection of MSC with different serotypes of virus rAAV-GFP

In this point, we have plasmid-DNA (viral vector with YFP-EAAT$_2$ or with Hag-tag-EAAT$_2$) available for viral encapsulation, however it was previously necessary to know the viral capside to get the cell infection (important in case MCSs).

With this aim, six viral serotypes (1, 2, 4, 5, 6 and 8) from rAAV-GFP were tested on cells (MCSs). Microscopy analysis showed that serotypes 2 and serotype 6 were the only ones that could infect the MCSs as it can be observe in the Figure 50. Therefore serotypes 2 and 6 were used for subsequently production.

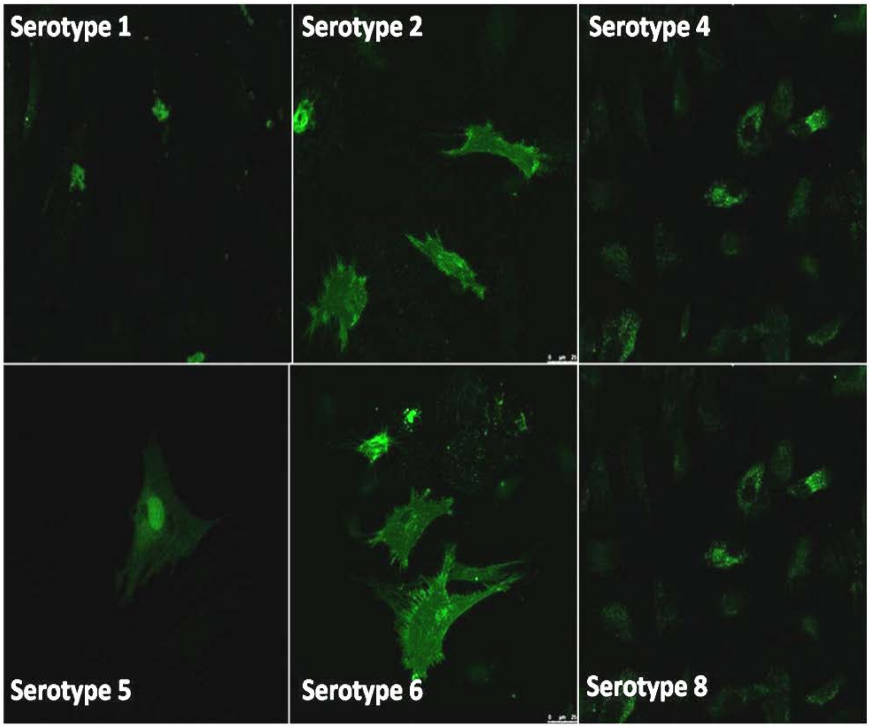

Figure 50: Transduction of MCSs with 6 different types of serotypes (rAAV-YFP), 1, 2, 4, 5, 6, 8. Serotype 2 and 6 were the ones which could infect the MSC.

8.3. Production and purification of recombinant adeno-associated viruses (rAAVs)

Based on the previous results of transduction with different serotypes in MSCs, serotypes 2 and 6 were chosen for the production of rAAV virus, which should incorporate the sequence Ha-tag-$EAAT_2$ and YFP-$EAAT_2$. Therefore 4 types of virus were generated: rAAV-YFP-$EAAT_2$ serotype 6, rAAV-Ha-tag-$EAAT_2$ serotype 6, rAAV-YFP-$EAAT_2$ serotype 2 and rAAV-Ha-tag serotype 2, according to the protocol described in Materials and Methods. Real-time PCR was used for the viral tittering as appear indicated in the Table 18.

	Serotype 6	Serotype 2
YFP-EAAT$_2$	1.227x10^{7}pv/ µl	6.538x10^7 pv/ µl
Ha-tag-EAAT$_2$	3.666x10^{8}pv/ µl	1.842x10^{8}pv/ µl

Table 18: Titer of virus.

8.4. Exogenous expression of EAAT$_2$ on MSCs cells through viral infection

In order to induce the exogenous EAAT$_2$ expression in MSCs, viral infection was performed as it is described in Material and Methods. Toxicity and efficiency of infection were also tested.

8.4.1. Infection with rAAV-YFP-EAAT$_2$ (serotypes 2, 6) and rAAV-Ha-Tag-EAAT$_2$ (serotypes 2, 6) of MSCs

The MSCs were infected with virus rAAV-YFP-EAAT$_2$ (serotypes 2, 6) and rAAV-Ha-Tag-EAAT$_2$ (serotypes 2, 6) and the toxicity was evaluated by LDH assay.

Infection of MCSs with rAAV6-YFP-EAAT$_2$ did not show toxicity effect respect to the control groups (% respect to control group) (Table 19 and Figure 51A).

rAAV6-YFP-EAAT$_2$	**24h**	**48h**	**72h**
Control	100±5	100±6	100±5
Vehicle	101±8	98±10	100±5
MOI: 1x10^{10}	101±3	96±6	98±16
MOI: 5x10^9	101±1	99±5	98±4
MOI: 1x10^9	99±9	100±11	99±6

Table 19: Toxicity analysis induced for different MOI of rAAV6-YFP-EAAT$_2$, determined by means of LDH assay. Data are represented as % respect to the control values (n=3)

The same result was obtained when the rAAV6-Ha-tag-EAAT$_2$ was used (Table 20 and Figure 51B).

rAAV6-Ha-tag -EAAT$_2$	24h	48h	72h
Control	100±5	100±6	100±5
Vehicle	89±10	88±12	92±7
MOI: 1x10^{10}	93±6	92±7	97±10
MOI: 5x10^9	92±6	93±3	96±8

Table 20: Toxicity analysis induced for different MOI of rAAV6-Ha-tag-EAAT$_2$ on MSCs, determined by means of LDH assay. Data are represented as % respect to the control values (n=3).

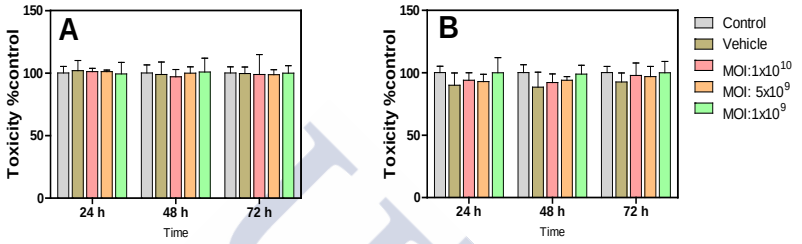

Figure 51: Toxicity analysis induced for different MOI of (A) rAAV6-YFP-EAAT$_2$ and (B) rAAV6-Ha-tag-EAAT$_2$ on MSCs, determined by means of LDH assay. Data are represented as % respect to the control values (n=3).

Analysis of the toxicity effect on MSCs induced for virus rAAV2-YFP-EAAT$_2$ (Table 21 and Figure 52A) and rAAV2-Ha-tag-EAAT$_2$ (Table 22 and Figure 52B) infection, showed that both infections did not cause toxicity respect to the control group.

rAAV2-YFP-EAAT$_2$	24h	48h	72h
Control	100±5	100±8	100±3
Vehicle	86,0±0,7	90,0±0,4	93±1
MOI: 1x10^{10}	90±4	89±11	90±13
MOI: 5x10^9	93±5	92±6	98±16
MOI: 1x10^9	118±9	100±3	101±6

Table 21: Analysis of toxicity induced for different MOI of rAAV2-YFP-EAAT$_2$ on MSCs determined by means LDH assay. Data are represented as % respect to the control group (n=3).

rAAV2-Ha-tag -EAAT$_2$	24h	48h	72h
Control	100±5	100±8	100±3
Vehicle	90±9	92±15	96±3
MOI: 1x10^{10}	92±10	92±7	97±14
MOI: 5x10^9	96±13	98±4	94±7

Table 22: Analysis of toxicity induced for different MOI of rAAV2-Ha-Tag -EAAT$_2$ on MSCs determined by means LDH assay. Data are represented as % respect to the control group (n=3).

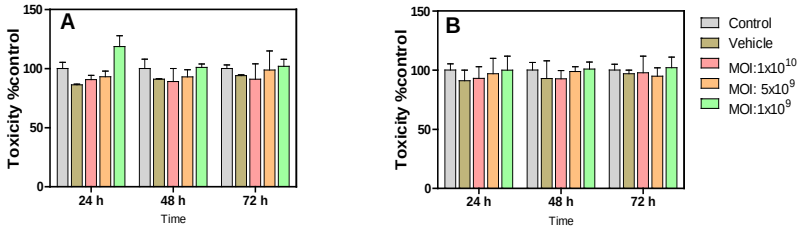

Figure 52: Analysis of toxicity induced for different MOI of (A) rAAV2-YFP-$EAAT_2$ and (B) rAAV2-Ha-Tag -$EAAT_2$ on MSCs determined by means LDH assay. Data are represented as % respect to the control group (n=3).

The three MOI tested in the experiments of toxicity were used on MSCs to induce the $EAAT_2$ expression. Unfortunately, all viruses probed, rAAV-YFP-$EAAT_2$ (serotypes 2 and 6) and rAAV-Ha-Tag-$EAAT_2$ (serotypes 2 and 6), did not show an efficient expression of the protein (YFP or Ha-Tag) analyzed by fluorescence microscopy (results not shown). Resume of the viral production and MSCs infection is represented in the Figure 53.

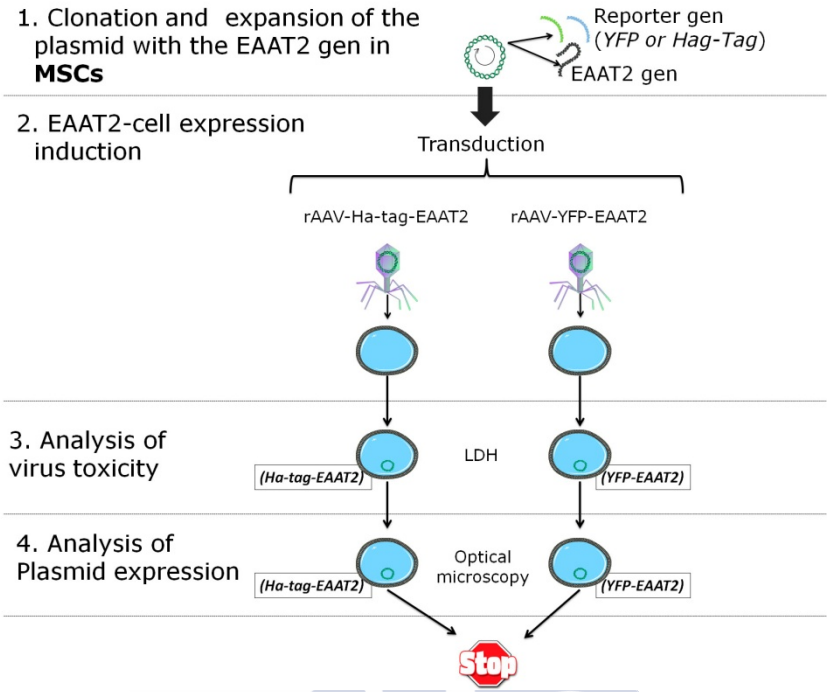

Figure 53: Resume of the viral production and MSCs infection. (1) Synthesis of constructors and viral production. (2) MSCs viral infection. (3) Analysis of viral toxicity (LDH). (4) Analysis of gen-reporter expression (microscopy analysis).

8.5. Exogenous expression of $EAAT_2$ on MSCs cells through transfection techniques

Due to the viral infection used to induce the $EAAT_2$ expression did not showed successful result, the following transfection techniques were probed: phosphate calcium transfection, lipofectamine transfection and electroporation transfection. The phosphate calcium technique was discarded because of the elevated toxicity and the low efficiency of transfection (data not shown), lipofectamine transfection had also to be discarded due to the low efficiency of transfection, therefore electroporation transfection was chosen.

8.5.1. Electroporation of MSCs

MSCs were submitted to electroporation procedure according the protocol described in Materials and Methods. Briefly, 4 µg of pRcCMVm-YFP-EAAT$_2$ plasmid per 1x10^6 MSCs were used in the electroporation procedure. Microscopy analysis showed YFP- positive cells (yellow fluorescence) demonstrating the efficacy of this transfection procedure (Figure 54).

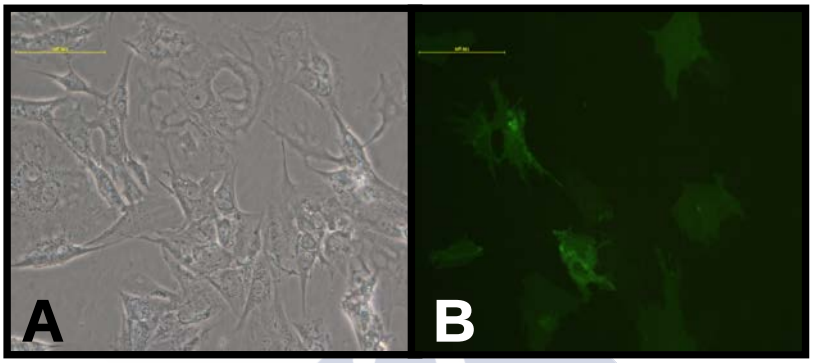

Figure 54: Microscopy analysis of the MSCs electroporation transfection. (A) Phase contrast image of MSCs.(B) MSC transfected positive YFP (scale bar 100µm).

To evaluate the harmful effect of the technique on the cells, the proliferation ratio and toxicity (LDH assay) were evaluated. Table 23 and Figure 55 show that the transfection produces a significant ($p<0.05$) reduction of proliferation rate 48h after assay, however this effect is reverted after 72 h.

	24h	48h	72h
Non-transfected MSCs	100±13	100±6	100±16
Transfected MSCs	69±5	71±11	89±12

Table 23: Analysis of the transfection on MSCs proliferation rate. Data are expressed as % respect to the non-transfected at 24 h. Data are compared at each time-point respect to the non-transfected cells.(n=3).

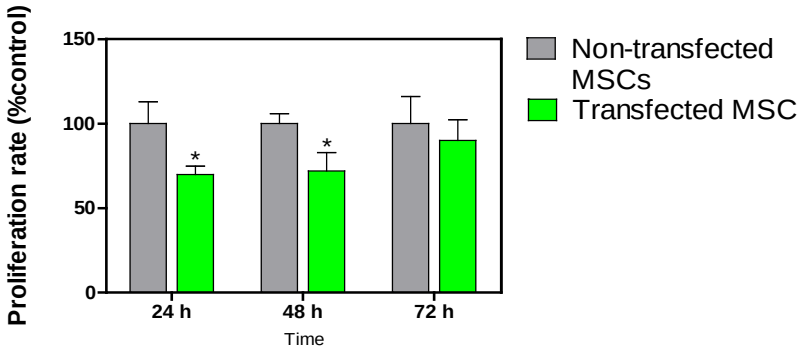

Figure 55: Analysis of the transfection on MSCs proliferation rate. Data was expressed as % respect to the un-transfected at 24 h. Data was compared at each time-point respect to the un-transfected cells. (n=3).

However, as it can be observed in Table 24 and Figure 56, there were not significant differences between non-transfected MSC (MSC-) and transfected MSC (MSC+) in terms toxicity (referred to control %) measured by LDH assay.

	24h	48h	72h
Non-transfected MSCs	100±13	100±11	100±9
Transfected MSCs	78±9	82±13	85±16

Table 24: Toxicity measured by means LDH assay demonstrates that there were significant differences between MSC- and MSC+, (n=3).

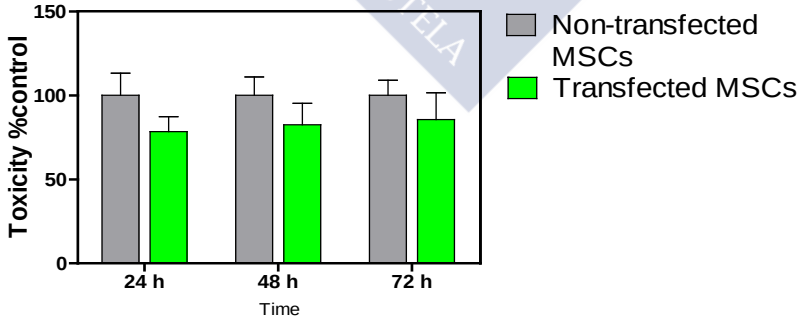

Figure 56: Toxicity measured by means LDH assay demonstrates that there were significant differences between MSC- and MSC+, (n=3).

8.5.2. Analysis of the reporter gen YFP in MSC

Through of fluorescence microscopy it was determined that the electroporation transfection induced an efficient expression of the gen-reporter (YFP) in transfected MSCs. The next step was to determine the time-point where the expression of the gen-reporter was higher. For that, the gen YFP expression was analyzed in the MSC+ by flow cytometry at various time-points (Figure 57). Flow cytometry analysis showed that the transfection efficiency of the electroporation was 60%, being the maximum expression at 48h after the transfection. After this point, the percentage of transfected cells (MSC+) started to decrease. Analysis of non-transfected cells (MSC-) showed that they were negatives for YFP analysis.

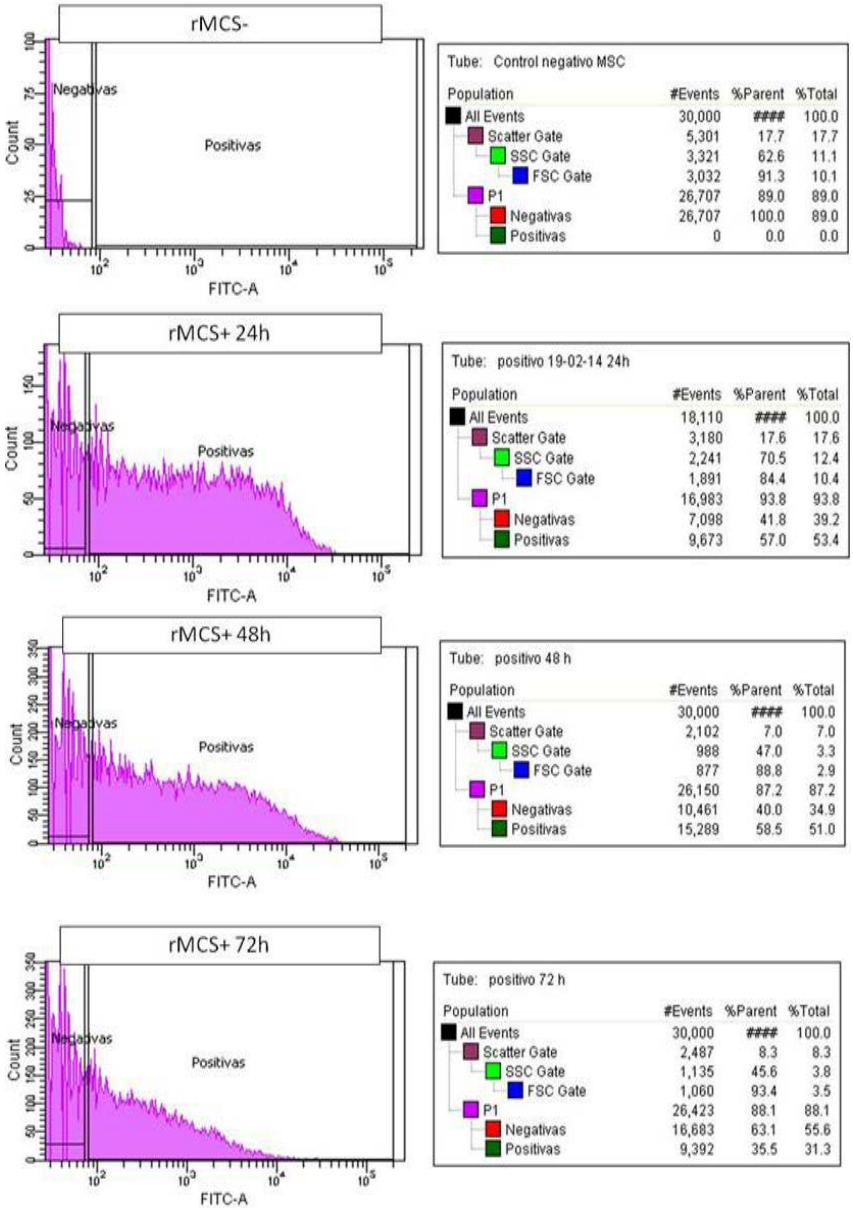

Figure 57: Analysis of gene expression YFP by flow cytometry. The maximum expression of YFP was at 48 h after electroporation. After this point, the percentage of transfected cells (MSC+) started to decrease. Analysis of MSC- (non-transfected cells) showed that they were negatives for YFP analysis

8.5.3. Analysis of the expression of $EAAT_2$ on MSC+

In order to assess the expression of $EAAT_2$ in MSC+, immunostaining of $EAAT_2$ and confocal microscopy were performed. The results showed in Figure 58 indicate that MSC+ was positive for YFP (Figure 58B) and $EAAT_2$. MSCs- (Figure 58A), YFP-negative cells, were negative for $EAAT_2$ staining. These results demonstrated the expression of $EAAT_2$ on MSC+.

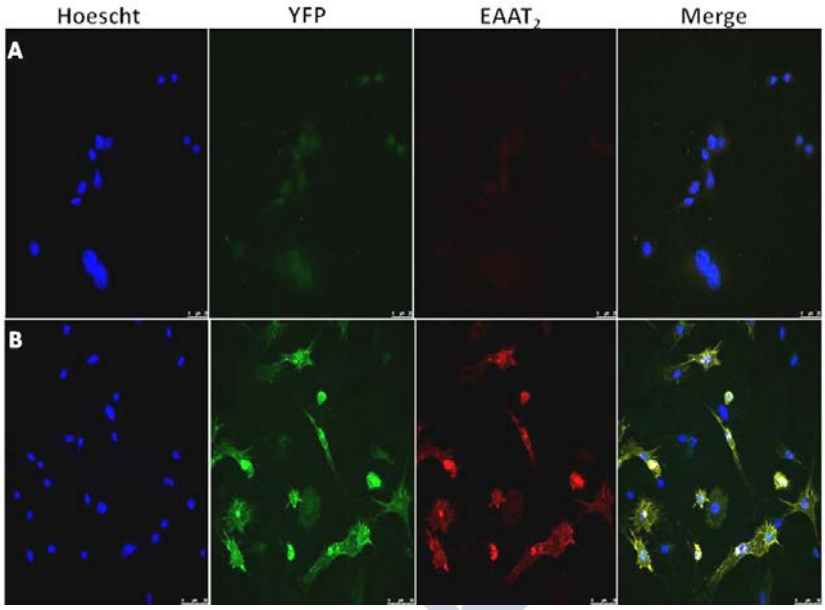

Figure 58: Immunostaining of $EAAT_2$.(A) MSCs- were negative for YFP expression and for $EAAT_2$ staining.(B) MSC+ expressed YFP that colocalize with the $EAAT_2$ staining.

Colocalization of YFP and $EAAT_2$ is showed in detail, in the Figure 59 and Figure 60.

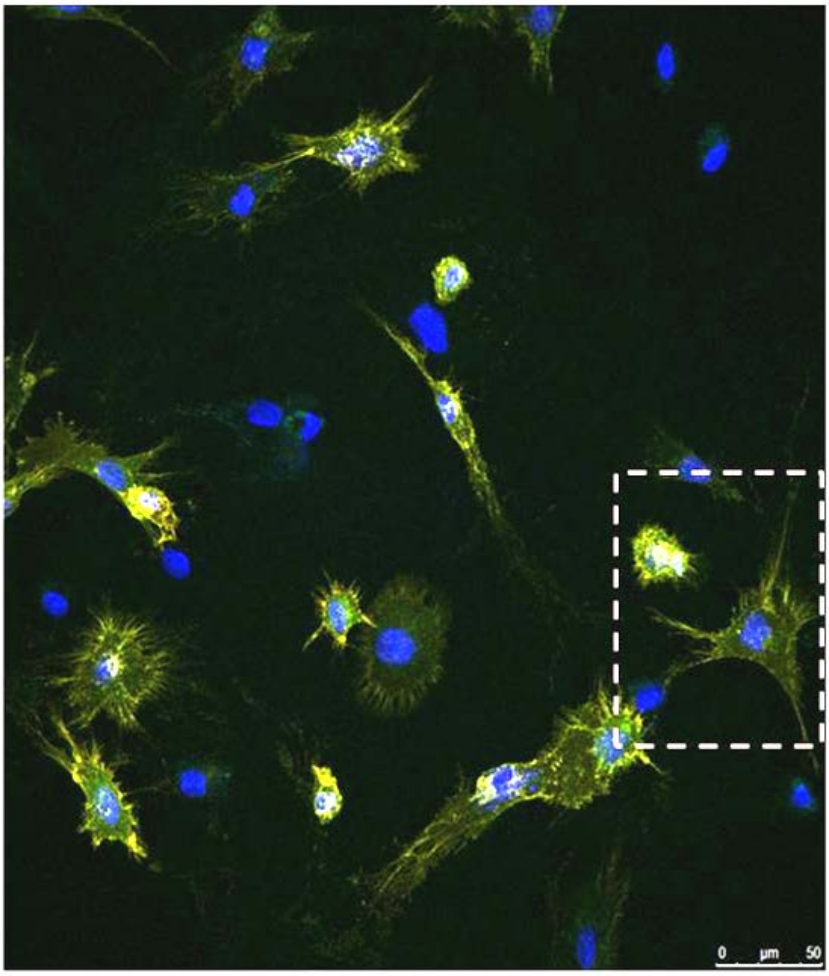

Figure 59: Colocalization of $EAAT_2$ and YFP on MSC+

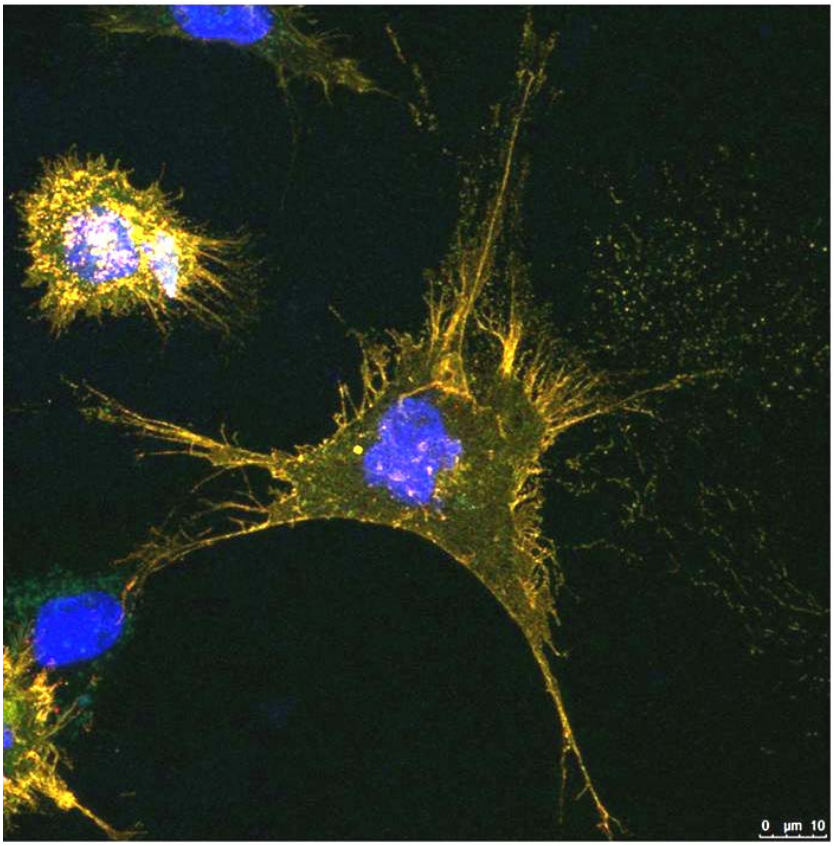

Figure 60: Detail of colocalization of $EAAT_2$ and YFP on MSC+

8.5.4. Characterization of the functionality of the $EAAT_2$ in MSC+

To verify the functionality of the $EAAT_2$ expressed in MSCs, glutamate uptake experiments were carried out. Previously, to optimize the experimental protocol, this assay was performed in astrocytes, cells that express endogenously the EAATs. We found that glutamate uptake in astrocytes was reduced significantly in the presence of excess of unlabeled glutamate (1mM) that demonstrated a specific uptake of glutamate (Table 25 and Figure 61). The uptake of glutamate was also measured in the presence of specific EAAT inhibitors, DHK and TBOA. DHK (dihydrokainic acid) is a selective inhibitor of $EAAT_2$, and TBOA (DL-threo-beta-Benzyloxyaspartate) a nonspecific inhibitor of EAAT1, 2, and 3. We found that 500µM DHK and 300µM TBOA inhibit the glutamate uptake into astrocytes.

Glutamate Concentration	Astrocytes	Astrocytes (DHK&TBOA)
1µM	100±1,4	4,0±0,70
10µM	93±3	3,0±0,8
50µM	67±15	3,0±0,3
100µM	26±5	2,0±0,5
250µM	15±4	2,0±0,6
500µM	7±1	2,0±0,3
1mM	4,0±1,8	2,0±0,3
10mM	2,0±0,6	1,0±0,4

Table 25: Glutamate uptake in astrocytes.

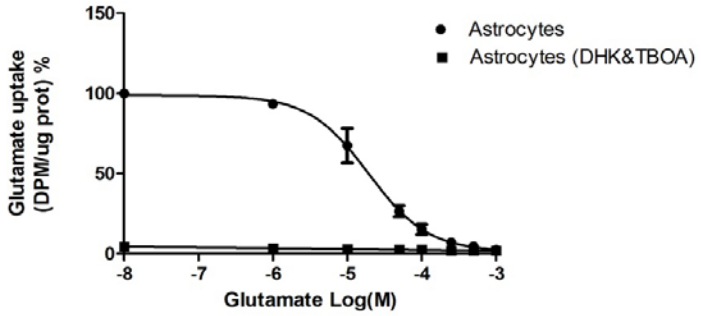

Figure 61: Glutamate uptake in astrocytes.

Analysis of glutamate uptake in MSC+, showed that the MSC+ were able to uptake glutamate specifically considering that the uptake was saturated at elevated concentrations of unlabeled glutamate (1mM) and the MSC- did not present an specific glutamate uptake (Table 26 and Figure 62).

Glutamate concentration	MSC+	MSC-
1µM	100±2	29±24
10µM	97± 3	25±21
50µM	128±21	24±20
100µM	74±44	19±16
250µM	51±38	17±14
500µM	35±21	15±12
1mM	24±17	14±12
10mM	22±19	15±13

Table 26: Glutamate uptake in MSC- and MSC+. Glutamate uptake observed in MSC+ is reduced at 1mM glutamate concentration (n=6).

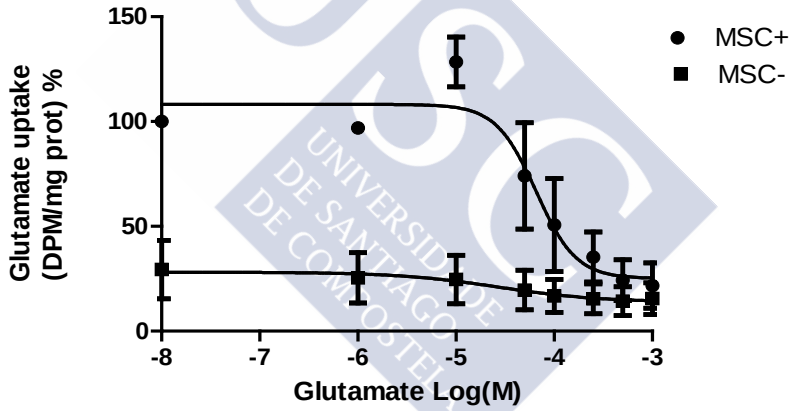

Figure 62: Glutamate uptake in MSC- and MSC+. Glutamate uptake observed in MSC+ is reduced at 1mM glutamate concentration (n=6).

To further characterize the glutamate uptake in MSC+ and determine whether the uptake was mediated by the $EAAT_2$ present on MSC+, glutamate uptake was measured in combination with specific EAATs inhibitors, DHK and TBOA. The results showed that when the assay was performed with 500µM DHK and 300µM TBOA, the glutamate uptake was abolished (Table 27 and Figure 63).

Glutamate concentration	MSC+	MSC+(DHK&TBOA)
1µM	100±2	37±7
10µM	97± 3	24,0±0,7
50µM	128±21	30±4
100µM	74±44	35±21
250µM	51±38	30±8
500µM	35±21	21±9
1mM	24±17	23±3
10mM	22±19	19±7

Table 27: Selective inhibition of uptake glutamate mediated by DHK and TOBA in MSC+, (n=6).

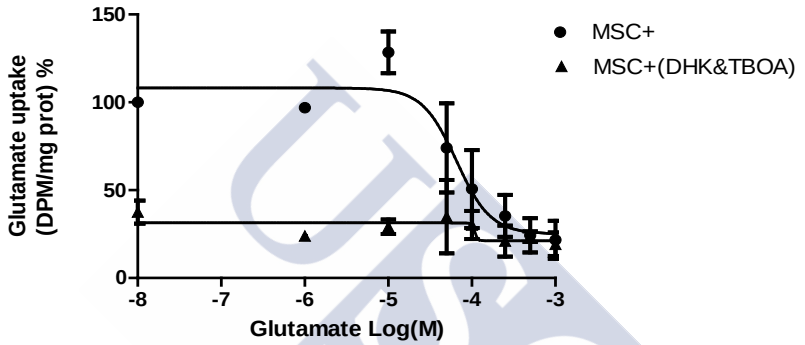

Figure 63: Selective inhibition of uptake glutamate mediated by DHK and TOBA in MSC+, (n=6).

The effect of DHK and TOBA were also evaluated individually on glutamate uptake. In Table 28 and Figure 64 it can be observed that glutamate uptake was inhibited ($p<0.05$) when DHK (500µM) alone or in combination TBOA (300µM) were used. However the glutamate uptake reduction observed with TBOA (300µM) alone was not significant.

Group	10µM
MSC+	13±5
MSC+ (DHK)	4,9±0,8
MSC+ (TBOA)	9,4±1,6
MSC+ (DHK&TBOA)	4,4±0,6

Table 28: Uptake assay of glutamate using specific inhibitors together and individually.

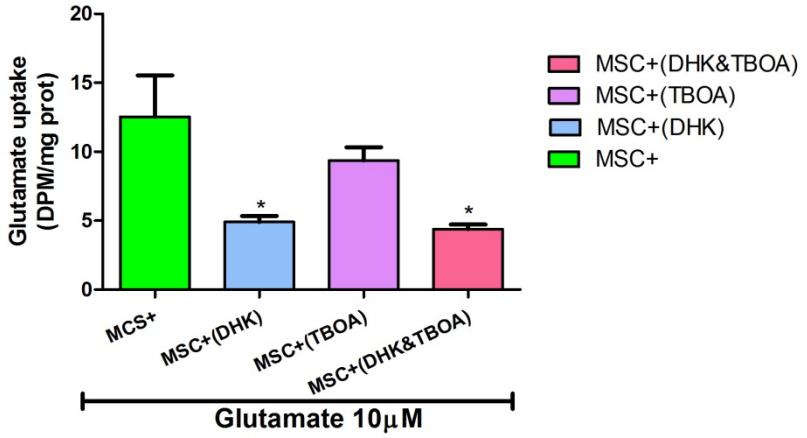

Figure 64: Uptake assay of glutamate using specific inhibitors together and individually.

8.6. Analysis of MSC+

The MSCs have endogenous characteristics that can be altered after transfection process. Therefore specific markers of MSCs phenotype, angiogenic capacity and secretion of VEGF were analyzed in MSC- and MSC+.

8.6.1. Flow cytometry

In order to evaluate phenotypic changes after transfection, CD45, CD90 and CD73 (membrane markers) were studied by means of flow cytometry in MSC- and MSC+. In Figure 65, it can observe $CD90^{+}$, $CD73^{+}$ and $CD45^{-}$ appear expressed in MSC- (that confirm the mesenchymal phenotype of the cells used). Analysis of MSC+ confirmed similar mesenchymal phenotype than MSC- after transfection.

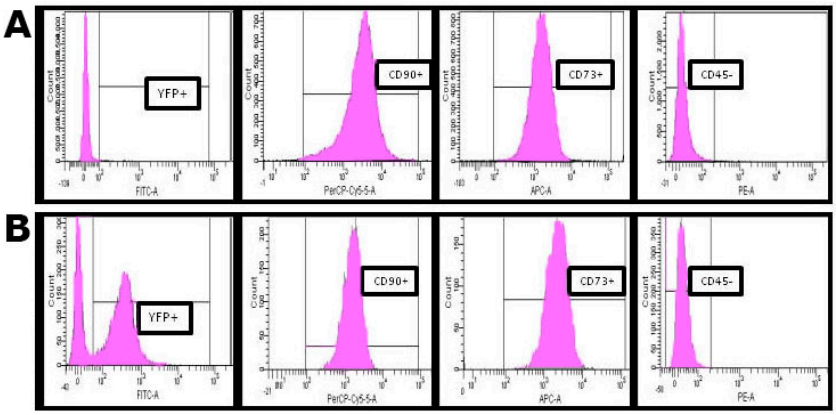

Figure 65: (A) Flow cytometry graphs of MSC- showed that the typical phenotype CD90^{+}, CD73^{+} and CD45^{+}. (B) Flow cytometry graphs of MSC+ demonstrated that the electroporation did not affected to the phenotype due to MSC+ were positive for CD90 and CD73 and negative for CD45.

8.6.2. Matrigel angiogenesis assay

The angiogenic capacity of MSC+ was also studied. In Figure 66B it can appreciate that MSC+ maintained the angiogenic properties without significant differences respect to MSC- (Figure 66A).

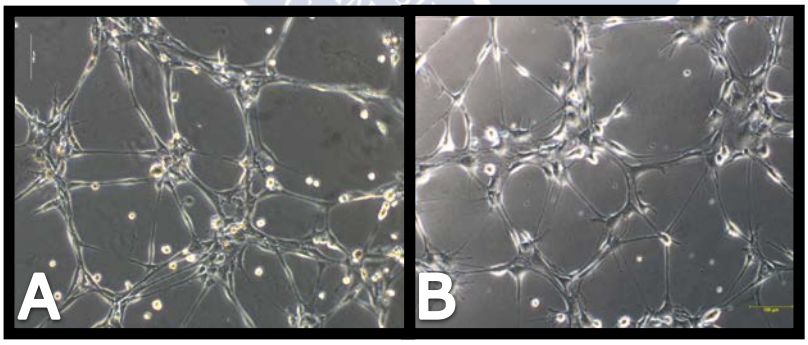

Figure 66: Microscopy contrast phase image of matrigel angiogenic assay with (A) MSC- and (B) MSC+, (scale bar 100µm).

The number of rings (an objective parameter of angiogenic activity) it was also analyzed and the results showed that there were not differences observed between MSC- and

MSC+ after the transfection, according with the microscopy image (Table 29 and Figure 67).

	Number of rings
MSC-	19,5±3,5
MSC+	18,5±0,7

Table 29: Number of rings formation of MSC- and MSC+ were analyzed by means of matrigel angiogenic assay with the aim to determine the influence of transfection of cell angiogenic activity, (n=3).

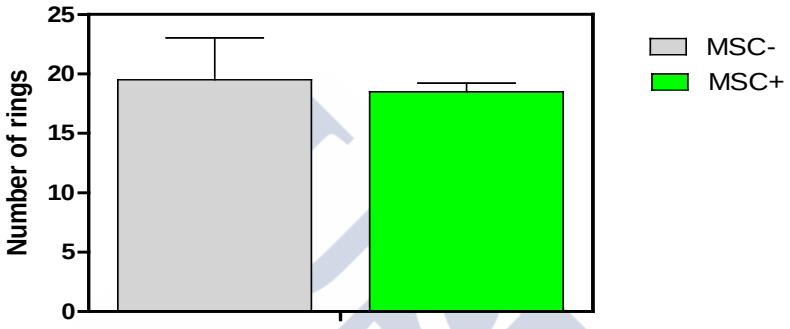

Figure 67: Number of rings formation of MSC- and MSC+ were analyzed by means of matrigel angiogenic assay with the aim to determine the influence of transfection of cell angiogenic activity, (n=3).

8.6.3. VEGF assay

VEGF, a growth factor released for MSCs were also measured. Levels of VEGF corrected for protein showed that there were not differences between MSC- and MSC+ at different time-points (Table 30 and Figure 68).

	24h	48h
MSC-	7,43±0,33	8,44±0,22
MSC+	7,98±0,43	8,13±0,15

Table 30: VEGF release (pg/ml per µg protein) were determined at different time-points in MSC- and MSC+, (n=6).

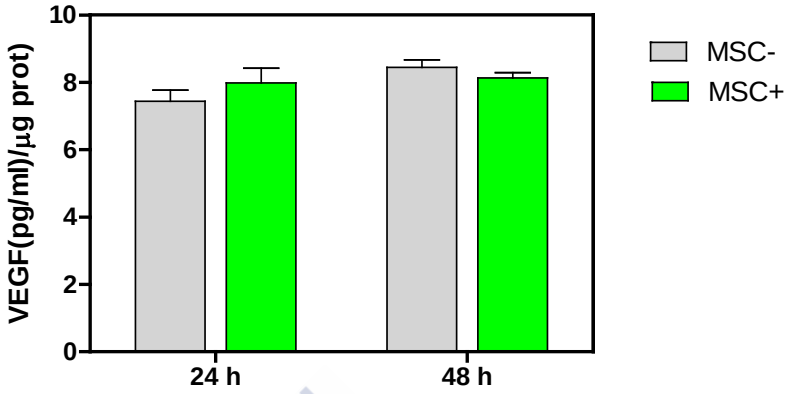

Figure 68: VEGF release (pg/ml per µg protein) were determined at different time-points in MSC- and MSC+, (n=6).

In Figure 69 it can be observed the resume of all employed techniques to express the $EAAT_2$ in MSCs. Only the electroporation turned out useful to induce the expression of $EAAT_2$ on MSCs.

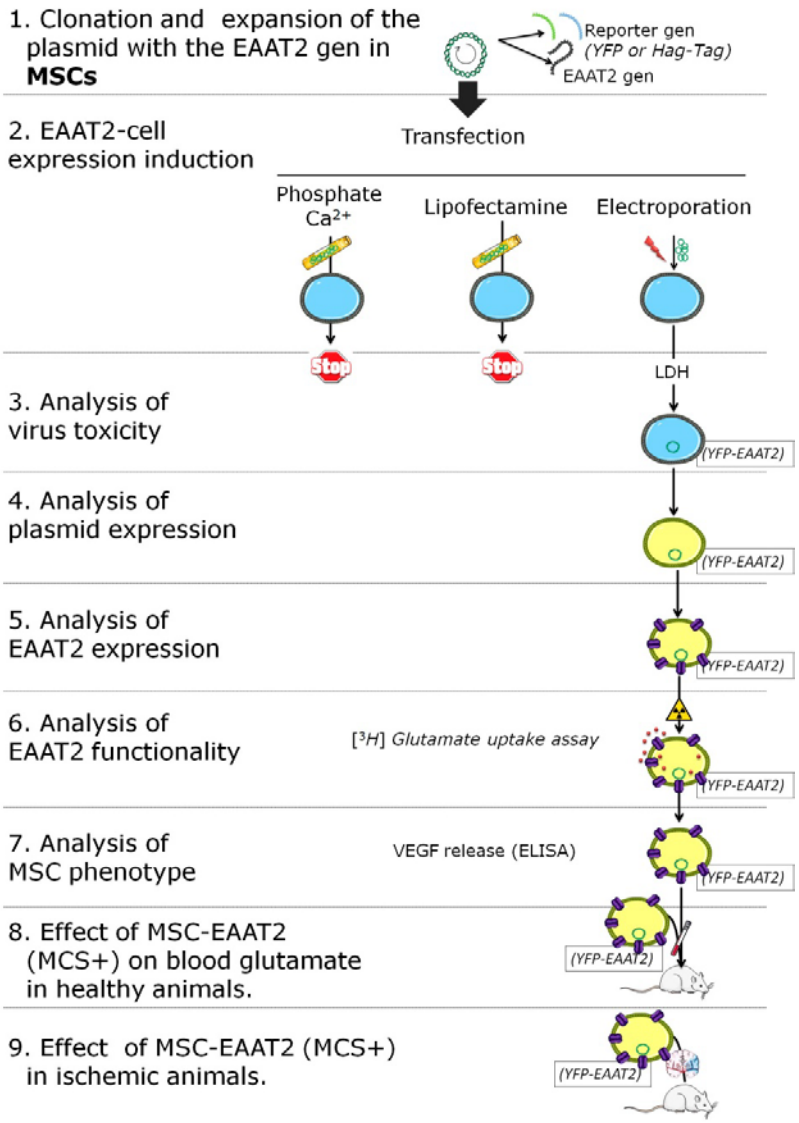

Figure 69: Resume of the procedures used to induce the expression of $EAAT_2$ in MSCs. (1) Synthesis of constructors and viral production. (2) MSCs transfection. (3) Analysis of transfection toxicity (LDH assay). (4) Analysis of gen-reporter expression (microscopy fluoresce and flow cytometry). (5) analysis of $EAAT_2$ expression (confocal microscopy).(6) analysis of $EAAT_2$ functionality ($[^3H]$ glutamate uptake. (7) Analysis mesenchymal phenotype (microscopy fluoresce and flow cytometry and VEGF release). Only the electroporation protocol could be used induce the expression of $EAAT_2$ on MSCs with the aim to test the effect of $EEAT_2$-cell on (8) blood glutamate and (9) in ischemic animal model.

8.7. Expression of $EAAT_2$ on HEK cells across viral infection

In addition to MSCs, exogenous expression of $EAAT_2$ was also tested in other type of cells without described effect on blood glutamate level and ischemic lesion.

With this purpose, HEK cells were chosen to induce the $EAAT_2$ exogenous expression by means of virus infection. Similar than MSCs, viral toxicity and infection efficiency were evaluated and $EAAT_2$ expression and the functionality of were studied.

8.7.1. Infection with rAAV-YFP-$EAAT_2$ (serotypes 2, 6) of HEK cells

HEK cells were infected with the virus rAAV6-YFP-$EAAT_2$ and rAAV2-YFP-$EAAT_2$ according to the protocol mentioned in section Materials and Methods and used for MSCs. After cell infection, cell toxicity was determined by LDH assay. Results showed that there was a not significant difference between the control and the groups after infection with rAAV2-YFP-$EAAT_2$ (Table 31 and Figure 70A) and rAAV6-YFP-$EAAT_2$ (Table 32 and Figure 70B).

rAAV2-YFP-$EAAT_2$	**24h**	**48h**	**72h**
Control	100±32	100±13	100±17
Vehicle	979	96±8	97±14
MOI: $1x10^{10}$	95±12	96±14	95±16
MOI: $5x10^{9}$	104±20	92±15	101±13
MOI: $1x10^{9}$	103±7	103±18	101±9

Table 31: Toxicity analysis induced for different MOI of rAAV6-$EAAT_2$ on HEK determined by means of LDH assay. Data are represented as % respect to the control values (n=3).

rAAV6-YFP-EAAT$_2$	24h	48h	72h
Control	100±7	100±9	100±5
Vehicle	88±8,90	81±3,50	90±9
MOI: 1x10^{10}	92±8	82±7	92±10
MOI: 5x10^{9}	99±5	98±8	96±9
MOI: 1x10^{9}	100±7	100±9	100±5

Table 32: Toxicity analysis induced for different MOI of rAAV6-YFP-EAAT$_2$ on HEK determined by means of LDH assay. Data are represented as % respect to the control values (n=3).

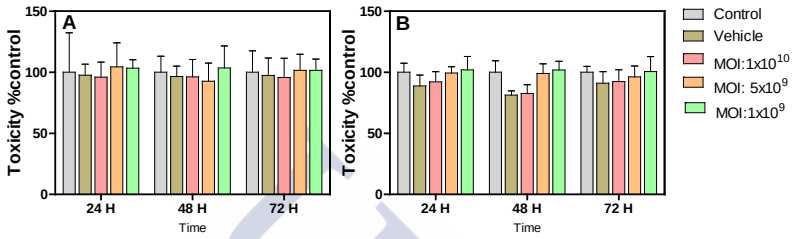

Figure 70: Toxicity analysis induced for different MOI of (A) rAAV6-EAAT$_2$ and (B) rAAV6-YFP-EAAT$_2$ on HEK determined by means of LDH assay. Data are represented as % respect to the control values (n=3).

8.7.2. Analysis of the reporter gene YFP in infected HEK cells

To analyze the YFP expression in HEK cells infected with the virus rAAV2-YFP-EAAT$_2$ was determined with fluorescence microscopy. The Figure 71A showed an image of phase contrast image of culture of HEK cells and in Figure 71B shows the same cell positive for YFP protein, which indicates the YFP-EAAT$_2$ plasmid expression. YFP protein expression was only observed with rAAV2-YFP-EAAT$_2$ virus but not with rAAV6-YFP-EAAT$_2$ (data not shown).

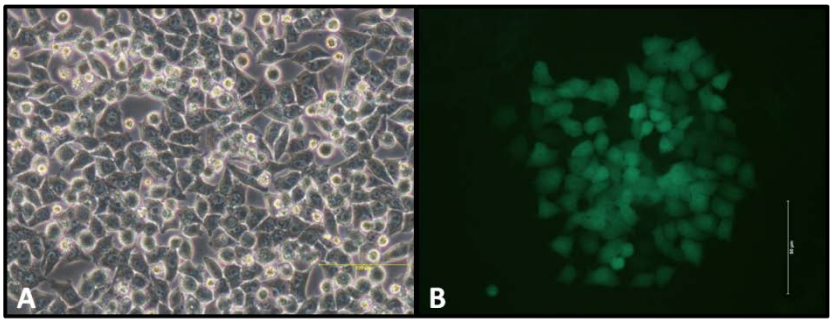

Figure 71: (A) Phase contrast image of culture of HEK cells. (B) HEK cells which expressed the YFP (scale bar 100µm) previously infected with rAAV2-YFP-EAAT$_2$. Infection with rAAV6-YFP-EAAT$_2$ did not showed YFP expression.

Flow cytometry analysis used to determine the infection efficacy of rAAV2-YFP-EAAT$_2$ demonstrated that the percentage of efficiency was around 0.5% after 7 days of infection, that shows the low efficiency of the virus used (Figure 72).

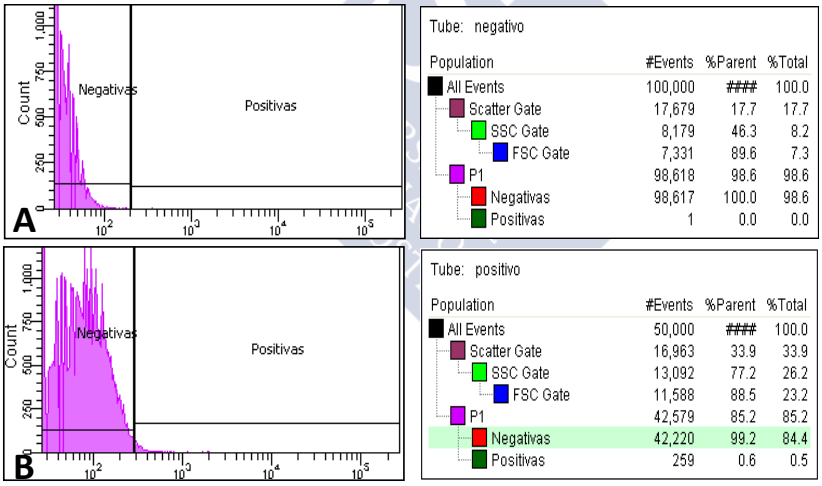

Figure 72: (A) Flow cytometry analysis of non-infected HEK cells and (B) Flow cytometry analysis of HEK cells infected with AAV2-YFP-EAAT$_2$. Only 0.5% of cells infected were positive for YFP expression.

Although the infection efficiency was very low, the culture could be purified and obtain a high percentage of HEK cells positive for YFP by sorting technique. Consequently, after

performing of sorting, the culture was purified to achieve a purity of 90%, which was analyzed by fluorescence microscopy (Figure 73) and flow cytometry (Figure 74).

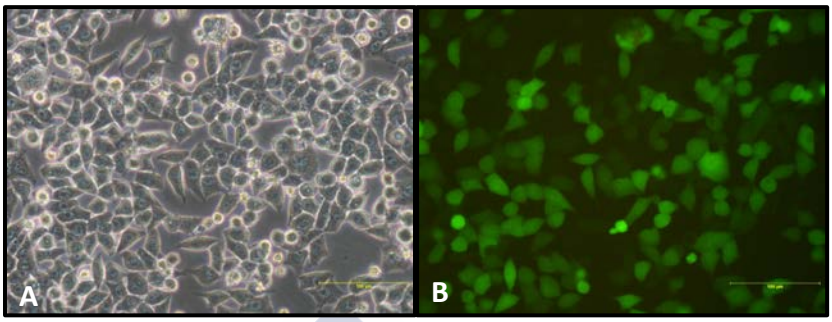

Figure 73: (A) Phase contrast image of HEK cells. (B) Fluorescence image of HEK cells that were submitted to sorting (scale bar 100µm)

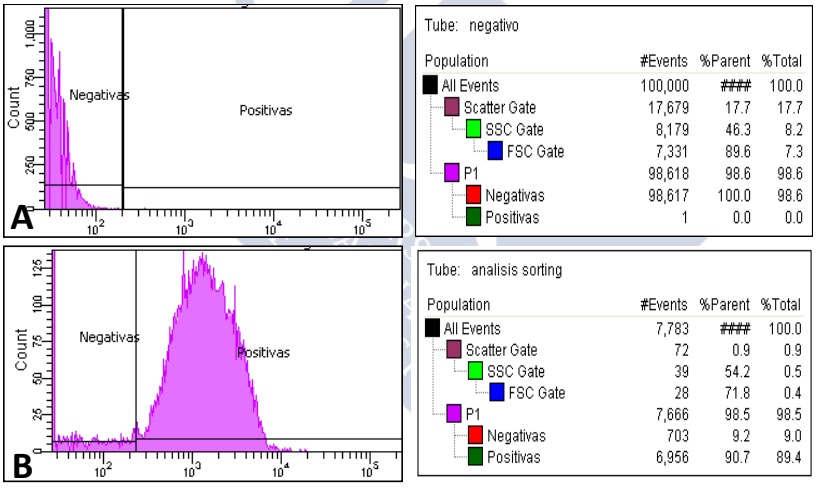

Figure 74: (A) Flow cytometry analysis of non-infected HEK cells and (B) flow cytometry analysis of infected HEK cells after sorting, positive for YFP expression

8.7.3. Analysis of expression of $EAAT_2$ in HEK cells positive for YFP

Sorted HEK cells, positive for YFP expression, infected with AAV2-YFP-$EAAT_2$, were analyzed to determine the expression of $EAAT_2$ by immunofluorescence. Figure 75, showed it could not be detect a clear positive staining for $EAAT_2$.

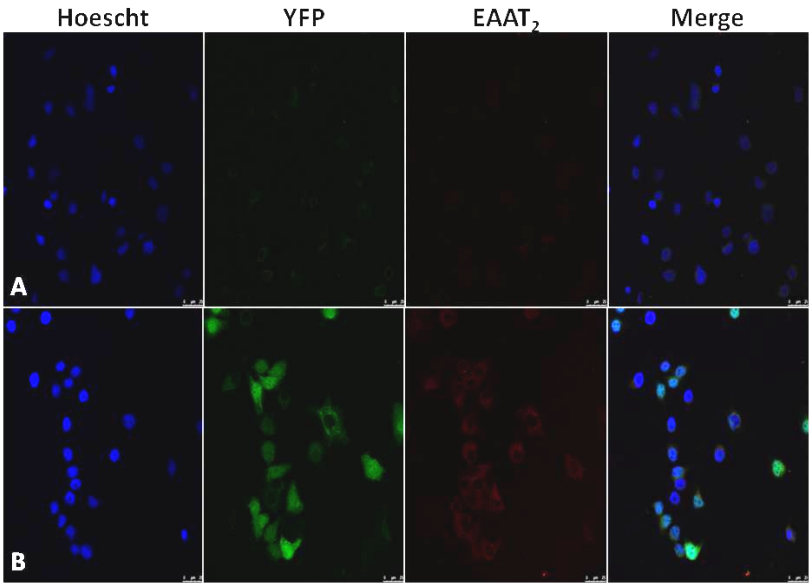

Figure 75: (A) Immunostaining for $EAAT_2$ in HEK negative for YFP. (B) Immunostaining for $EAAT_2$ HEK positive for YFP.

8.7.4. Characterization of the functionality of the $EAAT_2$ in HEK cells positive for YFP

Despite the fact that a clear signal of staining for $EAAT_2$ in HEK positive for YFP was not detected, the functionality of $EAAT_2$ was analyzed by glutamate uptake assay. In line with the previous stating results, HEK cells, positive for YFP, showed an unspecific glutamate uptake, as glutamate uptake was not reduced with higher glutamate concentrations (Table 33 and Figure 76).

Glutamate concentration	HEK-AAV2	HEK+AAV2
1µM	106±50	100±55
10µM	52±10	97±24
50µM	56±3	89±35
100µM	35±14	92±37
250µM	85±40	65±34
500µM	37±9	56±24
1mM	38±6	48±23
10mM	26±3	34±14

Table 33: Glutamate uptake assay with un-infected HEK cells (HEK-AAV2) and infected with virus AAV2-YFP-EAAT$_2$ (HEK+AAV2).

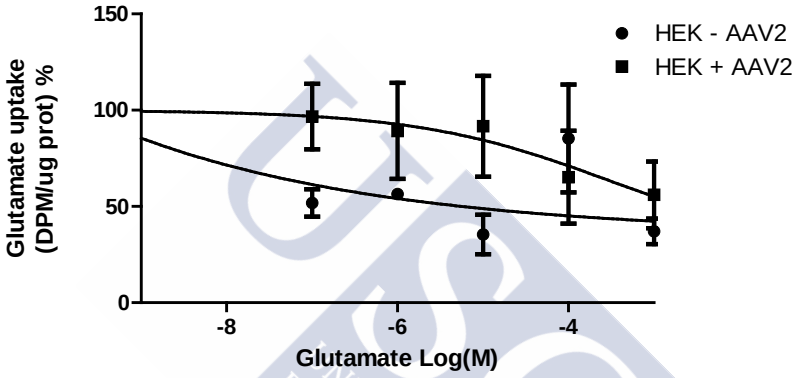

Figure 76: Glutamate uptake assay with un-infected HEK cells (HEK-AAV2) and infected with virus AAV2-YFP-EAAT$_2$ (HEK+AAV2).

Althought the virus did not produce a good results in terms of infection process, employing sorting techniques was achieved purify the culture until a very high percentage of HEK cells were positive for YFP. However, immunofluorescence techniques and glutamate uptake assay showed that the transporter EAAT$_2$ was not correctly expressed, thefore viral infection with AAV2-YFP-EAAT$_2$ used to induce the EAAT$_2$ expression in HEK cells was discarded.

In the Figure 77 it can be observed a summary of the procedures used to achieve expression of EAAT$_2$ by viral infection in HEK cells.

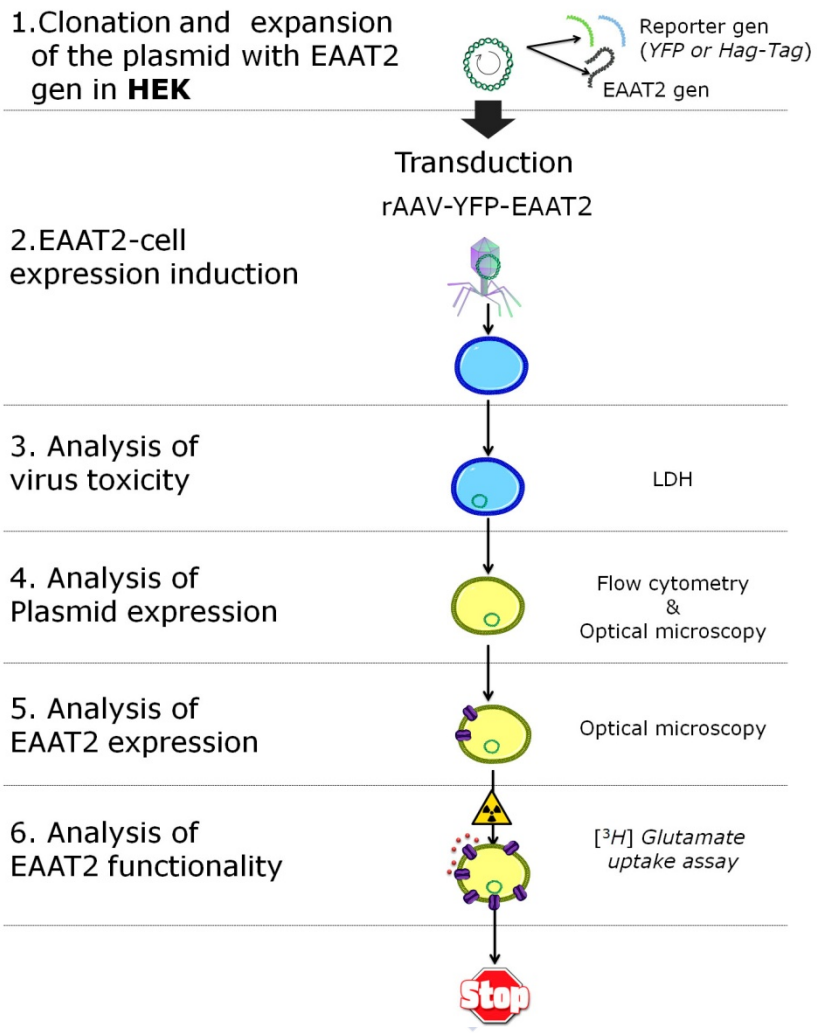

Figure 77: Summary of the procedures used to achieve expression of $EAAT_2$ by viral infection in HEK cells. (1) Synthesis of constructors and viral production. (2) HEK cells viral infection (3) Analysis of viral toxicity (LDH). (4) Analysis of gen-reporter expression (flow cytometry and microcopy). (5) Analysis of EAAT expression (confocal microscopy). (6) [^{3}H] glutamate uptake assay.

8.8. Calcium phosphate transfection of HEK cells

The calcium phosphate transfection with plasmid pRcCMVmYFPEAAT$_2$ was used as alternative technique to induce the expression of EAAT$_2$ in HEK cells. Other transfection technique (lipofectamine or eletroporation) were not cosidered as calcium phosphate was the most used for HEK cells trasnfection.

Microscopy analysis of transfected HEK cells (HEK+) with calcium phosphate transfection showed that they were express the gen-reporter (YFP) (Figure 78).

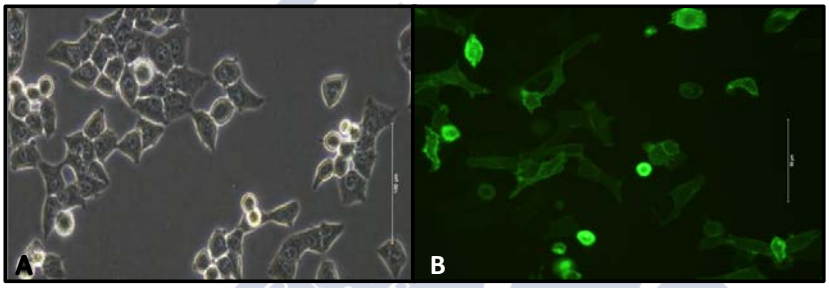

Figure 78: (A) Contrast phases image of HEK cells. (B) Culture of transfected HEK cells with calcium phosphate transfection (scale bar 100µm). Green cells indicate the successful expression of the gen-reporter (YFP).

To test the possible adverse effects of the calcium phosphate transfection on HEK cells, toxicity analysis by means of LDH assay was performed. In addition, the proliferation rate was evaluated. The LDH assay (Table 34 and Figure 79) showed that there was no significant difference between HEK– and HEK+, indicating low the toxicity of the transfection method used. There were not also significant differences between HEK- and HEK+ regarding to proliferation rate (Table 35 and Figure 80).

	24h	48h	72h
HEK-	100±24	100±16	100±18
HEK+	97±26	95±14	98±21

Table 34: Toxicity analysis of calcium phosphate transfection on HEK cells determined by means of LDH assay. Data are represented as % respect to the control values (n=3).

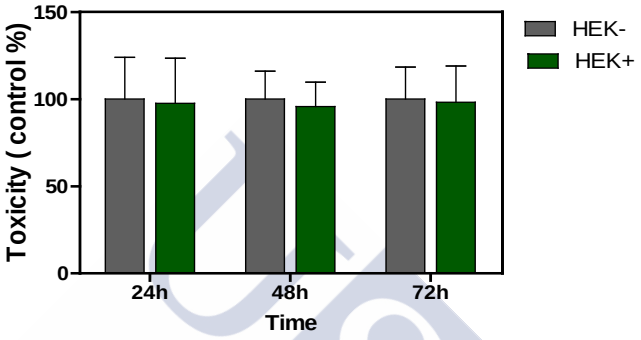

Figure 79: Toxicity analysis of calcium phosphate transfection on HEK cells determined by means of LDH assay. Data are represented as % respect to the control values (n=3).

	24h	48h	72h
HEK-	100±22	100±19	100±16
HEK+	97±15	98±22	99±10

Table 35: Proliferation rate analysis of calcium phosphate transfection on HEK cells (n=3).

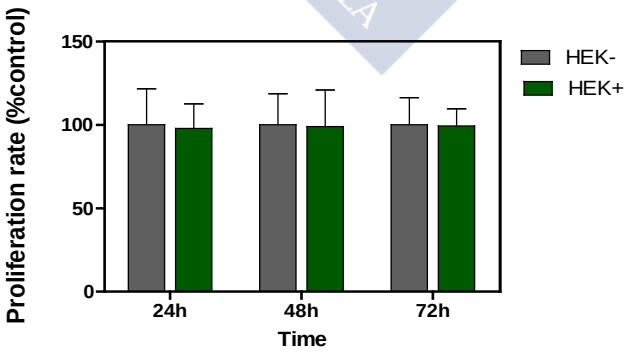

Figure 80: Proliferation rate analysis of calcium phosphate transfection on HEK cells (n=3).

8.8.1. Analysis of the reporter gen YFP in HEK+ transfected with calcium phosphate

Analysis of the percentage of efficiency of phosphate calcium in HEK cells, determined by means of flow cytometry, was around 50%. In the Figure 81, it can appreciate that the HEK-did not expresses YFP, while around 50% of the transfected cells were positive for YFP.

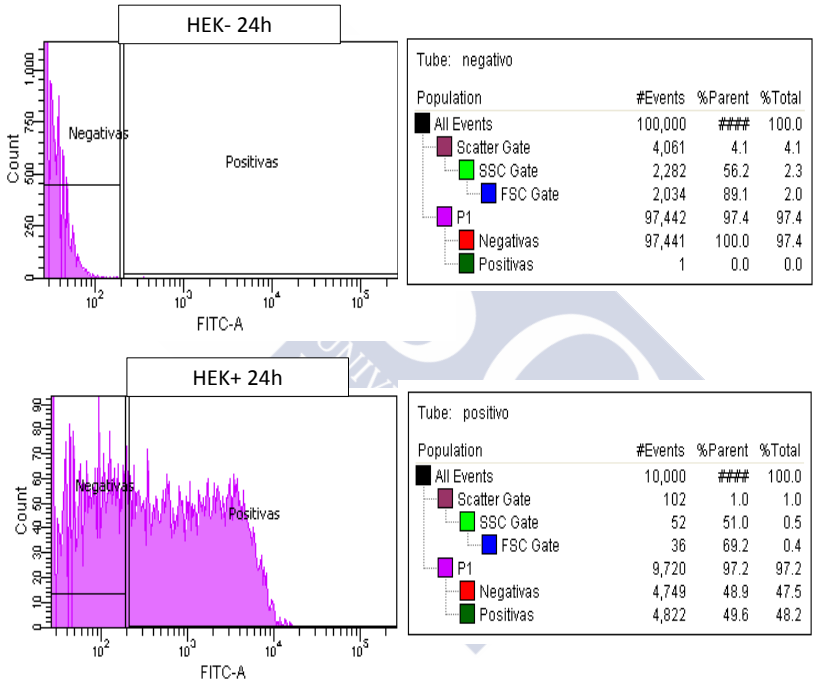

Figure 81: Analysis of YFP expression in of HEK- and HEK+ with calcium phosphate determined by flow cytometry.

The calcium phosphate technique for transfection of HEK cells proved to be very efficient for a highest number of transfected cells. In addition, many of the YFP-positive cells can be seleted based on their resistence to gentamicin (gentamicin resistence gene are included in the plasmid used) which allowed to separate. This procedure allowed to

select cells with plasmid integrated in the genome of the cells, therefore YFP (and subsecuently $EAAT_2$) are expressed constitutively. In the Figure 82, it can be observed a colony of HEK+ which expressed the gene YFP constitutively. This colony was picked and expanded in the optimum conditions.

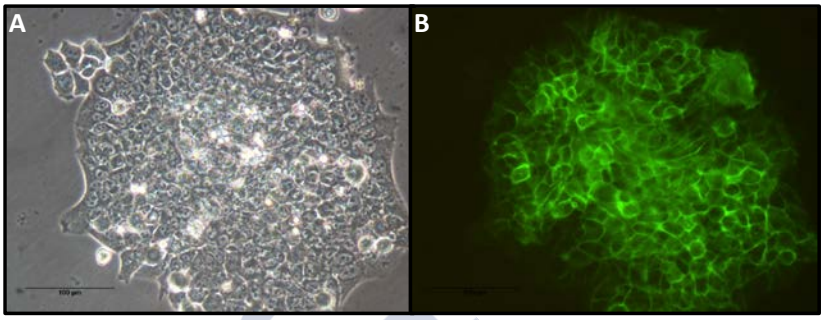

Figure 82: (A) Phase-contrast image of a colony of HEK+ selected with gentamincin. (B) Fluorescence microscopy image of a colony of HEK cells that express the gene YFP constitutively (HEK+) that selected with gentamicin.

8.8.2. Analysis of expression of $EAAT_2$ in HEK+

The expression of $EAAT_2$ in HEK+ was evaluated by immunostaining of $EAAT_2$ and confocal microscopy. The results are showed in Figure 83B, in which it can be observed that YFP positive cells were also positive for the expression of $EAAT_2$ and both labels colocalized Figure 83A).

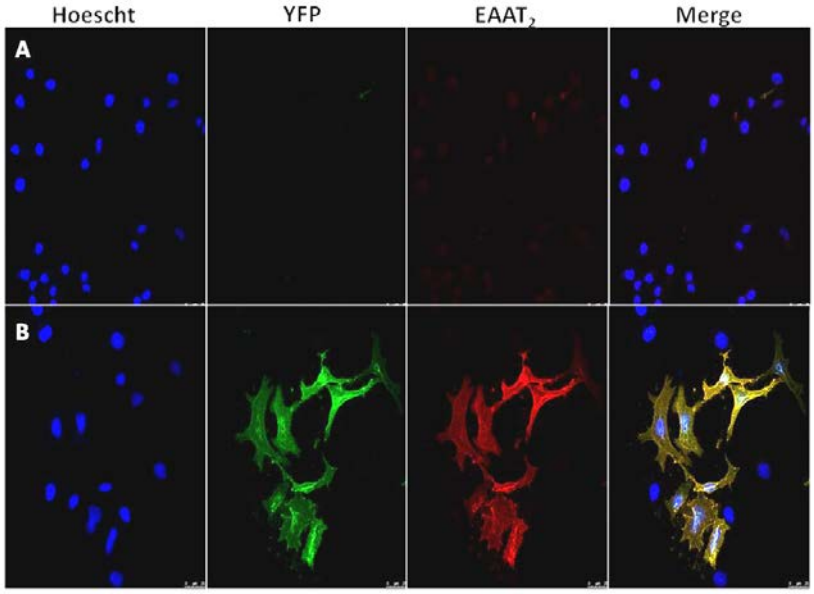

Figure 83: Immunostaining of $EAAT_2$ in (A) HEK- and in (B) HEK+.

8.8.3. Characterization of the functionality of the $EAAT_2$ in HEK+

Glutamate uptake assays were performed with the aim to determine the functionality of the $EAAT_2$ in HEK+. The results showed (Table 36 and Figure 84) that HEK+ are able to uptake glutamate in a specific way as the uptake was reduced when elevated concentrations of unlabeled glutamate were used (1mM). Specific glutamate uptake was not observer in HEK-.

Glutamate concentration	HEK-	HEK+
1µM	13±3	100±14
10µM	15±3	98±13
50µM	10±2	97±12
100µM	8±1	65±12
250µM	6±2	41±15
500µM	5±2	28±6
1mM	5±1	21±3
10mM	5±2	13±3

Table 36: Glutamate uptake assay for HEK- and HEK+.

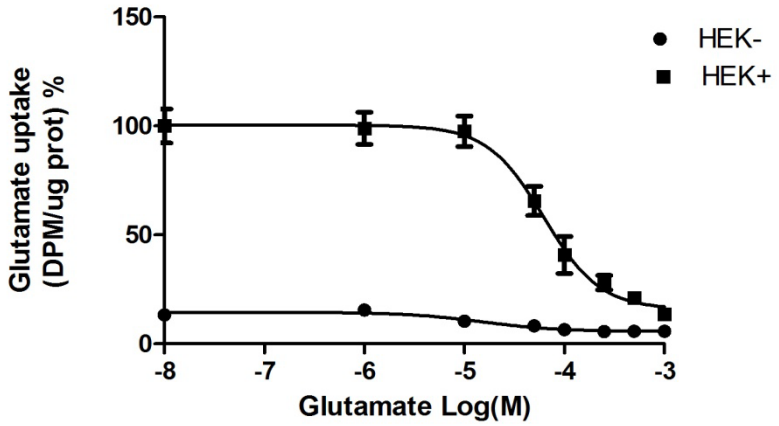

Figure 84: Glutamate uptake assay for HEK- and HEK+.

To be sure that glutamate uptake was mediated by $EAAT_2$, two selective inhibitors (DHK and TBOA) of the transporter were used. In Table 37 and Figure 6, it can observe that the

uptake of glutamate by HEK+ was blocked when both $EAAT_2$-blockers were used.

Glutamate concentration	HEK+	HEK+(TBOA+DHK)
1µM	100±14	8±3
10µM	98±13	8±3
50µM	97±12	9,0±0,9
100µM	65±12	8±2
250µM	41±15	9±2
500µM	28±6	7±2
1mM	21±3	5±0,5
10mM	13±3	6±0,7

Table 37: Selective inhibition of uptake glutamate mediated by DHK (500µM) and TBOA (300µM) in HEK+.

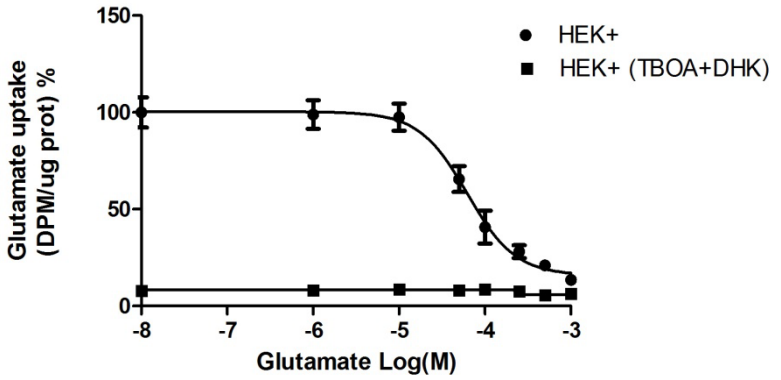

Figure 85: Selective inhibition of uptake glutamate mediated by DHK (500µM) and TBOA (300µM) in HEK+.

DHK and TBOA were tested independently (Table 38 and Figure 86). Glutamate uptake was inhibited ($p<0.05$), when both transporters inhibitors were used separately, the indicated the specific glutamate uptake observed.

Group	10µM
HEK+	98±12
HEK+ (DHK)	2,6±0,5
HEK+ (TBOA)	1,7±0,5
HEK+ (DHK&TBOA)	8,6±0,9

Table 38: Selective inhibition of uptake glutamate mediated by DHK and TBOA used in combination and separately HEK transfected cells (HEK+), (n=6).

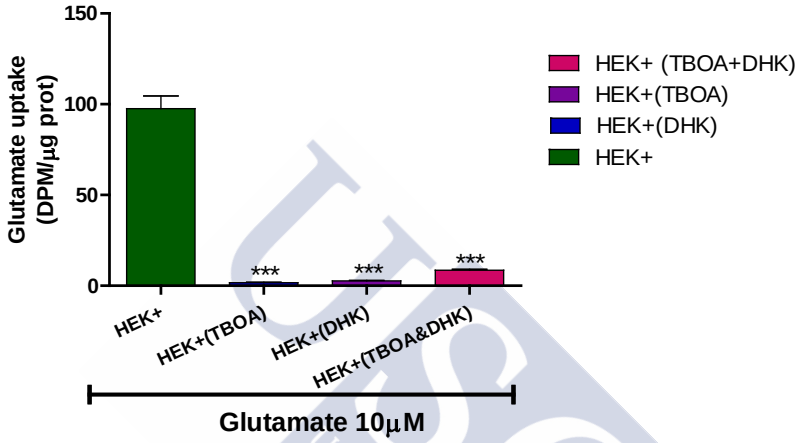

Figure 86: Selective inhibition of uptake glutamate mediated by DHK and TBOA used in combination and separately HEK transfected cells (HEK+), *(p<0.05, n=6)

Therefore, we can conclude that calcium phosphate transfection with pRcCMVmYFPEAAT$_2$, represents the optimal technique to obtain HEK cells with functional EAAT$_2$. In Figure 87 it is summarized the results obtained for HEK cells.

In the Figure 88 is represented all results and procedures involved in EAAT$_2$ gene expression in HEK cells and MSCs. Cells obtained were used to test their effect blood glutamate reduction in healthy animals and then their protective in ischemic animals.

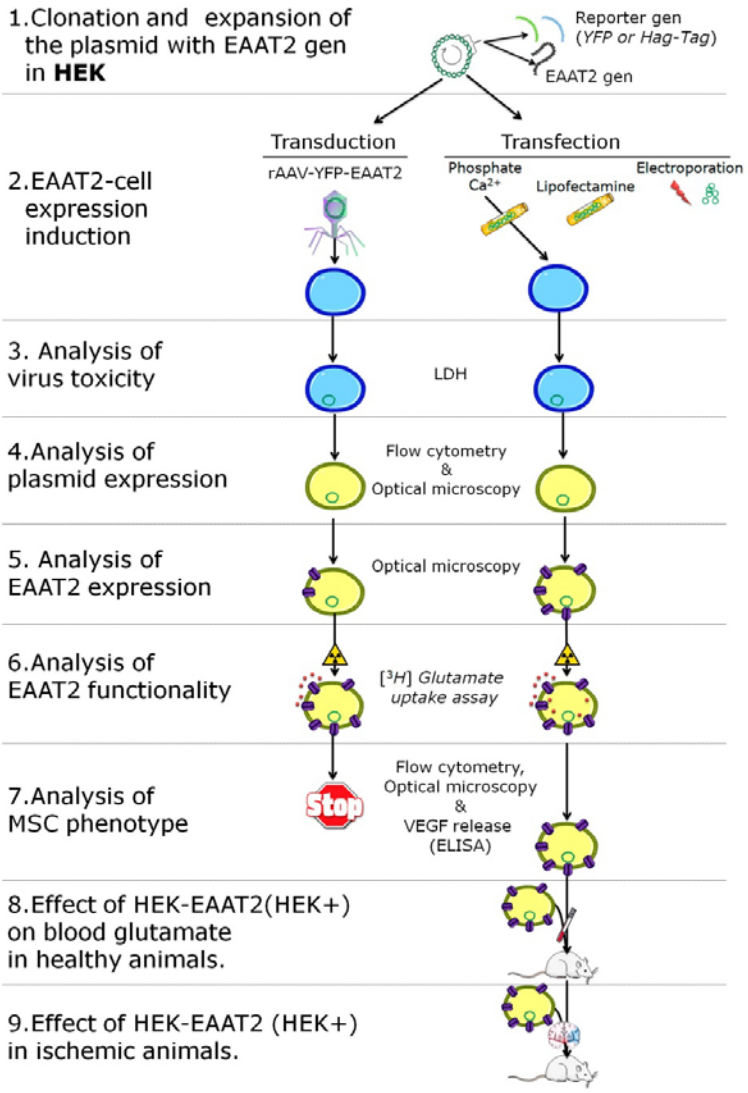

Figure 87: Resume of the procedures used to induce the expression of $EAAT_2$ in HEK cells by means of calcium phosphate transfection. (1) Synthesis of constructors and viral production. (2) HEK cells transfection. (3) Analysis of transfection toxicity (LDH assay). (4) Analysis of gen-reporter expression (microscopy fluoresce and flow cytometry). (5) Analysis of $EAAT_2$ expression (confocal microscopy). (6) Analysis of $EAAT_2$ functionality [^{3}H] glutamate uptake. (7) Analysis mesenchymal phenotype (microscopy fluoresce and flow cytometry and VEGF release). Calcium phosphate transfection was the optimal protocol to induce the expression of $EAAT_2$ on HEK cells with the aim to test the effect of $EAAT_2$-cell on blood glutamate (8) and in ischemic model (9).

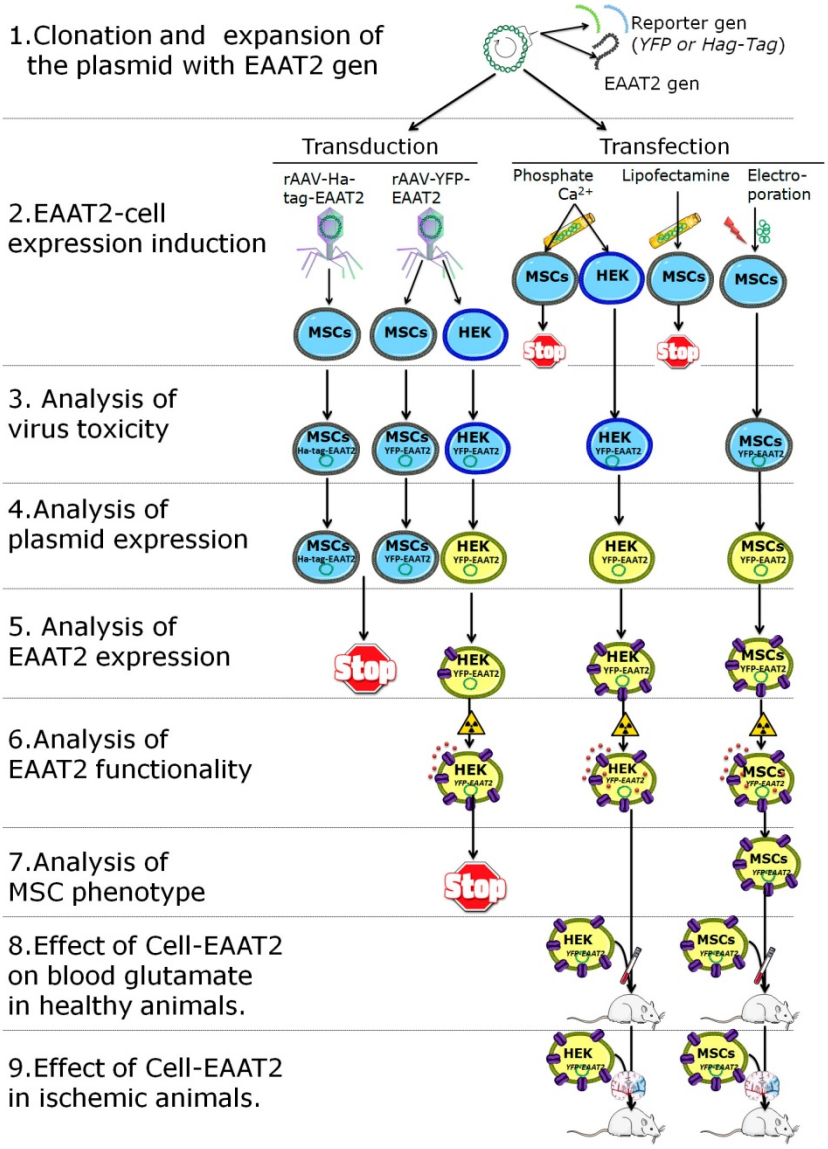

Figure 88: Procedures involved in $EAAT_2$ gene expression in HEK cells and MSCs.

8.9. Protective effect of HEK+ and MSC+ on ischemic animals model

8.9.1. Serum glutamate concentration in healthy animals

To determine the protective effect of HEK+ and MSC+, a previous dose-response assay in healthy animals was performed to determine the appropriate number of cells needed to induce a blood glutamate reduction.

The following experimental groups were studied: Vehicle (control group, treated with saline), oxaloacetate (3.5 mg/100g), $3x10^6$HEK- cells, $3x10^6$HEK+ cells, $3x10^6$MSCs- and $3x10^6$MSCs+. The serum glutamate was measured prior to administration of treatment (basal) and 1, 3 and 4h after. The oxaloacetate was used as positive control of blood glutamate grabber.

The results showed a reduction of glutamate in the animals treated with oxaloacetate at 1h ($p<0.05$) and 4h ($p<0.05$) after the administration compared with the vehicle. According with the $EAAT_2$ induced expression, administration of $3x10^6$HEK+ produced a reduction of glutamate levels at 1h ($p<0.05$) after administration, while $3x10^6$MSC+ decreased the glutamate levels at 1h ($p<0.01$) and 3h ($p<0.05$) after of the administration compared with the vehicle. The decrease of glutamate was maintained at least 3h after administration. In those animals treated with $3x10^6$HEK- and $3x10^6$MSC-, a reduction of glutamate was not observed (Table 38 and Figure 89).

In order to achieve a greater reduction of glutamate, in the second phase of the study, a dose of $9x10^6$ MSC- and $9x10^6$ MSC+ were also tested. The results demonstrated that a dose of $9x10^6$MSC+ could reduce the glutamate significantly ($p<0.05$) during 3 h compared with the vehicle, however this effect was not higher than $3x10^6$MSC+ dose. The dose of

9x10^{6}MSC- did not cause any effect on glutamate (Table 38 and Figure 89).

	Basal	1h	3h	4h
Vehicle	100±19	107±34	118±22	101±39
Oxal	100±6	64±24	84±55	54±2
3x10^6 HEK-	100±12	101±47	87±29	117±40
3x10^6 HEK+	100±8	88±4	72±7	97±28
3x10^6 MSC-	100±5	113±14	126±23	96±33
3x10^6 MSC+	100±20	56±13	73±30	104±57
9x10^6 MSC-	100±13	97±6	108±24	136±52
9x10^6 MSC+	100±5	64±9	70±7	82±12

Table 39: Effect of vehicle (control group, treated with saline), oxaloacetate (3.5 mg/100g), 3x10^{6}HEK- cells, 3x10^{6}HEK+ cells, 3x10^{6}MSCs-, 3x10^{6}MSCs+, 9x10^{6}MSCs- and 9x10^{6}MSCs+ on serum glutamate in healthy animals. Glutamate was determined in basal conditions (before treatment administration), and 1, 3 and 4 h after treatment. Data are shown as % respect to the basal levels (n=6).

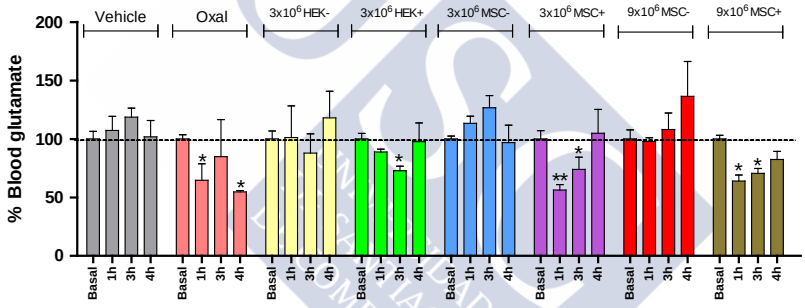

Figure 89: Effect of vehicle (control group, treated with saline), oxaloacetate (3.5 mg/100g), 3x10^{6}HEK- cells, 3x10^{6}HEK+ cells, 3x10^{6}MSCs-, 3x10^{6}MSCs+, 9x10^{6}MSCs- and 9x10^{6}MSCs+ on serum glutamate in healthy animals. Glutamate was determined in basal conditions (before treatment administration), and 1, 3 and 4 h after treatment. Data are shown as % respect to the basal levels (*p<0.05, **p<0.001, (n=6). Dashed line indicates the reference respect to basal levels.

8.9.2. Serum glutamate concentration in ischemic animals

Once determined their effect on blood glutamate reduction, their protective effect were analyzed in ischemic animals (Table 40 and Figure 90). The following groups were performed: Vehicle (control group, treated with saline), oxaloacetate (3.5 mg/100g), 3x10^{6}HEK- cells, 3x10^{6}HEK+

cells, 3x10^{6}MSCs-, 3x10^{6}MSCs+, 9x10^{6}MSCs- and 9x10^{6}MSCs+. Treatments were injected after the reperfusion (45 min). The analysis of serum glutamate was performed prior to MCAO (pre-ischemia), reperfussion and 1, 3, 4 and 24h after the administration of treatment. In Figure 90, it can be observed that in the animals treated with oxaloacetate and transfected cells (3x10^{6}HEK+, 3x10^{6}MSC+ and 9x10^{6}MSC+), all treatments caused a reduction (p<0.05) of blood glutamate 1h after the administration of treatment compared with the vehicle. None effect on blood glutamate levels were observed during the first 4 h after administration in those animals treated with non transfected cells (3x10^{6}HEK-, 3x10^{6}MSC- and 9x10^{6}MSC).

	Basal	Reperf	1h	3h	4h	24h
Vehicle	100±22	101±25	105±28	99±35	113±30	124±27
Oxal	100±32	97±31	73±14	84±36	84±29	91±30
3x10^6 HEK-	100±17	99±5	88±29	110±36	98±54	94±38
3x10^6 HEK+	100±8	115±34	76±11	89±18	105±20	105±14
3x10^6 MSC-	100±12	86±29	96±14	91±19	107±44	61±10
3x10^6 MSC+	100±16	91±45	74±23	63±27	74±22	69±29
9x10^6 MSC-	100±25	107±28	122±70	110±72	106±70	145±10
9x10^6 MSC+	100±9	107±12	73±5	67±6	78±11	119±45

Table 40: Serum glutamate in ischemic animals. Data are shown as the percentage relative to the basal level (*p<0.05, **p<0.01, ***p<0.001, n=6).

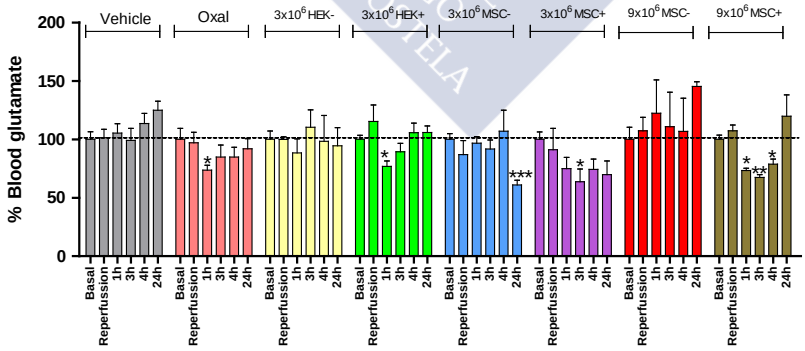

Figure 90: Serum glutamate in ischemic animals. Data are shown as the percentage relative to the basal level (*p<0.05, **p<0.01, ***p<0.001, n=6). Dashed line indicates the reference respect to basal levels.

8.9.3. Effects on ischemic lesion volume

Infarct volume sizes were measured on ADC maps, calculated from MR DWI, acquired during the occlusion (t=0), and on T_2 maps, obtained from T_2 weighted images at 1, 7 and 14 after the induction of the ischemia.

In Figure 91 it can be observed a representative MRI of each group at different time points. In Table 41 and Figure 92, infarct volume sizes are expressed in percentage respect the hemisphere volume corrected by edema factor. No statistically significant differences were found on infarct volumes of all groups at t=0. In those groups that were treated, except the animals injected with $3x10^6$ HEK-, the infarct volumes experiment a decrease compared to vehicle at 1, 7 and 14 days. These results were statistically significant only for animals which were administrated with oxaloacetate at 14days ($p<0.05$), $3x10^6$ MSC- at 7 and 14 days ($p<0.05$) and $9x10^6$ MSC- at 1, 7 and 14 days ($p<0.01$).

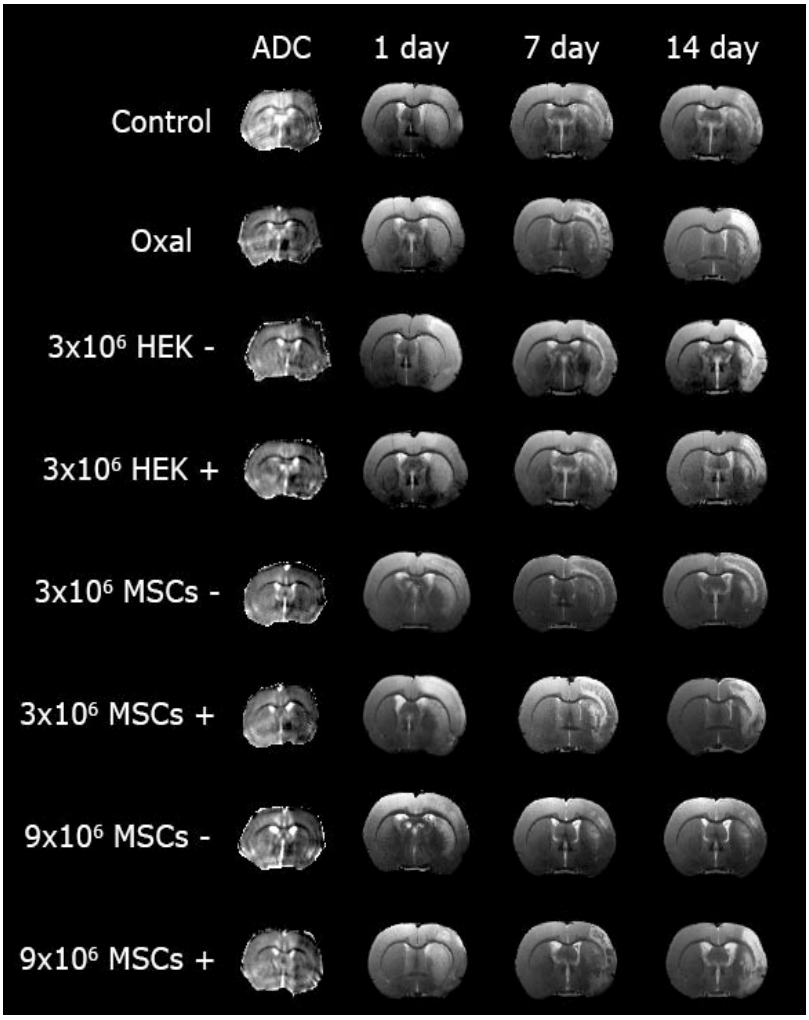

Figure 91: Representative MRI of each group at different time points. tMCAO corresponds to ADC maps and 1,7 and 14 days to T_2 weighed images.

	ADC	24h	7d	14d
Vehicle	43±3	41±7	33±8	30±10
Oxal	41±2	35±9	28±7	24±6
3x10^{6}HEK-	38±3	37±6	34±17	30±16
3x10^{6}HEK+	44±2	36±9	32±8	27±7
3x10^{6}MSC-	42±3	32±5	23±8	22±4
3x10^{6}MSC+	43±2	36±4	28±9	25±3
9x10^{6}MSC-	40±4	22±11	15±12	13±12
9x10^{6}MSC+	41±5	33±12	25±12	22±13

Table 41: Infarct size assessed by means of MRI in MCAO rats. MCAO rats were treated with vehicle (control group, treated with saline), oxaloacetate (3.5 mg/100g), 3x10^{6}HEK- cells, 3x10^{6}HEK+ cells, 3x10^{6}MSCs-, 3x10^{6}MSCs+, 9x10^{6}MSCs- and 9x10^{6}MSCs+. Treatments were injected after the reperfusion (45 min). Infarct sizes were measured at 24 h, 7 and 14 days after ischemia. ADC map were used to determine the basal ischemic lesion before treatment administration. Data are shown as % ± S.E.M respect to the hemisphere volume corrected by edema factor (n=6).

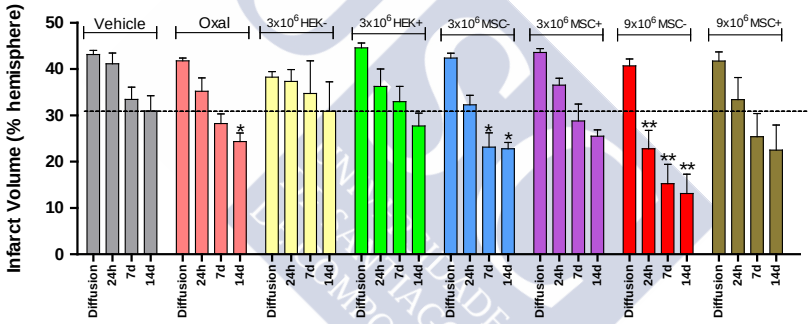

Figure 92: Infarct size assessed by means of MRI in MCAO rats. MCAO rats were treated with vehicle (control group, treated with saline), oxaloacetate (3.5 mg/100g), 3x10^{6}HEK- cells, 3x10^{6}HEK+ cells, 3x10^{6}MSCs-, 3x10^{6}MSCs+, 9x10^{6}MSCs- and 9x10^{6}MSCs+. Treatments were injected after the reperfusion (45 min). Infarct sizes were measured at 24 h, 7 and 14 days after ischemia. ADC map were used to determine the basal ischemic lesion before treatment administration. Data are shown as % ± S.E.M respect to the hemisphere volume corrected by edema factor.*p<0.05, **p<0.01 with respect to the control group at the same time point (n=6). Higher difference between groups was observed at 14 days (indicated with the dashed line).

Infarct volume was also analyzed considering the infarct size relative to the basal volume, with the aim to eliminate the basal difference between groups. The statistical analysis showed similar results than the previous analysis. In this case, higher protective effect seems to be observed in the

3x10^{6}HEK+ compared to 3x10^{6}HEK- respect to control group, however this differences are not significant (Figure 93).

	ADC	24h	7d	14d
Vehicle	100±7	95±17	77±19	71±24
Oxal	100±5	84±22	67±16	58±14
3x10^{6}HEK-	100±8	97±16	90±45	78±40
3x10^{6}HEK+	100±6	81±21	73±18	62±15
3x10^{6}MSC-	100±7	76±13	54±19	53±8
3x10^{6}MSC+	100±5	83±8	66±20	58±8
9x10^{6}MSC-	100±10	55±28	37±29	32±29
9x10^{6}MSC+	100±12	80±28	60±29	53±32

Table 42: Infarct size assessed by means of MRI in MCAO rats. MCAO rats were treated with vehicle (control group, treated with saline), oxaloacetate (3.5 mg/100g), 3x10^{6}HEK- cells, 3x10^{6}HEK+ cells, 3x10^{6}MSCs-, 3x10^{6}MSCs+, 9x10^{6}MSCs- and 9x10^{6}MSCs+. Treatments were injected after the reperfusion (45 min). Infarct sizes were measured at 24 h, 7 and 14 days after ischemia. ADC maps were used to determine the basal ischemic lesion before treatment administration. Data are shown as % ± S.E.M respect to the basal volume (n=6).

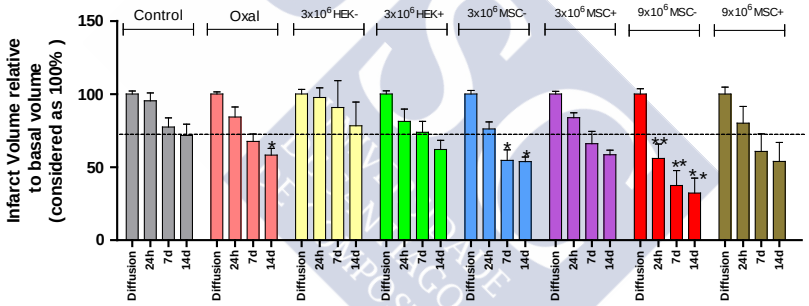

Figure 93: Infarct size assessed by means of MRI in MCAO rats. MCAO rats were treated with vehicle (control group, treated with saline), oxaloacetate (3.5 mg/100g), 3x10^{6}HEK- cells, 3x10^{6}HEK+ cells, 3x10^{6}MSCs-, 3x10^{6}MSCs+, 9x10^{6}MSCs- and 9x10^{6}MSCs+. Treatments were injected after the reperfusion (45 min). Infarct sizes were measured at 24 h, 7 and 14 days after ischemia. ADC maps were used to determine the basal ischemic lesion before treatment administration. Data are shown as % ± S.E.M respect to the basal volume.*p<0.05, **p<0.01 with respect to the control group at the same time point (n=6). Higher difference between groups was observed at 14 days (indicated with the dashed line).

8.9.4. Functional test

The overall effects on functional recovery were evaluated for cylinder and mNSS tests. Both tests were performed prior to tMCAO (pre-ischemia) and 7 and 14 days after the ischemia.

The cylinder test was done by counting the number of forelimb contacts. The number of impaired and non-impaired forelimb contacts was calculated as a percentage of total contacts. Attending to the obtained results (Table 43 and Figure 94), the administration of oxaloacetate, $3x10^6$HEK+, $3x10^6$MSC-, $3x10^6$MSC+, $9x10^6$MSC- and $9x10^6$MSC+ showed a reduction on the use of impaired forelimb compared with the vehicle at 7 and 14 days. But only there were significant differences at 7days in animals treated with $3x10^6$MSC- ($p<0.05$). At 14 days there were significant differences in the next animals: treated with oxoalocetate ($p<0.05$) $3x10^6$HEK+ ($p<0.05$), $3x10^6$MSC- ($p<0.01$) and $9x10^6$MSC-($p<0.01$). The effect on the cylinder test was detected for the treatment with $3x10^6$HEK- at 14 days, but the beneficial effect was less than the mentioned groups.

	Basal	7d	14d
Vehicle	48±4	25±13	26±12
Oxal	45±8	27±13	33±8
$3x10^6$HEK-	48±5	23±3	29±3
$3x10^6$HEK+	50±9	25±3	34±3
$3x10^6$MSC-	47±7	34±12	38±12
$3x10^6$MSC+	50±4	29±8	34±4
$9x10^6$MSC-	48±7	30±18	39±12
$9x10^6$MSC+	43±4	29±13	32±16

Table 43: Use of impaired forelimb (%) in the cylinder test.

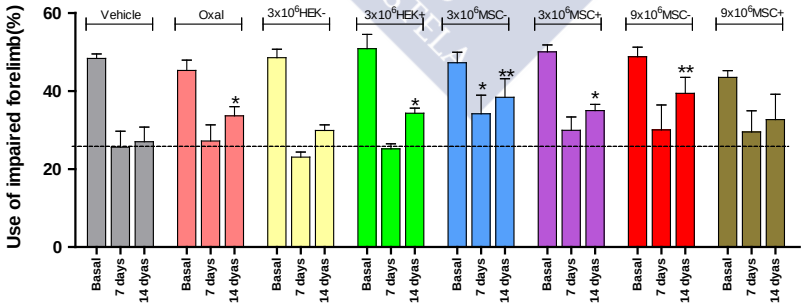

Figure 94: Use of impaired forelimb (%) in the cylinder test.

The results of the mNSS test are showed in Table 44 and Figure 95. It can be observed that there was a tendency to improve of the functional recovery for all groups at time points measured, being the differences between theirs minimal. The groups treated with oxaloacetate and 9x10^{6}MSC- showed the best result regarding to functional recovery.

	Basal	7d	14d
Vehicle	0,00±0,04	9,7±1,5	8±3
Oxal	0,00±0,03	8,0±1,4	7,0±1,1
3x10^{6}HEK-	0,00±0,02	8±2	8,0±1,3
3x10^{6}HEK+	0,00±0,05	10±2	9±2
3x10^{6}MSC-	0,00±0,03	8,0±1,1	6±2
3x10^{6}MSC+	0,00±0,01	9,0±1,4	8±2
9x10^{6}MSC-	0,00±0,06	8±2	6±2
9x10^{6}MSC+	0,00±0,03	8±2	7,0±1,3

Table 44: Points in the mNSS.

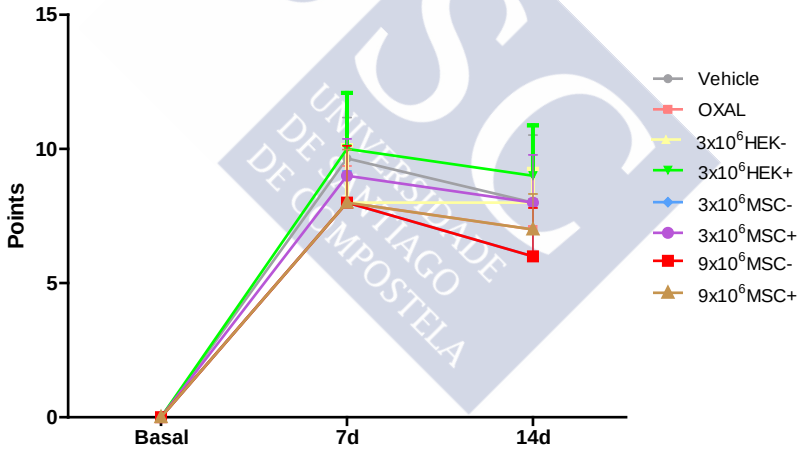

Figure 95: Points in the mNSS.

Discussion

USC
UNIVERSIDADE
DE SANTIAGO
DE COMPOSTELA

9.Section I: Analysis of protective effect of rGOT in ischemia

Nowadays, the concept of blood/brain glutamate scavenging is well recognized as a novel and attractive protective strategy to reduce the excitotoxic effect of excess extracellular glutamate that accumulates in the brain following an ischemic stroke. The efficacy of this strategy has been demonstrated in different types of ischemic animal models, and it has also been tested in other pathologies associated with an increase in brain glutamate levels, such as traumatic brain injury (TBI)[312] or glioma[170] with successful results.

GOT activation by means of exogenous administration of oxaloacetate has been used as the most common approach to reduce the serum glutamate concentration. In this study, we found that the i.v. administration of rGOT1 was also able to induce a reduction in serum and brain glutamate levels, which also resulted in a significant reduction in the infarct volume and improvement in the sensorimotor deficit after ischemia. These effects were similar to those observed with the higher doses of oxaloacetate[116]. Importantly, the protective effect of rGOT1 was more evident when it was administered in combination with a low concentration of oxaloacetate that had no effect by itself, indicating that the combined administration of rGOT1 and oxaloacetate could be an efficient serum glutamate-grabbing approach. The i.v. administration of an endogenous serum enzyme such as GOT1 as a new protective treatment against ischemia is an interesting strategy because it is unlikely that the administration of rGOT1 can induce toxic effects in humans as the levels of this enzyme varies among healthy human subjects (7–45 U/l), and has been shown to increase 10-fold in patients with liver damage. [313] On the other hand, the increase in the enzyme activity after the treatment is not much longer than 24 h, and serum glutamate concentrations

come back to normal within the first 6 h, which reduces long-term potential adverse effects. However, the effective dose of GOT (12.88 µg/100g) used in the animals cannot be extrapolated to humans, as GOT levels in rats are almost 10-fold higher than those in humans (10 U/l in humans versus 95 U/l in rats). In this regard, further (pre)-clinical studies based on the administration of GOT should be conducted in humans to determine the effective therapeutic dose of GOT able to induce a significant reduction in serum glutamate in humans. In line with this, we have previously observed that stroke patients who had high GOT activity (average of 17 U/l) at admission had reduced serum glutamate concentrations and a significantly better neurological outcome than patients with lower average activity of GOT of 11 U/l. [118, 314] Therefore, it can be hypothesized that the administration of rGOT1 doses able to increase the systemic GOT activity, at least two or three-fold, are necessary for clinical studies in stroke patients.

Regarding the use of oxaloacetate as a serum glutamate scavenging treatment, such a treatment could present some limitations associated with the high dose likely to be necessary in patients to achieve the same effects than those observed in experimental animals.[86] However, although to date there are no consistent data in humans confirming this toxic effect, a study published in the 60's,[315] in which oxaloacetate was used to treat diabetic patients (from 200 to 1000mg per day in three divided doses given orally) did not report any effect on liver function tests and blood acetone and cholesterol levels at the doses administered. Oral administration is not comparable to i.v. administration used in this study; nevertheless, this clinical study represents evidence for the relative safety of the administration of this molecule in humans. In this line, we also observed that oxaloacetate does not affect the viability of the neuronal culture, which is used as a current assay for neurotoxicity. [316] The protective effects of oxaloacetate have also been discussed. [114] As this molecule participates in the energy

metabolism and provides an antioxidant protection of cells subjected to stress, such as hydrogen peroxide, it has been suggested that the protective role of oxaloacetate could be related to other mechanisms different from serum glutamate reduction. Studies in a TBI model showed that the protective effect of oxaloacetate was abolished in the presence of excess glutamate in serum or when it was administered in combination with maleate (a GOT inhibitor),[136] which effectively demonstrate its serum glutamate-scavenging action.

Interestingly, the protective effect of rGOT1 (12.88 μg per 100 g) was potentiated when it was administered in combination with a non-effective low dose of oxaloacetate (1.5mg per 100 g) but not with higher doses of the enzyme (25.76 μg per 100 g). These findings are in agreement with a previous glioblastoma study reporting that the combination of rGOT1 with low amounts of oxaloacetate together with temozolodine significantly extends the lifespan of tumor-bearing animals. The therapeutic synergistic effect observed between oxaloacetate and GOT can be attributed to the fact that the endogenous oxaloacetate concentration can become a limiting factor of the enzymatic reaction when GOT activity is increased after treatment. Therefore, attending to the rapid and maintained reduction in serum glutamate concentration, treatments based on the combined administration of rGOT1 supplemented with a low concentration of oxaloacetate could be optimal to reach the maximum protective effect in ischemia. Of note, the low dose of oxaloacetate is sufficient to increase the glutamate-scavenging activity of rGOT1, which reduces the potential complications associated with a high dose of this molecule.

It is crucial to develop treatment approaches capable of overcoming the narrow therapeutic window in stroke in order to mitigate the detrimental effects of the excess of brain glutamate after ischemia, which represents a stumbling-block from a clinical point of view. Owing to this limitation, only those treatments (mainly, NMDA antagonists) with protective

effects beyond the first 1–2 h after the onset of ischemia have shown clinical interest. [317] In our ischemic experimental model, we have observed that brain and serum glutamate levels appear to be increased in the first 2 h after reperfusion. We observed that lowering of glutamate by means of GOT treatments had protective effects even when the treatment was delayed until 1 h after reperfusion. Further experiments need to be carried out to determine the length of the therapeutic window; however, based on our results, it may be speculated that the therapeutic window for the administration of rGOT1 could be up to 2 h after the onset of ischemia. As this treatment does not require a prior computerized tomography scan, it could be given as early as possible, perhaps even as ambulatory treatment suggesting potential clinical application. In this line, in a recently published model of brain hemorrhage, glutamate grabbers were shown to decrease the blood glutamate levels but did not affect the hemorrhagic hematoma, confirming that this treatment can be given without neuroimaging, in case of suspected stroke, which may potentially increases the number of patients treated within the therapeutic window. [121]

All preclinical studies on different models and the clinical observational analysis reported about the effect of rGOT and/or oxaloacetate, guarantee the therapeutic efficacy of the reduction of blood glutamate as well as the glutamate grabber drugs; however, translation to clinical practice has critical steps before their use in humans. These critical steps are those necessary to develop a clinical trial, which will involve high financial support and risk of investment for the sponsors interested in the study. In addition, the repeated failure of protective drugs against glutamate excitotoxicity in clinical trials has reduced the trust of pharmaceutical companies and other sponsors in stroke studies.

Aiming to demonstrate the clinical efficacy glutamate grabbers in humans and reduce the risk of investment in the study, a novel pharmacological strategy known as drug repositioning was used for our group one year ago to find

new grabbing drugs. This allowed researchers to search drugs already known and used for other pathologies and in which the clinical phase I and phase II were already completed, reducing the risk of investment for sponsors in case the clinical study result failed. Following this pharmacological strategy and, as purpose of other project ongoing in our group, we analyzed more than one thousand known drugs with the aim to determine whether any of them could act on GOT activity reducing glutamate levels, similar to treatment with OxAc. In this analysis, one drug (coded as CBG000592) was found with a high affinity for GOT (EC50 = 4.04 μM, Emax = 30 μM). A proof of concept (EudraCT Number: 2014-003123-22) in progress will allow us to check the protective efficacy of this drug and this mechanism.

In conclusion, in this study we show that oxaloacetate potentiates the protective effect of intravenously administered rGOT1 after ischemia. This effect is mediated through a reduction in serum and brain glutamate levels. The protective effect was observed even when the treatments were initiated as soon as 2 h after the onset of ischemia. The robust protection shown by the combination of rGOT1 and low doses of oxaloacetate proposes that this strategy may represent a valid approach for a successful acute-phase stroke treatment. Successful results with CBG000592 in the clinical proof of concept will allow us to get financial support to start a new clinical study based in the use if this enzymatic treatment, rGOT.

These data are already published in Cell Death Dis. 2014; 9;5:e992.

10. Section II: Effect of glutamate grabbers cells on ischemic damage.

Glutamate is an essential excitatory neurotransmitter regulating brain functions. Excitatory amino acid transporter ($EAAT_2$) is one of the major glutamate transporters expressed predominantly in astroglial cells and responsible for 90% of total glutamate uptake. Glutamate transporters tightly regulate glutamate concentration in the synaptic cleft. In fact, dysfunction of $EAAT_2$ leads to an accumulation of excessive extracellular glutamate implicated in the development of several neurodegenerative diseases including Alzheimer's disease, Huntington's disease, and amyotrophic lateral sclerosis. Analysis of the $EAAT_2$ promoter showed that the expression of this protein can be increased by means of transcriptional activators. Indeed, screening of approximately 1,040 FDA approved compounds and nutritionals led to the discovery that many β-lactam antibiotics are transcriptional activators of $EAAT_2$ resulting in increased $EAAT_2$ protein levels. Therefore, treatment with ceftriaxone (CEF) in animals, a β-lactam antibiotic, led to an increase of $EAAT_2$ expression and glutamate transport activity in the brain. Subsequent experimental studies showed that CEF has neuroprotective effects in both *in vitro* and *in vivo* models based on its ability to inhibit neuronal cell death by preventing glutamate excitotoxicity.[76]

Based on these previous studies where over-expression of $EAAT_2$ in astrocytes cells led a protection against glutamate excitotoxicity, we thought that if we could induce an expression of $EAAT_2$ in cells we could originate blood cell grabbers, potentially more efficient than the current treatments already tested, oxaloacetate or enzymes (rGOT).

On the other hand, mesenchymal stem cells (MSCs) represent the most common neurodegenerative experimental strategy in cerebral ischemia. Application MSCs resulted in an improved functional recovery and infarct reduction in experimental animals. The underlying precise mechanisms of this phenomenon remain elusive, although MSC transplantation is considered to affect many diverse events, e.g., by modulating the inflammatory milieu, stimulating endogenous neurogenesis and angiogenesis, and reducing glial scar formation. Because of these preclinical studies, first clinical trials confirmed improved functional recovery in patients who had received MSCs systemically.[318]

Therefore, given the high affinity of $EAAT_2$ for glutamate and the high beneficial effect of MSCs in stroke pathology, in this study we planned to combine both mechanisms with the aim to obtain a cellular therapy against stroke with neuroprotective and neurorecovery effect.

With this purpose, $EAAT_2$ protein expression was induced in MSCs and the functionality of these transporters to uptake glutamate was determined by means of *in vitro* assays and their capacity to reduce glutamate from blood *in vivo* experiments. The effect of $EAAT_2$-trasfected MSCs were also compared with a well know blood glutamate grabber, oxaloacetate, and with $EAAT_2$-trasfected HEK cells to eliminate the intrinsic beneficial effect of MSCs.

The *in vitro* experimental results showed that the transfection protocols used to induce the $EAAT_2$ expression in MSCs (electroporation transfection) and in HEK cells (phosphate calcium transfection) were efficient. Microscopy analysis and [^{3}H] glutamate uptake assay confirmed the expression and the functionality of the protein, while phenotypic analysis indicated that, apparently, the mesenchymal properties were not change after transfection

However, although, the transfection protocols used were successful to the $EAAT_2$ expression, viral infection strategy

used for the same purpose did not showed good results, as MSCs did not present expression of both gen-reporter, YFP , in case of the rAAV-YFP-$EAAT_2$ and Ha-tag, in case of rAAV-Ha-tag-$EAAT_2$. In this sense, there are numerous reports indicating the success of these vectors in transduction of MSCs from other species, but there seems to be no convincing evidence to suggest that AAV can effectively transduce rat MSCs at high levels. The reason for this species transduction efficiency difference is unclear at present, but it seems unlikely to be due to low expression of necessary cell-surface receptors, given that the low efficiency was seen with all the serotypes. It is possible, however, that it is the result of inefficient transport to the nucleus and limited second strand synthesis, since previous studies have shown that this is the major limiting factor in efficient gene expression after AAV transduction. [319]

In case of HEK cells, it was possible to observe the expression of the gen reporter YFP after viral transduction (infected with rAAV-YFP-$EAAT_2$) however, microscopy analysis and [^{3}H] glutamate uptake assay did not demonstrate a clear expression and functionality of the transporter. Although, sequence analysis should be perform to confirm this idea, we speculate that scission of the $EAAT_2$ from the plasmid could explain this results.

Our major interest to obtain $EAAT_2$-trasnducted cells by means of AVV infections was due to, this strategy allow to incorporate the $EAAT_2$-gen to the cell genome, and therefore the protein ($EAAT_2$) would be expressed constitutively, while the transfection procedure used to induce the protein expression made necessary to repeat the same protocol before to use the transfected in case of MSCs.

In line with the *in vitro* [^{3}H] glutamate uptake assay, administration of $EAAT_2$-transfected MSCs (MSCs+) and $EAAT_2$-transfected HEK cells (HEK+) induced a reduction of blood glutamate in healthy animals, that it was not observed in case of un-transfected cells. Therefore these results,

confirmed our original hypothesis, that the expression of $EAAT_2$ in cells originates cell grabbers of blood glutamate. With the aim to increase the effect of transfected MSCs on blood glutamate reduction, a higher dose of MSCs+ ($9x10^6$ cells) was also tested; however, we could not observe that the effect increased. We speculate that the dose used ($9x10^6$ cells), it was a really high dose (i.v. cell doses higher than $3x10^6$ cells is not commonly used in experimental studies with rats), therefore many cells could be trapped in the lung or the spleen, reducing their effect. In fact, future studies will be also necessary to perform in order to determinate the final destination of the administered cells.

It could be also tentative to speculate that, to increase the expression of the numbers of $EAAT_2$ per cell could be an alternative to increase the glutamate grabbing efficacy, however, as it was already explained in Material and Methods, the maximum amount of plasmid optimized for transfection protocol was already used to get the maximum expression of the protein per cell.

Analysis of the same treatments on ischemic animals showed that, in line with those results observed previously in healthy rats, oxaloacetate and transfected cells caused a significant reduction of blood glutamate levels after administration; however, this effect was not correlated with the infarct volume reduction. Thus, higher protective effect was observed with untransfected MSCs (MCSs-). Only, in case of HEK cells treatment, functional analysis measured by means of cylinder test, showed that HEK+ had better functional recovery than HEK- in agreement with the blood glutamate reduction observed.

We believe that MSCs have multiple intrinsic beneficial effects on ischemic stroke that can be altered after transfection procedure. This could explain why the protective effect of MCS- is better than MSC+. Thus, although MSC+ is able to reduce the glutamate excitotoxicity, the alteration of beneficial properties of MSCs is possibly much more relevant

in terms of protection. Phenotype analysis of MSCs (membrane markers, VEGF release and ring formation) did not showed deference respect MCS- after transfection, however although these properties are the most used to characterize the MSCs, other multiple protective molecular mechanism associated to these cells can be affected after transfection.

Interestingly, when HEK cells, a type of cells without described effect on cerebral ischemic lesion, express $EAAT_2$, they are able to reduce the blood glutamate levels and induce a functional improvement 14 days after ischemia. Once, this confirm by means of an alternative strategy, the effect of blood glutamate reduction as an efficient protective strategy against ischemic stroke.

In addition of cell glutamate grabbers here described, the use of grabbing drugs (oxaloacetate or rGOT) already tested, other alternatives to induce a reduction of blood glutamate has also been evaluated as blood glutamate grabbers with beneficial effects in ischemia. In this regard, the use of dialysis to filter the blood and remove excess glutamate has been suggested as an interesting and potentially useful method for reducing blood glutamate concentrations. Thus, compared with healthy controls, patients with end-stage renal failure on hemodialysis had higher concentrations of blood glutamate, and it has been described that, during hemodialysis (especially in the first hour), glutamate concentrations decreased regardless of the size of filter pores, blood flow rate, or gender.[320] Similarly, peritoneal dialysis resulted in decreases in blood glutamate with a corresponding increase of glutamate in the dialysis solution.[120] In agreement with these findings, in a rat model of ischemia, the reduction of blood glutamate levels observed with peritoneal dialysis was associated with a decrease in infarct area. In fact, this hypothesis is currently being tested in clinical trials in phase IIa (EudraCT Number: 2012-000791-42).

We have to note, that one important limitation of this study was that we did not analyzed the neurorecovery effect of MSC+ with the aim to determine its neuroprotective and neurorecovery effect. Since MSC- presented higher protective effect than MSC+, we considered not relevant to perform this analysis.

In conclusion, these results showed that the induced expression of EAATs on cells represents other novel an interesting alternative to reduce blood glutamate with potential beneficial effect after ischemia. However, blood glutamate cell grabbing did not present better beneficial effect trespect to other glutamate grabbers already well described, as their protective effect was not higher than oxaloacetate.

USC
UNIVERSIDADE
DE SANTIAGO
DE COMPOSTELA

Conclusions

USC
UNIVERSIDADE
DE SANTIAGO
DE COMPOSTELA

11. Conclusions

Based on the objectives cited at the beginning of this Thesis, and once completed the experiments and analyzed the results obtained; we can conclude that:

Section I: Analysis of protective effect of rGOT in ischemia

1. The administration of rGOT1 alone induces a reduction in serum and brain glutamate levels, which also resulted in a significant reduction in the infarct volume and improvement in the sensorimotor deficit after ischemia.
2. The beneficial effects mediated by rGOT1 were similar to those observed with the higher doses of oxaloacetate.
3. Combination of rGOT1 with a low dose of oxaloacetate potentiates the therapeutic effect of intravenously rGOT1 after ischemia.
4. The protective effect mediated by administration of rGOT1 was observed even when the treatments were initiated as soon as 2h after the onset of ischemia.
5. The robust protection shown by the combination of rGOT1 and low doses of oxaloacetate proposes that this strategy may represent a valid approach for a successful acute-phase stroke treatment.

Section II: Effect of glutamate grabbers cells on ischemic damage.

1. We have optimized a protocol to induce the exogenous expression of $EAAT_2$ in mesenchymal stem cells and HEK cells.
2. We have demonstrated the expression and functionality of $EAAT_2$ in mesenchymal stem cells and HEK cells.

3. The transfection of mesenchymal stem cells does not affect the membrane markers analyzed, angiogenic capacity or secretion of VEGF.
4. The administration of transfected cells with $EAAT_2$ is able to induce a lowering of serum glutamate levels *in vivo.*
5. The beneficial effect of mesenchymal stem cells is reduced after exogenous expression of $EAAT_2$, which limit the use of these cells like a cell grabber.
6. Blood glutamate cell grabbing do not present better benefit than other glutamate grabbers already well described, as their protective effect is not higher than oxaloacetate.
7. Results with EAAT2 transfected cells have confirmed the effect of blood glutamate reduction as an efficient alternative protective strategy against ischemic stroke.
8. Our results demonstrate that the transfection of mesenchymal stem cells with functional $EAAT_2$ may confer their a dual therapeutic action: neuroprotection and neurorepair.

12. Conclusiones

Basándonos en los objetivos citados al comienzo de esta Tesis, y una vez completados los experimentos y analizados los resultados obtenidos; podemos concluir que:

Sección I: Análisis del efecto protector de la rGOT1 en la isquemia

1. La administración de rGOT1 produce una reducción de los niveles de glutamato en suero y en cerebro, lo cual está asociado a una disminución del volumen de infarto y una mejora del déficit sensoriomotor después de la isquemia.
2. Los efectos beneficios mediados por rGOT1 fueron similares a los observados con el oxaloacetato a dosis elevadas.
3. La combinación de rGOT1 con una dosis baja de oxaloacetato, potencia los efectos terapéuticos de la rGOT1 intravenosa tras la isquemia.
4. El efecto protector mediado por la administración de la rGOT1 se observa incluso cuando los tratamientos se inician 2h después del comienzo de la isquemia.
5. La destacada protección mostrada por la combinación de rGOT1 y dosis bajas de oxaloacetato sugiere que esta estrategia puede representar una aproximación válida para el tratamiento exitoso del ictus en fase aguda.

Sección II: Efecto de los atrapadores celulares de glutamato en el daño isquémico

1. Hemos optimizado un protocolo para inducir la expresión exógena del $EAAT_2$ en células madre mesenquimales y células HEK.
2. Hemos demostrado la expresión y funcionalidad del $EAAT_2$ en células madre mesenquimales y células HEK.

3. La transfección de células madre mesenquimales no afecta a los marcadores de membrana analizados, a la capacidad angiogénica o a la secreción de VEGF.
4. La administración de células transfectadas con $EAAT_2$ induce una disminución de los niveles de glutamato sérico *in vivo*.
5. El efecto beneficioso de las células madre mesenquimales es reducido tras la expresión exógena del EAAT2, lo cual limita el uso de estas células como un atrapador celular.
6. Los atrapadores celulares de glutamato sanguíneo no presentan un mayor beneficio que los otros atrapadores de glutamato ya descritos, así como su efecto protector no es mayor que el del oxaloacetato.
7. Los resultados con células transfectadas con $EAAT_2$ confirman que, por medio de un procedimiento alternativo, la reducción del glutamato sanguíneo es una estrategia protectora eficiente en el ictus isquémico.
8. Nuestros resultados demuestran que la tranfección de células madre mesenquimales con un $EAAT_2$ funcional puede conferirles una acción terapéutica dual: neuroprotección y neurorreparación.

Appendix

USC
UNIVERSIDADE
DE SANTIAGO
DE COMPOSTELA

13. Resumen

Las enfermedades cerebrovasculares son la segunda causa de muerte y la primera de discapacidad en países desarrollados. Sin embargo, a pesar de su importancia socio-económica, las terapias disponibles son limitadas. La etiología más frecuente del ictus, el ictus isquémico, consiste en la reducción localizada del flujo cerebral tras la oclusión de una arteria cerebral. Este proceso desencadena una serie de eventos a nivel molecular y celular que culminan con un fallo energético en el área cerebral afectada, seguida de un proceso de muerte celular por necrosis. Esta área recibe el nombre de core isquémico. La región circundante al core, denominada penumbra isquémica, está constituida por tejido hipoperfundido pero todavía viable. Sin embargo, esta área está condicionada a una serie de procesos moleculares de excitotoxicidad, estrés oxidativo y respuesta inflamatoria que constituyen las dianas terapéuticas principales de neuroprotección en la isquemia cerebral.

Las terapias de reperfusión, bien por trombólisis farmacológica con el activador tisular del plasminógeno recombinante (rt-PA) o por trombectomía mecánica, constituyen las estrategias terapéuticas que logran mejores beneficios en los pacientes que sufren un ictus isquémico. Sin embargo, la estrecha ventana terapéutica (4.5 h tras el comienzo de los síntomas para la trombólisis farmacológica) los efectos secundarios asociados a esta terapia farmacológica y la necesidad de equipos altamente cualificados e infraestructuras de vanguardia para la trombectomía mecánica hacen que únicamente entre el 3 y el 7% de los pacientes con infarto cerebral pueden beneficiarse de esta terapia en los países más desarrollados. Por ello, urge la necesidad de desarrollar nuevas estrategias terapéuticas basadas en neuroprotección o neurorreparación.

La neuroprotección es un término que incluye todas las terapias dirigidas a reducir la muerte celular tras un proceso isquémico sin ejercer ningún tipo de influencia en la reperfusión del tejido durante la fase aguda del ictus. Los fármacos neuroprotectores se clasifican, en cuanto a sus mecanismos de acción, en los siguientes grupos: antagonistas de los canales de $Ca^{2+,}$ antagonistas de los receptores de glutamato, antioxidantes, precursores fosfolipídicos, inhibidores de la liberación de glutamato, agonistas del GABA y anti-inflamatorios. Hasta ahora, algunos fármacos han mostrado resultados prometedores en estudios experimentales, pero una vez trasladados a ensayos clínicos no han demostrado eficacia.

Por otro lado, las estrategias neurorreparadoras presentan una ventana terapéutica mayor que la fase aguda del ictus. Estas estrategias incluyen la restauración de la función cerebral, ya sea bien por regeneración del tejido cerebral dañado (neurorregeneración) o bien por la creación de nuevas conexiones neuronales o sinapsis (plasticidad cerebral). El fin de las terapias de neurorreparación es la restauración de la unidad neurovascular mediante estrategias farmacológicas o de terapia celular, enfocadas a la potenciación de la neurogénesis, angiogénesis y sinaptogénesis.

El glutamato constituye una de las principales dianas de neuroprotección en la isquemia cerebral. El glutamato es el principal neurotransmisor del sistema nervioso central. En el cerebro, el glutamato se encuentra compartimentado intracelularmente en neuronas y astrocitos; siendo una pequeña fracción del mismo extracelular. Esta homeostasis del glutamato es muy sensible a cambios de energía y está regulada principalmente por los transportadores de aminoácidos excitatorios (EAATs), presentes en astrocitos, neuronas y las células endoteliales que forman la barrera hematoencefálica; siendo el $EAAT_2$ el responsable del 90% de la recaptación de glutamato extracelular. La perturbación del equilibrio del glutamato está relacionada con daño del

sistema nervioso central, tal como ocurre en el ictus isquémico, el traumatismo craneoencefálico, la Esclerosis Lateral Amiotrófica (ELA) o la Enfermedad de Parkinson, entre otras.

Durante la isquemia cerebral, la despolarización de la membrana celular debido al fallo energético produce un incremento de glutamato en el espacio extracelular. Este exceso de glutamato induce un complejo proceso de mecanismos patogénicos, que conducen a la neuroexcitotoxicidad. Con el fin de mitigar los efectos deletéreos de la excitotoxicidad, se desarrollaron nuevos fármacos neuroprotectores para bloquear los receptores del glutamato o inhibir la liberación de glutamato a través del bloqueo de los canales presinápticos. Dichos tratamientos farmacológicos no mostraron eficacia en clínica humana, por lo que urge la necesidad de desarrollar nuevas estrategias terapéuticas contra la excitotoxicidad mediada por glutamato. Con este fin, surgieron los estudios que describen la existencia de un gradiente de concentración de glutamato entre las células endoteliales que forman la barrera hematoencefálica del cerebro y el torrente sanguíneo. Cuando la concentración de glutamato de las células endoteliales cerebrales es mayor que la concentración de glutamato sanguíneo, este es transportado desde el cerebro hacia el torrente sanguíneo. Debido a ello, surge la hipótesis de que la reducción de los niveles de glutamato sanguíneo incrementaría el gradiente de concentración entre el endotelio cerebral y la sangre; favoreciendo de este modo la eliminación de glutamato cerebral. Este mecanismo potencial de neuroprotección se denomina atrapamiento de glutamato sanguíneo. Así, el tratamiento de la isquemia cerebral con atrapadores de glutamato sanguíneo, podría generar una reducción del glutamato cerebral, lo que podría conllevar implicaciones terapéuticas tras la isquemia cerebral. En este sentido, diferentes estudios han descrito que la reacción metabólica mediada por la transaminasa glutámico oxalacética (GOT) podría constituir una importante diana

neuroprotectora en la isquemia cerebral. El potencial terapéutico asociado a la GOT se debe al hecho de que esta enzima, usando el oxalacetato como co-substrato, es capaz de metabolizar el glutamato a α-cetoglutarato y aspartato, conllevando a una disminución de los niveles de glutamato en sangre. Basándose en esta premisa, nuestro grupo demostró que la administración de oxalacetato induce una reducción de los niveles de glutamato sanguíneo, por medio de la activación de la GOT, lo cual media efectos neuroprotectores en un modelo animal en rata de isquemia cerebral. Sin embargo, desde un punto de vista clínico, el uso de oxalacetato como atrapador de glutamato puede tener importantes limitaciones como son sus potenciales efectos secundarios, debido a que el oxalacetato participa en el Ciclo de Krebs, su elevada dosis terapéutica y su estrecha ventana terapéutica.

La terapia celular ha surgido como una estrategia prometedora frente a tratamientos farmacológicos convencionales debido a sus múltiples y potenciales mecanismos de acción, entre los cuales destacan la integración de las células administradas en los tejidos, procesos de inmunomodulación o secreción de factores de crecimiento. Varias estirpes celulares han demostrado efectos beneficiosos en estudios preclínicos de isquemia cerebral, incluyendo células madre embrionarias, células madre neurales, células madre pluripotentes inducidas y células madre mesenquimales (MSCs), entre otras. De todas ellas, las MSCs han sido descritas como las más idóneas. Esto se debe, no solo a que son multipotentes, sino también a sus capacidades inmunomoduladoras y de secreción de factores de crecimiento, lo que les confiere mecanismos pleiotrópicos de acción entre los que destacan: diferenciación a células de estirpe neural; inducción de la neurogénesis, angiogénesis y sinaptogénesis; activación de procesos endógenos de plasticidad cerebral; regulación del flujo sanguíneo cerebral; reducción de la apoptosis; inmunomodulación de la inflamación; e incremento de la

supervivencia celular, entre otros. Además, diversos estudios preclínicos de isquemia cerebral en roedores han encontrado recuperación funcional y reducción del volumen de infarto.

Por todo lo anteriormente mencionado, la combinación de mecanismos de neuroprotección (por atrapadores de glutamato sanguíneo), y de neurorreparación (mediados por MSCs) constituiría una estrategia terapéutica prometedora en la isquemia cerebral. Por ello, el objetivo de este trabajo consistió en el desarrollo de nuevas alternativas de atrapadores de glutamato sanguíneo para su uso en el ictus isquémico. Para ello hemos utilizado dos estrategias: enzimática y celular. La estrategia enzimática se basó en el uso de la rGOT1 administrada individualmente y combinada con una dosis no terapéutica de oxaloacetato. La estrategia celular, consistió en expresar, por transfección celular, el transportador $EAAT_2$ en estirpes celulares. Para este fin, se usaron dos tipos celulares: células HEK (se busca el efecto neuroprotector por capatación de glutamato sanguíneo por $EAAT_2$) y las MSCs (efecto dual: neuroprotector, por captación de glutamato sanguíneo por $EAAT_2$, y neurorreparador, por sus propiedades endógenas de célula madre).

Para testar la eficacia de la rGOT1 en la disminución del glutamato sanguíneo y cerebral, y posteriormente determinar el efecto protector de la enzima, el estudio fue dividido en dos partes. En primer lugar, se realizó un estudio dosis-respuesta en animales sanos con el objetivo de determinar la dosis más efectiva de rGOT1 en la disminución de glutamato sanguíneo. Para simular el incremento de glutamato observado después de la isquemia cerebral, inyectamos glutamato, a una dosis de 15mM, en la yugular de ratas SD. Se ensayaron las siguientes dosis de rGOT1: 6.44 µg/100g, 12.88 µg/100g y 25.76 µg/100g. Para analizar las concentraciones de glutamato se obtuvieron muestras sanguíneas de la vena de la cola antes de la inyección de glutamato y a las 1, 2, 4, 6 y 24 h después de la inyección de glutamato. Los niveles de glutamato sérico se midieron

mediante técnicas de ELISA. Los resultados mostraron que la dosis de 12.88 µg/100g de rGOT1 fue la más efectiva en la reducción del glutamato sanguíneo ($p<0.01$). Con el objetivo de determinar si el efecto de la enzima podría ser potenciado por el oxalacetato, la dosis rGOT1 12.88 µg/100g se combinó con una dosis no terapéutica de oxalacetato (1.5mg/100g). La administración de dicha combinación indujo una mayor disminución del glutamato en sangre ($p<0.01$).

El siguiente paso fue examinar el efecto protector de la rGOT1 (12.88 µg/100g) y rGOT1 (12.88 µg/100g) suplementada con oxalacetato (1.5 mg/100g) en ratas SD, sometidas a isquemia cerebral mediante filamento intraluminal, comparado con animales tratados con oxalacetato a una dosis de 3.5 mg/100g (dosis terapéutica). Para determinar la capacidad terapéutica de los tratamientos, los cuales fueron administrados justo después de la reperfusión, se avaluó el volumen de infarto por imagen de Resonacia Magnética (MRI) y el déficit funcional por el Test del Cilindro. Asimismo, se midió la reducción del glutamato sanguíneo por técnicas de ELISa y la actividad de GOT fue determinada por Reflotron GOT, y la reducción de glutamato cerebral por espectroscopia de MRI. Los resultados mostraron que el incremento del glutamato sérico tras la isquemia cerebral fue reducido por los tratamientos: rGOT1 (12.88 µg/100g), oxaloacetato (3.5 mg/100g) y rGOT1 más oxaloacetato (12.88 µg/100g y 1.5 mg/100g, respectivamente), sin haber diferencias significativas entre ellos. Esta disminución de glutamato sérico causada por los tratamientos se asoció a una reducción del glutamato cerebral ($p<0.05$). Todos los tratamientos indujeron una disminución del volumen de infarto a las 24 h y a los 7 d después de la isquemia ($p<0.05$), siendo este efecto mayor en los animales tratados con rGOT1+oxaloacetato ($p<0.05$). En los animales a los cuales se les administró rGOT1, la actividad enzimática de la misma estaba aumentada ($p<0.01$).

Con el fin de determinar la ventana terapéutica óptima para la administración de la rGOT1, las ratas isquémicas fueron tratadas también 1 h después de la reperfusión. Los grupos de tratamientos fueron: rGOT1 (12.88 µg/100g) y rGOT1+oxaloacetato (12.88 µg/100g y 1.5 mg/100g, respectivamente). Ambos tratamientos causaron una reducción significativa ($p<0.05$) de los niveles de glutamato sanguíneo. Sin embargo, el análisis del volumen de infarto reveló que la administración de los tratamientos 1 hora después de la reperfusión tiene un menor efecto protector que la administración justo después de la reperfusión.

En cuanto a los test somatosensoriales, el tratamiento combinado de rGOT1 con oxaloacetato está asociado a un mejor pronóstico funcional a los 7 días ($p<0.05$).

Por otro lado, para inducir la expresión de EAAT2 en diversas estirpes celulares empleamos diferentes técnicas de transfección. Mediante microscopía de fluorescencia y citometría de flujo, se analizó la presencia del gen reporter YFP, que confirmaba la eficiencia del proceso de transfección del $EAAT_2$. En un primer paso, se utilizaron diferentes vectores virales para tratar de expresar el $EAAT_2$ en células HEK y MSCs. Los resultados de la infección no mostraron una expresión del YFP en dichas células. Debido a ello, se emplearon otras técnicas de transfección. Por un lado, en las MSCs se ensayaron las siguientes técnicas: fosfato cálcico, lipofección y electroporación; siendo esta última la que ofreció resultados positivos para la expresión de $EAAT_2$ y el YFP asociado. En lo que se refiere a las células HEK, se consiguió expresar $EAAT_2$ y el YFP asociado mediante la transfección con fosfato cálcico. La posterior selección con gentamicina permitió seleccionar aquellas células HEK que habían integrado el $EAAT_2$ en su genoma.

Mediante técnicas de inmunofluorescencia y microscopía confocal, se observó que tanto las HEK como la MSCs co-expresaban el gen reporter YFP y $EAAT_2$. Además, se determinó la funcionalidad del gen $EAAT_2$ en las células

transfectadas mediante experimentos de captación de glutamato tritiado. Los resultados de estos experimentos demostraron que las células transfectadas eran capaces de captar glutamato de una forma eficiente. Para confirmar que dicha captación estaba mediada por $EAAT_2$, se determinó la captación del glutamato en combinación con inhibidores específicos del $EAAT_2$, DHK y TBOA. Los resultados de estos experimentos demostraron que la utilización de los inhibidores impedía la captación de glutamato en las células transfectadas, confirmando que dicha captación estaba mediada por $EAAT_2$.

Debido a que las MSCs presentan propiedades endógenas neurorreparadoras, fue necesario determinar que dicho fenotipo celular no fue modificado tras el proceso de electroporación. Para ello se analizaron, por citometría de flujo, la expresión de marcadores específicos del fenotipo de MSCs (CD90+, CD45- y CD73+), la capacidad angiogénica por matrigel y la secreción de VEGF por técnicas de ELISA. Los resultados mostraron que no existen diferencias entre las MSC+ y MSC-, en cuanto a las propiedades mencionadas anteriormente.

Una vez demostrada la capacidad de las células transfectadas para captar glutamato in vitro, fue necesario determinar su efecto *in vivo*. Para ello, previamente a la utilización de las células transfectadas en ratas Wistar sometidas a isquemia cerebral, se determinó la dosis celular adecuada para inducir una reducción de los niveles de glutamato plasmático. Con esta finalidad, los siguientes grupos experimentales fueron analizados en ratas sanas: 3.5 mg/100g de oxalacetato (dosis terapéutica, control positivo), $3x10^6$ HEK-, $3x10^6$ HEK+, $3x10^6$ MSC- y $3x10^6$ MSC+. La concentración de glutamato sérico fue medida mediante técnicas de ELISA, previamente a la administración del tratamiento y a las 1, 3 y 4 h después de la administración del tratamiento. Los resultados mostraron una reducción de glutamato sérico en los animales tratados con oxalacetato a 1 y 4 h después de la administración. En cuanto a los grupos tratados con células,

la administración de $3x10^6$ HEK+ indujo una disminución de los niveles de glutamato 1 h después, mientras que el grupo tratado con $3x10^6$ MSC+ disminuyó los niveles de glutamato sérico 1 y 3 h después de la administración del tratamiento (todas las $p<0.05$). Con el objetivo de conseguir una mayor reducción de glutamato, se analizaron 2 grupos más, $9x10^6$ MSC- y $9x10^6$ MSC+. Los resultados mostraron que en el grupo tratado con $9x10^6$ MSC+ disminuye los niveles de glutamato a las 3 h ($p<0.05$) respecto al grupo control, pero dicha disminución no era mayor a la inducida por la dosis de $3x10^6$ MSC+.

Finalmente, se estudió el efecto terapéutico de las estirpes celulares transfectadas con $EAAT_2$, administradas intravenosamente, en ratas Wistar sometidas a isquemia cerebral mediante filamento intraluminal. Para determinar los efectos beneficiosos de esta terapia se avaluó el volumen de infarto por imagen de Resonacia Magnética (MRI) y el déficit funcional. Asimismo, se analizaron los niveles de glutamato sistémico mediante ELISA. Se realizaron los siguientes grupos de estudio: vehículo (PBS), oxalacetato (3.5 mg/100g), $3x10^6$ HEK-, $3x10^6$ HEK+, $3x10^6$ MSC-, $3x10^6$ MSC+, $9x10^6$ MSC- y $9x10^6$ MSC+. Los tratamientos fueron inyectados en yugular justo después de la reperfusión. El análisis de glutamato sérico fue realizado previamente a la cirugía, inmediatamente tras la reperfusión y a las 1, 3, 4 y 24 h después de la administración del tratamiento. Los resultados mostraron una reducción del glutamato sérico, a 1 hora tras la administración del tratamiento, en los grupos tratados con oxalacetato y células transfectadas ($p<0.05$). Sin embargo, de estos grupos que indujeron una reducción del glutamato sanguíneo, únicamente el grupo tratado con oxalacetato mostró una reducción del volumen del infarto ($p<0.05$). Otros grupos que indujeron una reducción del volumen del infarto al día 7 fueron $3x10^6$ MSC- y $9x10^6$ MSC-. En cuanto a los test funcionales, los animales tratados con oxalacetato, $3x10^6$ HEK+, $3x10^6$ MSC- y $9x10^6$ MSC-

mostraron una mejoría funcional a los 14 días tras la isquemia.

En base a todos los resultados anteriormente indicados, concluimos que:

- La administración de rGOT1 produce una reducción de los niveles de glutamato en suero y en cerebro, lo cual está asociado a una disminución del volumen de infarto y una mejora del déficit sensoriomotor después de la isquemia.

- Los efectos beneficios mediados por rGOT1 fueron similares a los observados con el oxaloacetato a dosis elevadas.

- La combinación de rGOT1 con una dosis baja de oxaloacetato, potencia los efectos terapéuticos de la rGOT1 intravenosa tras la isquemia.

- El efecto protector mediado por la administración de la rGOT1 se observa incluso cuando los tratamientos se inician 2h después del comienzo de la isquemia.

- La destacada protección mostrada por la combinación de rGOT1 y dosis bajas de oxaloacetato sugiere que esta estrategia puede representar una aproximación válida para el tratamiento exitoso del ictus en fase aguda.

- Hemos optimizado un protocolo para inducir la expresión exógena del EAAT2 en células madre mesenquimales y células HEK.

- Hemos demostrado la expresión y funcionalidad del EAAT2 en células madre mesenquimales y células HEK.

- La transfección de células madre mesenquimales no afecta a los marcadores de membrana analizados, a la capacidad angiogénica o a la secreción de VEGF.

- La administración de células transfectadas con EAAT2 induce una disminución de los niveles de glutamato sérico in vivo.

- El efecto beneficioso de las células madre mesenquimales es reducido tras la expresión exógena del EAAT2, lo cual limita el uso de estas células como un atrapador celular.

- Los atrapadores celulares de glutamato sanguíneo no presentan un mayor beneficio que los otros atrapadores de glutamato ya descritos, así como su efecto protector no es mayor que el del oxaloacetato.

- Los resultados con células transfectadas con EAAT2 confirman que, por medio de un procedimiento alternativo, la reducción del glutamato sanguíneo es una estrategia protectora eficiente en el ictus isquémico.

- Nuestros resultados demuestran que la tranfección de células madre mesenquimales con un EAAT2 funcional puede conferirles una acción terapéutica dual: neuroprotección y neurorreparación.

14. Summary

Cerebrovascular disease is the second leading cause of death and disability in the first developed countries. However, despite its socio-economic importance, available therapies are limited. The most common etiology of stroke, ischemic stroke, is localized reduction of cerebral blood flow following cerebral artery occlusion. This process triggers a series of events at the molecular and cellular level that culminate with a power failure in the area of the brain affected, followed by a process of cell death by necrosis. This area is called the ischemic core. The region surrounding the core, called the ischemic penumbra, consists hypoperfused tissue but still viable tissue. However, this area is subject to a number of molecular processes excitotoxicity, oxidative stress and inflammatory response are the main therapeutic targets for neuroprotection in cerebral ischemia.

Reperfusion therapies, by pharmacologic thrombolysis with tissue recombinant plasminogen activator (rt-PA) or mechanical thrombectomy, are the treatment strategies that achieve better benefits in patients suffering ischemic stroke. However, the narrow therapeutic window (4.5 h after onset of symptoms you for pharmacological thrombolysis), the side effects associated with this drug therapy and the need for highly qualified equipment and infrastructure for mechanical thrombectomy make only between 3 and 7% of patients with cerebral infarction may benefit from this therapy in most developed countries. Therefore, there is urgent need to develop new therapeutic strategies based on neuroprotection or neurorepair.

Neuroprotection is a term that includes all therapies aimed at reducing death after ischemia without exerting any influence on tissue reperfusion during the acute phase of stroke. Neuroprotective drugs are classified in terms of their mechanisms actions in the following groups: antagonists of Ca^{2+} channel, antagonists of glutamate receptor,

antioxidants, phospholipid precursors, inhibitors of the release of glutamate, GABA agonists and anti -inflammatory. So far, some drugs have shown promising results in experimental studies, taken once per clinical trials have not demonstrated efficacy.

Furthermore, the neurorepair strategies present a therapeutic window larger than the acute phase of stroke. These strategies include the restoration of brain function, whether good by regeneration of brain tissue damaged (neuroregeneration) or by creating new neural connections or synapses (brain plasticity). The purpose of the neurorepair therapies is the restoration of the neurovascular unit using pharmacological or cell therapy strategies, focused on enhancing neurogenesis, angiogenesis and synaptogenesis.

Glutamate is one of the major targets of neuroprotection in cerebral ischemia. Glutamate is the primary neurotransmitter of the central nervous system. In the brain, glutamate is compartmentalized intracellularly in neurons and astrocytes, as a small extracellular fraction thereof. This glutamate homeostasis is very sensitive to energy changes and is mainly regulated by excitatory amino acid transporters (EAATs) present in astrocytes, neurons and endothelial cells which form the blood brain barrier; EAAT being responsible for 90% of the reuptake of extracellular glutamate. The disturbance of equilibrium of glutamate is related central nervous system damage, such as occurs in ischemic stroke, head injury, amyotrophic lateral sclerosis (ALS) and Parkinson's Disease, among others.

During cerebral ischemia, depolarization of the cell membrane due to power failure causes an increase of glutamate into the extracellular space. This excess glutamate induces a complex process pathogenic mechanisms leading to neuroexcitotoxicity. To mitigate the deleterious effects of excitotoxicity, novel neuroprotective drugs developed to block glutamate receptors or inhibit glutamate release by blocking presynaptic channels. These drug treatments did not

show efficacy in human clinical, because of this urgent need to develop new therapeutic strategies against excitotoxicity mediated by glutamate. To this end, different studies described the existence of glutamate concentration gradient between the endothelial cells that form the blood-brain barrier and the bloodstream. When glutamate concentration of the brain endothelial cells is greater than the concentration of blood glutamate, this is carried from the brain to the bloodstream. Because of that a new hypothesis arise, which postulate that the reducing blood levels of glutamate would increase the concentration gradient between brain endothelium and blood; thereby favoring the elimination of cerebral glutamate. This potential mechanism of neuroprotection is called grabbing of blood glutamate. Thus, treatment of cerebral ischemia with blood glutamate grabbers, could lead to a reduction of cerebral glutamate, which could lead to therapeutic implications after cerebral ischemia. In this regard, various studies have reported that the metabolic reaction mediated by glutamic oxaloacetic transaminase (GOT) could be an important neuroprotective target in cerebral ischemia. The therapeutic potential associated with the GOT is due to the fact that this enzyme, using oxaloacetate as co-substrate, is able to metabolize glutamate to α-ketoglutarate and aspartate, leading to a decrease in blood levels of glutamate. Based on this premise, our group demonstrated that administration of oxaloacetate induces a reduction in blood glutamate levels through the activation of the GOT, which average neuroprotective effects in an animal model of cerebral ischemia in rat. However, from a clinical point of view, the use of oxaloacetate as a glutamate grabber can have important limitations due to their potential side effects, because the oxaloacetate participates in the Krebs cycle, its high therapeutic dose and narrow therapeutic window.

Cell therapy has emerged as a promising strategy against conventional medical treatments because of its many potential mechanisms of action, among which the integration

of the administered cells in tissues, immunomodulation processes or secretion of growth factors. Several cell lines have shown beneficial effects in preclinical studies of cerebral ischemia, including embryonic stem cells, neural stem cells, induced pluripotent stem cells and mesenchymal stem cells (MSCs), among others. Of these, MSCs have been described as the most suitable. This is because not only they are multipotent, but also their immunomodulatory abilities and secretion of growth factors, giving them pleiotropic mechanisms of action, among them: differentiation into neural lineage cells; induction of neurogenesis, angiogenesis and synaptogenesis; activation of endogenous processes of brain plasticity; regulation of cerebral blood flow; reduced apoptosis; immunomodulation of inflammation; and increased cell survival, among others. Moreover, several preclinical studies of cerebral ischemia in rodents found functional recovery and reduced infarct volume.

For all the above, the combination of mechanisms of neuroprotection (by blood glutamate grabbing) and neurorepair (mediated by MSCs) constitute a promising therapeutic strategy in cerebral ischemia. Therefore, the objective of this work was the development of new alternatives of blood glutamate grabbers for use in ischemic stroke. So we have used two strategies: enzymatic and cellular. The enzymatic strategy was based on the use of rGOT1 administered individually and combined with a non-therapeutic dose of oxaloacetate. The cell strategy was to express, through cell transfection, the transporter $EAAT_2$ in cell lines. For this purpose, two cell lines were used: HEK cells (it seeks the neuroprotective effect for blood glutamate uptake by $EAAT_2$) and MSCs (dual effect: neuroprotective, by uptake of blood glutamate by $EAAT_2$ and neurorepair, by endogenous properties of mesenchymal stem cells).

To test the effectiveness of rGOT1 in decreased of blood glutamate and brain glutamate, and then determine the protective effect of the enzyme, the study was divided into two parts. First, a dose response study in healthy animals

was performed in order to determine the most effective dose of rGOT1 in reducing blood glutamate. To simulate of increase of glutamate observed after cerebral ischemia, glutamate was injected, at a dose of 15 mM, in the jugular of SD rats. The following doses were tested rGOT1: 6.44 µg/ 100g, 12.88 µg /100g and 25.76 µg /100g. To determine the concentrations of glutamate, the blood samples were obtained from the tail vein before glutamate injection and at 1, 2, 4, 6 and 24 h after glutamate injection. Serum levels glutamate were measured by ELISA. The results showed that the dose of 12.88 µg /100g rGOT1 was the most effective in reducing blood glutamate ($p < 0.01$). In order to determine whether the effect of the enzyme could be powered by oxaloacetate, rGOT1 dose 12.88 µg /100g was combined with a non-therapeutic dose of oxaloacetate (1.5mg /100g). The administration of such combination induced a larger decrease in blood glutamate ($p < 0.01$).

The next step was to examine the protective effect of rGOT1 (12.88 µg/100g) and rGOT1 (12.88 µg /100g) supplemented with oxaloacetate (1.5 mg/100g) in SD rats subjected to cerebral ischemia by intraluminal filament, compared with animals treated oxaloacetate with a dose of 3.5 mg/100g (therapeutic dose). To determine the therapeutic capacity of the treatments, which were administered immediately after reperfusion, the infarct volume was valued by Magnetic Resonance image (MRI) and the functional deficit by Cylinder Test. Likewise, the reduction of blood glutamate was measured by ELISA and GOT activity was determined by means of Reflotron GOT, and the reduction of cerebral glutamate was measured MRI spectroscopy. The results showed that the increase in serum glutamate following cerebral ischemia was reduced by treatments: rGOT1 (12.88 µg/100g), oxaloacetate (3.5 mg/100g) and rGOT1 more oxaloacetate (12.88 µg/100g and 1.5mg/100g respectively), without significant differences between them. This decrease in serum glutamate caused by treatment was associated with a reduction in brain glutamate ($p < 0.05$). All treatments

induced a decrease in infarct volume at 24 h and 7 d after ischemia ($p < 0.05$), with the greatest effect in animals treated with rGOT1 + oxaloacetate ($p < 0.05$). In animals which were administered rGOT1, the enzymatic activity thereof was increased ($p < 0.01$).

In order to determine the optimal therapeutic window for the administration of rGOT1, ischemic rats were also treated 1 h after reperfusion. The treatment groups were: rGOT1 (12.88 µg/100g) and rGOT1 + oxaloacetate (12.88 µg/100 g and 1.5 mg/100g, respectively). Both treatments caused a significant reduction ($p < 0.05$) of blood glutamate levels. However, the infarct volume analysis revealed that the administration of treatment 1 h after reperfusion has less protective effect that the administration right after reperfusion.

As somatosensory test, combination therapy of rGOT1 with oxaloacetate is associated with better functional outcome 7 d ($p < 0.05$).

Moreover, to induce expression of $EAAT_2$ in various cell lines employ different transfection techniques. By fluorescence microscopy and flow cytometry the presence of the YFP reporter gene was analyzed to test the efficiency of the transfection process of $EAAT_2$. In a first step, different viral vectors to try to express the $EAAT_2$ in HEK cells and MSCs were used. The results of infection did not show expression of YFP in such cells. As a result, other transfection techniques were used. On one hand, in MSCs the following techniques were tested: calcium phosphate, lipofection and electroporation; the latter being offered positive results for the expression of $EAAT_2$ and associated YFP. As it regards the HEK cells, the expression of $EAAT_2$ and YFP was achieved by calcium phosphate transfection. The subsequent selection with gentamicin allowed to select those HEK cells that had integrated the $EAAT_2$ in its genome.

By immunofluorescence and confocal microscopy, we found that both HEK as MSCs co-expressing the YFP reporter gene and $EAAT_2$. Furthermore, the functionality of $EAAT_2$ gene in transfected cells was determined by experiments of glutamate uptake. The results of these experiments showed that the transfected cells were able to uptake glutamate efficiently. To confirm that the uptake was mediated by $EAAT_2$, glutamate uptake in combination with specific inhibitors of $EAAT_2$, DHK and TBOA, was determined. The results of these experiments demonstrated that the use of the inhibitors prevented the glutamate uptake in transfected cells, confirming that this uptake was mediated by $EAAT_2$.

Because of MSCs exhibit endogenous neurorepairs properties was necessary to determine that the electroporation process not change the characteristic of MSCs. To this, the expression of specific markers of the phenotype of MSCs (CD90 +, CD45- and CD73 +) were analyzed by flow cytometry, the angiogenic capacity by matrigel and VEGF secretion by ELISA. The results showed no differences between the MSC- and MSC+, regarding the above mentioned properties.

Having demonstrated the ability of transfected cells to uptake glutamate *in vitro*, it was necessary to determine their effect *in vivo*. For this, prior to the use of transfected cells in Wistar rats subjected to cerebral ischemia, adequate cell dose was determined to induce a reduction of blood glutamate. To this end, the following experimental groups were analyzed in healthy rats: 3.5 mg/100g of oxaloacetate (therapeutic dose, positive control), $3x10^6$ HEK-, $3x10^6$ HEK+, $3x10^6$ MSC- and $3x10^6$ MSC +. Serum glutamate concentration was measured by ELISA prior to the administration of treatment and at 1, 3 and 4 h after administration of the treatment. The results showed a reduction in serum glutamate in animals treated with oxaloacetate at 1 and 4 h after administration. As for the groups treated with cells, administration of $3x10^6$ HEK+ induced a decrease in glutamate levels 1 hour after, while $3x10^6$ MSC+ treated group decreased serum glutamate levels

1 and 3 h after administration (all $p < 0.05$). With the aim of achieving greater reductions glutamate, two more groups, $9x10^6$ MSC- and $9x10^6$ MSC+, were analyzed. The results showed that in the group treated with $9x10^6$ MSC+ reduces glutamate levels at 3 h ($p < 0.05$) respect to the control group, but this reduction was not greater than the dose of $3x10^6$ MSC+.

Finally, the therapeutic effect of cell lines transfected with $EAAT_2$, administered intravenously, in Wistar rats subjected to cerebral ischemia by intraluminal filament was studied. To determine the beneficial effects of this therapy, infarct volume was valued by Magnetic Resonance image (MRI) and functional deficits by functional test. Likewise, blood glutamate levels were analyzed by ELISA. The following study groups were conducted: Vehicle (PBS), oxaloacetate (3.5 mg/100g), $3x10^6$ HEK-, $3x10^6$ HEK+, $3x10^6$ MSC-, $3x10^6$ MSC+, $9x10^6$ MSC- and $9x10^6$ MSC+. Treatments were injected into right jugular after reperfussion. Analysis of serum glutamate was conducted prior to surgery, immediately after reperfusion and 1, 3, 4 and 24 h after treatment administration. The results showed a reduction in serum glutamate, 1 h after treatment administration, in the groups treated with oxaloacetate and transfected cells ($p < 0.05$). However, the animals treated with oxaloacetate showed a reduction of infarct volume ($p < 0.05$). Other groups that induced a reduction of infarct volume were $3x10^6$ MSC- and $9x10^6$ MSC+ at 7d. As for the functional test, the animals treated with oxaloacetate, $3x10^6$ HEK+, $3x10^6$ MSC- and $9x10^6$ MSC- functional improvement showed 14 d after ischemia.

Based on all the above results, we conclude that:

Section I: Analysis of protective effect of rGOT in ischemia

6. The administration of rGOT1 alone induces a reduction in serum and brain glutamate levels, which also resulted in a significant reduction in the infarct

volume and improvement in the sensorimotor deficit after ischemia.

7. The beneficial effects mediated by rGOT1 were similar to those observed with the higher doses of oxaloacetate.
8. Combination of rGOT1 with a low dose of oxaloacetate potentiates the therapeutic effect of intravenously rGOT1 after ischemia.
9. The protective effect mediated by administration of rGOT1 was observed even when the treatments were initiated as soon as 2h after the onset of ischemia.
10. The robust protection shown by the combination of rGOT1 and low doses of oxaloacetate proposes that this strategy may represent a valid approach for a successful acute-phase stroke treatment.

Section II: Effect of glutamate grabbers cells on ischemic damage.

9. We have optimized a protocol to induce the exogenous expression of $EAAT_2$ in mesenchymal stem cells and HEK cells.
10. We have demonstrated the expression and functionality of $EAAT_2$ in mesenchymal stem cells and HEK cells.
11. The transfection of mesenchymal stem cells does not affect the membrane markers analyzed, angiogenic capacity or secretion of VEGF.
12. The administration of transfected cells with $EAAT_2$ is able to induce a lowering of serum glutamate levels *in vivo.*
13. The beneficial effect of mesenchymal stem cells is reduced after exogenous expression of $EAAT_2$, which limit the use of these cells like a cell grabber.
14. Blood glutamate cell grabbing do not present better benefit than other glutamate grabbers already well described, as their protective effect is not higher than oxaloacetate.

15. Results with EAAT2 transfected cells have confirmed the effect of blood glutamate reduction as an efficient alternative protective strategy against ischemic stroke.
16. Our results demonstrate that the transfection of mesenchymal stem cells with functional $EAAT_2$ may confer their a dual therapeutic action: neuroprotection and neurorepair.

USC
UNIVERSIDADE
DE SANTIAGO
DE COMPOSTELA

Bibliography

USC
UNIVERSIDADE
DE SANTIAGO
DE COMPOSTELA

1. The world health organization monica project (monitoring trends and determinants in cardiovascular disease): A major international collaboration. Who monica project principal investigators. *J Clin Epidemiol*. 1988;41:105-114
2. Bonita R. Epidemiology of stroke. *Lancet*. 1992;339:342-344
3. Feigin VL, Lawes CM, Bennett DA, Anderson CS. Stroke epidemiology: A review of population-based studies of incidence, prevalence, and case-fatality in the late 20th century. *Lancet Neurol*. 2003;2:43-53
4. Diaz-Guzman J, Egido-Herrero JA, Fuentes B, Fernandez-Perez C, Gabriel-Sanchez R, Barbera G, Abilleira S. [incidence of strokes in spain: The ibericTUS study. Data from the pilot study]. *Rev Neurol*. 2009;48:61-65
5. Feigin VL, Lawes CM, Bennett DA, Barker-Collo SL, Parag V. Worldwide stroke incidence and early case fatality reported in 56 population-based studies: A systematic review. *Lancet Neurol*. 2009;8:355-369
6. Diaz-Guzman J, Bermejo-Pareja F, Benito-Leon J, Vega S, Gabriel R, Medrano MJ. Prevalence of stroke and transient ischemic attack in three elderly populations of central spain. *Neuroepidemiology*. 2008;30:247-253
7. Rodríguez-Yáñez M, Fernández Maiztegui C, Pérez-Concha T, Castillo J, Zarranz J. Enfermedades vasculares cerebrales. *Neurología*. Madrid, España: Elsevier España; 2008:337-411.
8. Arboix A, Díaz J, Pérez-Sempere A, Álvarez-Sabín J. Ictus: Tipos etiológicos y criterios diagnósticos. *Rev Neurol*. 2002;17:3-12
9. Arias-Rivas S, Vivancos-Mora J, Castillo J. Epidemiología de los subtipos de ictus en pacientes hospitalizados atendidos por neurólogos: Resultados del registro epices (i). *Rev Neurol*. 2012;54:385-393
10. Del Zoppo GJ, Saver JL, Jauch EC, Adams HP, Jr., American Heart Association Stroke C. Expansion of the time window for treatment of acute ischemic stroke with intravenous tissue plasminogen activator: A science advisory from the american heart association/american stroke association. *Stroke*. 2009;40:2945-2948
11. Adams HP, Jr., Bendixen BH, Kappelle LJ, Biller J, Love BB, Gordon DL, Marsh EE, 3rd. Classification of subtype of acute ischemic stroke. Definitions for use in a multicenter clinical trial. Toast. Trial of org 10172 in acute stroke treatment. *Stroke*. 1993;24:35-41
12. Feinberg WM, Albers GW, Barnett HJ, Biller J, Caplan LR, Carter LP, Hart RG, Hobson RW, 2nd, Kronmal RA, Moore WS, Robertson JT, Adams HP. Guidelines for the management of transient ischemic attacks. From the ad hoc committee on guidelines for the management of transient

ischemic attacks of the stroke council of the american heart association. *Circulation*. 1994;89:2950-2965
13. Calandre L, Arnal C, Ortega JF, Bermejo F, Felgeroso B, del Ser T, Vallejo A. Risk factors for spontaneous cerebral hematomas. Case-control study. *Stroke*. 1986;17:1126-1128
14. Castillo J. Fisiopatología de la isquemia cerebral. *Rev Neurol*. 2000;30:459-464
15. Back T. Pathophysiology of the ischemic penumbra--revision of a concept. *Cell Mol Neurobiol*. 1998;18:621-638
16. Astrup J, Symon L, Branston NM, Lassen NA. Cortical evoked potential and extracellular k+ and h+ at critical levels of brain ischemia. *Stroke*. 1977;8:51-57
17. Hansen AJ. Effect of anoxia on ion distribution in the brain. *Physiol Rev*. 1985;65:101-148
18. Blank WF, Jr., Kirshner HS. The kinetics of extracellular potassium changes during hypoxia and anoxia in the cat cerebral cortex. *Brain Res*. 1977;123:113-124
19. Choi DW. Ionic dependence of glutamate neurotoxicity. *J Neurosci*. 1987;7:369-379
20. Choi DW, Rothman SM. The role of glutamate neurotoxicity in hypoxic-ischemic neuronal death. *Annu Rev Neurosci*. 1990;13:171-182
21. White BC, Sullivan JM, DeGracia DJ, O'Neil BJ, Neumar RW, Grossman LI, Rafols JA, Krause GS. Brain ischemia and reperfusion: Molecular mechanisms of neuronal injury. *J Neurol Sci*. 2000;179:1-33
22. Choi DW. Excitotoxic cell death. *J Neurobiol*. 1992;23:1261-1276
23. Schiene K, Bruehl C, Zilles K, Qu M, Hagemann G, Kraemer M, Witte OW. Neuronal hyperexcitability and reduction of gabaa-receptor expression in the surround of cerebral photothrombosis. *J Cereb Blood Flow Metab*. 1996;16:906-914
24. Banasiak KJ, Xia Y, Haddad GG. Mechanisms underlying hypoxia-induced neuronal apoptosis. *Prog Neurobiol*. 2000;62:215-249
25. Grandati M, Verrecchia C, Revaud ML, Allix M, Boulu RG, Plotkine M. Calcium-independent no-synthase activity and nitrites/nitrates production in transient focal cerebral ischaemia in mice. *Br J Pharmacol*. 1997;122:625-630
26. Nogawa S, Zhang F, Ross ME, Iadecola C. Cyclo-oxygenase-2 gene expression in neurons contributes to ischemic brain damage. *J Neurosci*. 1997;17:2746-2755
27. McDonald ES, Windebank AJ. Mechanisms of neurotoxic injury and cell death. *Neurol Clin*. 2000;18:525-540
28. Jander S, Kraemer M, Schroeter M, Witte OW, Stoll G. Lymphocytic infiltration and expression of intercellular

adhesion molecule-1 in photochemically induced ischemia of the rat cortex. *J Cereb Blood Flow Metab*. 1995;15:42-51

29. Rami A, Agarwal R, Botez G, Winckler J. Mu-calpain activation, DNA fragmentation, and synergistic effects of caspase and calpain inhibitors in protecting hippocampal neurons from ischemic damage. *Brain Res*. 2000;866:299-312
30. Adams HP, Jr., del Zoppo G, Alberts MJ, Bhatt DL, Brass L, Furlan A, Grubb RL, Higashida RT, Jauch EC, Kidwell C, Lyden PD, Morgenstern LB, Qureshi AI, Rosenwasser RH, Scott PA, Wijdicks EF, American Heart Association/American Stroke Association Stroke C, American Heart Association/American Stroke Association Clinical Cardiology C, American Heart Association/American Stroke Association Cardiovascular R, Intervention C, Atherosclerotic Peripheral Vascular Disease Working G, Quality of Care Outcomes in Research Interdisciplinary Working G. Guidelines for the early management of adults with ischemic stroke: A guideline from the american heart association/american stroke association stroke council, clinical cardiology council, cardiovascular radiology and intervention council, and the atherosclerotic peripheral vascular disease and quality of care outcomes in research interdisciplinary working groups: The american academy of neurology affirms the value of this guideline as an educational tool for neurologists. *Circulation*. 2007;115:e478-534
31. Dirks M, Niessen LW, van Wijngaarden JD, Koudstaal PJ, Franke CL, van Oostenbrugge RJ, Huijsman R, Lingsma HF, Minkman MM, Dippel DW, Investigators PRATiIS. Promoting thrombolysis in acute ischemic stroke. *Stroke*. 2011;42:1325-1330
32. Donnan GA, Davis SM, Parsons MW, Ma H, Dewey HM, Howells DW. How to make better use of thrombolytic therapy in acute ischemic stroke. *Nat Rev Neurol*. 2011;7:400-409
33. Lees KR, Bluhmki E, von Kummer R, Brott TG, Toni D, Grotta JC, Albers GW, Kaste M, Marler JR, Hamilton SA, Tilley BC, Davis SM, Donnan GA, Hacke W, Ecass AN, Group Er-PS, Allen K, Mau J, Meier D, del Zoppo G, De Silva DA, Butcher KS, Parsons MW, Barber PA, Levi C, Bladin C, Byrnes G. Time to treatment with intravenous alteplase and outcome in stroke: An updated pooled analysis of ecass, atlantis, ninds, and epithet trials. *Lancet*. 2010;375:1695-1703
34. Wahlgren N, Ahmed N, Davalos A, Ford GA, Grond M, Hacke W, Hennerici MG, Kaste M, Kuelkens S, Larrue V, Lees KR, Roine RO, Soinne L, Toni D, Vanhooren G, investigators S-M. Thrombolysis with alteplase for acute ischaemic stroke in the safe implementation of thrombolysis in stroke-

monitoring study (sits-most): An observational study. *Lancet*. 2007;369:275-282
35. Rodriguez-Yáñez M, Sobrino T, Arias S, Vazquez-Herrero F, Brea D, Blanco M, Leira R, Castellanos M, Serena J, Vivancos J, Davalos A, Castillo J. Early biomarkers of clinical-diffusion mismatch in acute ischemic stroke. *Stroke*. 2011;42:2813-2818
36. Kaur H, Prakash A, Medhi B. Drug therapy in stroke: From preclinical to clinical studies. *Pharmacology*.92:324-334
37. Ginsberg MD. Current status of neuroprotection for cerebral ischemia: Synoptic overview. *Stroke*. 2009;40:S111-114
38. Jia M, Njapo SA, Rastogi V, Hedna VS. Taming glutamate excitotoxicity: Strategic pathway modulation for neuroprotection. *CNS Drugs*.29:153-162
39. Shuaib A, Lees KR, Lyden P, Grotta J, Davalos A, Davis SM, Diener HC, Ashwood T, Wasiewski WW, Emeribe U. Nxy-059 for the treatment of acute ischemic stroke. *N Engl J Med*. 2007;357:562-571
40. Chamorro A, Amaro S, Castellanos M, Segura T, Arenillas J, Marti-Fabregas J, Gallego J, Krupinski J, Gomis M, Canovas D, Carne X, Deulofeu R, Roman LS, Oleaga L, Torres F, Planas AM. Safety and efficacy of uric acid in patients with acute stroke (urico-ictus): A randomised, double-blind phase 2b/3 trial. *Lancet Neurol*.13:453-460
41. Secades JJ, Frontera G. Cdp-choline: Pharmacological and clinical review. *Methods Find Exp Clin Pharmacol*. 1995;17 Suppl B:1-54
42. Hurtado O, Moro MA, Cardenas A, Sanchez V, Fernandez-Tome P, Leza JC, Lorenzo P, Secades JJ, Lozano R, Davalos A, Castillo J, Lizasoain I. Neuroprotection afforded by prior citicoline administration in experimental brain ischemia: Effects on glutamate transport. *Neurobiol Dis*. 2005;18:336-345
43. Hurtado O, Cardenas A, Pradillo JM, Morales JR, Ortego F, Sobrino T, Castillo J, Moro MA, Lizasoain I. A chronic treatment with cdp-choline improves functional recovery and increases neuronal plasticity after experimental stroke. *Neurobiol Dis*. 2007;26:105-111
44. Davalos A, Castillo J, Alvarez-Sabin J, Secades JJ, Mercadal J, Lopez S, Cobo E, Warach S, Sherman D, Clark WM, Lozano R. Oral citicoline in acute ischemic stroke: An individual patient data pooling analysis of clinical trials. *Stroke*. 2002;33:2850-2857
45. Davalos A, Alvarez-Sabin J, Castillo J, Diez-Tejedor E, Ferro J, Martinez-Vila E, Serena J, Segura T, Cruz VT, Masjuan J, Cobo E, Secades JJ. Citicoline in the treatment of acute ischaemic stroke: An international, randomised, multicentre, placebo-controlled study (ictus trial). *Lancet*.380:349-357

46. J. Castillo, M. Blanco, M. Rodríguez-Yáñez, T. Sobrino, R. Leira, J. Montaner. Estrategias neuroprotectoras en tratamiento del ictus isquémico. ICG Marge, SL. Barcelona 2009; 109-124.
47. Alvarez-Buylla A, Garcia-Verdugo JM. Neurogenesis in adult subventricular zone. *J Neurosci*. 2002;22:629-634
48. Zhang ZG, Chopp M. Neurorestorative therapies for stroke: Underlying mechanisms and translation to the clinic. *Lancet Neurol*. 2009;8:491-500
49. Marti-Fabregas J, Romaguera-Ros M, Gomez-Pinedo U, Martinez-Ramirez S, Jimenez-Xarrie E, Marin R, Marti-Vilalta JL, Garcia-Verdugo JM. Proliferation in the human ipsilateral subventricular zone after ischemic stroke. *Neurology*. 2010;74:357-365
50. Le Belle JE, Orozco NM, Paucar AA, Saxe JP, Mottahedeh J, Pyle AD, Wu H, Kornblum HI. Proliferative neural stem cells have high endogenous ros levels that regulate self-renewal and neurogenesis in a pi3k/akt-dependant manner. *Cell Stem Cell*. 2011;8:59-71
51. Arenillas JF, Sobrino T, Castillo J, Davalos A. The role of angiogenesis in damage and recovery from ischemic stroke. *Curr Treat Options Cardiovasc Med*. 2007;9:205-212
52. Brea D, Sobrino T, Ramos-Cabrer P, Castillo J. Reorganización de la vasculatura cerebral tras la isquemia. *Rev Neurol*. 2009;49:645-654
53. Seevinck PR, Deddens LH, Dijkhuizen RM. Magnetic resonance imaging of brain angiogenesis after stroke. *Angiogenesis*. 2010;13:101-111
54. Sobrino T, Hurtado O, Moro MA, Rodriguez-Yanez M, Castellanos M, Brea D, Moldes O, Blanco M, Arenillas JF, Leira R, Davalos A, Lizasoain I, Castillo J. The increase of circulating endothelial progenitor cells after acute ischemic stroke is associated with good outcome. *Stroke*. 2007;38:2759-2764
55. Zacharek A, Chen J, Cui X, Li A, Li Y, Roberts C, Feng Y, Gao Q, Chopp M. Angiopoietin1/tie2 and vegf/flk1 induced by msc treatment amplifies angiogenesis and vascular stabilization after stroke. *J Cereb Blood Flow Metab*. 2007;27:1684-1691
56. Font MA, Arboix A, Krupinski J. Angiogenesis, neurogenesis and neuroplasticity in ischemic stroke. *Curr Cardiol Rev*. 2010;6:238-244
57. Liu XS, Chopp M, Zhang RL, Hozeska-Solgot A, Gregg SC, Buller B, Lu M, Zhang ZG. Angiopoietin 2 mediates the differentiation and migration of neural progenitor cells in the subventricular zone after stroke. *J Biol Chem*. 2009;284:22680-22689
58. Teng H, Zhang ZG, Wang L, Zhang RL, Zhang L, Morris D, Gregg SR, Wu Z, Jiang A, Lu M, Zlokovic BV, Chopp M.

Coupling of angiogenesis and neurogenesis in cultured endothelial cells and neural progenitor cells after stroke. *J Cereb Blood Flow Metab*. 2008;28:764-771

59. Chopp M, Zhang ZG, Jiang Q. Neurogenesis, angiogenesis, and mri indices of functional recovery from stroke. *Stroke*. 2007;38:827-831
60. Jiang Q, Zhang ZG, Ding GL, Zhang L, Ewing JR, Wang L, Zhang R, Li L, Lu M, Meng H, Arbab AS, Hu J, Li QJ, Pourabdollah Nejad DS, Athiraman H, Chopp M. Investigation of neural progenitor cell induced angiogenesis after embolic stroke in rat using mri. *Neuroimage*. 2005;28:698-707
61. Parr AM, Tator CH, Keating A. Bone marrow-derived mesenchymal stromal cells for the repair of central nervous system injury. *Bone Marrow Transplant*. 2007;40:609-619
62. Moriyama Y, Hayashi M, Yamada H, Yatsushiro S, Ishio S, Yamamoto A. Synaptic-like microvesicles, synaptic vesicle counterparts in endocrine cells, are involved in a novel regulatory mechanism for the synthesis and secretion of hormones. *J Exp Biol*. 2000;203:117-125
63. Schousboe A. Transport and metabolism of glutamate and gaba in neurons are glial cells. *Int Rev Neurobiol*. 1981;22:1-45
64. Boyko M, Gruenbaum SE, Gruenbaum BF, Shapira Y, Zlotnik A. Brain to blood glutamate scavenging as a novel therapeutic modality: A review. *J Neural Transm*.121:971-979
65. Rodriguez-Rodriguez P, Almeida A, Bolanos JP. Brain energy metabolism in glutamate-receptor activation and excitotoxicity: Role for apc/c-cdh1 in the balance glycolysis/pentose phosphate pathway. *Neurochem Int*.62:750-756
66. Mangia S, Giove F, Dinuzzo M. Metabolic pathways and activity-dependent modulation of glutamate concentration in the human brain. *Neurochem Res*.37:2554-2561
67. Hawkins RA. The blood-brain barrier and glutamate. *Am J Clin Nutr*. 2009;90:867S-874S
68. Cooper AJ, McDonald JM, Gelbard AS, Gledhill RF, Duffy TE. The metabolic fate of 13n-labeled ammonia in rat brain. *J Biol Chem*. 1979;254:4982-4992
69. Cooper AJ, Plum F. Biochemistry and physiology of brain ammonia. *Physiol Rev*. 1987;67:440-519
70. Martinez-Hernandez A, Bell KP, Norenberg MD. Glutamine synthetase: Glial localization in brain. *Science*. 1977;195:1356-1358
71. Shigeri Y, Seal RP, Shimamoto K. Molecular pharmacology of glutamate transporters, eaats and vgluts. *Brain Res Brain Res Rev*. 2004;45:250-265

72. Krzyzanowska W, Pomierny B, Filip M, Pera J. Glutamate transporters in brain ischemia: To modulate or not? *Acta Pharmacol Sin*.35:444-462
73. Zhou Y, Danbolt NC. Glutamate as a neurotransmitter in the healthy brain. *J Neural Transm*.121:799-817
74. Cederberg HH, Uhd NC, Brodin B. Glutamate efflux at the blood-brain barrier: Cellular mechanisms and potential clinical relevance. *Arch Med Res*.45:639-645
75. Maragakis NJ, Dietrich J, Wong V, Xue H, Mayer-Proschel M, Rao MS, Rothstein JD. Glutamate transporter expression and function in human glial progenitors. *Glia*. 2004;45:133-143
76. Kim K, Lee SG, Kegelman TP, Su ZZ, Das SK, Dash R, Dasgupta S, Barral PM, Hedvat M, Diaz P, Reed JC, Stebbins JL, Pellecchia M, Sarkar D, Fisher PB. Role of excitatory amino acid transporter-2 (eaat2) and glutamate in neurodegeneration: Opportunities for developing novel therapeutics. *J Cell Physiol*.226:2484-2493
77. Zou J, Wang YX, Dou FF, Lu HZ, Ma ZW, Lu PH, Xu XM. Glutamine synthetase down-regulation reduces astrocyte protection against glutamate excitotoxicity to neurons. *Neurochem Int*.56:577-584
78. Westbrook GL. Glutamate receptors and excitotoxicity. *Res Publ Assoc Res Nerv Ment Dis*. 1993;71:35-50
79. Beretta S, Begni B, Ferrarese C. Pharmacological manipulation of glutamate transport. *Drug News Perspect*. 2003;16:435-445
80. Zerangue N, Kavanaugh MP. Flux coupling in a neuronal glutamate transporter. *Nature*. 1996;383:634-637
81. Fremeau RT, Jr., Voglmaier S, Seal RP, Edwards RH. Vgluts define subsets of excitatory neurons and suggest novel roles for glutamate. *Trends Neurosci*. 2004;27:98-103
82. McBean GJ. Cerebral cystine uptake: A tale of two transporters. *Trends Pharmacol Sci*. 2002;23:299-302
83. Oldendorf WH, Szabo J. Amino acid assignment to one of three blood-brain barrier amino acid carriers. *Am J Physiol*. 1976;230:94-98
84. Mann GE, Yudilevich DL, Sobrevia L. Regulation of amino acid and glucose transporters in endothelial and smooth muscle cells. *Physiol Rev*. 2003;83:183-252
85. Zauner A, Bullock R, Kuta AJ, Woodward J, Young HF. Glutamate release and cerebral blood flow after severe human head injury. *Acta Neurochir Suppl*. 1996;67:40-44
86. Leibowitz A, Boyko M, Shapira Y, Zlotnik A. Blood glutamate scavenging: Insight into neuroprotection. *Int J Mol Sci*.13:10041-10066
87. Castillo MR, Babson JR. Ca(2+)-dependent mechanisms of cell injury in cultured cortical neurons. *Neuroscience*. 1998;86:1133-1144

88. Castillo J, Davalos A, Naveiro J, Noya M. Neuroexcitatory amino acids and their relation to infarct size and neurological deficit in ischemic stroke. *Stroke*. 1996;27:1060-1065
89. Castillo J, Davalos A, Noya M. Progression of ischaemic stroke and excitotoxic aminoacids. *Lancet*. 1997;349:79-83
90. Castillo J, Davalos A, Noya M. Aggravation of acute ischemic stroke by hyperthermia is related to an excitotoxic mechanism. *Cerebrovasc Dis*. 1999;9:22-27
91. Zlotnik A, Sinelnikov I, Gruenbaum BF, Gruenbaum SE, Dubilet M, Dubilet E, Leibowitz A, Ohayon S, Regev A, Boyko M, Shapira Y, Teichberg VI. Effect of glutamate and blood glutamate scavengers oxaloacetate and pyruvate on neurological outcome and pathohistology of the hippocampus after traumatic brain injury in rats. *Anesthesiology*.116:73-83
92. Andreadou E, Kapaki E, Kokotis P, Paraskevas GP, Katsaros N, Libitaki G, Zis V, Sfagos C, Vassilopoulos D. Plasma glutamate and glycine levels in patients with amyotrophic lateral sclerosis: The effect of riluzole treatment. *Clin Neurol Neurosurg*. 2008;110:222-226
93. Stojanovic IR, Kostic M, Ljubisavljevic S. The role of glutamate and its receptors in multiple sclerosis. *J Neural Transm*.121:945-955
94. Campos F, Sobrino T, Blanco M, Lopez-Arias E, Baluja A, Alvarez J, Castillo J. Glutamate neurotoxicity is involved in the neurological damage in patients undergoing extracorporeal circulation. *Int J Cardiol*.172:481-483
95. O'Kane RL, Martinez-Lopez I, DeJoseph MR, Vina JR, Hawkins RA. Na(+)-dependent glutamate transporters (eaat1, eaat2, and eaat3) of the blood-brain barrier. A mechanism for glutamate removal. *J Biol Chem*. 1999;274:31891-31895
96. Caldeira MV, Salazar IL, Curcio M, Canzoniero LM, Duarte CB. Role of the ubiquitin-proteasome system in brain ischemia: Friend or foe? *Prog Neurobiol*.112:50-69
97. Sattler R, Tymianski M. Molecular mechanisms of calcium-dependent excitotoxicity. *J Mol Med (Berl)*. 2000;78:3-13
98. Lau A, Tymianski M. Glutamate receptors, neurotoxicity and neurodegeneration. *Pflugers Arch*.460:525-542
99. Campos F, Sobrino T, Perez-Mato M, Rodriguez-Osorio X, Leira R, Blanco M, Mirelman D, Castillo J. Glutamate oxaloacetate transaminase: A new key in the dysregulation of glutamate in migraine patients. *Cephalalgia*.33:1148-1154
100. Zlotnik A, Gurevich B, Cherniavsky E, Tkachov S, Matuzani-Ruban A, Leon A, Shapira Y, Teichberg VI. The contribution of the blood glutamate scavenging activity of pyruvate to its

neuroprotective properties in a rat model of closed head injury. *Neurochem Res*. 2008;33:1044-1050
101. Aarts M, Liu Y, Liu L, Besshoh S, Arundine M, Gurd JW, Wang YT, Salter MW, Tymianski M. Treatment of ischemic brain damage by perturbing nmda receptor- psd-95 protein interactions. *Science*. 2002;298:846-850
102. Jones N. Stroke: Disruption of the nnos-psd-95 complex is neuroprotective in models of cerebral ischemia. *Nat Rev Neurol*.7:61
103. Zhou L, Li F, Xu HB, Luo CX, Wu HY, Zhu MM, Lu W, Ji X, Zhou QG, Zhu DY. Treatment of cerebral ischemia by disrupting ischemia-induced interaction of nnos with psd-95. *Nat Med*.16:1439-1443
104. Lee JM, Zipfel GJ, Choi DW. The changing landscape of ischaemic brain injury mechanisms. *Nature*. 1999;399:A7-14
105. Dykens JA. Isolated cerebral and cerebellar mitochondria produce free radicals when exposed to elevated ca2+ and na+: Implications for neurodegeneration. *J Neurochem*. 1994;63:584-591
106. Ogden KK, Traynelis SF. New advances in nmda receptor pharmacology. *Trends Pharmacol Sci*.32:726-733
107. Kalia LV, Kalia SK, Salter MW. Nmda receptors in clinical neurology: Excitatory times ahead. *Lancet Neurol*. 2008;7:742-755
108. Muir KW. Glutamate-based therapeutic approaches: Clinical trials with nmda antagonists. *Curr Opin Pharmacol*. 2006;6:53-60
109. Ikonomidou C, Turski L. Why did nmda receptor antagonists fail clinical trials for stroke and traumatic brain injury? *Lancet Neurol*. 2002;1:383-386
110. Danbolt NC. Glutamate uptake. *Prog Neurobiol*. 2001;65:1-105
111. Lipton P. Ischemic cell death in brain neurons. *Physiol Rev*. 1999;79:1431-1568
112. Castillo J, Martinez F, Corredera E, Aldrey JM, Noya M. Amino acid transmitters in patients with headache during the acute phase of cerebrovascular ischemic disease. *Stroke*. 1995;26:2035-2039
113. Nagy D, Marosi M, Kis Z, Farkas T, Rakos G, Vecsei L, Teichberg VI, Toldi J. Oxaloacetate decreases the infarct size and attenuates the reduction in evoked responses after photothrombotic focal ischemia in the rat cortex. *Cell Mol Neurobiol*. 2009;29:827-835
114. Campos F, Sobrino T, Ramos-Cabrer P, Castillo J. Oxaloacetate: A novel neuroprotective for acute ischemic stroke. *Int J Biochem Cell Biol*.44:262-265
115. Marosi M, Fuzik J, Nagy D, Rakos G, Kis Z, Vecsei L, Toldi J, Ruban-Matuzani A, Teichberg VI, Farkas T. Oxaloacetate

restores the long-term potentiation impaired in rat hippocampus ca1 region by 2-vessel occlusion. *Eur J Pharmacol*. 2009;604:51-57

116. Campos F, Sobrino T, Ramos-Cabrer P, Argibay B, Agulla J, Perez-Mato M, Rodriguez-Gonzalez R, Brea D, Castillo J. Neuroprotection by glutamate oxaloacetate transaminase in ischemic stroke: An experimental study. *J Cereb Blood Flow Metab*.31:1378-1386
117. Boyko M, Zlotnik A, Gruenbaum BF, Gruenbaum SE, Ohayon S, Kuts R, Melamed I, Regev A, Shapira Y, Teichberg VI. Pyruvate's blood glutamate scavenging activity contributes to the spectrum of its neuroprotective mechanisms in a rat model of stroke. *Eur J Neurosci*.34:1432-1441
118. Campos F, Rodriguez-Yanez M, Castellanos M, Arias S, Perez-Mato M, Sobrino T, Blanco M, Serena J, Castillo J. Blood levels of glutamate oxaloacetate transaminase are more strongly associated with good outcome in acute ischaemic stroke than glutamate pyruvate transaminase levels. *Clin Sci (Lond)*.121:11-17
119. Campos F, Perez-Mato M, Agulla J, Blanco M, Barral D, Almeida A, Brea D, Waeber C, Castillo J, Ramos-Cabrer P. Glutamate excitoxicity is the key molecular mechanism which is influenced by body temperature during the acute phase of brain stroke. *PLoS One*.7:e44191
120. Godino Mdel C, Romera VG, Sanchez-Tomero JA, Pacheco J, Canals S, Lerma J, Vivancos J, Moro MA, Torres M, Lizasoain I, Sanchez-Prieto J. Amelioration of ischemic brain damage by peritoneal dialysis. *J Clin Invest*.123:4359-4363
121. Silva-Candal A, Vieites-Prado A, Gutierrez-Fernandez M, Rey RI, Argibay B, Mirelman D, Sobrino T, Rodriguez-Frutos B, Castillo J, Campos F. Blood glutamate grabbing does not reduce the hematoma in an intracerebral hemorrhage model but it is a safe excitotoxic treatment modality. *J Cereb Blood Flow Metab*.35:1206-1212
122. Ghajar J. Traumatic brain injury. *Lancet*. 2000;356:923-929
123. Cole TB. Global road safety crisis remedy sought: 1.2 million killed, 50 million injured annually. *JAMA*. 2004;291:2531-2532
124. Warden DL, French L. Traumatic brain injury in the war zone. *N Engl J Med*. 2005;353:633-634
125. Xydakis MS, Fravell MD, Nasser KE, Casler JD. Analysis of battlefield head and neck injuries in iraq and afghanistan. *Otolaryngol Head Neck Surg*. 2005;133:497-504
126. Stonesifer LD. Mild traumatic brain injury in u.S. Soldiers returning from iraq. *N Engl J Med*. 2008;358:2178; author reply 2179
127. Mock C, Quansah R, Krishnan R, Arreola-Risa C, Rivara F. Strengthening the prevention and care of injuries worldwide. *Lancet*. 2004;363:2172-2179

128. Maas AI, Stocchetti N, Bullock R. Moderate and severe traumatic brain injury in adults. *Lancet Neurol*. 2008;7:728-741
129. Hutchinson PJ, O'Connell MT, Rothwell NJ, Hopkins SJ, Nortje J, Carpenter KL, Timofeev I, Al-Rawi PG, Menon DK, Pickard JD. Inflammation in human brain injury: Intracerebral concentrations of il-1alpha, il-1beta, and their endogenous inhibitor il-1ra. *J Neurotrauma*. 2007;24:1545-1557
130. Kroemer G, Galluzzi L, Brenner C. Mitochondrial membrane permeabilization in cell death. *Physiol Rev*. 2007;87:99-163
131. Rose ME, Huerbin MB, Melick J, Marion DW, Palmer AM, Schiding JK, Kochanek PM, Graham SH. Regulation of interstitial excitatory amino acid concentrations after cortical contusion injury. *Brain Res*. 2002;943:15-22
132. Bullock R, Zauner A, Woodward JJ, Myseros J, Choi SC, Ward JD, Marmarou A, Young HF. Factors affecting excitatory amino acid release following severe human head injury. *J Neurosurg*. 1998;89:507-518
133. Richards DA, Tolias CM, Sgouros S, Bowery NG. Extracellular glutamine to glutamate ratio may predict outcome in the injured brain: A clinical microdialysis study in children. *Pharmacol Res*. 2003;48:101-109
134. Orrenius S, Zhivotovsky B, Nicotera P. Regulation of cell death: The calcium-apoptosis link. *Nat Rev Mol Cell Biol*. 2003;4:552-565
135. Zlotnik A, Gurevich B, Tkachov S, Maoz I, Shapira Y, Teichberg VI. Brain neuroprotection by scavenging blood glutamate. *Exp Neurol*. 2007;203:213-220
136. Zlotnik A, Gruenbaum SE, Artru AA, Rozet I, Dubilet M, Tkachov S, Brotfain E, Klin Y, Shapira Y, Teichberg VI. The neuroprotective effects of oxaloacetate in closed head injury in rats is mediated by its blood glutamate scavenging activity: Evidence from the use of maleate. *J Neurosurg Anesthesiol*. 2009;21:235-241
137. Cross DT, 3rd, Tirschwell DL, Clark MA, Tuden D, Derdeyn CP, Moran CJ, Dacey RG, Jr. Mortality rates after subarachnoid hemorrhage: Variations according to hospital case volume in 18 states. *J Neurosurg*. 2003;99:810-817
138. van Gijn J, Kerr RS, Rinkel GJ. Subarachnoid haemorrhage. *Lancet*. 2007;369:306-318
139. Harmsen P, Tsipogianni A, Wilhelmsen L. Stroke incidence rates were unchanged, while fatality rates declined, during 1971-1987 in goteborg, sweden. *Stroke*. 1992;23:1410-1415
140. Stegmayr B, Eriksson M, Asplund K. Declining mortality from subarachnoid hemorrhage: Changes in incidence and case fatality from 1985 through 2000. *Stroke*. 2004;35:2059-2063

141. Sehba FA, Bederson JB. Mechanisms of acute brain injury after subarachnoid hemorrhage. *Neurol Res*. 2006;28:381-398
142. Johnston MV, Trescher WH, Ishida A, Nakajima W. Neurobiology of hypoxic-ischemic injury in the developing brain. *Pediatr Res*. 2001;49:735-741
143. Hillered L, Vespa PM, Hovda DA. Translational neurochemical research in acute human brain injury: The current status and potential future for cerebral microdialysis. *J Neurotrauma*. 2005;22:3-41
144. Huang CY, Wang LC, Wang HK, Pan CH, Cheng YY, Shan YS, Chio CC, Tsai KJ. Memantine alleviates brain injury and neurobehavioral deficits after experimental subarachnoid hemorrhage. *Mol Neurobiol*.51:1038-1052
145. Schulz MK, Wang LP, Tange M, Bjerre P. Cerebral microdialysis monitoring: Determination of normal and ischemic cerebral metabolisms in patients with aneurysmal subarachnoid hemorrhage. *J Neurosurg*. 2000;93:808-814
146. Park S, Yamaguchi M, Zhou C, Calvert JW, Tang J, Zhang JH. Neurovascular protection reduces early brain injury after subarachnoid hemorrhage. *Stroke*. 2004;35:2412-2417
147. Sehba FA, Chereshnev I, Maayani S, Friedrich V, Jr., Bederson JB. Nitric oxide synthase in acute alteration of nitric oxide levels after subarachnoid hemorrhage. *Neurosurgery*. 2004;55:671-677; discussion 677-678
148. Dawson VL, Kizushi VM, Huang PL, Snyder SH, Dawson TM. Resistance to neurotoxicity in cortical cultures from neuronal nitric oxide synthase-deficient mice. *J Neurosci*. 1996;16:2479-2487
149. Kandratavicius L, Balista PA, Lopes-Aguiar C, Ruggiero RN, Umeoka EH, Garcia-Cairasco N, Bueno-Junior LS, Leite JP. Animal models of epilepsy: Use and limitations. *Neuropsychiatr Dis Treat*.10:1693-1705
150. Rosenow F, Knake S. Status epilepticus in adults. *Handb Clin Neurol*.108:813-819
151. Lee SK. Treatment strategy for the patient with hippocampal sclerosis who failed to the first antiepileptic drug. *J Epilepsy Res*.4:1-6
152. Eid T, Tu N, Lee TS, Lai JC. Regulation of astrocyte glutamine synthetase in epilepsy. *Neurochem Int*.63:670-681
153. Carvalho AS, Torres LB, Persike DS, Fernandes MJ, Amado D, Naffah-Mazzacoratti Mda G, Cavalheiro EA, da Silva AV. Neuroprotective effect of pyruvate and oxaloacetate during pilocarpine induced status epilepticus in rats. *Neurochem Int*.58:385-390
154. Bloudek LM, Stokes M, Buse DC, Wilcox TK, Lipton RB, Goadsby PJ, Varon SF, Blumenfeld AM, Katsarava Z, Pascual J, Lanteri-Minet M, Cortelli P, Martelletti P. Cost of

healthcare for patients with migraine in five european countries: Results from the international burden of migraine study (ibms). *J Headache Pain*.13:361-378
155. Ferrari A, Spaccapelo L, Pinetti D, Tacchi R, Bertolini A. Effective prophylactic treatments of migraine lower plasma glutamate levels. *Cephalalgia*. 2009;29:423-429
156. Martinez F, Castillo J, Rodriguez JR, Leira R, Noya M. Neuroexcitatory amino acid levels in plasma and cerebrospinal fluid during migraine attacks. *Cephalalgia*. 1993;13:89-93
157. Edvinsson L, Villalon CM, MaassenVanDenBrink A. Basic mechanisms of migraine and its acute treatment. *Pharmacol Ther*.136:319-333
158. Goadsby PJ, Classey JD. Glutamatergic transmission in the trigeminal nucleus assessed with local blood flow. *Brain Res*. 2000;875:119-124
159. Ramadan NM. The link between glutamate and migraine. *CNS Spectr*. 2003;8:446-449
160. Kertesz S, Kapus G, Gacsalyi I, Levay G. Deramciclane improves object recognition in rats: Potential role of nmda receptors. *Pharmacol Biochem Behav*.94:570-574
161. Wang M, Chazot PL, Ali S, Duckett SF, Obrenovitch TP. Effects of nmda receptor antagonists with different subtype selectivities on retinal spreading depression. *Br J Pharmacol*.165:235-244
162. de Groot J, Sontheimer H. Glutamate and the biology of gliomas. *Glia*.59:1181-1189
163. Sontheimer H. Malignant gliomas: Perverting glutamate and ion homeostasis for selective advantage. *Trends Neurosci*. 2003;26:543-549
164. Sontheimer H. Ion channels and amino acid transporters support the growth and invasion of primary brain tumors. *Mol Neurobiol*. 2004;29:61-71
165. Ye ZC, Sontheimer H. Glioma cells release excitotoxic concentrations of glutamate. *Cancer Res*. 1999;59:4383-4391
166. Ye ZC, Rothstein JD, Sontheimer H. Compromised glutamate transport in human glioma cells: Reduction-mislocalization of sodium-dependent glutamate transporters and enhanced activity of cystine-glutamate exchange. *J Neurosci*. 1999;19:10767-10777
167. Behrens PF, Langemann H, Strohschein R, Draeger J, Hennig J. Extracellular glutamate and other metabolites in and around rg2 rat glioma: An intracerebral microdialysis study. *J Neurooncol*. 2000;47:11-22
168. Rijpkema M, Schuuring J, van der Meulen Y, van der Graaf M, Bernsen H, Boerman R, van der Kogel A, Heerschap A. Characterization of oligodendrogliomas using short echo

time 1h mr spectroscopic imaging. *NMR Biomed*. 2003;16:12-18
169. Roslin M, Henriksson R, Bergstrom P, Ungerstedt U, Bergenheim AT. Baseline levels of glucose metabolites, glutamate and glycerol in malignant glioma assessed by stereotactic microdialysis. *J Neurooncol*. 2003;61:151-160
170. Ruban A, Berkutzki T, Cooper I, Mohar B, Teichberg VI. Blood glutamate scavengers prolong the survival of rats and mice with brain-implanted gliomas. *Invest New Drugs*.30:2226-2235
171. Pandit V, Seshadri S, Rao SN, Samarasinghe C, Kumar A, Valsalan R. A case of organophosphate poisoning presenting with seizure and unavailable history of parenteral suicide attempt. *J Emerg Trauma Shock*.4:132-134
172. Santos MD, Pereira EF, Aracava Y, Castro NG, Fawcett WP, Randall WR, Albuquerque EX. Low concentrations of pyridostigmine prevent soman-induced inhibition of gabaergic transmission in the central nervous system: Involvement of muscarinic receptors. *J Pharmacol Exp Ther*. 2003;304:254-265
173. Lallement G, Delamanche IS, Pernot-Marino I, Baubichon D, Denoyer M, Carpentier P, Blanchet G. Neuroprotective activity of glutamate receptor antagonists against soman-induced hippocampal damage: Quantification with an omega 3 site ligand. *Brain Res*. 1993;618:227-237
174. McDonough JH, Jr., McLeod CG, Jr., Nipwoda MT. Direct microinjection of soman or vx into the amygdala produces repetitive limbic convulsions and neuropathology. *Brain Res*. 1987;435:123-137
175. Raveh L, Brandeis R, Gilat E, Cohen G, Alkalay D, Rabinovitz I, Sonego H, Weissman BA. Anticholinergic and antiglutamatergic agents protect against soman-induced brain damage and cognitive dysfunction. *Toxicol Sci*. 2003;75:108-116
176. Tattersall J. Seizure activity post organophosphate exposure. *Front Biosci (Landmark Ed)*. 2009;14:3688-3711
177. Lallement G, Denoyer M, Collet A, Pernot-Marino I, Baubichon D, Monmaur P, Blanchet G. Changes in hippocampal acetylcholine and glutamate extracellular levels during soman-induced seizures: Influence of septal cholinoceptive cells. *Neurosci Lett*. 1992;139:104-107
178. Capacio BR, Shih TM. Anticonvulsant actions of anticholinergic drugs in soman poisoning. *Epilepsia*. 1991;32:604-615
179. Gilat E, Kadar T, Levy A, Rabinovitz I, Cohen G, Kapon Y, Sahar R, Brandeis R. Anticonvulsant treatment of sarin-induced seizures with nasal midazolam: An electrographic, behavioral, and histological study in freely moving rats. *Toxicol Appl Pharmacol*. 2005;209:74-85

180. Ruban A, Mohar B, Jona G, Teichberg VI. Blood glutamate scavenging as a novel neuroprotective treatment for paraoxon intoxication. *J Cereb Blood Flow Metab*.34:221-227
181. Griesmaier E, Keller M. Glutamate receptors - prenatal insults, long-term consequences. *Pharmacol Biochem Behav*.100:835-840
182. Zlotnik A, Tsesis S, Gruenbaum BF, Ohayon S, Gruenbaum SE, Boyko M, Sheiner E, Brotfain E, Shapira Y, Teichberg VI. Relationship between glutamate, got and gpt levels in maternal and fetal blood: A potential mechanism for fetal neuroprotection. *Early Hum Dev*.88:773-778
183. Holopainen IE, Lauren HB. Glutamate signaling in the pathophysiology and therapy of prenatal insults. *Pharmacol Biochem Behav*.100:825-834
184. Ruban A, Cohen-Kashi Malina K, Cooper I, Graubardt N, Babakin L, Jona G, Teichberg VI. Combined treatment of an amyotrophic lateral sclerosis rat model with recombinant got1 and oxaloacetic acid: A novel neuroprotective treatment. *Neurodegener Dis*.
185. de Peppo GM, Marolt D. State of the art in stem cell research: Human embryonic stem cells, induced pluripotent stem cells, and transdifferentiation. *J Blood Transfus*.2012:317632
186. Kim SU, de Vellis J. Stem cell-based cell therapy in neurological diseases: A review. *J Neurosci Res*. 2009;87:2183-2200
187. Marti M, Mulero L, Pardo C, Morera C, Carrio M, Laricchia-Robbio L, Esteban CR, Izpisua Belmonte JC. Characterization of pluripotent stem cells. *Nat Protoc*.8:223-253
188. Desai N, Rambhia P, Gishto A. Human embryonic stem cell cultivation: Historical perspective and evolution of xeno-free culture systems. *Reprod Biol Endocrinol*.13:9
189. Miki T, Ring A, Gerlach J. Hepatic differentiation of human embryonic stem cells is promoted by three-dimensional dynamic perfusion culture conditions. *Tissue Eng Part C Methods*.17:557-568
190. Swijnenburg RJ, Schrepfer S, Govaert JA, Cao F, Ransohoff K, Sheikh AY, Haddad M, Connolly AJ, Davis MM, Robbins RC, Wu JC. Immunosuppressive therapy mitigates immunological rejection of human embryonic stem cell xenografts. *Proc Natl Acad Sci U S A*. 2008;105:12991-12996
191. Takahashi K, Tanabe K, Ohnuki M, Narita M, Ichisaka T, Tomoda K, Yamanaka S. Induction of pluripotent stem cells from adult human fibroblasts by defined factors. *Cell*. 2007;131:861-872
192. Yu J, Vodyanik MA, Smuga-Otto K, Antosiewicz-Bourget J, Frane JL, Tian S, Nie J, Jonsdottir GA, Ruotti V, Stewart R,

Slukvin, II, Thomson JA. Induced pluripotent stem cell lines derived from human somatic cells. *Science*. 2007;318:1917-1920
193. Liang P, Du J. Human induced pluripotent stem cell for modeling cardiovascular diseases. *Regen Med Res*.2:4
194. Marti-Fabregas J, Romaguera-Ros M, Gomez-Pinedo U, Martinez-Ramirez S, Jimenez-Xarrie E, Marin R, Marti-Vilalta JL, Garcia-Verdugo JM. Proliferation in the human ipsilateral subventricular zone after ischemic stroke. *Neurology*.74:357-365
195. Gage FH, Ray J, Fisher LJ. Isolation, characterization, and use of stem cells from the cns. *Annu Rev Neurosci*. 1995;18:159-192
196. Sobrino T, Campos F, Castillo J. The role of endothelial progenitor cells in stroke. In: Zhao L-R, Zhang JH, eds. *Cellular therapy for stroke and cns injuries*. Springer International Publishing; 2015:109-123.
197. Takagi Y, Nishimura M, Morizane A, Takahashi J, Nozaki K, Hayashi J, Hashimoto N. Survival and differentiation of neural progenitor cells derived from embryonic stem cells and transplanted into ischemic brain. *J Neurosurg*. 2005;103:304-310
198. Buhnemann C, Scholz A, Bernreuther C, Malik CY, Braun H, Schachner M, Reymann KG, Dihne M. Neuronal differentiation of transplanted embryonic stem cell-derived precursors in stroke lesions of adult rats. *Brain*. 2006;129:3238-3248
199. Shen LH, Li Y, Chen J, Cui Y, Zhang C, Kapke A, Lu M, Savant-Bhonsale S, Chopp M. One-year follow-up after bone marrow stromal cell treatment in middle-aged female rats with stroke. *Stroke*. 2007;38:2150-2156
200. Chen J, Li Y, Wang L, Zhang Z, Lu D, Lu M, Chopp M. Therapeutic benefit of intravenous administration of bone marrow stromal cells after cerebral ischemia in rats. *Stroke*. 2001;32:1005-1011
201. Mehler MF, Rozental R, Dougherty M, Spray DC, Kessler JA. Cytokine regulation of neuronal differentiation of hippocampal progenitor cells. *Nature*. 1993;362:62-65
202. Wei X, Du Z, Zhao L, Feng D, Wei G, He Y, Tan J, Lee WH, Hampel H, Dodel R, Johnstone BH, March KL, Farlow MR, Du Y. Ifats collection: The conditioned media of adipose stromal cells protect against hypoxia-ischemia-induced brain damage in neonatal rats. *Stem Cells*. 2009;27:478-488
203. Borlongan CV, Kaneko Y, Maki M, Yu SJ, Ali M, Allickson JG, Sanberg CD, Kuzmin-Nichols N, Sanberg PR. Menstrual blood cells display stem cell-like phenotypic markers and exert neuroprotection following transplantation in experimental stroke. *Stem Cells Dev*. 2010;19:439-452

204. Martino G, Pluchino S. The therapeutic potential of neural stem cells. *Nat Rev Neurosci*. 2006;7:395-406
205. Sheikh AM, Nagai A, Wakabayashi K, Narantuya D, Kobayashi S, Yamaguchi S, Kim SU. Mesenchymal stem cell transplantation modulates neuroinflammation in focal cerebral ischemia: Contribution of fractalkine and il-5. *Neurobiol Dis*. 2011;41:717-724
206. Bacigaluppi M, Pluchino S, Peruzzotti-Jametti L, Kilic E, Kilic U, Salani G, Brambilla E, West MJ, Comi G, Martino G, Hermann DM. Delayed post-ischaemic neuroprotection following systemic neural stem cell transplantation involves multiple mechanisms. *Brain*. 2009;132:2239-2251
207. Hirko AC, Dallasen R, Jomura S, Xu Y. Modulation of inflammatory responses after global ischemia by transplanted umbilical cord matrix stem cells. *Stem Cells*. 2008;26:2893-2901
208. Arvidsson A, Collin T, Kirik D, Kokaia Z, Lindvall O. Neuronal replacement from endogenous precursors in the adult brain after stroke. *Nat Med*. 2002;8:963-970
209. Mine Y, Tatarishvili J, Oki K, Monni E, Kokaia Z, Lindvall O. Grafted human neural stem cells enhance several steps of endogenous neurogenesis and improve behavioral recovery after middle cerebral artery occlusion in rats. *Neurobiol Dis*. 2013;52:191-203
210. Goldman SA, Chen Z. Perivascular instruction of cell genesis and fate in the adult brain. *Nat Neurosci*. 2011;14:1382-1389
211. Chopp M, Li Y, Zhang ZG. Mechanisms underlying improved recovery of neurological function after stroke in the rodent after treatment with neurorestorative cell-based therapies. *Stroke*. 2009;40:S143-145
212. Lee SH, Lumelsky N, Studer L, Auerbach JM, McKay RD. Efficient generation of midbrain and hindbrain neurons from mouse embryonic stem cells. *Nat Biotechnol*. 2000;18:675-679
213. Nagai N, Kawao N, Okada K, Okumoto K, Teramura T, Ueshima S, Umemura K, Matsuo O. Systemic transplantation of embryonic stem cells accelerates brain lesion decrease and angiogenesis. *Neuroreport*. 2010;21:575-579
214. Tae-Hoon L, Yoon-Seok L. Transplantation of mouse embryonic stem cell after middle cerebral artery occlusion. *Acta Cir Bras*. 2012;27:333-339
215. Seyed Jafari SS, Ali Aghaei A, Asadi-Shekaari M, Nematollahi-Mahani SN, Sheibani V. Investigating the effects of adult neural stem cell transplantation by lumbar puncture in transient cerebral ischemia. *Neurosci Lett*. 2011;495:1-5

216. Guzman R, De Los Angeles A, Cheshier S, Choi R, Hoang S, Liauw J, Schaar B, Steinberg G. Intracarotid injection of fluorescence activated cell-sorted cd49d-positive neural stem cells improves targeted cell delivery and behavior after stroke in a mouse stroke model. *Stroke*. 2008;39:1300-1306
217. Chen SJ, Chang CM, Tsai SK, Chang YL, Chou SJ, Huang SS, Tai LK, Chen YC, Ku HH, Li HY, Chiou SH. Functional improvement of focal cerebral ischemia injury by subdural transplantation of induced pluripotent stem cells with fibrin glue. *Stem Cells Dev*. 2010;19:1757-1767
218. Wang J, Chao F, Han F, Zhang G, Xi Q, Li J, Jiang H, Wang J, Yu G, Tian M, Zhang H. Pet demonstrates functional recovery after transplantation of induced pluripotent stem cells in a rat model of cerebral ischemic injury. *J Nucl Med*. 2013;54:785-792
219. Chen J, Sanberg PR, Li Y, Wang L, Lu M, Willing AE, Sanchez-Ramos J, Chopp M. Intravenous administration of human umbilical cord blood reduces behavioral deficits after stroke in rats. *Stroke*. 2001;32:2682-2688
220. Kozlowska H, Jablonka J, Janowski M, Jurga M, Kossut M, Domanska-Janik K. Transplantation of a novel human cord blood-derived neural-like stem cell line in a rat model of cortical infarct. *Stem Cells Dev*. 2007;16:481-488
221. Li Y, Chen J, Wang L, Lu M, Chopp M. Treatment of stroke in rat with intracarotid administration of marrow stromal cells. *Neurology*. 2001;56:1666-1672
222. Kurozumi K, Nakamura K, Tamiya T, Kawano Y, Ishii K, Kobune M, Hirai S, Uchida H, Sasaki K, Ito Y, Kato K, Honmou O, Houkin K, Date I, Hamada H. Mesenchymal stem cells that produce neurotrophic factors reduce ischemic damage in the rat middle cerebral artery occlusion model. *Mol Ther*. 2005;11:96-104
223. Oki K, Tatarishvili J, Wood J, Koch P, Wattananit S, Mine Y, Monni E, Tornero D, Ahlenius H, Ladewig J, Brustle O, Lindvall O, Kokaia Z. Human-induced pluripotent stem cells form functional neurons and improve recovery after grafting in stroke-damaged brain. *Stem Cells*. 2012;30:1120-1133
224. Robinton DA, Daley GQ. The promise of induced pluripotent stem cells in research and therapy. *Nature*. 2012;481:295-305
225. Shinozuka K, Dailey T, Tajiri N, Ishikawa H, Kaneko Y, Borlongan CV. Stem cell transplantation for neuroprotection in stroke. *Brain Sci*. 2013;3:239-261
226. Lee JM, Jung J, Lee HJ, Jeong SJ, Cho KJ, Hwang SG, Kim GJ. Comparison of immunomodulatory effects of placenta mesenchymal stem cells with bone marrow and adipose mesenchymal stem cells. *Int Immunopharmacol*. 2012;13:219-224

227. Netto CA, Hodges H, Sinden JD, Le Peillet E, Kershaw T, Sowinski P, Meldrum BS, Gray JA. Effects of fetal hippocampal field grafts on ischaemic-induced deficits in spatial navigation in the water maze. *Neuroscience*. 1993;54:69-92
228. Darsalia V, Kallur T, Kokaia Z. Survival, migration and neuronal differentiation of human fetal striatal and cortical neural stem cells grafted in stroke-damaged rat striatum. *Eur J Neurosci*. 2007;26:605-614
229. Hoehn M, Kustermann E, Blunk J, Wiedermann D, Trapp T, Wecker S, Focking M, Arnold H, Hescheler J, Fleischmann BK, Schwindt W, Buhrle C. Monitoring of implanted stem cell migration in vivo: A highly resolved in vivo magnetic resonance imaging investigation of experimental stroke in rat. *Proc Natl Acad Sci U S A*. 2002;99:16267-16272
230. Fischer UM, Harting MT, Jimenez F, Monzon-Posadas WO, Xue H, Savitz SI, Laine GA, Cox CS, Jr. Pulmonary passage is a major obstacle for intravenous stem cell delivery: The pulmonary first-pass effect. *Stem Cells Dev*. 2009;18:683-692
231. Lee ST, Chu K, Jung KH, Kim SJ, Kim DH, Kang KM, Hong NH, Kim JH, Ban JJ, Park HK, Kim SU, Park CG, Lee SK, Kim M, Roh JK. Anti-inflammatory mechanism of intravascular neural stem cell transplantation in haemorrhagic stroke. *Brain*. 2008;131:616-629
232. Li L, Jiang Q, Ding G, Zhang L, Zhang ZG, Li Q, Panda S, Lu M, Ewing JR, Chopp M. Effects of administration route on migration and distribution of neural progenitor cells transplanted into rats with focal cerebral ischemia, an mri study. *J Cereb Blood Flow Metab*. 2010;30:653-662
233. Guo L, Ge J, Wang S, Zhou Y, Wang X, Wu Y. A novel method for efficient delivery of stem cells to the ischemic brain. *Stem Cell Res Ther*. 2013;4:116
234. Keimpema E, Fokkens MR, Nagy Z, Agoston V, Luiten PG, Nyakas C, Boddeke HW, Copray JC. Early transient presence of implanted bone marrow stem cells reduces lesion size after cerebral ischaemia in adult rats. *Neuropathol Appl Neurobiol*. 2009;35:89-102
235. Gutierrez-Fernandez M, Rodriguez-Frutos B, Alvarez-Grech J, Vallejo-Cremades MT, Exposito-Alcaide M, Merino J, Roda JM, Diez-Tejedor E. Functional recovery after hematic administration of allogenic mesenchymal stem cells in acute ischemic stroke in rats. *Neuroscience*. 2011;175:394-405
236. Gorelik M, Orukari I, Wang J, Galpoththawela S, Kim H, Levy M, Gilad AA, Bar-Shir A, Kerr DA, Levchenko A, Bulte JW, Walczak P. Use of mr cell tracking to evaluate targeting of glial precursor cells to inflammatory tissue by exploiting the very late antigen-4 docking receptor. *Radiology*. 2012;265:175-185

237. Suarez-Monteagudo C, Hernandez-Ramirez P, Alvarez-Gonzalez L, Garcia-Maeso I, de la Cuetara-Bernal K, Castillo-Diaz L, Bringas-Vega ML, Martinez-Aching G, Morales-Chacon LM, Baez-Martin MM, Sanchez-Catasus C, Carballo-Barreda M, Rodriguez-Rojas R, Gomez-Fernandez L, Alberti-Amador E, Macias-Abraham C, Balea ED, Rosales LC, Del Valle Perez L, Ferrer BB, Gonzalez RM, Bergado JA. Autologous bone marrow stem cell neurotransplantation in stroke patients. An open study. *Restor Neurol Neurosci*. 2009;27:151-161
238. Savitz SI, Dinsmore J, Wu J, Henderson GV, Stieg P, Caplan LR. Neurotransplantation of fetal porcine cells in patients with basal ganglia infarcts: A preliminary safety and feasibility study. *Cerebrovasc Dis*. 2005;20:101-107
239. Li WY, Choi YJ, Lee PH, Huh K, Kang YM, Kim HS, Ahn YH, Lee G, Bang OY. Mesenchymal stem cells for ischemic stroke: Changes in effects after ex vivo culturing. *Cell Transplant*. 2008;17:1045-1059
240. Savitz SI, Misra V, Kasam M, Juneja H, Cox CS, Jr., Alderman S, Aisiku I, Kar S, Gee A, Grotta JC. Intravenous autologous bone marrow mononuclear cells for ischemic stroke. *Ann Neurol*. 2011;70:59-69
241. Honmou O, Houkin K, Matsunaga T, Niitsu Y, Ishiai S, Onodera R, Waxman SG, Kocsis JD. Intravenous administration of auto serum-expanded autologous mesenchymal stem cells in stroke. *Brain*. 2011;134:1790-1807
242. Bhasin A, Srivastava MV, Kumaran SS, Mohanty S, Bhatia R, Bose S, Gaikwad S, Garg A, Airan B. Autologous mesenchymal stem cells in chronic stroke. *Cerebrovasc Dis Extra*. 2011;1:93-104
243. Moniche F, Montaner J, Gonzalez-Marcos JR, Carmona M, Pinero P, Espigado I, Cayuela A, Escudero I, de la Torre-Laviana FJ, Boada C, Rosell A, Mayol A, Jimenez MD, Gil-Peralta A, Gonzalez A. Intra-arterial bone marrow mononuclear cell (bm-mnc) transplantation correlates with gm-csf, pdgf-bb and mmp-2 serum levels in stroke patients: Results from a clinical trial. *Cell Transplant*. 2014
244. Friedrich MA, Martins MP, Araujo MD, Klamt C, Vedolin L, Garicochea B, Raupp EF, Sartori El Ammar J, Machado DC, Costa JC, Nogueira RG, Rosado-de-Castro PH, Mendez-Otero R, Freitas GR. Intra-arterial infusion of autologous bone marrow mononuclear cells in patients with moderate to severe middle cerebral artery acute ischemic stroke. *Cell Transplant*. 2012;21 Suppl 1:S13-21
245. Battistella V, de Freitas GR, da Fonseca LM, Mercante D, Gutfilen B, Goldenberg RC, Dias JV, Kasai-Brunswick TH, Wajnberg E, Rosado-de-Castro PH, Alves-Leon SV, Mendez-Otero R, Andre C. Safety of autologous bone marrow

mononuclear cell transplantation in patients with nonacute ischemic stroke. *Regen Med*. 2011;6:45-52
246. Friedenstein AJ, Chailakhjan RK, Lalykina KS. The development of fibroblast colonies in monolayer cultures of guinea-pig bone marrow and spleen cells. *Cell Tissue Kinet*. 1970;3:393-403
247. Dominici M, Le Blanc K, Mueller I, Slaper-Cortenbach I, Marini F, Krause D, Deans R, Keating A, Prockop D, Horwitz E. Minimal criteria for defining multipotent mesenchymal stromal cells. The international society for cellular therapy position statement. *Cytotherapy*. 2006;8:315-317
248. Williams AR, Hare JM. Mesenchymal stem cells: Biology, pathophysiology, translational findings, and therapeutic implications for cardiac disease. *Circ Res*.109:923-940
249. Popa-Wagner A, Buga AM, Doeppner TR, Hermann DM. Stem cell therapies in preclinical models of stroke associated with aging. *Front Cell Neurosci*.8:347
250. He Z, Hua J, Song Z. Concise review: Mesenchymal stem cells ameliorate tissue injury via secretion of tumor necrosis factor-alpha stimulated protein/gene 6. *Stem Cells Int*.2014:761091
251. Salvolini E, Orciani M, Vignini A, Mattioli-Belmonte M, Mazzanti L, Di Primio R. Skin-derived mesenchymal stem cells (s-mscs) induce endothelial cell activation by paracrine mechanisms. *Exp Dermatol*.19:848-850
252. Yang M, Li Q, Sheng L, Li H, Weng R, Zan T. Bone marrow-derived mesenchymal stem cells transplantation accelerates tissue expansion by promoting skin regeneration during expansion. *Ann Surg*.253:202-209
253. Madrigal M, Rao KS, Riordan NH. A review of therapeutic effects of mesenchymal stem cell secretions and induction of secretory modification by different culture methods. *J Transl Med*.12:260
254. Kyurkchiev D, Bochev I, Ivanova-Todorova E, Mourdjeva M, Oreshkova T, Belemezova K, Kyurkchiev S. Secretion of immunoregulatory cytokines by mesenchymal stem cells. *World J Stem Cells*.6:552-570
255. Bartholomew A, Sturgeon C, Siatskas M, Ferrer K, McIntosh K, Patil S, Hardy W, Devine S, Ucker D, Deans R, Moseley A, Hoffman R. Mesenchymal stem cells suppress lymphocyte proliferation in vitro and prolong skin graft survival in vivo. *Exp Hematol*. 2002;30:42-48
256. Griffin MD, Ritter T, Mahon BP. Immunological aspects of allogeneic mesenchymal stem cell therapies. *Hum Gene Ther*.21:1641-1655
257. Castro-Manrreza ME, Montesinos JJ. Immunoregulation by mesenchymal stem cells: Biological aspects and clinical applications. *J Immunol Res*.2015:394917

258. Le Blanc K, Davies LC. Mesenchymal stromal cells and the innate immune response. *Immunol Lett*.
259. Li Y, Chopp M, Chen J, Wang L, Gautam SC, Xu YX, Zhang Z. Intrastriatal transplantation of bone marrow nonhematopoietic cells improves functional recovery after stroke in adult mice. *J Cereb Blood Flow Metab*. 2000;20:1311-1319
260. Vu Q, Xie K, Eckert M, Zhao W, Cramer SC. Meta-analysis of preclinical studies of mesenchymal stromal cells for ischemic stroke. *Neurology*.82:1277-1286
261. Ishizaka S, Horie N, Satoh K, Fukuda Y, Nishida N, Nagata I. Intra-arterial cell transplantation provides timing-dependent cell distribution and functional recovery after stroke. *Stroke*.44:720-726
262. Famakin BM. The immune response to acute focal cerebral ischemia and associated post-stroke immunodepression: A focused review. *Aging Dis*.5:307-326
263. Dirnagl U, Klehmet J, Braun JS, Harms H, Meisel C, Ziemssen T, Prass K, Meisel A. Stroke-induced immunodepression: Experimental evidence and clinical relevance. *Stroke*. 2007;38:770-773
264. Huang P, Gebhart N, Richelson E, Brott TG, Meschia JF, Zubair AC. Mechanism of mesenchymal stem cell-induced neuron recovery and anti-inflammation. *Cytotherapy*.
265. Yoo SW, Chang DY, Lee HS, Kim GH, Park JS, Ryu BY, Joe EH, Lee YD, Kim SS, Suh-Kim H. Immune following suppression mesenchymal stem cell transplantation in the ischemic brain is mediated by tgf-beta. *Neurobiol Dis*.58:249-257
266. Nogueira AB, Sogayar MC, Colquhoun A, Siqueira SA, Marchiori PE, Teixeira MJ. Existence of a potential neurogenic system in the adult human brain. *J Transl Med*.12:75
267. Lin R, Cai J, Nathan C, Wei X, Schleidt S, Rosenwasser R, Iacovitti L. Neurogenesis is enhanced by stroke in multiple new stem cell niches along the ventricular system at sites of high bbb permeability. *Neurobiol Dis*.74:229-239
268. Darsalia V, Heldmann U, Lindvall O, Kokaia Z. Stroke-induced neurogenesis in aged brain. *Stroke*. 2005;36:1790-1795
269. Thored P, Arvidsson A, Cacci E, Ahlenius H, Kallur T, Darsalia V, Ekdahl CT, Kokaia Z, Lindvall O. Persistent production of neurons from adult brain stem cells during recovery after stroke. *Stem Cells*. 2006;24:739-747
270. Jin KL, Mao XO, Greenberg DA. Vascular endothelial growth factor: Direct neuroprotective effect in in vitro ischemia. *Proc Natl Acad Sci U S A*. 2000;97:10242-10247
271. Butti E, Bacigaluppi M, Rossi S, Cambiaghi M, Bari M, Cebrian Silla A, Brambilla E, Musella A, De Ceglia R, Teneud

L, De Chiara V, D'Adamo P, Garcia-Verdugo JM, Comi G, Muzio L, Quattrini A, Leocani L, Maccarrone M, Centonze D, Martino G. Subventricular zone neural progenitors protect striatal neurons from glutamatergic excitotoxicity. *Brain*.135:3320-3335

272. Jeong CH, Kim SM, Lim JY, Ryu CH, Jun JA, Jeun SS. Mesenchymal stem cells expressing brain-derived neurotrophic factor enhance endogenous neurogenesis in an ischemic stroke model. *Biomed Res Int*.2014:129145
273. Tsai MJ, Tsai SK, Hu BR, Liou DY, Huang SL, Huang MC, Huang WC, Cheng H, Huang SS. Recovery of neurological function of ischemic stroke by application of conditioned medium of bone marrow mesenchymal stem cells derived from normal and cerebral ischemia rats. *J Biomed Sci*.21:5
274. Yiu G, He Z. Glial inhibition of cns axon regeneration. *Nat Rev Neurosci*. 2006;7:617-627
275. Takano T, Oberheim N, Cotrina ML, Nedergaard M. Astrocytes and ischemic injury. *Stroke*. 2009;40:S8-12
276. Grade S, Weng YC, Snapyan M, Kriz J, Malva JO, Saghatelyan A. Brain-derived neurotrophic factor promotes vasculature-associated migration of neuronal precursors toward the ischemic striatum. *PLoS One*.8:e55039
277. Tang G, Liu Y, Zhang Z, Lu Y, Wang Y, Huang J, Li Y, Chen X, Gu X, Yang GY. Mesenchymal stem cells maintain blood-brain barrier integrity by inhibiting aquaporin-4 upregulation after cerebral ischemia. *Stem Cells*.32:3150-3162
278. Xin H, Chopp M, Shen LH, Zhang RL, Zhang L, Zhang ZG, Li Y. Multipotent mesenchymal stromal cells decrease transforming growth factor beta1 expression in microglia/macrophages and down-regulate plasminogen activator inhibitor 1 expression in astrocytes after stroke. *Neurosci Lett*.542:81-86
279. Li Y, Chen J, Zhang CL, Wang L, Lu D, Katakowski M, Gao Q, Shen LH, Zhang J, Lu M, Chopp M. Gliosis and brain remodeling after treatment of stroke in rats with marrow stromal cells. *Glia*. 2005;49:407-417
280. Shen LH, Li Y, Gao Q, Savant-Bhonsale S, Chopp M. Down-regulation of neurocan expression in reactive astrocytes promotes axonal regeneration and facilitates the neurorestorative effects of bone marrow stromal cells in the ischemic rat brain. *Glia*. 2008;56:1747-1754
281. Krupinski J, Kaluza J, Kumar P, Wang M, Kumar S. Prognostic value of blood vessel density in ischaemic stroke. *Lancet*. 1993;342:742
282. Lin YC, Ko TL, Shih YH, Lin MY, Fu TW, Hsiao HS, Hsu JY, Fu YS. Human umbilical mesenchymal stem cells promote recovery after ischemic stroke. *Stroke*.42:2045-2053
283. Gutierrez-Fernandez M, Rodriguez-Frutos B, Ramos-Cejudo J, Teresa Vallejo-Cremades M, Fuentes B, Cerdan S, Diez-

Tejedor E. Effects of intravenous administration of allogenic bone marrow- and adipose tissue-derived mesenchymal stem cells on functional recovery and brain repair markers in experimental ischemic stroke. *Stem Cell Res Ther*.4:11

284. Miki Y, Nonoguchi N, Ikeda N, Coffin RS, Kuroiwa T, Miyatake S. Vascular endothelial growth factor gene-transferred bone marrow stromal cells engineered with a herpes simplex virus type 1 vector can improve neurological deficits and reduce infarction volume in rat brain ischemia. *Neurosurgery*. 2007;61:586-594; discussion 594-585
285. Onda T, Honmou O, Harada K, Houkin K, Hamada H, Kocsis JD. Therapeutic benefits by human mesenchymal stem cells (hmscs) and ang-1 gene-modified hmscs after cerebral ischemia. *J Cereb Blood Flow Metab*. 2008;28:329-340
286. Dulamea AO. The potential use of mesenchymal stem cells in stroke therapy--from bench to bedside. *J Neurol Sci*.352:1-11
287. Lalu MM, McIntyre L, Pugliese C, Fergusson D, Winston BW, Marshall JC, Granton J, Stewart DJ. Safety of cell therapy with mesenchymal stromal cells (safecell): A systematic review and meta-analysis of clinical trials. *PLoS One*.7:e47559
288. Schenborn ET, Goiffon V. Deae-dextran transfection of mammalian cultured cells. *Methods Mol Biol*. 2000;130:147-153
289. Holmen SL, Vanbrocklin MW, Eversole RR, Stapleton SR, Ginsberg LC. Efficient lipid-mediated transfection of DNA into primary rat hepatocytes. *In Vitro Cell Dev Biol Anim*. 1995;31:347-351
290. Washbourne P, McAllister AK. Techniques for gene transfer into neurons. *Curr Opin Neurobiol*. 2002;12:566-573
291. Mehier-Humbert S, Guy RH. Physical methods for gene transfer: Improving the kinetics of gene delivery into cells. *Adv Drug Deliv Rev*. 2005;57:733-753
292. Martinou I, Fernandez PA, Missotten M, White E, Allet B, Sadoul R, Martinou JC. Viral proteins e1b19k and p35 protect sympathetic neurons from cell death induced by ngf deprivation. *J Cell Biol*. 1995;128:201-208
293. Ikeda SR, Lovinger DM, McCool BA, Lewis DL. Heterologous expression of metabotropic glutamate receptors in adult rat sympathetic neurons: Subtype-specific coupling to ion channels. *Neuron*. 1995;14:1029-1038
294. Inoue T, Krumlauf R. An impulse to the brain--using in vivo electroporation. *Nat Neurosci*. 2001;4 Suppl:1156-1158
295. Shirahata Y, Ohkohchi N, Itagak H, Satomi S. New technique for gene transfection using laser irradiation. *J Investig Med*. 2001;49:184-190
296. Barrett LE, Sul JY, Takano H, Van Bockstaele EJ, Haydon PG, Eberwine JH. Region-directed phototransfection reveals

the functional significance of a dendritically synthesized transcription factor. *Nat Methods*. 2006;3:455-460
297. Yao CP, Zhang ZX, Rahmanzadeh R, Huettmann G. Laser-based gene transfection and gene therapy. *IEEE Trans Nanobioscience*. 2008;7:111-119
298. Schneckenburger H, Hendinger A, Sailer R, Strauss WS, Schmitt M. Laser-assisted optoporation of single cells. *J Biomed Opt*. 2002;7:410-416
299. Kim HJ, Greenleaf JF, Kinnick RR, Bronk JT, Bolander ME. Ultrasound-mediated transfection of mammalian cells. *Hum Gene Ther*. 1996;7:1339-1346
300. Dobson J. Gene therapy progress and prospects: Magnetic nanoparticle-based gene delivery. *Gene Ther*. 2006;13:283-287
301. Scherer F, Anton M, Schillinger U, Henke J, Bergemann C, Kruger A, Gansbacher B, Plank C. Magnetofection: Enhancing and targeting gene delivery by magnetic force in vitro and in vivo. *Gene Ther*. 2002;9:102-109
302. Daya S, Berns KI. Gene therapy using adeno-associated virus vectors. *Clin Microbiol Rev*. 2008;21:583-593
303. Srivastava A, Lusby EW, Berns KI. Nucleotide sequence and organization of the adeno-associated virus 2 genome. *J Virol*. 1983;45:555-564
304. Tan I, Ng CH, Lim L, Leung T. Phosphorylation of a novel myosin binding subunit of protein phosphatase 1 reveals a conserved mechanism in the regulation of actin cytoskeleton. *J Biol Chem*. 2001;276:21209-21216
305. Longa EZ, Weinstein PR, Carlson S, Cummins R. Reversible middle cerebral artery occlusion without craniectomy in rats. *Stroke*. 1989;20:84-91
306. Schaar KL, Brenneman MM, Savitz SI. Functional assessments in the rodent stroke model. *Exp Transl Stroke Med*.2:13
307. Higuchi T, Graham SH, Fernandez EJ, Rooney WD, Gaspary HL, Weiner MW, Maudsley AA. Effects of severe global ischemia on n-acetylaspartate and other metabolites in the rat brain. *Magn Reson Med*. 1997;37:851-857
308. Tkac I, Starcuk Z, Choi IY, Gruetter R. In vivo 1h nmr spectroscopy of rat brain at 1 ms echo time. *Magn Reson Med*. 1999;41:649-656
309. Romera C, Hurtado O, Botella SH, Lizasoain I, Cardenas A, Fernandez-Tome P, Leza JC, Lorenzo P, Moro MA. In vitro ischemic tolerance involves upregulation of glutamate transport partly mediated by the tace/adam17-tumor necrosis factor-alpha pathway. *J Neurosci*. 2004;24:1350-1357
310. Chen C, Okayama H. High-efficiency transformation of mammalian cells by plasmid DNA. *Mol Cell Biol*. 1987;7:2745-2752

311. Cohen-Kashi-Malina K, Cooper I, Teichberg VI. Mechanisms of glutamate efflux at the blood-brain barrier: Involvement of glial cells. *J Cereb Blood Flow Metab*.32:177-189
312. Teichberg VI, Cohen-Kashi-Malina K, Cooper I, Zlotnik A. Homeostasis of glutamate in brain fluids: An accelerated brain-to-blood efflux of excess glutamate is produced by blood glutamate scavenging and offers protection from neuropathologies. *Neuroscience*. 2009;158:301-308
313. Tian Z, Liu H, Su X, Fang Z, Dong Z, Yu C, Luo K. Role of elevated liver transaminase levels in the diagnosis of liver injury after blunt abdominal trauma. *Exp Ther Med*.4:255-260
314. Campos F, Sobrino T, Ramos-Cabrer P, Castellanos M, Blanco M, Rodriguez-Yanez M, Serena J, Leira R, Castillo J. High blood glutamate oxaloacetate transaminase levels are associated with good functional outcome in acute ischemic stroke. *J Cereb Blood Flow Metab*.31:1387-1393
315. Yoshikawa K. Studies on the anti-diabetic effect of sodium oxaloacetate. *Tohoku J Exp Med*. 1968;96:127-141
316. Llorens J, Li AA, Ceccatelli S, Sunol C. Strategies and tools for preventing neurotoxicity: To test, to predict and how to do it. *Neurotoxicology*.33:796-804
317. Ginsberg MD. Neuroprotection for ischemic stroke: Past, present and future. *Neuropharmacology*. 2008;55:363-389
318. Togel F, Westenfelder C. Adult bone marrow-derived stem cells for organ regeneration and repair. *Dev Dyn*. 2007;236:3321-3331
319. McMahon JM, Conroy S, Lyons M, Greiser U, O'Shea C, Strappe P, Howard L, Murphy M, Barry F, O'Brien T. Gene transfer into rat mesenchymal stem cells: A comparative study of viral and nonviral vectors. *Stem Cells Dev*. 2006;15:87-96
320. Rogachev B, Tsesis S, Gruenbaum BF, Gruenbaum SE, Boyko M, Klein M, Shapira Y, Vorobiev M, Zlotnik A. The effects of peritoneal dialysis on blood glutamate levels: Implementation for neuroprotection. *J Neurosurg Anesthesiol*.25:262-266